University of Naples Federico II

Polytechnic and Basic Sciences School

Department of Chemical Sciences

Ph.D. in Chemical Sciences

Sustainable production of functional materials from agri-food by-products

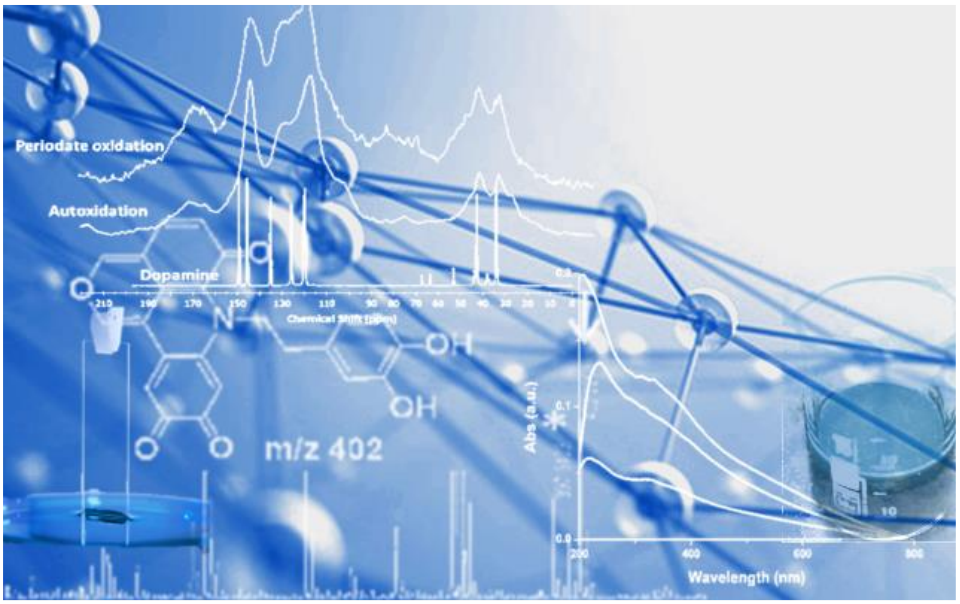

Federica Moccia

Advisor

Prof. Lucia Panzella

Prof. Andreas Schieber

Dr. Samuele Giovando

Examiner

Prof. Gerardino D'Errico

XXXIV Cycle 2018-2021

Coordinator: prof. Angela Lombardi

Index

ABSTRACT

This PhD research project was aimed at the exploitation of phenolic compounds from agri-food by-products for applications in human health or as additives for functional materials. Agri-food industry is responsible for the generation of high volumes of organic by-products along the entire supply chain, whose disposal represents a cost to the food processor and has a negative impact on the environment. On the other hand, these waste products are becoming increasingly attractive as easily available, low cost and sustainable sources of functional compounds, first of all phenolic compounds, which are finding increasing applications not only as food supplements but also as additives for the implementation of functional materials.

In this context, specific aims of the PhD project were:

a) Characterization of the antioxidant and functional properties and of the main phenolic constituents of selected agri-food by-products;
b) Improvement of the antioxidant properties of agri-food by-products by hydrolytic activation treatments or bioprocessing (e.g. fermentation) and characterization of the main structural modifications induced on the phenolic constituents;
c) Exploitation of agri-food by-products derived phenolic compounds as additives for the implementation of functional materials.

Main outcomes can be summarized as follows:

- Hydrolytic treatments induced specific boosting effects on the antioxidant properties of agri-food by-products as a consequence of the removal of non-active components (mainly polysaccharides) and of structural modifications induced on lignin and hydrolyzable tannins, whereas fermentation processes led, in the case of

pomegranate wastes, to a material with a very high content of the bioactive ellagic acid, likely as a result of hydrolytic phenomena.

- Incorporation of extracts from pecan nut shell, an agri-food by-product endowed with very potent antioxidant properties in poly(lactic acid) and whey protein films, provided materials with enhanced antioxidant and antimicrobial properties for use in food-related applications, such as active packaging, whereas functionalization of chitosan films with hydrolyzed spent coffee ground/silver nanoparticles led to materials with antioxidant and antibacterial activities for use in the biomedical sector.

In the frame of the collaboration with the industrial partner of the PhD project "Centro di Ricerche per la Chimica Fine", particular attention was devoted to tannins and by-products of the tannin industry. In particular, the research activity was directed to:

d) Improvement of the antioxidant and antipollutant properties of exhausted woods and chestnut wood fiber, that is the residual materials after industrial tannin extraction, by hydrolytic activation.
e) Comparative evaluation of the antioxidant properties of wood tannin-based coated substrates, which showed the superior ability of condensed tannins to form a functional and robust antioxidant coating for material functionalization.
f) Development of a rational and tunable deep eutectic solvent-based processing for valorization of chestnut wood fiber as a source of ellagic acid and lignin.

Finally, as part of the project carried out in collaboration with the foreign partner of the project, Prof. Andreas Schieber (Institute of Nutritional and Food Science, Molecular Food Technology, University of Bonn), new facile and low-cost protocols for the synthesis of anthocyanin metabolites of biological interest were developed.

Research work on related topics concerning food pigments resulted in the preparation and characterization of a new cyanine from oxidative coupling of chlorogenic acid with tryptophan with potential properties for use as a red dye for food coloring.

List of publications

1. L. Panzella, **F. Moccia**, M. Toscanesi, M. Trifuoggi, S. Giovando, A. Napolitano "Exhausted woods from tannin extraction as an unexplored waste biomass: evaluation of the antioxidant and pollutant adsorption properties and activating effects of hydrolytic treatments" *Antioxidants*, 8 (**2019**), 84; doi: 10.3390/antiox8040084.

2. **F. Moccia**, A.C. Flores-Gallegos, M.L. Ch vez-Gonz le, L. Sep lveda, S. Marzorati, L. Verotta, L. Panzella, J.A. Ascacio-Valdes, C.N. Aguilar, A. Napolitano "Ellagic acid recovery by solid state fermentation of pomegranate wastes by *Aspergillus niger* and *Saccharomyces cerevisiae*: a comparison" *Molecules*, 24 (**2019**), 3689; doi: 10.3390/molecules24203689.

3. **F. Moccia**, S. Agustin-Salazar, L. Verotta, E. Caneva, S. Giovando, G. D'Errico, L. Panzella, M. d'Ischia, A. Napolitano "Antioxidant properties of agri-food by-products and specific boosting effects of hydrolytic treatments", *Antioxidants*, 9 (**2020**), 438; doi: 10.3390/antiox9050438.

4. **F. Moccia**, S. Agustin-Salazar, A.-L. Berg, B. Setaro, R. Micillo, E. Pizzo, F. Weber, N. Gamez-Meza, A. Schieber, P. Cerruti, L. Panzella, A. Napolitano "Pecan (*Carya illinoinensis* (Wagenh.) K. Koch) nut shell as an accessible polyphenol source for active packaging and food colorant stabilization", *ACS Sustain. Chem. Eng.*, 8 (**2020**), 6700–6712; doi: 10.1021/acssuschemeng.0c00356.

5. L. Panzella, **F. Moccia**, R. Nasti, S. Marzorati, L. Verotta, A. Napolitano "Bioactive phenolic compounds from agri-food wastes: an update on green and sustainable extraction methodologies", *Front. Nutr.*, 7 (**2020**), 60; doi: 10.3389/fnut.2020.00060.

6. L. Panzella, P. Cerruti, P. Aprea, R. Paolillo, G. Pellegrino, **F. Moccia**, G. G. Condorelli, A. Vollaro, V. Ambrogi, M. R. Catania, M. d'Ischia, A. Napolitano

"Silver nanoparticles on hydrolyzed spent coffee grounds (HSCG) for green antibacterial devices", *J. Clean. Prod*, 268 (**2020**), 122352; doi: 10.1016/j.jclepro.2020.122352.

7. **F. Moccia**, A. Piscitelli, S. Giovando, P. Giardina, L. Panzella, M. d'Ischia, A. Napolitano "Hydrolyzable *vs*. Condensed wood tannins for bio-based antioxidant coatings: superior properties of quebracho tannins", *Antioxidants*, 9 (**2020**), 804; doi: 10.3390/antiox9090804.

8. M. L.Alfieri, **F. Moccia**, G. D'Errico, L. Panzella, M. d'Ischia, A. Napolitano "Acid treatment enhances the antioxidant activity of enzymatically synthesized phenolic polymers", *Polymers*, 12 (**2020**), 2544; doi: 10.3390/polym12112544.

9. **F. Moccia**, M. Á. Martín, S. Ramos, L. Goya, S. Marzorati, M. DellaGreca, L. Panzella, A. Napolitano "A new cyanine from oxidative coupling of chlorogenic acid with tryptophan: assessment of the potential as red dye for food coloring", *Food Chem.*, 348 (**2020**), 129152; doi: 10.1016/j.foodchem.2021.129152.

10. A. Arciello, L. Panzella, E. Dell'Olmo, M. Abdalrazeq, **F. Moccia**, R. Gaglione, S. Agustin-Salazar, A. Napolitano, L. Mariniello, C. V. L. Giosafatto "Development and characterization of antimicrobial and antioxidant whey protein-based films functionalized with Pecan (*Carya illinoinensis*) nut shell extract", *Food Packag. Shelf Life*, 29 (**2021**), 100710; doi: 10.1016/j.fpsl.2021.100710.

Manuscripts in preparation

1. **F. Moccia**, N. Gallucci, S. Giovando, A. Zuorro, R. Lavecchia, G. D'Errico, L. Panzella, A. Napolitano "A rational and tunable deep eutectic solvent-based processing for valorization of chestnut wood fiber as a clean and largely available source of ellagic acid and lignin". Manuscript in preparation.

2. V. Maresca, G. Salbitani, **F. Moccia**, P. Cianciullo, S. Sorbo, M. Insolvibile, S. Carfagna, L. Panzella, A. Basile "Antioxidant response to heavy metal pollution of Regi Lagni freshwater in *Conocephalum conicum* L. (Dum.)". Manuscript in preparation.

Chapter 1

Introduction

1.1 Natural compounds: primary and secondary metabolites

Natural compounds can be defined as all compounds that are synthesized/produced by living organisms. They are usually divided into two classes: primary and secondary metabolites. Primary metabolites can be found in all plants and are directly involved in the physiological processes occurring in the organism, such as its growth, development, and reproduction. Examples of primary metabolites include sugars, amino acids, and nucleosides. On the other hand, secondary metabolites are compounds that are not directly involved in primary metabolic processes of an organism and are produced by the plant cell through metabolic pathways derived from the primary metabolism. Compared to the primary metabolites which are highly conserved, the synthesis of secondary metabolites depends on the type of species, organs, tissues, cellular functions and cellular developmental stages.[1]

According to their chemical structures, secondary plant metabolites are divided into several classes, including:[2]

- Phenolics
- Alkaloids
- Terpenes

1.2 Antioxidants

An antioxidant is a substance (small molecule or complex system) that, when added to oxidizable molecules in small amounts (for small molecules, usually <1% of the quantity of the material requiring protection), is able to protect such molecules by delaying, retarding or inhibiting their autoxidation.[3] From a biological point of view,

antioxidants are molecules able to prevent or slow damage cells caused by reactive radical species. Oxidation is a chemical reaction that transfers electrons from a substance to an oxidizing agent. Oxidation reactions can produce radical species, commonly known in living organisms as reactive oxygen species (ROS). ROS are produced as result of normal cellular metabolism.[4] At high concentrations, under oxidative stress conditions, these reactive species produce adverse modifications to cell components, such as lipids, proteins, and DNA,[4–7] contributing to different pathological conditions, including cancer, neurological and cardio-respiratory disorders.[5,8] ROS include radicals such as superoxide ($\bullet O^{2-}$) and hydroxyl radicals ($\bullet OH$), as well as non-radical reactive intermediate molecules, like hydrogen peroxide (H_2O_2). $\bullet OH$, in particular, can react with organic molecules (RH) that in presence of oxygen are converted into peroxyl radicals ($ROO\bullet$), giving rise to chain reactions that can induce multiple chemical changes in lipid membranes, DNA and proteins.[4,6,7] (Figure 1.2.1). Nitrogen reactive species (nitric oxide, peroxynitrite, and related compounds) also can be produced by living organisms and, at high concentrations, have adverse effects on cells.[9]

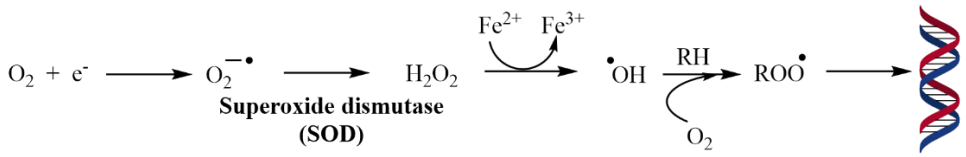

Figure 1.2.1. Main reactive oxygen species (ROS).

Antioxidants play an important role in terminating the radical chain reactions, thus inhibiting their dangerous effects on biomolecules. Antioxidants are usually classified into:

- **Endogenous antioxidants,** that are autonomously synthesized by organisms. This category includes enzymes, such as superoxide dismutase, glutathione peroxidase and catalase.

- **Exogenous antioxidants,** that are assumed with the diet. This category includes, among others, ascorbic acid, vitamin E and phenolic compounds.

Depending on the different mechanism of action, antioxidants can be also classified as primary and secondary antioxidants:

- **Primary antioxidants,** also known as preventive antioxidants, react rapidly with reactive radicals and convert them into more stable products. Usually, their mode of action is based on the donation of an electron or a hydrogen atom to the radical species. The resulting antioxidant radical is much less reactive than initial radical, and therefore do not promote oxidation. These antioxidant radicals can also react with others radicals, such as peroxyl, hydroxyl and other antioxidant radicals, terminating the chain reaction.[10]

- **Secondary antioxidants** react with hydroperoxides to yield non-radical, non-reactive products. They can also act as metal chelators.

Among antioxidants, phenolic compounds are particularly interesting for several applications.[10]

1.2.1 Phenolic compounds: properties and applications

Phenolic compounds are a group of ubiquitous secondary metabolites found mainly in plants and with a wide range of structures and functions. Structurally, natural phenolic compounds contain one or more aromatic rings functionalized with one or more hydroxyl groups and are characterized by a wide structural variety, ranging from a simple phenolic molecule to a complex high-molecular weight polymer (for example tannins and lignins).[11]

Phenolic compounds play important roles in plant growth, reproduction and protection against pathogens and predators, and confer colour and sensory characteristics to fruits and vegetables.

Antioxidant activity is among the most studied property of phenolic compounds. Indeed, they are able to slow down or completely inhibit oxidative processes promoted by ROS and reactive nitrogen species. The antioxidant mechanisms of phenolics include donation of hydrogen atoms or electrons, scavenging of free radicals and chelation of transition metal ions.[11] Of course their properties are strictly related to their structures.[11–13]

Natural phenolic compounds typically exert their beneficial effects through their circulating metabolites and exhibit a large number of beneficial properties for human health, such as anti-allergenic, anti-atherogenic, anti-inflammatory, anti-thrombotic, cardioprotective and vasodilatory activities.[11] Beneficial effects against human cancer cell lines have been also widely investigated, and several studies have demonstrated the ability to reduce or inhibit the growth of different tumours, including those of mouth, stomach, duodenum, colon, liver, lung, mammary gland or skin.[13–15]

Phenolic compounds have been also reported to display marked antimicrobial activities against different microorganisms involved in human diseases and deterioration of foods.[13] Therefore, in this context, many studies have evaluated the possible use of phenolic compounds as natural antimicrobial food preservatives.[16–18]

Remaining in an application context, natural phenolic compounds have been also investigated as natural dyes, providing shades of red, yellow-orange, blue and green. For example, anthocyanin, are commonly applied as food colorants in different liquid and solid matrices.[19]

The facile incorporation of antioxidant phenolic compounds into polymers and biopolymers, both for stabilization and functionalization purposes, is particularly relevant for food packaging applications. Indeed, oxidation is one of the main degradation reactions that may occur in food, and active packaging, that is packaging functionalized with antioxidant and/or antimicrobial additives such as natural phenolic compounds is attracting increasing attention.[17,20,21]

Considerable attention has been directed to the exploitation of phenolic compounds in cosmetics, too, since they have been found to be able to prevent skin aging and hyperpigmentation, provide photoprotective action, and, thanks to their anti-inflammatory activity, act as support in the treatment of sensitive or sun-stressed skin.[22,23]

Finally, natural phenolic compounds have been also used as functional additives for a broad range of other applications, including hydrogels, biocompatible and biomimetic glues, nanostructures for drug delivery, sensors, semiconductors, photo- and thermostabilizing agents, and other devices for biomedicine and organic electronics.[24–27]

1.2.2 Main classes of phenolic compounds

Phenolics comprise a wide variety of compounds that can be divided into several classes, according to the number of phenol rings and to the structural elements that bind these rings to one another. The main groups of natural phenolic compounds are described below.

Flavonoids. Flavonoids are one of the most widely distributed class of phenolic compounds, which account for approximately two-thirds of the dietary phenols,[12,28] and confer colour to many species of flowers and fruits. Flavonoids are present in nature predominantly as glycosides,[29] in which one or more sugar groups is bound to a phenolic group by glycosidic linkage. Flavonoids are divided into seven

subgroups: flavones, flavonols, flavanols, flavanones, isoflavones, chalcones, and anthocyanins, depending on the position of the linkage between the B and the C rings, as well as on the degree of unsaturation and oxidation of the C ring (Table 1.2.2.1).[30]

Flavonoids play a variety of biological and health beneficial activities. In plants, they are responsible for the colour and scent of flowers, protect them from different biotic and abiotic stresses, and act as signal molecules and phytoalexins. Furthermore, flavonoids are able to stimulate seed and spore germination, attract pollinator and act as UV filter.[31] Flavonoids are also associated with a wide range of biological effects on human health, as a result of their antioxidant, anticancer, anti-aging, cardio- and neuro-protective, antibacterial, anti-inflammatory, anti-allergic, antidiabetic and anti-thrombotic activities.[32]

Table 1.2.2.1. Basic structure of flavonoids and their classes. Adapted from Ref.[33]

Groups	Structure	Examples
Flavones	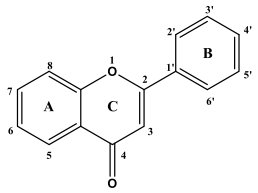	Apigenin Luteolin Tangeretin Nobiletin
Flavonols	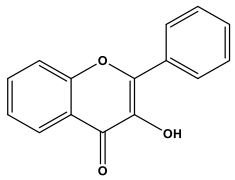	Kaempferol Myricetin Quercetin Isorhamnetin
Flavanols	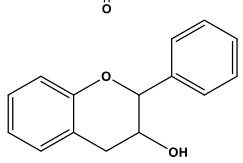	Catechin Gallocatechin Epicatechin, epigallocatechin-3- gallate
Flavanones	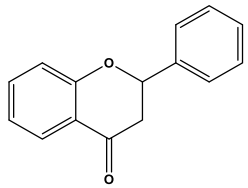	Naringenin Hesperetin Eriodictyo
Isoflavones	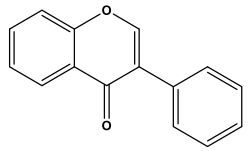	Daidzein Genistein Glycitein
Chalcones	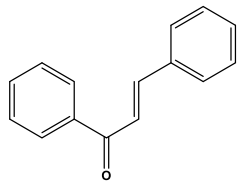	Phloridzin Arbutin Phloretin Chalconaringenin
Anthocyanidins	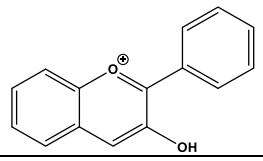	Cyanidin Delphinidin Pelargonidin

Flavones. Flavones are widely present as glucosides in leaves, flowers, and fruits. Luteolin and apigenin are the main flavones in diet.[30] High content of these compounds have been identified in celery, sweet red pepper, parsley and other herbs (Figure 1.2.2.1).[34] They are characterized by a double bond between positions 2 and 3 and a ketone in position 4 of the C ring. Different substitutions, such as hydroxylation, methylation, O- and C-alkylation and glycosylation can occur, increasing the number of possible molecules.[30]

Flavonols. Flavonols are characterized by the presence of a ketone group at C-4 and a hydroxyl group on position 3 of the C ring, which can be glycosylated. Flavonols are commonly found in a wide range of fruits, vegetables and beverages, in particular onions, tomatoes, apples, grapes and berries but also tea and red wine (Figure 1.2.2.1).[30] Due to the different glycosylation, methylation and hydroxylation patterns, flavonols are the largest subgroup of flavonoids, with myricetin, quercetin and kaempferol the most widely distributed in nature.

Flavanones and flavanols. Differently from flavonols and flavones, flavanones are characterized by the absence of the double bond between C2 and C3. These compounds are particularly present in citrus fruits and juices and exert an important role in generating the bitter taste of these fruits (Figure 1.2.2.1). Hesperitin, naringenin and eriodictyol are the main examples of this class of flavonoids. Flavanols, also known as dihydroflavonols or catechins, are the 3-hydroxy derivatives of flavanones.[30]

Isoflavones. Isoflavones are flavonoids characterized by a different position of the B ring, that is bonded to the C-3 of the C ring. Isoflavones are mainly represented by daidzein and genistein, predominantly found in soybeans and other leguminous plants (Figure 1.2.2.1).[30]

Chalcones. Chalcones are characterised by the absence of the C-ring of the basic flavonoid skeleton structure. Major examples of chalcones include phloridzin,

arbutin, phloretin and chalconaringenin, found in significant amounts in tomatoes, pears, strawberries, bearberries and wheat products.[30]

Anthocyanidins. Anthocyanins are the main class of flavonoids responsible for colours ranging from pink, red and purple to dark blue of most fruits, flowers and leaves,[35] in particular cranberries, black currants, red grapes, merlot grapes, raspberries, strawberries, blueberries, bilberries and blackberries (Figure 1.2.2.1). Cyanidin, delphinidin, malvidin, pelargonidin and peonidin are the most commonly found anthocyanins. Anthocyanins differ in the number of hydroxyl groups, the methylation degree of their hydroxyl groups, the nature and number of sugars bonded to the molecule, as well as the nature and number of aliphatic or aromatic acids attached to the sugars.[36] These flavonoids exist also in the aglycone forms, known as anthocyanidins.

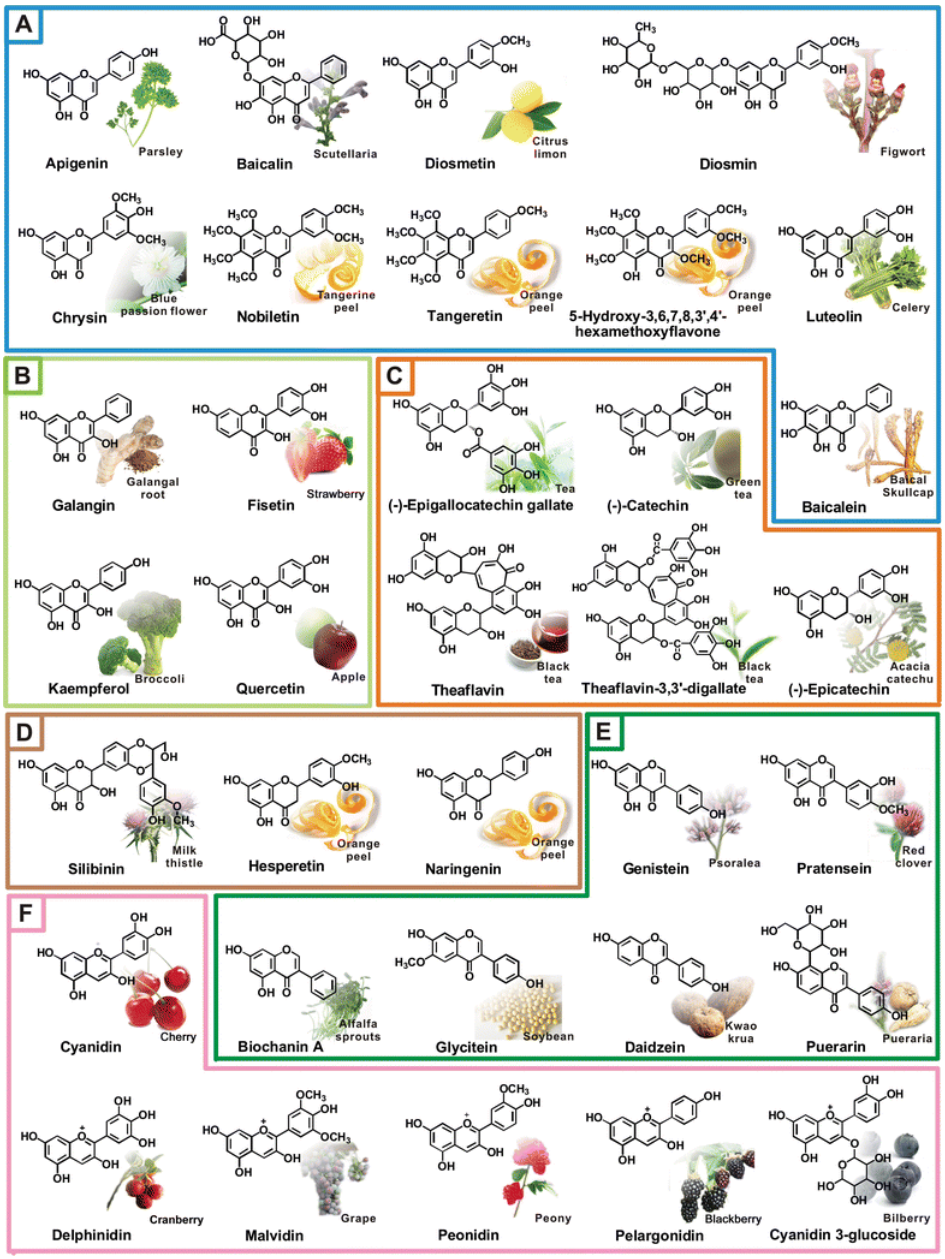

Figure 1.2.3.1. Representative natural flavonoids and their dietary sources. (A) flavones, (B) flavonols, (C) flavanols, (D) flavanones, (F) isoflavones, (G) anthocyanidins.[33]

Phenolic acids. Phenolic acids are phenolic compounds containing a carboxyl group. They constitute about one-third of the dietary phenols,[28] and generally occur rarely in free form and most frequently in the form of esters, glycosides or amides.[37] Phenolic acids are divided into two sub-groups, the hydroxybenzoic acids and the hydroxycinnamic acids.

The most common hydroxybenzoic acids are *p*-hydroxybenzoic, vanillic, protocatechuic, syringic and gallic acids, characterized by the common C6-C1 structure. Among hydroxycinnamic acids, characterized by a three-carbon side chain, the most abundant are caffeic, ferulic, *p*-coumaric and sinapic acids (Figure 1.2.2.2).[38]

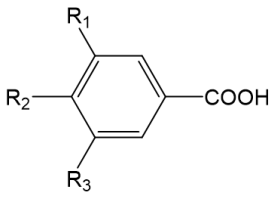

Hydroxybenzoic acid

Acid	R1	R2	R3
p-Hydroxybenzoic	H	OH	H
Protocatechuic	OH	OH	H
Vanillic	OCH_3	OH	H
Syringic	OCH_3	OH	OCH_3
Gallic	OH	OH	OH

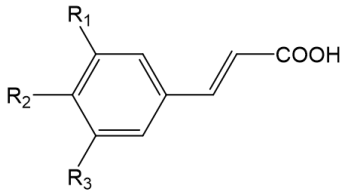

Hydroxycinnamic acid

Acid	R1	R2	R3
p-Coumaric	H	OH	H
Ferulic	OH	OH	H
Caffeic	OCH_3	OH	H
Sinapic	OCH_3	OH	OCH_3

Figure 1.2.2.2. Chemical structures of most abundant naturally occurring phenolic acids**.**

Phenolic acids act as potent antioxidants[39–41] and exhibit antidiabetic,[39,42] antimicrobial,[39,43,44] anticancer,[39,45,46] anti-inflammatory[39,47,48] and neuro- and cardio-protective activities.[39]

Stilbenes. Stilbenes are compounds characterized by a 1,2-diphenylethylene basic structure. Among the antioxidant stilbenes present in nature, a prominent role is occupied by 3,4',5-trihydroxystilbene, also known as resveratrol. This compound

exists in *cis*- or *trans*-configuration, but the latter is the most widely studied.[49] Resveratrol is found in different fruits, in particular mulberries, peanuts, grapes and red wine.[50] Others natural stilbenes are pterostilbene (*trans*-4'-hydroxy-3,5-dimethoxystilbene), the hydroxylate analogue of resveratrol piceatannol (*trans*-3,3′,4,5′-tetrahydroxystilbene) and pinosylvin (*trans*-3,5-dihydroxystilbene), which widely occur in plant sources such as grapes, peanuts, passion fruit and white tea[50] (Figure 1.2.2.3).

Natural stilbenes have received much attention for their remarkable potential in the prevention and treatment of different diseases, including cancer, due to their ability to induce cell death and their anti-inflammatory properties, associated with low toxicity in vivo.[50]

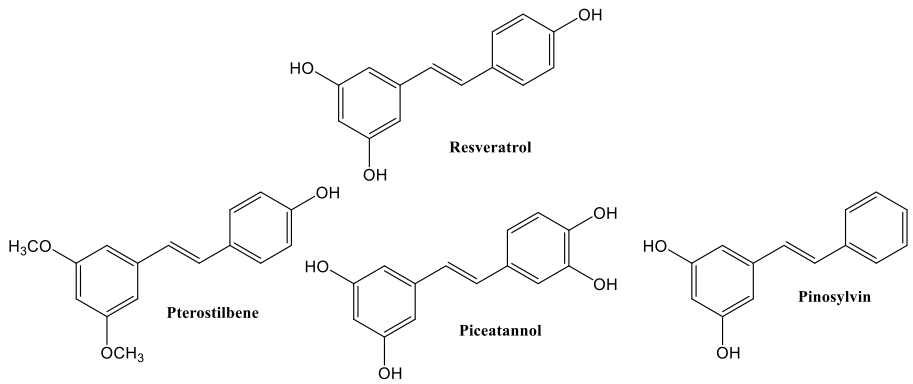

Figure 1.2.2.3. Chemical structure of the main naturally occurring stilbenes.

Tannins. Tannins are a class of phenolic polymers, responsible of the astringent taste of different foods.[51] They are traditionally divided into hydrolyzable and condensed or non-hydrolyzable tannins.[52]

Condensed tannins are polymeric flavonoids, and their most frequent basic units are derivatives of the flavanols (+)-catechin, (-)-epicatechin, (+)-gallocatechin, (-)-epigallocatechin and (-)-epigallocatehin gallate. They are characterized by a wide structural diversity due to possible O-methylation, C-and O-glycosylation, and O-

galloylation. In addition, condensed tannins can be further distinguished into procyanidins and profisetinidins.[52] Procyanidins, predominantly present in grape,[53] can be classified in the B-type (dimeric) and C-type (trimeric), characterized by single bond between units, usually between the C4 and the C6 or C8 of the flavanol units, or the A-type, characterized by an additional bond between C-2 and 7 or 5-OH (Figure 1.2.2.4). Profisetinidins, predominantly found in some type of wood, such as quebracho (*Schinopsis lorentzii*) e mimosa (*Acacia mollissima*),[54] differ from the procyanidins by the absence of a hydroxyl group at C5 position of the A ring.[52]

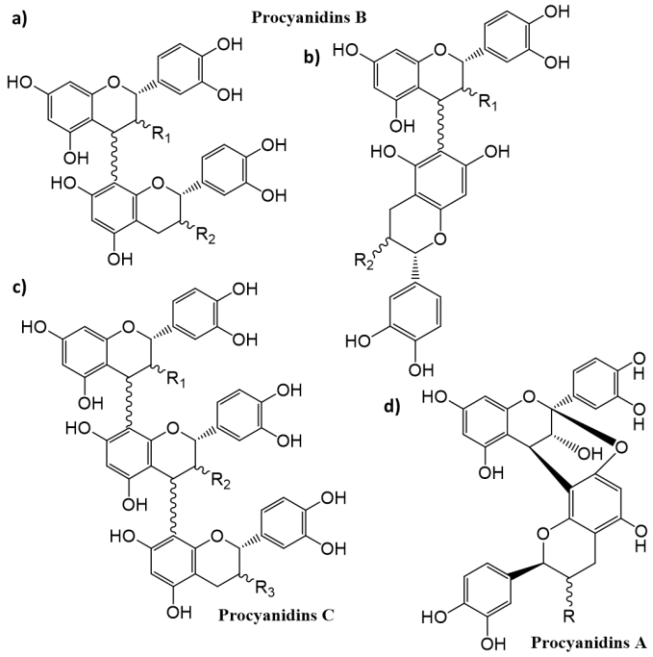

Figure 1.2.2.4. General structures of a) and b) B-type, c) C-type and d) A-type procyanidins.

Condensed tannins can contain up to 100 units of monomers, with a molecular weight ranging from 500 to over 2000 Da.[55]

Hydrolyzable tannins represent the other main class of tannins. They are usually found in plants in lower concentrations than condensed tannins. The structural motif

contains a monosaccharide as a central core, generally D-glucose, whose hydroxy groups are esterified with phenolic compounds, such as ellagic acid (EA) or gallic acid to give ellagitannins and gallotannins, respectively[52] (Figure 1.2.2.5). Their name is attributed to the facile hydrolysis induced by acids and some enzymes, such as tannase, resulting in gallic acid and EA release. Gallotannins are generally found in galls (*Quercus infectoria* and *Rhus semialata*),[56–58] in sumac fruits (*Rhus coriaria*),[56,59] and tara (*Caesalpinia spinosa*),[56,60] whereas ellagitannins are present in oak wood (*Quercus robur*, *Quercus petraea* and *Quercus alba*),[61] chestnut (*Castanea sativa*)[56,61,62] and myrobalan (*Terminalia chebula*).[56,63]

Phlorotannins are a third class of tannins and are polymers of phloroglucinol. They have been isolated from several genera of brown algae,[64] but are not relevant for the human diet.

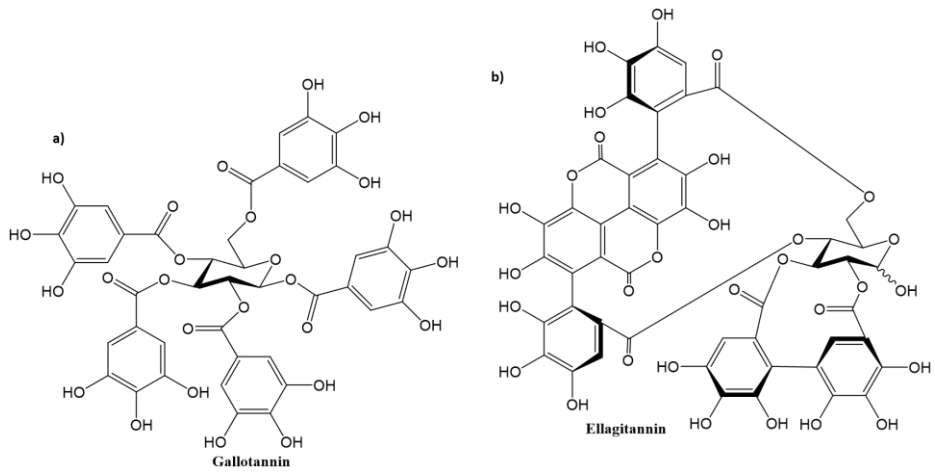

Figure 1.2.2.5. General structure of hydrolyzable tannins: a) gallotannin and b) ellagitannin.

Tannins occupy a prominent role among natural phenolic compounds due to their remarkable antioxidant, antimicrobial, and anticancer activities.[64–66] These compounds have been also well known for their ability to strongly interact with proteins, which has prompted their use in the leather tanning industry, as good substitute for the toxic chromium.[67,68] Tannins are also extensively used as food

additives, for example to improve wine colour stability, protect foods against oxidation, or to confer astringent taste and flavor.[67] Tannins are currently exploited as adhesive,[67,69,70] to replace formaldehyde-based materials and some of them are also used in animal food and feeds,[67] producing useful benefits in ruminants, such as faster growth rates of liveweight or wool, higher milk yields, increased fertility, and improved animal welfare and health through prevention of bloat and lowering of worm burdens. In particular, the ability of tannins to bind proteins can reduce the amount of protein that is digested in the rumen and enhance the amount of protein that is available for digestion in the small intestine, thus allowing higher absorption of dietary amino acids. On the other hand, some tannins can have harmful nutritional effects, acting as antinutritional agents and impacting negatively on animal production.[71]

Wood protection properties of tannins have been also investigated,[67,72–76] while different studies have evaluated the possibility to use tannins for the production of almost totally biosourced foams and resins.[67] Tannins have been found also to be able to act as anti-corrosion materials for metals.[67,69,77–80]

Several papers have reported the use of wood tannins for the production of functional films and coatings for a wide range of applications,[81–85] and, in virtue of their capability of interact with a wide variety of different compounds, hybrid and hybrid-like nanomaterials have been prepared and used in catalysis, in functional food packaging, as well as in UV-shielding.[86]

Lignin. Lignin is an irregular, water-insoluble, three-dimensional high molecular mass biopolymer (600–15000 kDa), composed of three different hydroxycinnamyl alcohol monomers, that is coniferyl, sinapyl and *p*-coumaryl alcohols, differing in the degree of methoxylation (Figure 1.2.2.6).[87] These monolignols lead, through a series of oxidation steps, to the formation of guaiacyl (G), syringyl (S), and *p*-hydroxyphenyl (H) lignin units, respectively. Lignin is, after cellulose, the second

most abundant terrestrial biopolymer, accounting for approximately 30% of the organic carbon on the planet.[87] The composition of lignins depends essentially on the type of plant species. For example, angiosperm lignins, classified as hardwood, consist mainly of G (50%) and S (50%) units, whereas gymnosperm lignins, classified as softwood, are composed mostly of G units with low levels of S units (ca. 5-10%). On the other hand, grass lignins is constituted of a mixture of G, H and S units.[88] Also the stage of cell development, as well as the environmental conditions can affect the lignin composition.[89]

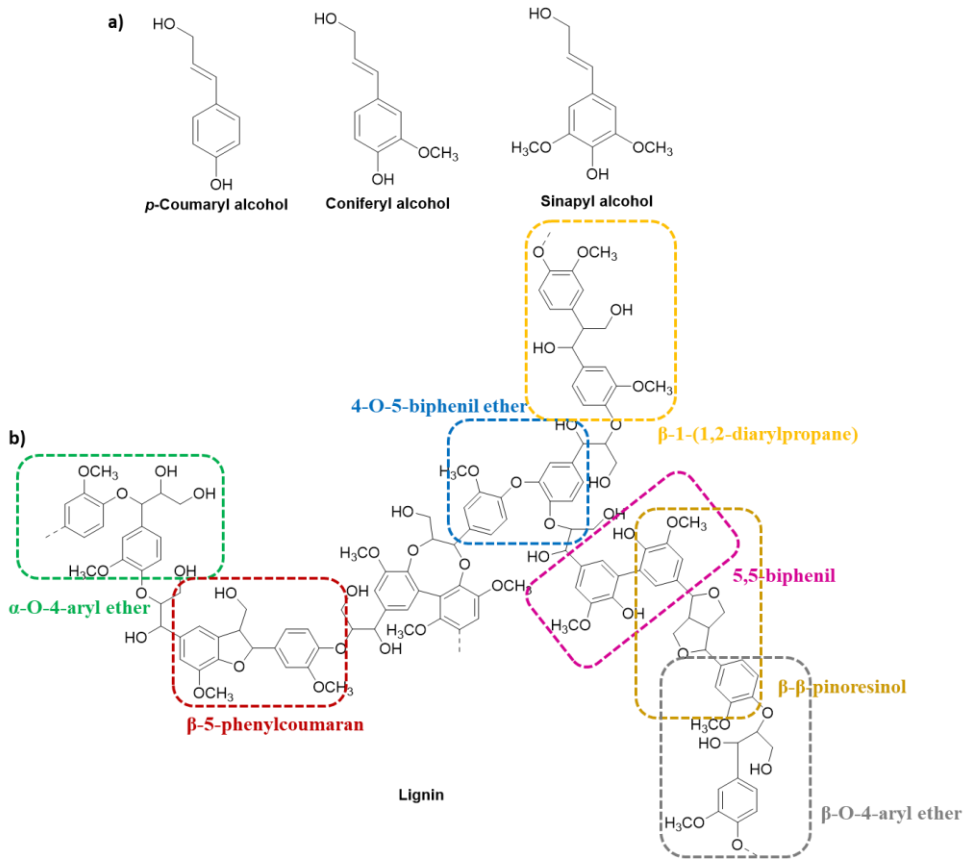

Figure 1.2.2.6. a) Chemical structures of lignin monomers and b) lignin scaffold. Adapted from Ref.[90]

The lignification process proceeds via radical coupling reactions, in which a new monomer binds to the growing polymer.[91] The most frequent inter-unit bond is the β–O–4-aryl ether linkage but β-5-phenylcoumaran, 5,5-biphenil, 4-O-5-biphenil ether, β-1-(1,2-diarylpropane), β-β-pinoresinol and α-O-4-aryl ether can be also found (Figure 1.2.3.6).[91,92]

Lignins exert many biological functions in plants, such as water transport, mechanical support and resistance to pathogens or stresses.[93]

Lignins also showed beneficial effects on human health, such as antioxidant, antifungal, antibiotic, anticarcinogenic, and anti-HIV activities.[94,95] Furthermore, they have been found to be able to control coronary heart diseases and Alzheimer's disease and reduce cholesterol, obesity and diabetes.[96] Lignin-rich fraction of brewer's spent grain has been found to be able to significantly reduce body weight gain, cholesterol and to improve insulin resistance in mice.[97]

Lignins have attracted great interests mainly in the production of functional materials. As an example, lignin-based carbon fibers and lignin-based porous carbon materials have been prepared and used for development of devices with efficient mechanical properties, to be used as gas and liquid purifiers, catalyst carriers, and in energy storage and electrode material applications.[98,99]

Lignins can be used also as reinforcers in polymer composites, as flame retardants in polymer or as additives in formaldehyde adhesive.[98,100]

The absorption properties of lignins make them suitable for application in biodegradable UV-shielding films for agricultural or food packaging applications, also due to the strong antimicrobial and antioxidant activities.[99,101] In addition, great attention has been focused on the capacity of lignins to act as sun blockers in sunscreens and cosmetic products.[98]

Recently, a wide range of lignin-based nanocomposites has been prepared by the association of lignins with cellulose, starch, chitosan, or proteins. The functionality provided by lignin to composite films typically includes UV-barrier, mechanical reinforcement, water resistance, adsorption and antifouling capacity, antioxidant and antimicrobial activity.[99]

Lignin shows high adsorption capacity towards metal ions and organic dyes, for pollutant remediation. Furthermore, different metal oxide-lignin o metal-lignin hybrids have been prepared as platform for the design of advanced sensing materials for e.g. biomedical applications.[99,101,102]

Lignin nanoparticles have been used as drug delivery systems, UV absorbents, and in tissue engineering.[96,99,103]

1.3 Agri-food by-products as sources of phenolic compounds

The wide distribution of phenolic compounds in different natural sources, such as fruits, vegetables, and lignocellulosic biomasses, has stimulated intense research work aimed at studying their properties and possible applications.

Recently, also agri-food by-products have been considered with increasing interest as easily accessible and sustainable sources of phenolic compounds.[104] Indeed, global food waste approximates 1.3 billion tons per year as the result of processes occurring along the entire supply chain.[105] In particular, agri-food industry is responsible for the generation of high volumes of organic biomass, of which a considerable part, composed of leaves, roots, stalks, bark, bagasse, straw residues, seeds, wood and animal residues, is classified as food waste.[106] Disposal of these by-products represents a cost to the food processor and has a negative impact on the environment. It has been calculated that the decomposition of only one metric ton of organic solid waste results in the release into the atmosphere of 50–110 m^3 of CO_2 and 90–140 m^3 of methane.[107] Moreover, organic wastes can be responsible of

phytotoxicity phenomena, including water contamination and deterioration, death of sensitive marine organisms, inhibition of seed germination, and intestinal disorders in animals.[108] On the other hand, these materials can be considered as a largely available, low-cost source of value-added compounds, in particular phenolic compounds, whose recovery represents therefore a valuable opportunity.[105] However, it has to be pointed out that agri-food by-product derived phenolic compounds may exhibit low/moderate bioavailability and may undergo extensive bacterial and human metabolism, that could affect their beneficial properties for human health.

1.3.1 Fruit by-products

Fruits and vegetable wastes constitute a significant portion (about 42%) of the total globally produced waste.[109] Most of fruit by-products contain equal or greater quantities of phenolic compounds than the fruit itself. The main fruit by-products are listed below.

Grape and wine by-products. Grape represent the largest fruit crop throughout the world, used most often as table grapes, raisins, juices and, above all, for wine production.[110] Wine and winery industries generate approximately 9 million tons of wastes *per* year in the world, which represents about 20% w/w of the total grapes used in the wine processing.[111] The grape by-product is known as grape pomace and consists mainly of grape seeds (about 20-26%), skin, stems, and remaining pulp.[112]

Grape pomace is rich in polyphenols and contains different phenolic compounds such as (+)-catechin, (-)-epicatechin, quercetin, myricetin, rutin, kaempferol, EA, hydroxytyrosol, *trans*-resveratrol,[111] but also phenolic acids such as caffeic, gallic, protocatechuic, 4-hydroxybenzoic, and syringic acid, well known for their beneficial properties on human health, including cardioprotective, neuroprotective, anti-inflammatory, anticarcinogenic, and antimicrobial activities.[112]

Condensed tannins (mainly procyanidins) represent another main class of polyphenols present in grape pomace. Indeed, oenological tannins are among the most important high-value compounds present in this by-product, widely used as additives in the food and beverage industry.[20] Grape pomace tannins are able to control the metabolism of lipid and glucose and are also used as feed supplements.[20]

Anthocyanins, mainly malvidin, peonidin, and cyanidin, are other polyphenols abundant in grape pomace, from which are commonly recovered and used as food colorants.[104]

Finally, about 16-24% w/w of lignins have been reported in grape by-products (Figure 1.3.1.1).[113]

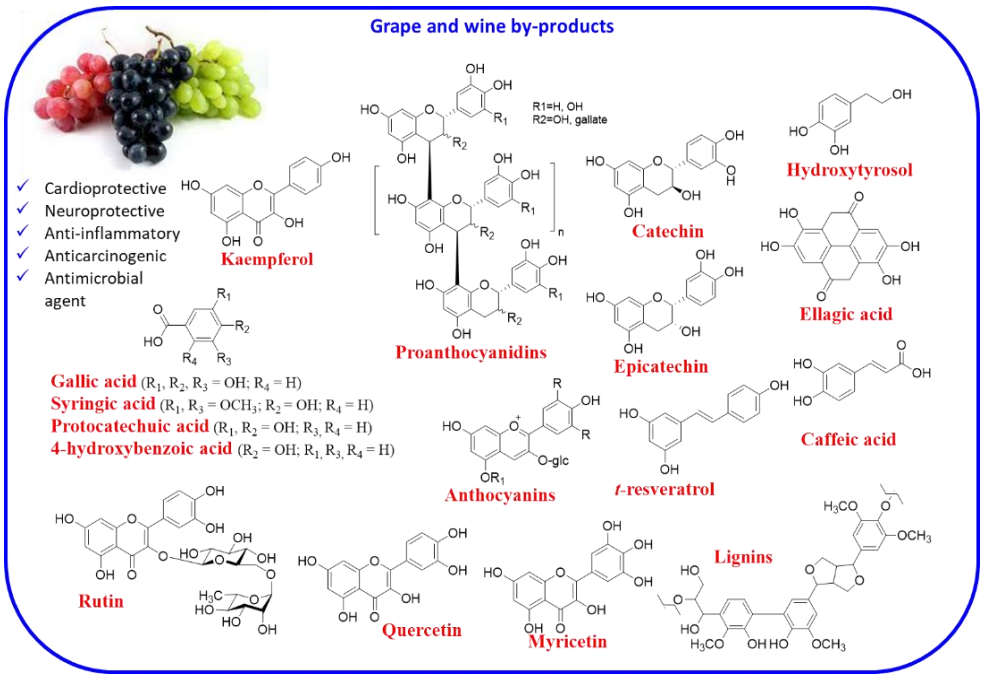

Figure 1.3.1.1. Main phenolic constituents of grape by-products.[112]

Orange and lemon by-products. Citrus family includes several fruits, such as *Citrus sinensis* (orange), *Citrus reticulata* (mandarin), *Citrus tangerine* (tangerine), *Citrus*

aurantifulia (lime), *Citrus limon* (lemon), *Citrus limetta* (sweet lime), and *Citrus paradisi* (grapefruit).[114]

Approximately one-third of citrus fruits is used to produce fresh juice or drinks,[110] and since the yield of citrus juice represents half the weight of the fruit, a large amounts of waste, up to 15 million tons (mainly peel, seeds and pulp), are globally produced each year.[111]

Citrus residues contain large amounts of polyphenols and citrus peels exhibit a total phenolic content 15% higher than the peeled fruit.[111] Citrus peels, as well as seeds and pulp, are an important source of hydroxycinnamic acids and flavonoids, mainly flavanone glycosides (hesperidin, naringin and narirutin), flavanones (hesperetin and naringenin), and flavone aglycons (sinensetin, nobiletin, luteolin and tangeretin) (Figure 1.3.1.2).[104,111,112] Extracts obtained from citrus by-products have been proposed as antioxidant, antibacterial and antimicrobials or as food additives, to impart bitter taste to food and beverages.[115]

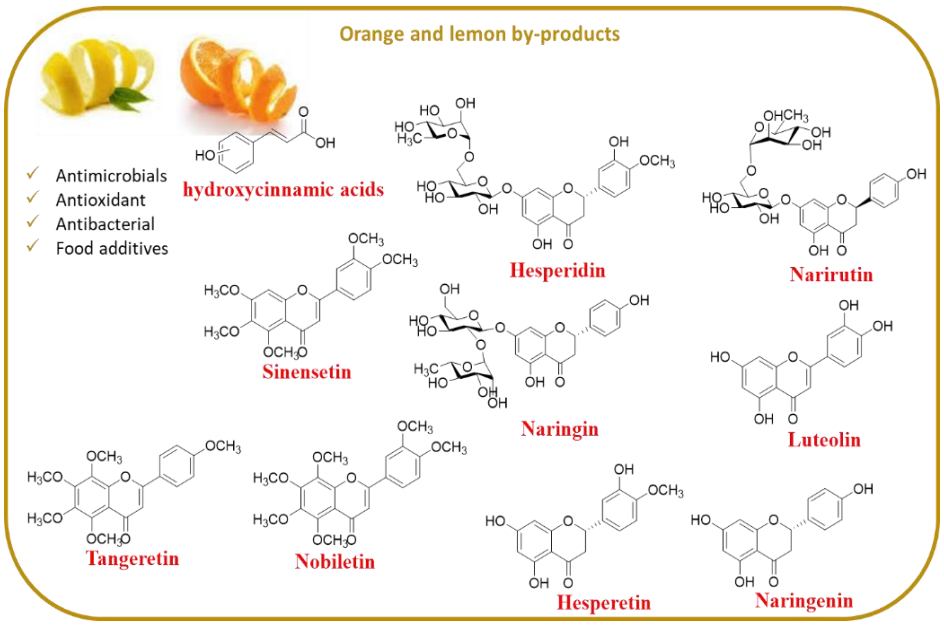

Figure 1.3.1.2. Main phenolic constituents of citrus by-products.[112]

Pomegranate by-products. *Punica granatum* L., better known as pomegranate, is another fruit widely used in the juice industry. For each ton of pomegranate juice produced, 9 tons of by-products are formed.[111] Peels, pomace and seeds are the main constituents of pomegranate by-products and show a 10-fold higher phenolic content than the pulp, which make this waste material one of the most interesting industrial by-products.[111]

Pomegranate by-products are rich in different polyphenols, such as anthocyanins, flavonoids, but also specific ellagitannins, punicalagin and punicalin, which contribute to a very high antioxidant activity (Figure 1.3.1.3).[12,20,111,112] Several studies have demonstrated the health-promoting activities of pomegranate by-products, including anticancer and antibacterial activities.[116–119]

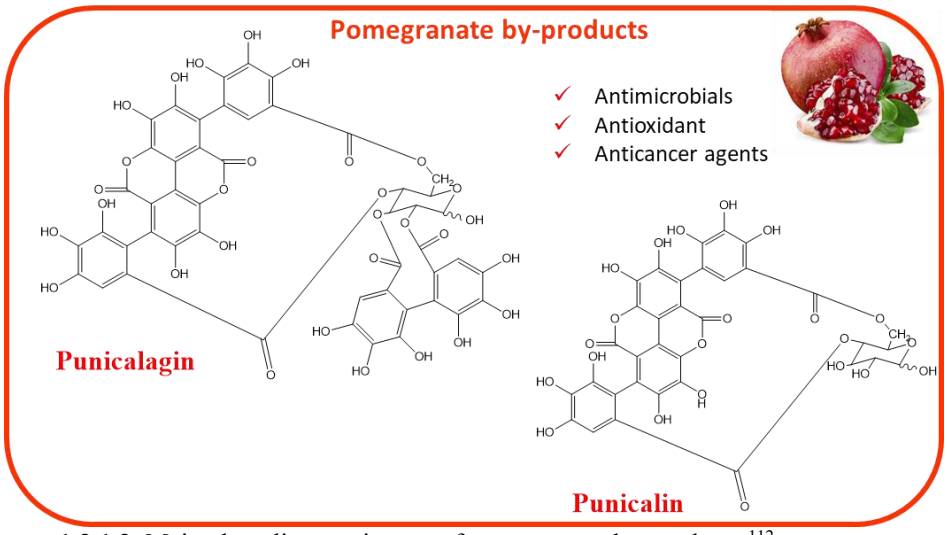

Figure 1.3.1.3. Main phenolic constituents of pomegranate by-products.[112]

Apple by-products. Apple pomace, peels and seeds are the main by-products of the apple industry and represent a low-cost source of phenolic compounds. Among these, a prominent role is played by quercetin glycosides, kaempferol, catechin, procyanidins, and especially the dihydrochalcone phlorizin. Other polyphenols, such as anthocyanins and phenolic acids, mainly chlorogenic and caffeic acids, are also

present.[104,111,112] Apple by-products exhibit antimicrobial, anticancer, and cardioprotective activities (Figure 1.3.1.4).[120,121]

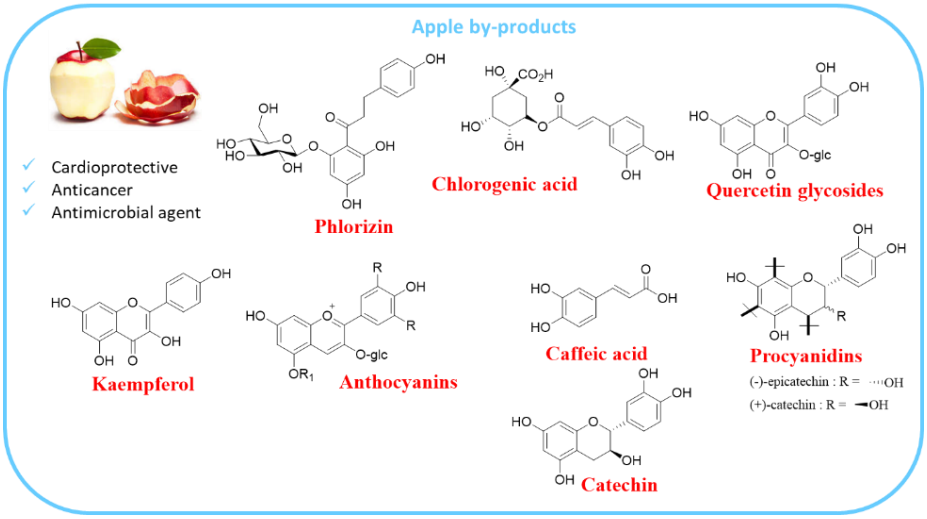

Figure 1.3.1.4. Main phenolic constituents of apple by-products.[112]

Pineapple by-products. Pineapple (*Ananas comosus*) is a tropical fruit whose processing produces large amounts of by-products, consisting mainly of peel and pomace. Pineapple by-products represent approximately 30–35% of the pineapple fruit[110] and are rich in phenolic compounds, particularly catechin, epicatechin and gallic and ferulic acids (Figure 1.3.1.5).[104,112] Pineapple by-products exhibit efficient antioxidant properties and good antibacterial, anticancer and antifungal activites.[122]

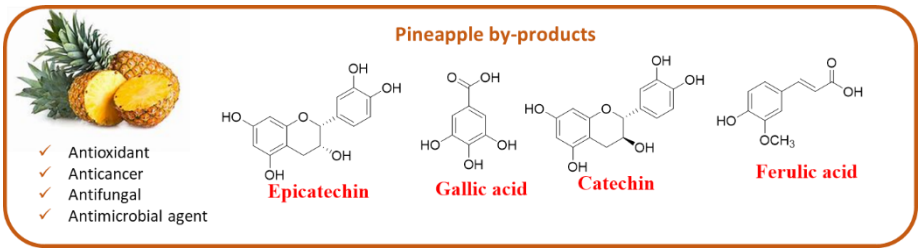

Figure 1.3.1.5. Main phenolic constituents of pineapple by-products.[112]

Banana by-products. Banana peels constitute around 30–40% of the total weight of the fruit and represent another important source of phenolic compounds, with high

added value, in particular flavonoids and proanthocyanidins (Figure 1.3.1.6).[104,110,112] Applications as antioxidant and antimicrobial agents are reported in literature.[123]

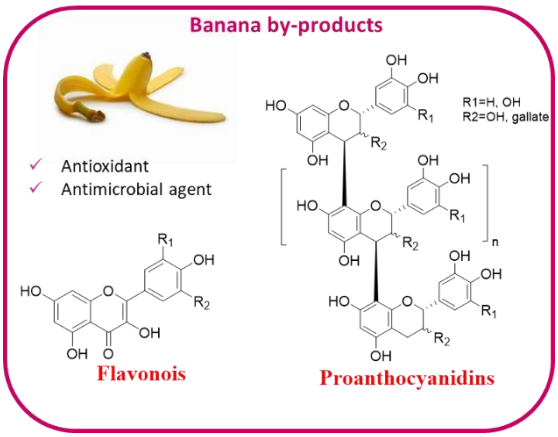

Figure 1.3.1.6. Main phenolic constituents of banana by-products.[112]

Berry fruit by-products. Blueberry is a popular fruit suitable for processing into wine or juice. Blueberry processing produces high amount of wastes, in particular skin and seeds (19% and 2% in weight of the whole fruit, respectively). The skin and seeds contain glycosides of malvidin, delphinidin, petunidin, cyanidin, and peonidin but also phenolic acids, in particular cinnamic acids.[124]

Blackcurrant pomace, obtained from blackcurrant juice processing, is another fruit by-product rich in glycosylated anthocyanins (delphinidin and cyanidin), flavonoids in glycosylated and aglycone form (quercetin, myceretin and kaempferol), and phenolic acids (caffeic, *p*-coumaric and ferulic acids).[125]

On the other hand, bilberry by-products are rich in glucosides, galactosides, arabinosides and acetylgalactosides derivatives of delphinidin, cyanidin, petunidin, peonidin and malvidin.[126]

Raspberry and cranberry pomace are also rich in anthocyanins, in particular cyanidin-3-O-sophoroside, and contain significant amounts of EA, too. Cranberry

pomace is composed of, above all, peonidin 3-O-galactoside and cyanidin 3-O-galactoside. In addition, considerable levels of flavonols, such as quercetin and myricetin 3-O-galactoside and quercetin 3-O-rhamnoside have been found.[127]

In blackberry residues, phenolic acids (chlorogenic and gallic acids), flavonoids (luteolin and quercetin) and anthocyanins have been reported.[128]

Finally, strawberry by-products are characterized by a very interesting pattern of phenolic molecules. The agro-industrial strawberry chain reaches up a production of around 8 million tons of fruit *per* year, and the amount of generated waste represents up to 20% of the total production. Strawberries by-products consist mainly of the sepals, stems, and other part of the fruit, rich in metabolites of great interest. The distribution of these molecules depends on part of the fruit but also on the strawberry *cultivar*. In general, strawberry by-products are rich in hydrolyzable tannins, EA in bound and free form, flavonols, mainly quercetin and kaempferol, and anthocyanins (Figure 1.3.1.7).[129]

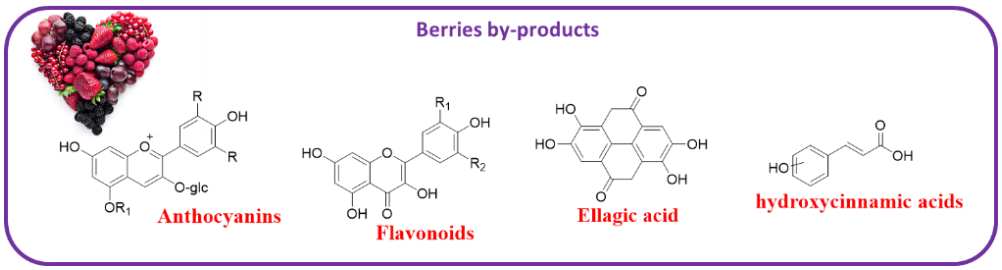

Figure 1.3.1.7. Main phenolic constituents of berry by-products.

Nut fruit by-products. Significant amounts of waste are produced also from pistachio, peanut, pecan, hazelnut and chestnut processing.

Pistachio is an important commercial crop. The fruit consists of an edible seed and a lignified shell. According to the final use, the edible seeds are separated from the shell, that is the waste material. Pistachio shell contain cellulose (30–55%), hemicelluloses (20–32%) and lignin (12–38%),[130] but also phenolic compounds,

mainly gallic acid, protocatechuic acid, catechin, epicatechin, rutin, naringin, luteolin, eriodictyol, quercetin, and naringenin.[131,132]

Peanut shell is another abundant and inexpensive by-product, produced in about 5 million tonnes every year in China alone.[133] This waste material also consists of cellulose (48%), hemicellulose (3%) and lignin (28%),[134] although luteolin and eriodictyol have been also identified.[133]

Chestnut industry also generates a large amount of by-products, constituted mainly of the chestnut inner and outer shells, which holds about 10% to 15% of the whole chestnut weight.[135] Chestnut by-products are rich in lignin, cellulose and hemicelluloses.[136] As several nut fruits, chestnut waste materials contain phenolic acids (mainly gallic acid and protocatechuic acid), flavonoids (quercetin, rutin, catechin and epicatechin) and hydrolyzable tannins (vescalagin, castalagin and gallocatechin). High content of EA is also found in inner and outer chestnut shells.[137]

Pecan nuts are another important agricultural product of some states in South America. Nut shell, the not-edible part of pecan nut, represents up to 49% of the entire fruit.[138] This by-product contains several phenolic compounds including gallic acid, EA, *p*-hydroxybenzoic acid, protocatechuic acid and epigallocatechin gallate.[139] Furthermore, high contents of condensed tannins have been found.[20]

Hazelnut shell represents more than 50% of the total nut weight and the major by-product in hazelnut industry production. Hazelnut shells are composed of about 30% hemicelluloses, 27% celluloses, and 43% lignin.[140] Several bioactive molecules have been also identified, such as catechin, epicatechin gallate, and gallic acid (Figure 1.3.1.8).[140]

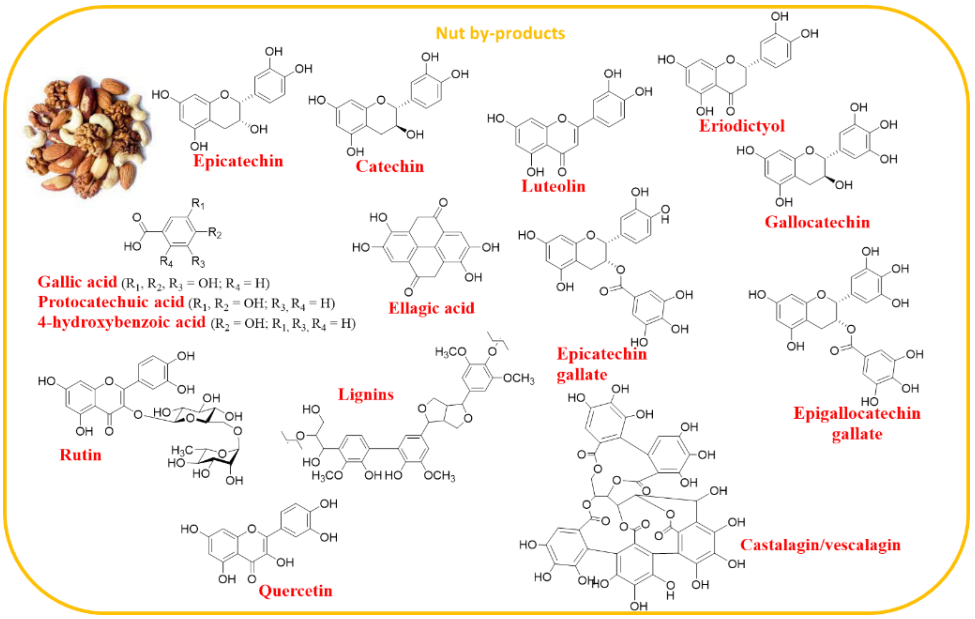

Figure 1.3.1.8. Main phenolic constituents of nut by-products.

1.3.2 Vegetable by-products

As in the case of fruit by-products, vegetables industry produces high amounts of waste materials that may exert health benefits comparable to the starting samples.[104]

Tomato by-products. Tomatoes are one of the most important crops in the world, but approximately one-third of the total weight is discarded in the form of skin and seeds during industrial processing. Tomato residues are a good source of bioactive molecules, especially carotenoids, such as β-carotene and lycopene, but also phenolic compounds. Peels and seeds contain flavanones, such as naringenin glycosylated derivatives and flavonols, mainly quercetin, rutin and kaempferol glycoside derivatives.[104,112,141] In addition, hydroxycinnamic acids such as caffeic, chlorogenic, ferulic and *p*-coumaric acids have been identified (Figure 1.3.2.1).[142] Tomato by-products have proved to be potent antioxidant and antimicrobial agents.[143]

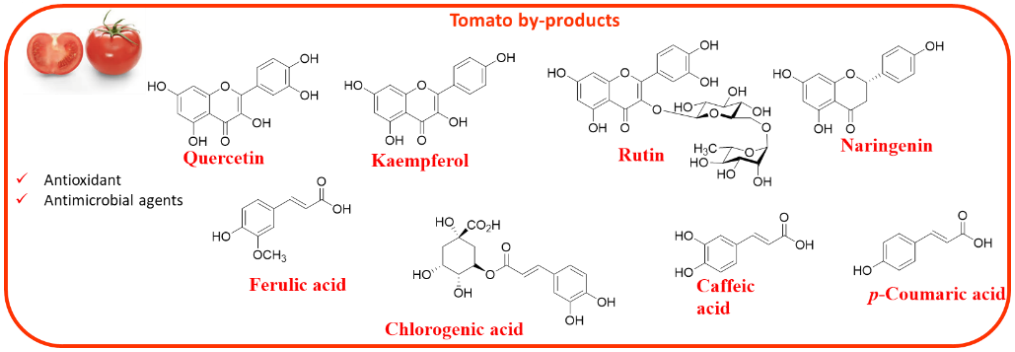

Figure 1.3.2.1. Main phenolic constituents of tomato by-products.[112]

Potato. Potato is one of the main vegetables consumed in European and American diets.[142] Potato peels are a potato processing by-product therefore available in very large amounts. This waste material possesses about 50% of the phenolic compounds of the whole tuber,[142] and contains mainly chlorogenic, gallic, protocatechuic and caffeic acids in free and bound form. The high content of polyphenols makes this by-product an interesting antioxidant, antibacterial and anticarcinogenic agent (Figure 1.3.2.2).[144] Recently, potato peels have been also used as a biosorbent for the removal of toxic metal agents from water.[145]

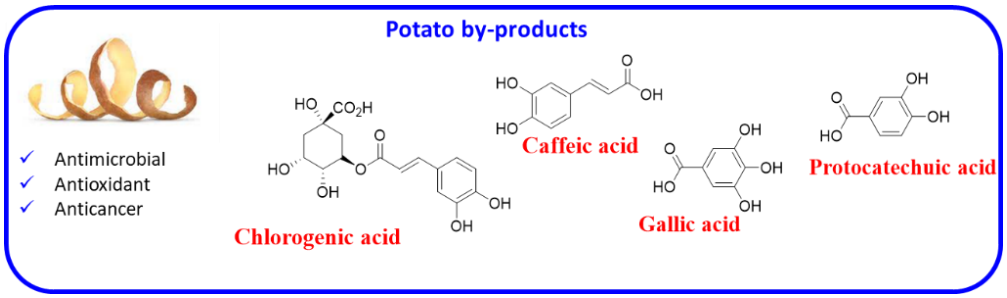

Figure 1.3.2.2. Main phenolic constituents of potato by-products.[112]

1.3.3 Lignocellulosic by-products

Lignocellulosic by-products have been widely described as sources of phenolic compounds. This category includes among other, coffee and wood industry by-products.

Coffee by-products. Coffee is one of most popular beverages, whose annual worldwide production is over 105 million tons.[146] Industrial processing of coffee generates large amounts of coffee by-products, in particular spent coffee grounds (SCG) and coffee silverskin (CS), that represent more than 50% of the coffee fruit dry weight.[147]

SCG is the residual material derived from the production of espresso beverages or soluble coffee, with a worldwide annual generation amount of six million tons,[20] while CS is the residue obtained during the bean roasting step.[148] Because of their easy availability and chemical composition, these by-products have attracted great attention as possible active components to be exploited in different fields.

SCG contain mainly carbohydrates (38−42%), melanoidins (25%) and proteins (8%).[149,150] Furthermore, significant amounts of phenolic acids have been also found in SCG, in particular chlorogenic acid and its isomers and derivatives, as well as caffeic acid, protocatechuic acids and flavonoids.[151–155] SCG contains also 20-26% of lignins and a low content of condensed tannins.[156]

CS is composed of polysaccharides, mainly cellulose and hemicelluloses, monosaccharides, proteins, and phenolic compounds such as chlorogenic acid and its isomers (Figure 1.3.3.1).[157,158]

SCG and CS exhibit high health beneficial properties, such as, among other, protective effects against cardiovascular and gastrointestinal diseases, anti-inflammatory, anticarcinogenic, and antimicrobial activities.[157,159–164] Recently,

coffee by-products have found application as thermo- and photo-oxidative stabilizers in the development of packaging materials.[150]

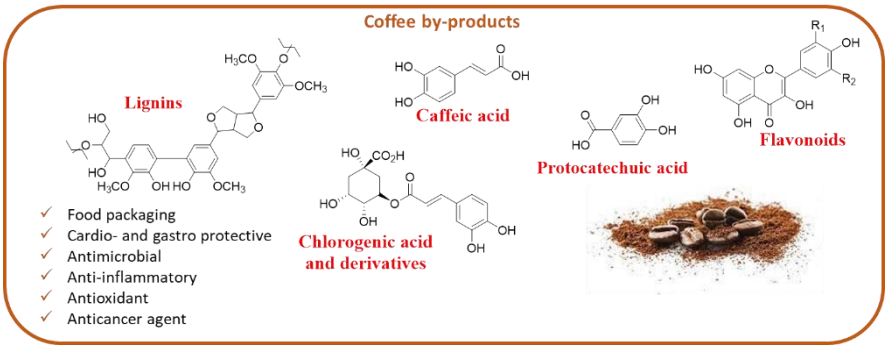

Figure 1.3.3.1. Main phenolic constituents of coffee by-products.[112]

Wood by-products. Forest industry generates large volume of wood residues (sawdust, off-cuts, and bark). It has been estimated that about 5 billion tons of biomass residues from agroforestry and food industries are produced worldwide, with an emission of 3.3 billion tonnes of CO_2, each year.[165] The biomass wastes generated from wood industries are commonly used for heating, energy or pellet production.[166] Wood traditionally represents a rich source of biopolymers, in particular tannins and lignin, that account for approximately 30% of wood weight.[90]

1.4 Aims of the PhD project

Within the context briefly described in the previous paragraphs, this PhD work was aimed mainly at the exploitation of phenolic compounds from different agri-food wastes for applications as additives for functional materials or in human health (e.g. as food supplements).

In particular, the following results were achieved:

a) Characterization of the antioxidant properties and of the main phenolic constituents of selected agri-food and wood by-products.

b) Improvement of the antioxidant properties of selected agri-food by-products or bio-inspired phenolic polymers by hydrolytic activation treatments or bioprocessing (e.g. fermentation).
c) Exploitation of agri-food by-products derived phenolic compounds as additives for the implementation of functional materials to be used in the food, biomedical, environmental or dermocosmetic sector.
d) Development of new eco-friendly extraction protocols to recover value-added compounds (phenolics and lignins) from selected agri-food by-products.
e) Development of synthetic strategies for the preparation of anthocyanin metabolites.
f) Preparation and characterization of a red pigment from oxidative coupling of chlorogenic acid and tryptophan for use as a food colorant.

The characterization of the antioxidant properties was performed by validated chemical assays. For the structural characterization of the phenolic compounds, solid state spectroscopic techniques and chemical degradation methods were applied, whereas the extractable components were identified and quantified by customary chromatographic and spectro(photo)metric methods. The functional properties of the agri-food derived phenolic compounds and of the additivated materials were evaluated by validated specific assays, often in collaboration with other research groups.

Part of the work described under the research lines a), c), and d) was carried out during a six-month stage at "Centro Ricerche per la Chimica Fine S.r.l." of Silvateam S.p.a. (San Michele Mondovì, Cuneo, Italy), whereas part of the work described under the research lines c) and e) was run in collaboration with Professor Andreas Schieber of the Institute of Nutritional and Food Sciences, University of Bonn (Bonn, Germany), as envisaged by the PON Ricerca e Innovazione 2014-

2020, Azione I.1 “Dottorati Innovativi con caratterizzazione Industriale”) PhD project.

Chapter 2

Hydrolytic treatments: a straightforward strategy to improve the functional properties of phenolic compounds

2.1 Introduction

As mentioned in the Introduction, agri-food industry is responsible for the generation of high volumes of organic wastes, consisting mainly of fruit and vegetable by-products. For example, grape and banana processing generates approximately 9 million tons of by-products per year,[111,167] while citrus and apple industry produce about 15 and 3 million tons of waste per year, respectively.[111,167] Other notable examples are pomegranate (about 4.2 million tons of wastes per 1 ton of juice),[111] pineapple and nuts such as pecan nuts, for which up to 50% of the whole fruit is discarded.[168,169] Regarding vegetable processing, considerable amounts of wastes are produced every year, as in the case of potato and tomato processing.[170,171]

As again mentioned in the Introduction, on the other hand these materials can be considered as a largely available, low-cost source of value-added natural compounds, among which a prominent role is occupied by phenolic compounds, which are well-known for their potent antioxidant properties and beneficial effects on human health.[172]

The wide distribution of phenolic compounds in agri-food by-products has therefore attracted great interest, and intense research work has been focused on the characterization of their properties and their exploitation in several application fields.[173]

With the aim of further improving specific properties of agri-food by-products and phenolics thereof, with particular reference to the antioxidant properties, recently, an expedient acid hydrolysis protocol has been developed (Figure 2.1.1).

A remarkable example is represented by spent coffee grounds (SCG), which, further to treatment with 6 M HCl, at 100 °C, for 18 h, was converted into a hydrolyzed material (HSCG), with an antioxidant efficiency up to 30 times higher compared to untreated SCG.[150] Comparative structural and morphological analysis proved that the hydrolytic treatment not only led to a removal of the polysaccharidic fraction and hence to an enrichment of the sample in the phenolic constituents, but also to a depolymerization/repolymerization of the lignin component, making the phenolic OH functionalities more available for interaction with oxidized species, thus resulting in an increase of the antioxidant properties.[150] The same hydrolytic treatment has been performed also on the solid residues from pomegranate fermentation, leading again to a material with enhanced antioxidant activity, mainly due, in this case, to the release of free ellagic acid (EA) from ellagitannins degradation.[174]

Based on these findings, the possibility to exploit the hydrolytic treatment as a tool to boost the antioxidant properties of selected agri-food wastes was investigated, as described in the present Chapter. In a related study, the effects of the acid treatment were evaluated also on synthetic, bioinspired phenolic polymers.

Specifically, the research activities were directed to:

a) Evaluation of the antioxidant properties of the acid-treated samples with respect to starting materials, using validated chemical assays.
b) Characterization of the main chemical modifications induced by the acid treatment on the different samples by using spectroscopic, chromatographic, and chemical degradation methods.

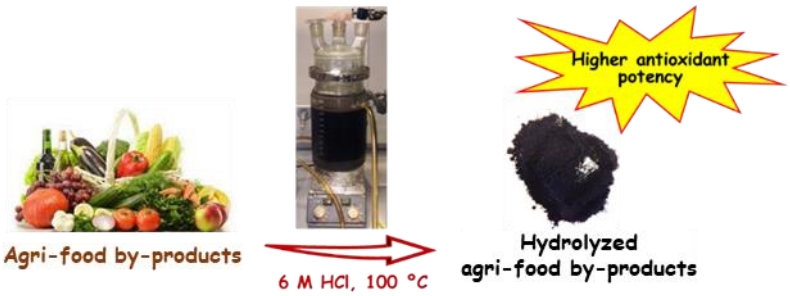

Figure 2.1.1. Hydrolytic treatment of agri-food by-products.

2.2 Evaluation of the antioxidant properties of the selected agri-food by-products

In a first series of experiments, the antioxidant properties of selected agri-food by-products were investigated by two widely used assays, i.e., the 2,2-diphenyl-1-picrylhydrazyl (DPPH) and ferric reducing/antioxidant power (FRAP) assay, following the "QUENCHER" method, , which allows to measure the efficiency of electron transfer processes from a solid antioxidant. [175–177] Although these *in vitro* assays do not involve a biological target to be protected and therefore they are not biologically relevant, they are currently employed in the literature for a preliminary evaluation of the antioxidant properties of a sample. Pecan nut shell, pomegranate peel and seeds, grape pomace, apple peel, seeds and core, orange peel and albedo, banana peel, pineapple peel and stem, tomato peel and seeds and potato peel were selected as fruit and vegetable by-products.

The results of the antioxidant assays are reported in Table 2.2.1. In the DPPH assay, pecan nut shell, pomegranate peel and seeds, and grape pomace showed EC_{50} values of 0.14, 0.29 and 0.49 mg/mL, in that order, and were found to be significantly more active than apple, orange, banana, pineapple, tomato, and potato wastes, that showed EC_{50} values higher than 1.5 mg/mL.

A similar trend was observed in the FRAP assay, with pecan nut shell, pomegranate peel and seeds, and grape pomace characterized by the highest reducing power among the fruit and vegetable by-products.

To obtain information on the amounts of phenolic compounds present in the different by-products, the total phenolic content (TPC) was determined for each sample by the Folin-Ciocalteu assay.[178] As expected on the basis of the antioxidant assays, pomegranate peel and seeds, grape pomace and pecan nut shell showed the highest TPC values (Table 2.2.1).

Table 2.2.1. Antioxidant properties and TPC values of the selected agri-food wastes. Reported are the mean ± SD values of at least three experiments.

	Sample	DPPH assay EC_{50} (mg/mL)	FRAP assay (mg of Trolox/mg of sample)	TPC (mg of gallic acid/g of sample) (Folin-Ciocalteu assay)
Fruit by-products	Pomegranate peel and seeds	0.29 ± 0.04	0.044 ± 0.009	125.6 ± 0.9
	Apple peel, seeds and core	>1.5	0.0006 ± 0.0007	23 ± 1
	Orange peel and albedo	>1.5	0.0008 ± 0.0002	17 ± 1
	Banana peel	> 1.5	0.0044 ± 0.0002	20 ± 2
	Pineapple peel and stem	> 1.5	0.00141 ± 0.00004	6.4 ± 0.3
	Grape pomace	0.49 ± 0.05	0.0116 ± 0.0007	124 ± 5
	Pecan nut shell	0.14 ± 0.01	0.061 ± 0.002	82 ± 4
Vegetable by-products	Tomato peel and seeds	> 1.5	0.00046 ± 0.00001	25 ± 3
	Potato peel	> 1.5	0.00023 ± 0.00001	27.7 ± 0.8
	Trolox	0.011 ± 0.001	-	

2.3 Acid treatment on the selected agri-food by-products

The acid treatment on the fruit and vegetable by-products was performed as reported,[150,174,179] by incubating each sample in 6 M HCl at 100 ◦C for 1 h. The hydrolyzed materials were then collected by centrifugation, extensively washed with

water until neutrality, and lyophilized. The yields of recovered samples are reported in Table 2.3.1.

Table 2.3.1. Recovery yields of agri-food by-products subjected to hydrolytic treatment.

	Sample	Yields (w/w)
Fruit and vegetable by-products	Pomegranate peel and seeds	10%
	Apple peel, seeds and core	2%
	Orange peel and albedo	9%
	Banana peel	7%
	Pineapple peel and stem	20%
	Grape pomace	30%
	Pecan nut shell	45%
Vegetable by-products	Tomato peel and seeds	12%
	Potato peel	2%

Grape pomace and pecan nut shell showed the highest recovery yields further to the acid treatment, probably due to the high content of phenolic polymers, such as lignins and condensed tannins, which are insoluble in water and not easily hydrolyzable compared to polysaccharides. In agreement with this observation, potato, and apple wastes, rich in polysaccharidic components, exhibited very low recovery yields after the acid treatment.

2.3.1 Evaluation of the antioxidant properties of the acid-treated agri-food by-products

The antioxidant properties of the hydrolyzed agri-food by-products were characterized by DPPH and FRAP assays and compared to those of the untreated samples. The acid hydrolysis exerted an activating effect on almost all fruit and vegetable by-products, that showed a remarkable decrease in the EC_{50} values determined in the DPPH assay (Figure 2.3.1.1a). Notably, however, no significant effects were observed for grape pomace, while a remarkable weakening in the antioxidant properties was observed for pecan nut shell, with a 8-fold increase of the EC_{50} value after the treatment.

FRAP assay (Figure 2.3.1.1b) showed an increase of the antioxidant properties for apple, potato, and tomato wastes, whereas less significant effects were observed on orange, banana and pomegranate by-products. In agreement with the DPPH assay results, the acid treatment led to a material with an 80% decrease of Trolox equivalents (eqs) in the case of pecan nut shell. A 50% decrease in the Trolox eqs was observed also for grape pomace (Figure 2.3.1.1b).

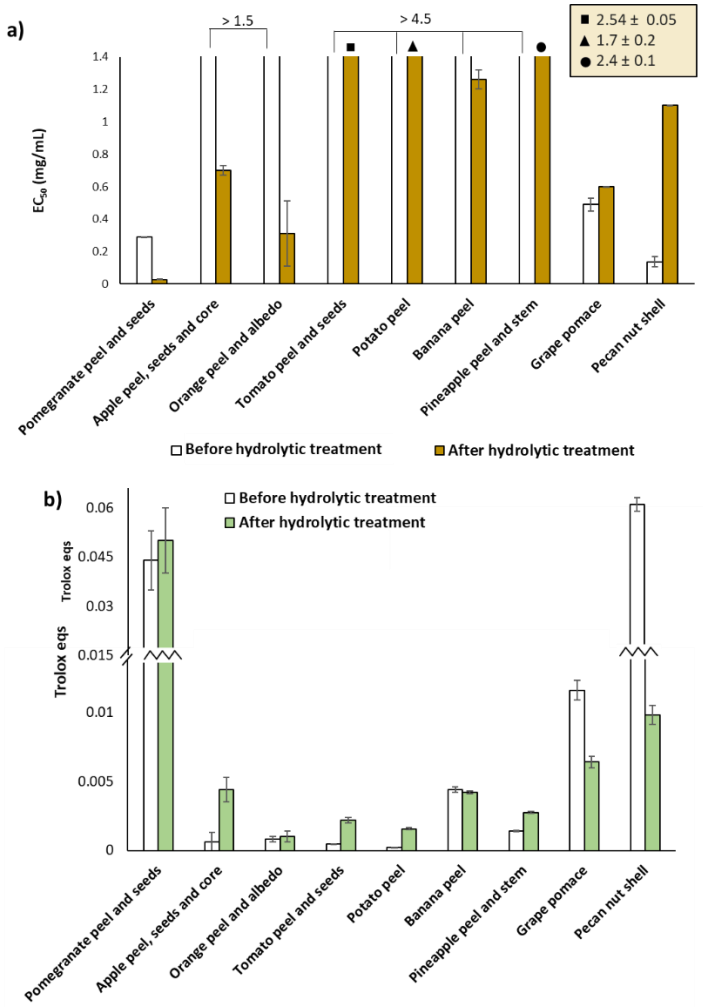

Figure 2.3.1.1. Antioxidant properties of agri-food by-products before and after hydrolytic treatment, determined by (a) DPPH and (b) FRAP assays. Reported are the mean ± SD values of at least three experiments.

Acid-treated fruit and vegetable by-products were analyzed also for their phenolic content. Pomegranate, apple and pineapple wastes showed a significant increase of TPC values after treatment, while hydrolyzed grape pomace and pecan nut shell showed a 3-fold decrease of TPC values with respect to the untreated materials, indicating substantial chemical modifications induced by the hydrolytic treatment on these agri-food by-products, likely responsible for the lowering of the antioxidant properties (Figure 2.3.1.2).

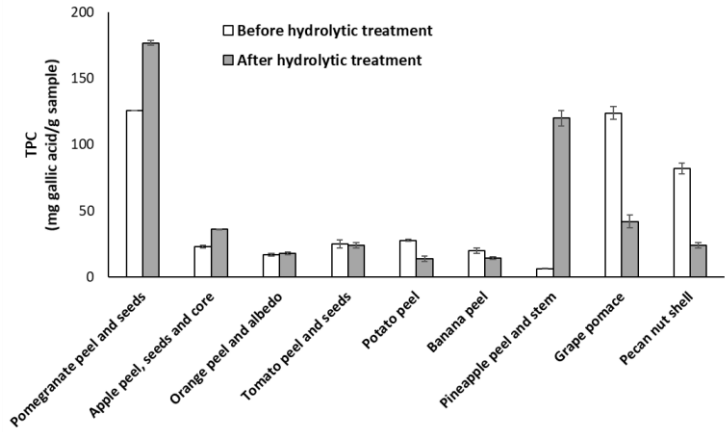

Figure 2.3.1.2. TPC values of agri-food by-products before and after hydrolytic treatment. Reported are the mean ± SD values of at least three experiments.

Since pecan nut shell and grape pomace are well known for their high content of condensed tannins, in order to investigate the effects of the hydrolytic treatment on the main constituents of these by-products, the antioxidant properties of pure tannins were evaluated before and after the acid treatment.

Chestnut (CT) and quebracho (QT) tannins, composed of ellagitannins and profisetinidins, respectively,[20,54,62] were used as models of hydrolyzable and condensed tannins. As shown in Figure 2.3.1.3, the acid treatment led to a decrease in the antioxidant properties and TPC values of quebracho tannins, perfectly in

agreement with what observed on the condensed tannin-rich materials grape pomace and pecan nut shell.

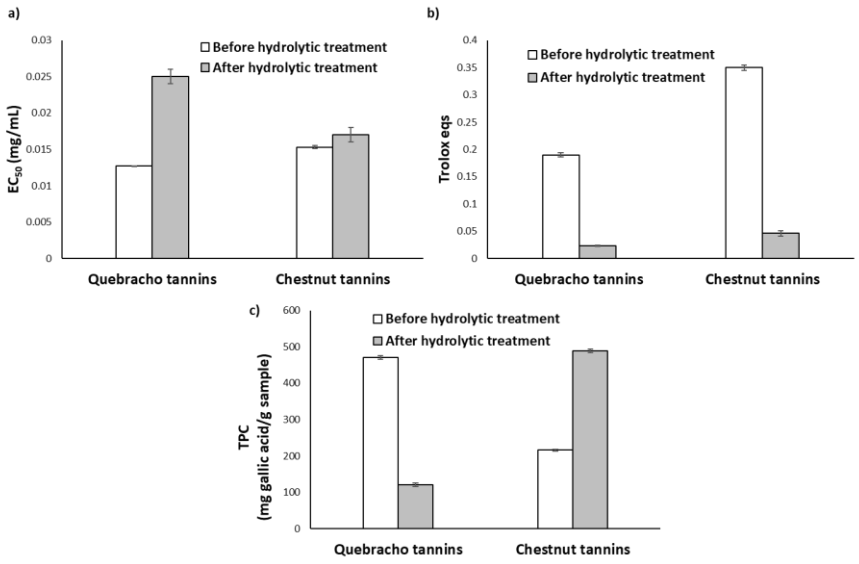

Figure 2.3.1.3. Antioxidant properties of pure tannins before and after the acid treatment determined by (a) DPPH, (b) FRAP and (c) TPC assays. Reported are the mean ± SD values of at least three experiments.

2.3.2 Characterization of the structural modifications induced by the hydrolytic treatment on the agri-food by-products

2.3.2.1 UV-Vis and HPLC analysis

To obtain further information on the nature of the chemical modifications induced by the acid treatment on the agri-food by-products, the DMSO-soluble fractions of the different materials, before and after the treatment, were analyzed by UV-Vis spectroscopy and HPLC. As an example, here are reported the spectra of pomegranate peel and seeds, selected as hydrolyzable tannin-rich material, grape pomace and pecan nut shells, selected as condensed tannin-rich materials, and potato peels, containing high amounts of polysaccharides (about 30% w/w), starch (about

25% w/w) and lignin (about 20%).[180] For pomegranate and potato wastes, a general increase in absorbance was observed after the hydrolytic treatment (Figure 2.3.2.1.1a,b), suggesting that this latter efficiently cleave phenolic polymers such as lignins and hydrolyzable tannins into low-molecular weight, extractable compounds. In particular, in the case of pomegranate, the hydrolyzed sample showed an increase in the absorbance at 355 nm, suggestive of the release of EA as a result of punicalagin and punicalin hydrolysis, as already reported for pomegranate wastes,[174] whereas the hydrolyzed potato waste spectrum showed the appearance of two absorption maxima at around 280 and 310 nm, typical of lignin moieties with hydroxycinnamic acid type structures.[181,182] On the other hand, the UV-Vis spectra of the DMSO-extractable fractions from grape pomace and pecan nut shell (Figure 2.3.2.1.1c,d) showed a significant decrease in the maximum at ca. 280 nm further to the acid treatment, probably related to the degradation of condensed tannins, as expected based on the observed decrease in the antioxidant properties.

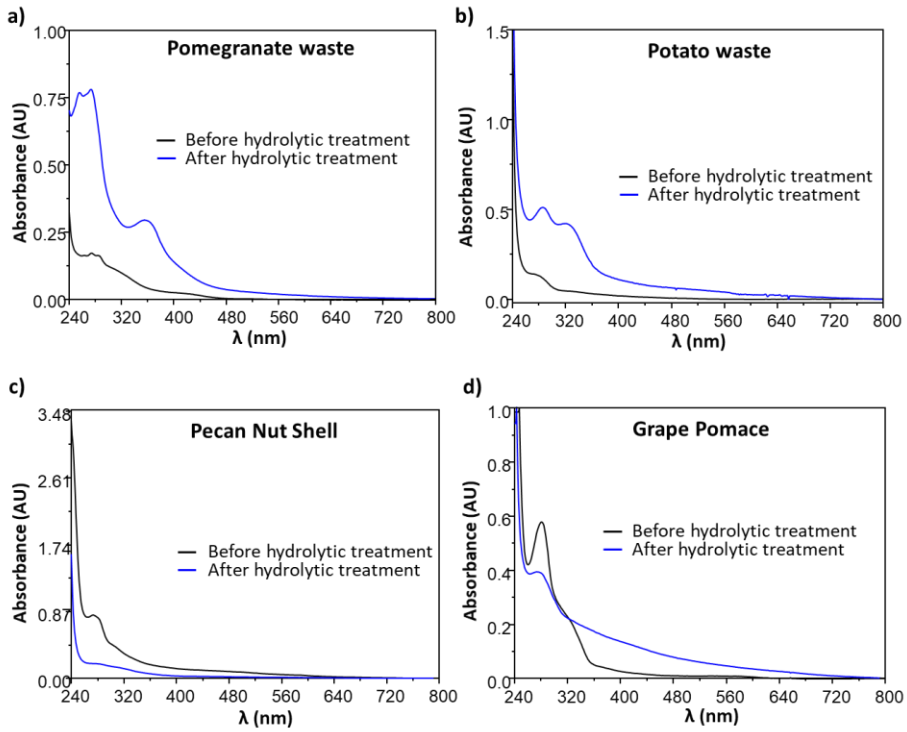

Figure 2.3.2.1.1. UV-Vis spectra of the DMSO-soluble fractions of selected fruit and vegetable by-products, before and after the hydrolytic treatment.

To confirm this hypothesis, pure CT and QT were analyzed by UV-Vis analysis before and after the acid treatment and results superimposable to those of hydrolyzable and condensed tannin-rich by-products were obtained, as shown in Figure 2.3.2.1.2a,c.

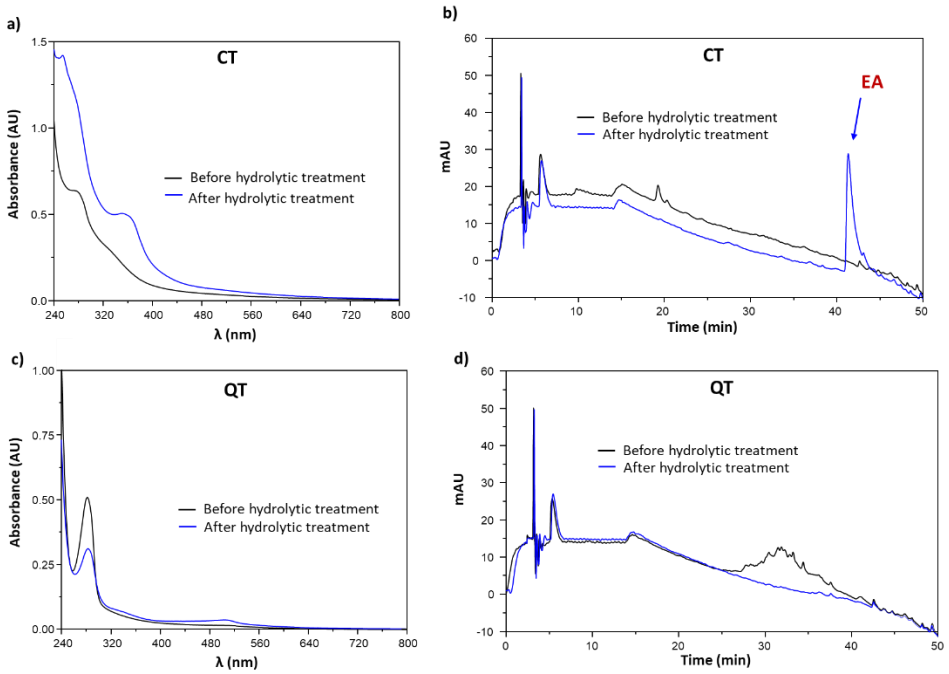

Figure 2.3.2.1.2. UV-Vis spectra of the DMSO-soluble fractions of (a) hydrolyzable and (c) condensed tannins and HPLC profiles of the DMSO-soluble fractions of (b) hydrolyzable and (d) condensed tannins, before and after the acid treatment.

HPLC analysis of the DMSO-extractable fractions confirmed all the previous observations. Here are reported the HPLC profile of DMSO-extractable fraction of pomegranate waste, which after hydrolysis exhibited the appearance of a compound eluted at around 41 min, due to the release of EA, as observed for the hydrolyzed CT sample (Figure 2.3.2.1.3 and Figure 2.3.2.1.2b). Formation of EA could be presumably associated to the increase of the antioxidant properties observed for this sample in the DPPH and FRAP assay. On the other hand, the HPLC profile of the extractable fraction of QT appeared more complex, with a broad peak eluting between 25 and 40 min, which disappeared after the acid treatment, likely as the result of QT depolymerization. This process probably led to a release of flavanol monomers, which could be washed away and/or degraded due to the harsh conditions of the acid treatment.

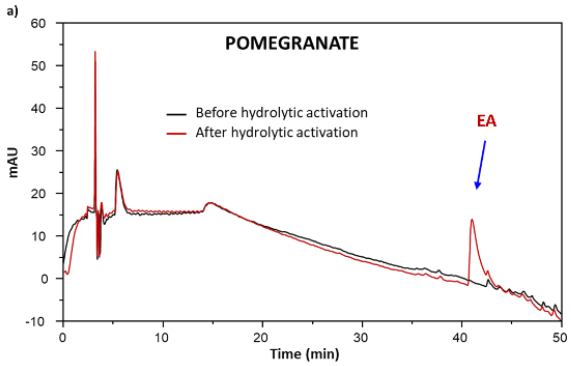

Figure 2.3.2.1.3. HPLC profiles of the DMSO-soluble fraction of pomegranate waste before and after hydrolytic treatment.

2.3.2.2. ATR-FTIR analysis

With the aim of further characterizing the structural modifications induced by the acid treatment, in other experiments the agri-food by-products were directly analyzed by ATR-FTIR analysis, before and after hydrolysis. As an example, the FTIR spectra of potato waste, pecan nut shell and grape pomace are shown in Figure 2.3.2.2.1. In the first case, a marked increase of the two sharp peaks at 2950–2850 cm^{-1} was observed further to the hydrolytic treatment, as evident also from the subtracted spectrum (hydrolyzed minus untreated, black dashed line), (Figure 2.3.2.2.1a). These signals are typically associated to the C−H stretching vibration of lignins,[150,181] so the observed increase is likely to indicate an enrichment in the lignin component as a result of polysaccharide hydrolysis and removal. Notably, the peaks at 2950–2850 cm^{-1} were less significantly affected or even reduced by the hydrolytic treatment in the case of grape pomace and pecan nut shell (Figure 2.3.2.2.1b,c).

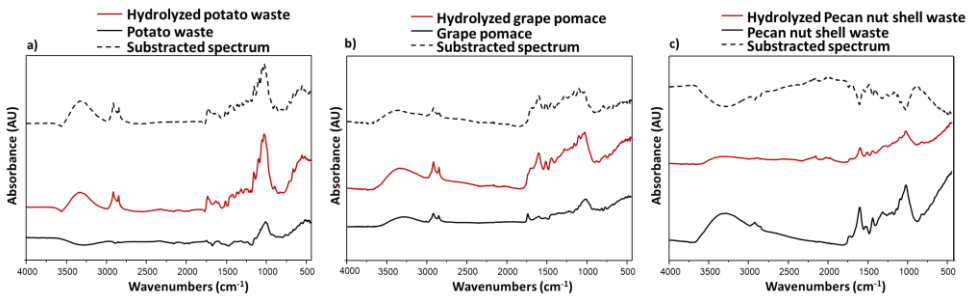

Figure 2.3.2.2.1. ATR-FTIR spectra of selected agri-food by-products, before and after hydrolytic activation.

2.3.2.3. Chemical degradation analysis

In a last series of experiments, agri-food by-products were subjected to chemical degradation treatments commonly adopted for the qualitative and quantitative analysis of phenolic polymers, that is alkaline hydrogen peroxide degradation, alkali fusion and acid degradation (Figure 2.3.2.3.1). The first two methods are commonly employed to analyze insoluble and structurally complex phenolic polymers and are based on the HPLC identification of low-molecular weight markers deriving from oxidative breakdown of the polymer,[183] whereas acid degradation has been reported as a strategy for the identification of extractable and non-extractable ellagitannins.[184]

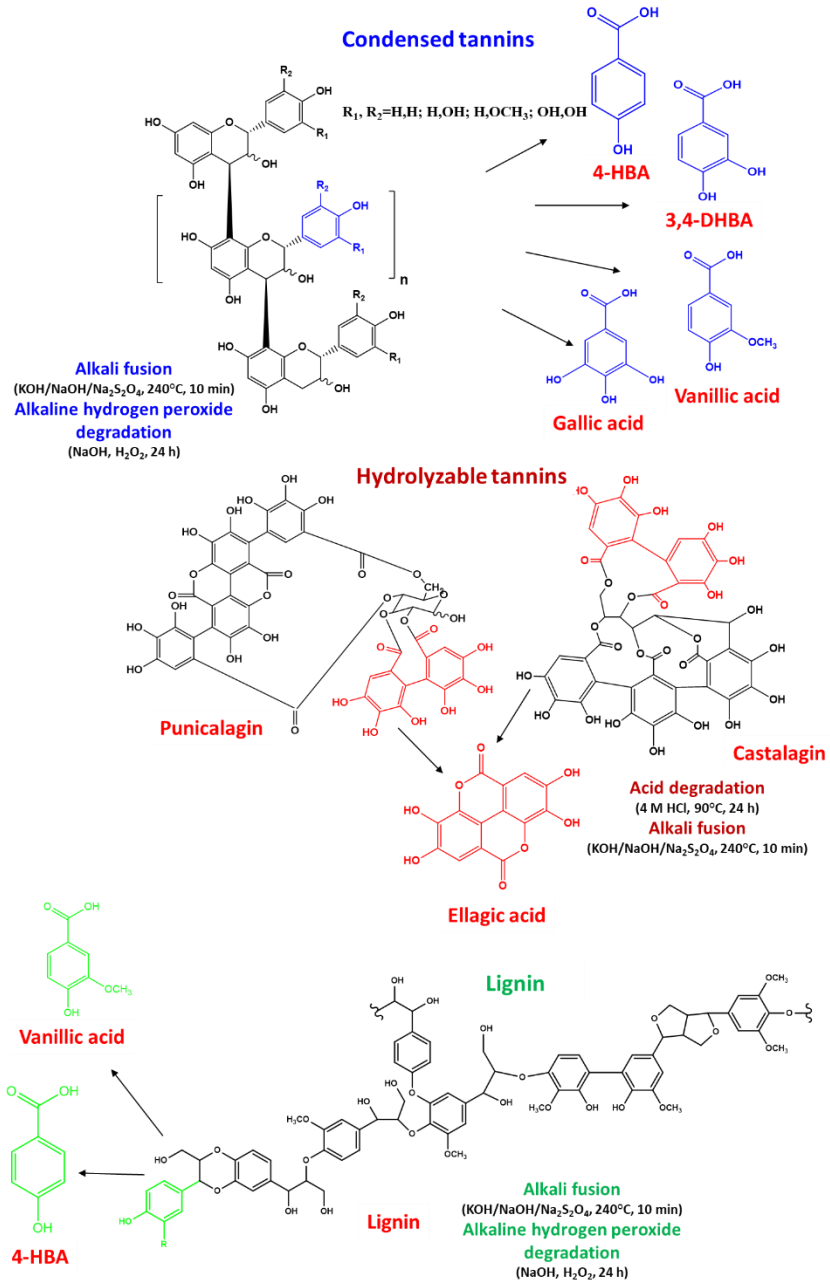

Figure 2.3.2.3.1. Possible chemical degradation pathways under acid and alkaline conditions.

In general, the hydrolyzed materials showed chromatographic profiles characterized by more intense and/or a greater number of peaks, suggesting again the occurrence of breaking/cleavage processes of high molecular weight components, leading to the release of small units more susceptible to the attack by the chemical degradation agents and responsible for the improved antioxidant properties. 3,4-dihydroyxbenzoic acid (3,4-DHBA), 4-hydroxybenzoic acid (4-HBA) and gallic acid were identified as the main chemical degradation products, by comparison of chromatographic properties with those of authentic standards. The elutographic profiles of the chemical degradation mixtures of pomegranate waste are shown as a remarkable example in Figures 2.3.2.3.2. The HPLC profile of the alkaline hydrogen peroxide degradation mixture of treated and untreated pomegranate waste showed a single peak eluted at 18 min and identified as 3,4-DHBA, detected in higher amounts in the case of the hydrolyzed sample (Figure 2.3.2.3.2a). EA was found to be the major peak of HPLC profile of alkali fusion of hydrolyzed sample and was practically absent in the untreated sample (Figure 2.3.2.3.2b). EA represented the main component also of the solid residue deriving from the acid degradation mixture, with an intensity about seven-fold higher than that obtained from the untreated pomegranate (Figure 2.3.2.3.2c). On the other hand, the supernatant from the acid degradation mixture of untreated pomegranate showed a series of peaks eluted at around 18–23 min (Figure 2.3.2.3.2d), likely due to partially hydrolyzed ellagitannins, which were found to be absent in the HPLC profile of pomegranate waste after the hydrolytic treatment, probably because this treatment had already removed these components.

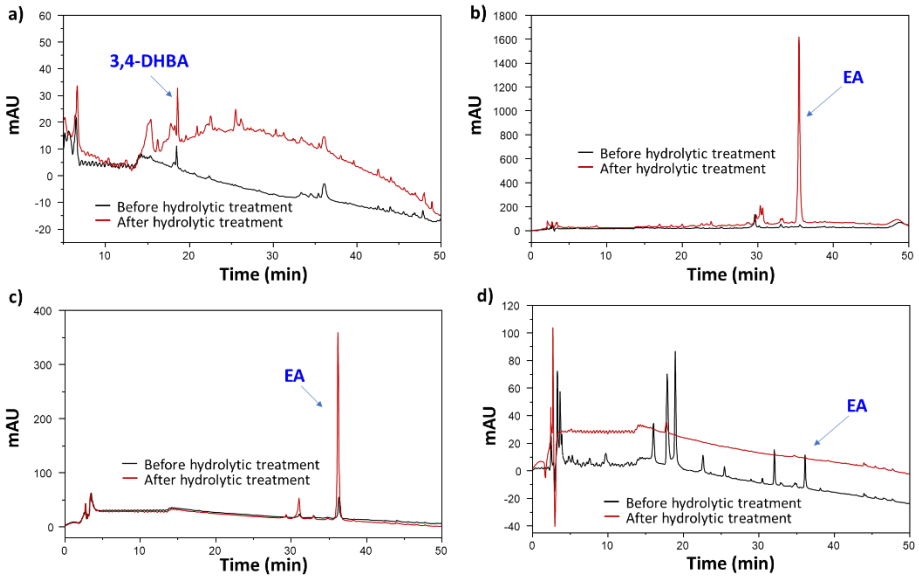

Figure 2.3.2.3.2. HPLC profiles of chemical degradation mixtures of pomegranate wastes before and after the acid treatment. (a) Alkaline hydrogen peroxide degradation mixture. (b) Alkali fusion mixture. (c) Solid residue from the acid degradation mixture. (d) Supernatant from the acid degradation mixture.

The same degradation experiments were carried out on pure CT. In Figure 2.3.2.3.3 the HPLC profiles of alkali fusion and acid degradation mixtures are reported, and the hydrolyzed material showed, as in the case of pomegranate waste, chromatographic profiles characterized by EA as the main peak, which was present only in very low amount in the mixtures of the untreated sample (Figure 2.3.2.3.3).

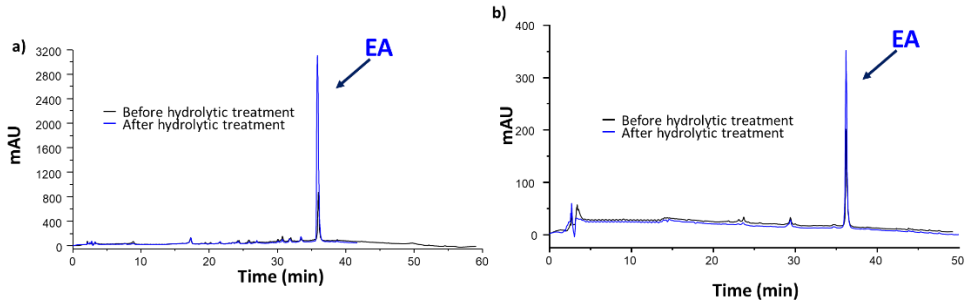

Figure 2.3.2.3.3. HPLC profiles of chemical degradation mixtures of CT, before and after the acid treatment. (a) Alkali fusion mixture. (b) Solid residue from the acid degradation mixture.

2.4. Evaluation of the effects of the acid treatment on enzymatically synthesized phenolic polymers

In another series of experiments, the same hydrolytic treatment adopted for the agri-food by-products was performed on synthetic polymers obtained from enzymatic, biomimetic oxidation of natural starting phenolic compounds.

Whereas in the past, intense research has been focused on these monomers, less attention has been directed to the possible exploitation of their polymers. Recently, these polymers have attracted remarkable interest for their potent antioxidant properties,[20] which have prompted their exploitation for different applications, including e.g. the use as active components in packaging,[185–187] and biomaterials.[26,188] Phenolic polymers exhibit several advantages over the corresponding monomers, including in some cases increased antioxidant activity, lower bioactivity and toxicity, better stability properties, and hence more practical processing, and lower solubility that reduces the tendency to leak, for e.g. for packaging applications.[20,187–189]

Among polymerization strategies, peroxidase-catalyzed reactions have been used e.g. for the preparation of poly(caffeic acid methyl ester) (PolyCAME),

polypyrogallol and polyguaiacol, proposed as active ingredients for stabilization of synthetic polymers against thermal and photo-oxidative degradation,[187,190,191] and of polytyrosol, endowed with osteogenic activity.[188]

In a recent work, horseradish peroxidase (HRP) coupled with H_2O_2 has been adopted as an easily available, eco-friendly and low-cost oxidant for the polymerization of mono-, di- and tri-phenolic compounds, and a systematic investigation of the antioxidant properties of the thus obtained phenolic polymers has been reported.[192]

Based on these findings and on the results described in the previous paragraphs, the effects of the acid treatment on the antioxidant and radical-scavenging properties of the above-mentioned phenolic polymers were evaluated.

2.4.1 Preparation of the enzymatically synthesized phenolic polymers

Mono-, di- and tri-phenols (Figure 2.4.1.1) were polymerized using HRP and H_2O_2 in phosphate buffer at pH 6.8. The mixtures were kept under magnetic stirring overnight and the polymers collected by acidification with 3 M HCl up to pH 3, centrifugation and lyophilization.

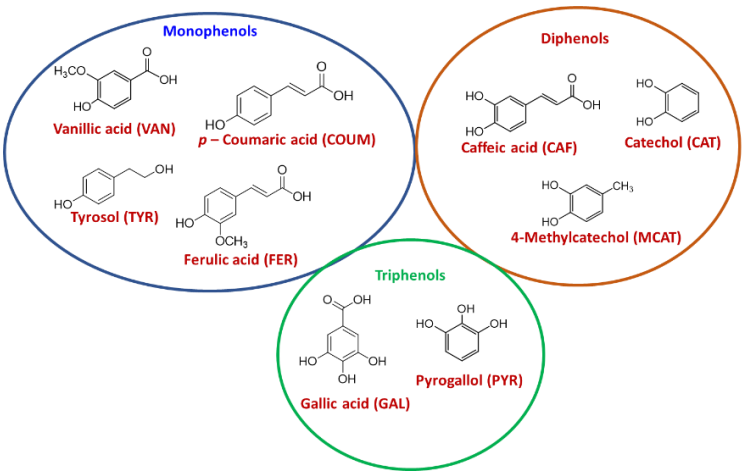

Figure 2.4.1.1. Mono-, di- and tri-phenols used for polymer preparation.

The phenolic polymers were then subjected to an acid treatment with 6 M HCl at 100 ◦C for 24 h. The recovery yields of the treated materials are reported in Table 2.4.1.1.

Table 2.4.1.1. Recovery yields of phenolic polymers subjected to the acid treatment.

Polymer	Yields (w/w)
PolyGAL	65%
PolyPYR	100%
PolyCAT	70%
PolyMCAT	67%
PolyCAF	83%
PolyFER	67%
PolyCOUM	29%
PolyVAN	62%
PolyTYR	75%

2.4.2 Characterization of the antioxidant and scavenging properties of the acid treated-phenolic polymers

2.4.2.1 DPPH and FRAP assays

Treated and untreated phenolic polymers were analyzed for their antioxidant properties by DPPH and FRAP assays. As shown in Figure 2.4.2.1.1a, untreated PolyGAL showed the lowest EC_{50} value in the DPPH assay, followed by untreated PolyPYR, PolyCAT, PolyCAF and PolyMCAT. This trend is in line with what expected on the basis of the number of phenolic groups in the monomers: indeed, triphenolic-based polymers, followed by diphenolic-based polymers, showed more efficient antioxidant properties than the monophenolic-based polymers. After the acid treatment, an increase in the DPPH-reducing properties was observed for all polymers, with the exception of PolyCOUM, for which a decrease was actually obtained, and PolyTYR and PolyVAN, for which the effects of the acid treatment were found to be less significant. The most significant effects were observed on PolyFER, which exhibited an EC_{50} value 3.4-fold lower with respect to the untreated material, very close to those of tri- and diphenolic-based polymers.

In the case of the FRAP assay, PolyGAL, PolyPYR, PolyCAT and PolyCAF were found to be again the most active among untreated polymers. Despite the activating effect of the acid treatment was found to be less specific on the Fe^{3+}-reducing power (Figure 2.4.2.1.1b), all the materials showed an improvement of reducing power and again the most significant effect was observed on PolyFER.

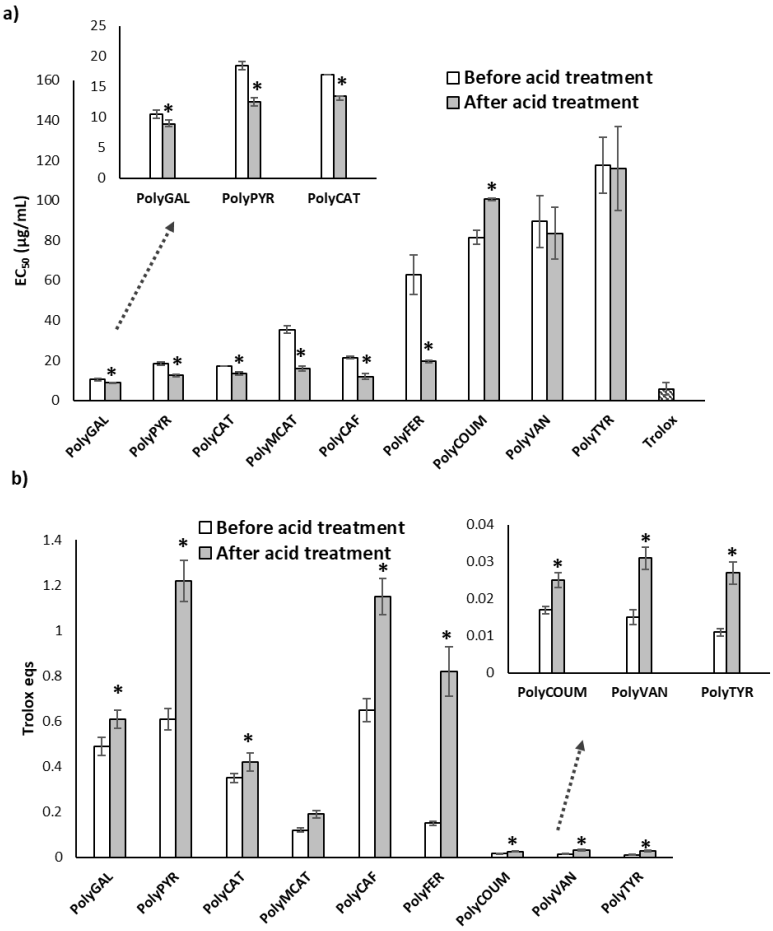

Figure 2.4.2.1.1. Antioxidant properties of the enzymatically synthesized phenolic polymers, before and after the acid treatment, determined by (a) DPPH and (b) FRAP assay. Reported are the mean ± SD values of at least three experiments. Values marked with asterisks are significantly different from those of the untreated polymer ($p < 0.05$).

2.4.2.2 Superoxide-and NO-scavenging assays

As evidenced in Chapter 1, many studies have shown the key role of ROS in the initiation and progression of different human diseases and superoxide anion radical, is one of the most important and biologically relevant ROS in living organisms. Nitric oxide (NO) is another radical species, actively produced in human body. Despite low concentrations are considered physiological and exert crucial roles in vascular and neuronal signal transduction, smooth muscle contractility, platelet adhesion and aggregation, immunity, and cell death regulation, high concentrations of this radical are directly involved in different pathologies, such as hypertension, cardiovascular dysfunctions, neurodegeneration, arthritis, asthma and septic shock.[193] Indeed, NO can lead to the formation of reactive nitrogen species (RNS) by reaction with oxygen, generating the strong oxidizing species nitrogen dioxide, or superoxide ions, leading to peroxynitrite, a well-known cytotoxic agent.

In this context, in a further series of experiments the superoxide- and nitric oxide scavenging properties of the acid treated enzymatically synthesized polymers were investigated and compared with those previously reported for the untreated polymers.[192,194]

The superoxide-scavenging assay is based on the rapid autoxidation of pyrogallol under alkaline conditions, leading to superoxide anion radical generation. This latter reacts with nitroblue tetrazolium, which is reduced by superoxide anion radical to a diformazan which is spectrophotometrically detected at 560 nm (Figure 2.4.2.2.1).

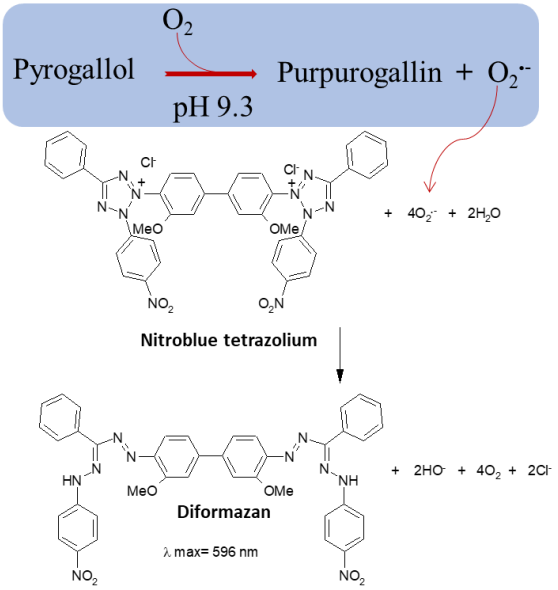

Figure 2.4.2.2.1. Superoxide-scavenging assay.

In the NO-scavenging assay, NO is generated by decomposition of sodium nitroprusside in phosphate buffer at pH 7.4. Under aerobic conditions NO reacts with oxygen to produce nitrite ions. NO scavengers compete with oxygen leading to a lower production of nitrite ions, which are detected by reaction with Griess's reagent, composed of sulphanilamide and *N*-1-naphtylethylendiamine in phosphoric acid: in acidic medium, sulphanilamide is diazotized by the nitrite ions and the diazocompound then reacts with *N*-1-naphtylethylendiamine giving rise to a conjugated compound with an absorption maximum at 540 nm (Figure 2.4.2.2.2).

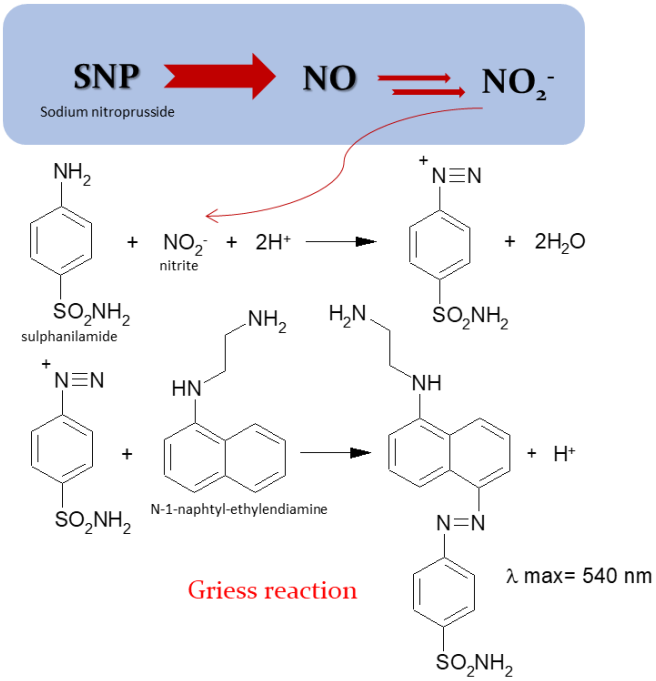

Figure 2.4.2.2.2. NO-scavenging assay.

As evident from Figure 2.4.2.2.3a, the results of the superoxide-scavenging assay showed a remarkable increase in the superoxide trapping ability of PolyMCAT and PolyVAN, that exhibited a 4- and 20-fold improvement, respectively of the activity after the acid treatment, whereas a significant decrease (ca. 70%) in the superoxide-trapping ability was observed for PolyCOUM.

The results of the NO-scavenging assay confirmed the higher efficiency of the triphenolic-based polymers PolyGAL and PolyPYR, followed by PolyCAT. After the acid treatment, a remarkable increase in the NO-trapping capacity was found in the case of PolyCAF, which showed a 5-fold higher activity after the treatment, whereas a significant decrease of the NO-scavenging ability was observed in the case of PolyCOUM and PolyTYR, which, in particular, completely lost its already poor effectiveness (Figure 2.4.2.2.3b).

Actually, the chemical mechanisms behind NO and superoxide scavenging are not known, and indeed different pathways could be operative, leaving a full interpretation of these results still incomplete.[194]

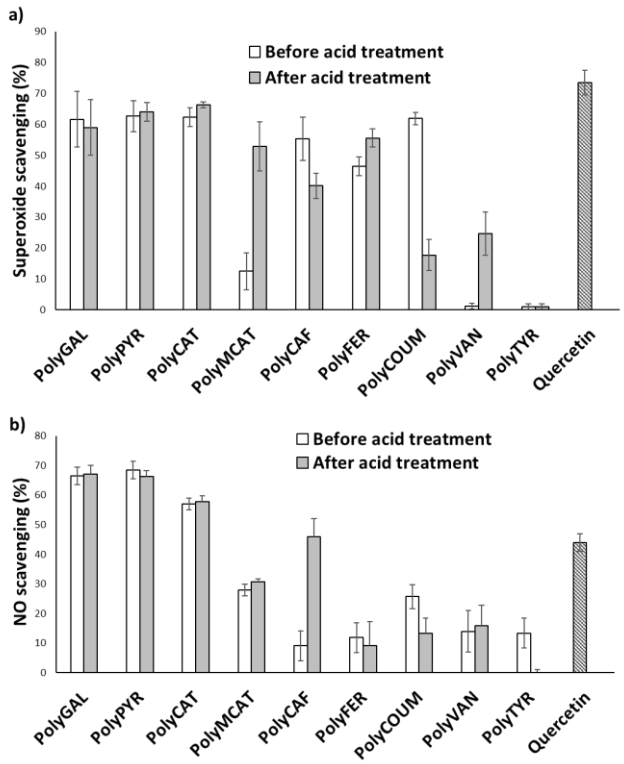

Figure 2.4.2.2.3. (a) Superoxide and (b) NO-scavenging properties of the enzymatically synthesized phenolic polymers, before and after the acid treatment. Reported are the mean ± SD values of at least three experiments.

2.4.3 Spectroscopic investigation of the structural modifications induced by the acid treatment on the enzymatically synthesized phenolic polymers

2.4.3.1 UV-Vis analysis

In order to better understand the chemical modifications induced by the acid treatment, DMSO solutions of the different polymers were analyzed by UV–vis

spectroscopy. Figure 2.4.3.1.1 showed no significant changes in the spectra of monophenol-derived PolyTYR and PolyVAN and the diphenol-derived PolyMCAT. On the contrary, the hydroxycinnamic acid-derived PolyCOUM and PolyCAF showed an almost total abatement of the absorption further to the acid treatment, indicative of remarkable structural modifications of the polymer backbone. The triphenol-derived PolyGAL and PolyPYR as well as PolyFER showed a general loss of the spectroscopic features, whereas an increase in the absorbance with no significant modifications in the spectrum, was observed for PolyCAT.

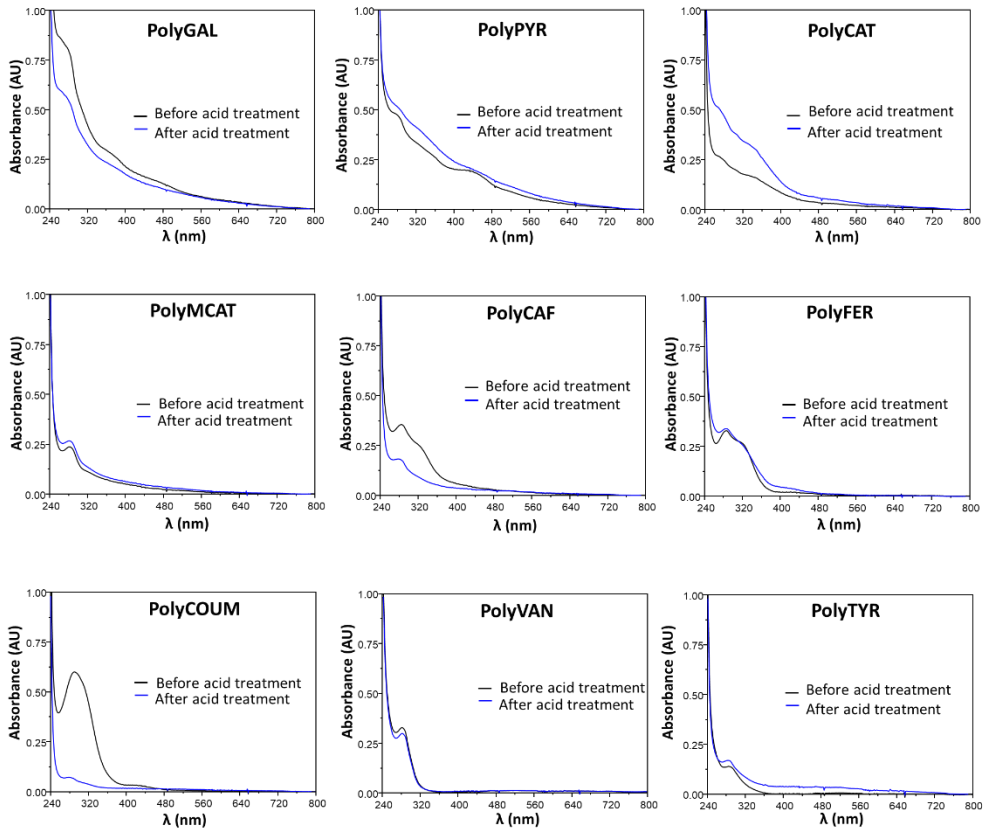

Figure 2.4.3.1.1. UV-Vis spectra of the enzymatically synthesized polymers, before and after the acid treatment.

All these results are in line with those of the antioxidant assays, showing in general an abatement of the reducing and radical scavenging properties for PolyCOUM, likely as a consequence of detrimental extensive structural modifications induced by the acid treatment, reflected also in the low recovery yields reported in Table 2.4.1.1. On the other hand, the broadening of the UV-Vis spectrum observed for PolyGAL, PolyPYR and PolyFER would be indicative of the occurrence of chemical reactions resulting in the formation of more varied species or structural units, possibly characterized by a more extended π-electron conjugation, and hence endowed with higher antioxidant properties.

2.4.3.2 EPR analysis

Phenolic polymers before and after the acid treatment were also analyzed by EPR spectroscopy (Table 2.4.3.2.1 and Figure 2.4.3.2.1), which has been recently reported as a promising approach to inquire into the structural basis of the antioxidant properties of these samples, being characterized by the presence of intrinsic free radical centers.[192] Indeed, natural or synthetic pehnolic polymers are characterized by the presence of stable organic free radicals, due to the redox equilibria between fully reduced, fully oxidized, and semi-oxidized phenolic units.[195] All the samples were characterized by g values compatible with carbon-centered radicals.[196] A general increase of spin density was observed for most of the polymers further to the acid treatment, ranging from 4.5-6.6-fold for the triphenol- and diphenol-derived samples, to 2.8-fold for the monophenolic polymers PolyCOUM and PolyTYR. The spin density of PolyVAN and PolyFER was instead not significantly affected by the treatment. Concerning the signal amplitude (ΔB), this was less affected by the acid treatment, even if a slight increase was observed for almost all polymers. However, marked differences were observed between untreated and treated PolyFER, with the first showing a ΔB value 2-fold higher. On the contrary, PolyCOUM, PolyVAN and PolyTyr showed a lower ΔB in comparison with untreated materials. Based on these data, it can be concluded, again, that the

acid treatment significantly affected the structure of triphenolic and hydroxycinnamic-derived polymers. In particular, the broader signals of the treated polymers could be the result of a greater number of π-stacking interactions in aromatic (planar) units, as a consequence of dehydration and/or oxidation processes occurring under strong acidic and high temperature conditions.[192,197] In agreement with this hypothesis is also the observed increase in the spin density, which would be indicative of the generation of structural features able to stabilize unpaired electrons and hence to sustain electron transfer processes, such as highly π-conjugated systems.[192] The possibility that the acid treatment breaks weak C-O linkages, inducing depolymerization processes and hence leading to an increase in low molecular weight molecules exhibiting a higher number of phenolic OH moieties and, as a consequence, a higher spin density, cannot be ruled out.

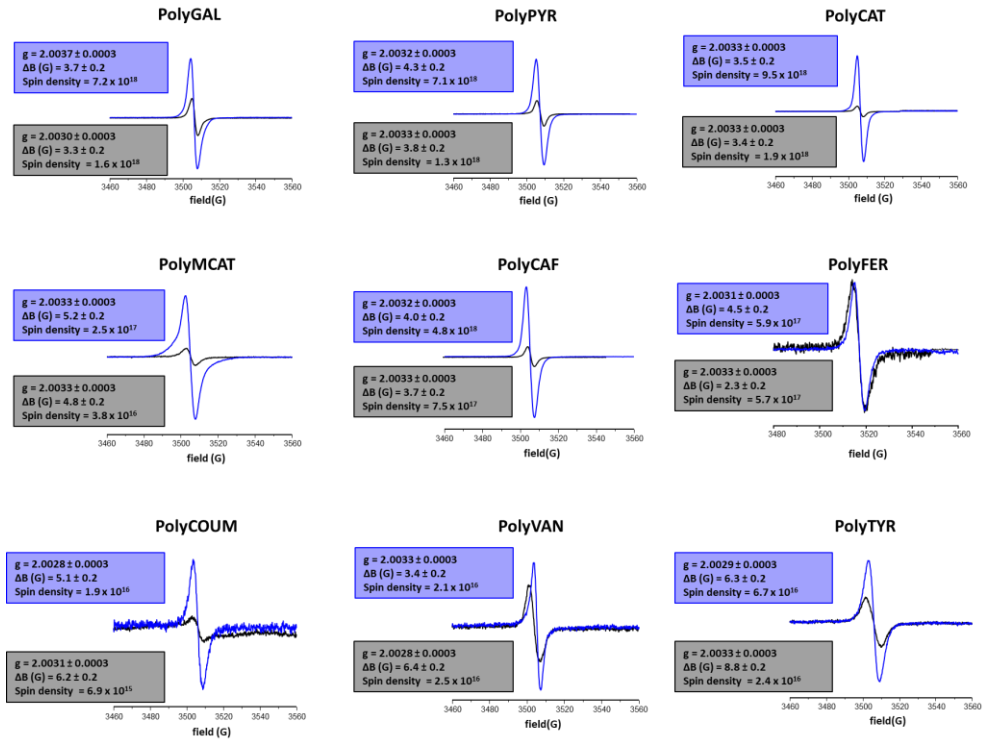

Figure 2.4.3.2.1. Solid-state EPR spectra of the enzymatically synthesized phenolic polymer before (black traces) and after (blue traces) acid treatment.

Table 2.4.3.2.1. EPR parameters of the phenolic polymers before and after the acid treatment. Experimental uncertainties are ± 0.0003 on g-factor, ± 10% on spin-density and ± 0.2 g on ΔB.

Precursor	g-factor	Spin density (spin g^{-1})	ΔB (G)
PolyGAL	2.0030	1.6×10^{18}	3.3
Treated PolyGAL	2.0037	7.2×10^{18}	3.7
PolyPYR	2.0033	1.3×10^{18}	3.8
Treated PolyPYR	2.0032	7.1×10^{18}	4.3
PolyCAT	2.0033	1.9×10^{18}	3.4
Treated PolyCAT	2.0033	9.5×10^{18}	3.5
PolyMCAT	2.0033	3.8×10^{16}	4.8
Treated PolyMCAT	2.0033	2.5×10^{17}	5.2
PolyCAF	2.0033	7.5×10^{17}	3.7
Treated PolyCAF	2.0032	4.8×10^{18}	4.0
PolyFER	2.0033	5.7×10^{17}	2.3
Treated PolyFER	2.0032	5.9×10^{17}	4.5
PolyCOUM	2.0031	6.9×10^{15}	6.2
Treated PolyCOUM	2.0028	1.9×10^{16}	5.1
PolyVAN	2.0028	2.5×10^{16}	6.4
Treated PolyVAN	2.0033	2.1×10^{16}	3.4
PolyTYR	2.0033	2.4×10^{16}	8.8
Treated PolyTYR	2.0029	6.7×10^{16}	6.3

2.4.3.3 ATR-FTIR analysis

ATR-FTIR analysis was carried out on representative examples of each class of polymers, that is PolyPYR (triphenol), PolyCAT (diphenol) and PoyTYR (monophenol). As reported in Figure 2.4.3.3.1, no significant modifications in the FTIR spectrum of PolyTYR, before and after the acid treatment, were observed, in accordance with UV-Vis analysis (Figure 2.4.3.1.1) and antioxidant assays, showing no remarkable increase in the antioxidant properties for this polymer. On the other hand, PolyPYR and PolyCAT spectra evidenced the appearance of new bands at 1000–900 cm^{-1}, associated to =C–H bending vibrations, due to the probable formation of additional double bond further to the acid treatment, likely resulting in more extended π-conjugation systems. Treated PolyPYR also showed signals in the region 1670–1600 cm^{-1}, due to C=C stretching bands.

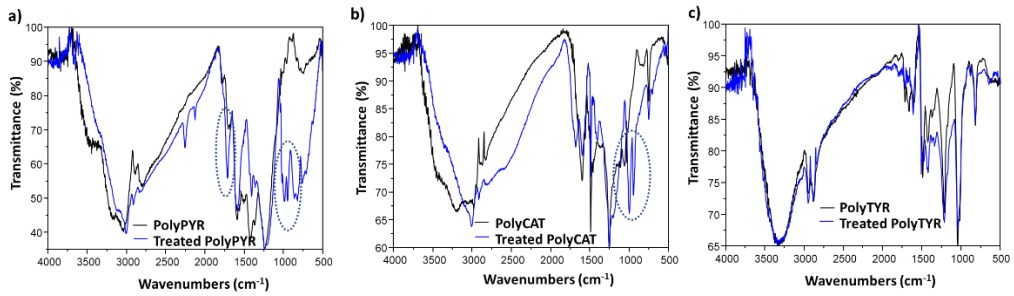

Figure 2.4.3.3.1. ATR-FTIR spectra of selected phenolic polymers before and after the acid treatment.

2.4.3.4 NMR analysis

In another series of experiments, the same selected polymers, before and after acid treatment, were analyzed also by ^{1}HNMR (Figure 2.4.3.4.1). The spectra did not show significant variations in the case of PolyTYR and PolyCAT. On the other hand, treated PolyPYR showed an almost complete loss of proton signals, in agreement with the hypothesis of formation of new C-C/C=C bonds, as evidenced also in the ATR-FTIR spectrum.

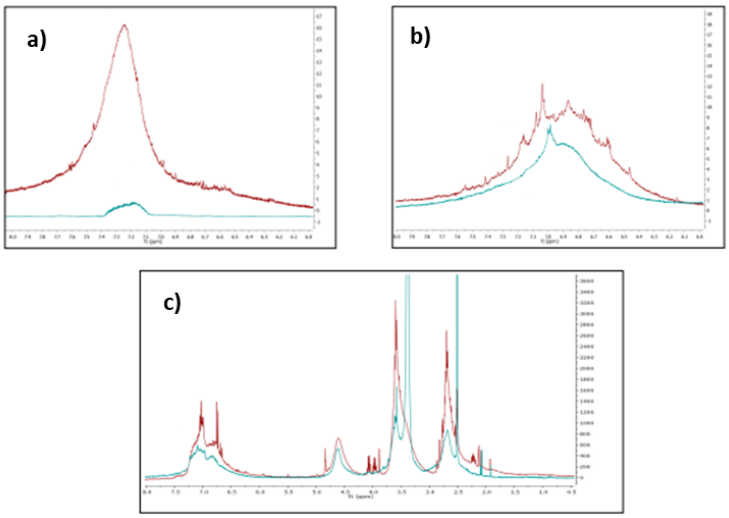

Figure 2.4.3.4.1. ^{1}H NMR spectra of (a) PolyPYR, (b) PolyCAT and (c) PolyTYR, before (red trace) and after (green trace) acid treatment, recorded in DMSO-d_6.

Finally, PolyFER and PolyCAF, before and after the acid treatment, were analyzed by solid state ^{13}C NMR spectroscopy, run in the cross-polarization magic angle spinning (CP-MAS) mode. These two polymers were chosen on the basis of the remarkable improvement of their antioxidant properties and the significant increase of spin density highlighted by EPR analysis. PolyFER and PolyCAF showed quite similar spectra (Figure 2.4.3.4.2). The first was characterized by broad signals around 172 and 56 ppm, due to carboxyl and methoxyl groups, respectively. The signal at 56 ppm was obviously lacking in the spectrum of PolyCAF. Other signals were present at around 150 and 135–125, assigned to quaternary aromatic carbons, and 120–110 ppm, attributed to the C-H carbon of the benzene moiety. The spectra also showed the presence of signals in the aliphatic region at 75−90 ppm, indicative of the presence of dihydrobenzofuran units, as previously reported for other phenolic polymers.[187,198] The acidic treatment led to the almost complete disappearance of the broad signals at 75–90 ppm (Figure 2.4.3.4.2), probably due to furane ring opening resulting in more extended π-electron conjugated species as supposed also based on the evidence reported in the previous paragraphs (Figure 2.4.3.4.3)**.**

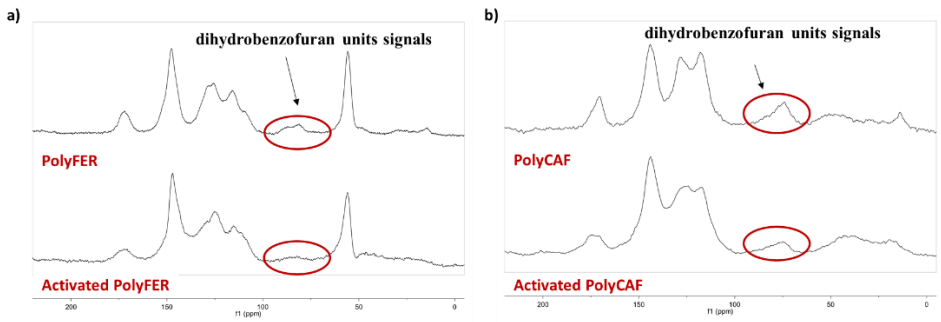

Figure 2.4.3.4.2. Solid state ^{13}C NMR spectra, recorded in the CP-MAS mode, of (a) PolyFER and (b) PolyCAF, before and after acid treatment.

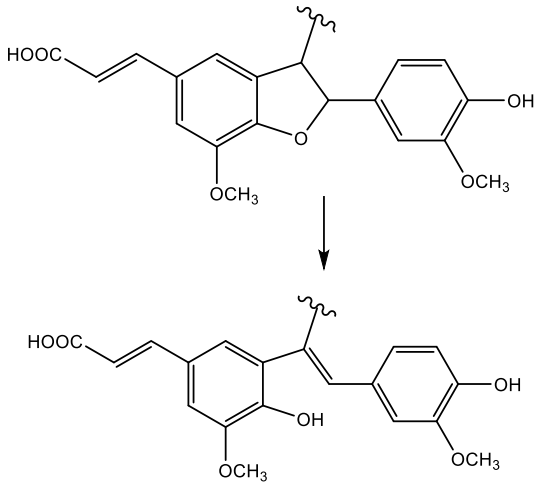

Figure 2.4.3.4.3. Proposed structural modifications induced on PolyFER by the acid treatment.

2.5 Conclusions

Fruit and vegetable wastes and by-products are cheap and largely available sources of phenolic compounds, endowed with remarkable antioxidant properties. Of particular interest is the possibility to improve these and other functional properties *via* a hydrolytic treatment, involving the use of concentrated HCl and high temperatures.[150,174]

Most of the analyzed agri-food by-products exhibited a marked enhancement of the antioxidant properties after the hydrolytic treatment, as a consequence of both the removal of inert components (mainly carbohydrates) and structural modifications of the active phenolic fraction enhancing H-atom- and electron-donor properties of the lignin and/or hydrolyzable tannin-rich materials, as deduced based on the results of extensive spectroscopic analysis run also on model systems. Conversely, the same hydrolytic treatment induced a marked decrease in the antioxidant capacity of agri-food by-products rich in condensed tannins, likely as a result of partial loss of the low molecular weight, more accessible, antioxidant components (Figure 2.5.1).

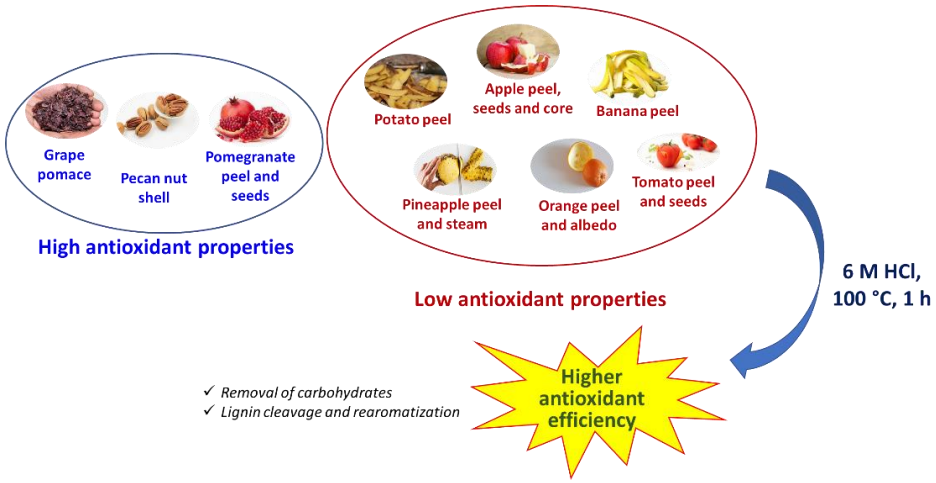

Figure 2.5.1. Overview of the boosting effects of hydrolytic treatments on agri-food by-products.

Parallel studies on bio-inspired synthetic phenolic polymers confirmed that the acid treatment may selectively induce significant structural modifications resulting in the generation of more extended π-conjugated systems, responsible for an improvement of the antioxidant and radical scavenging properties (Figure 2.5.2).

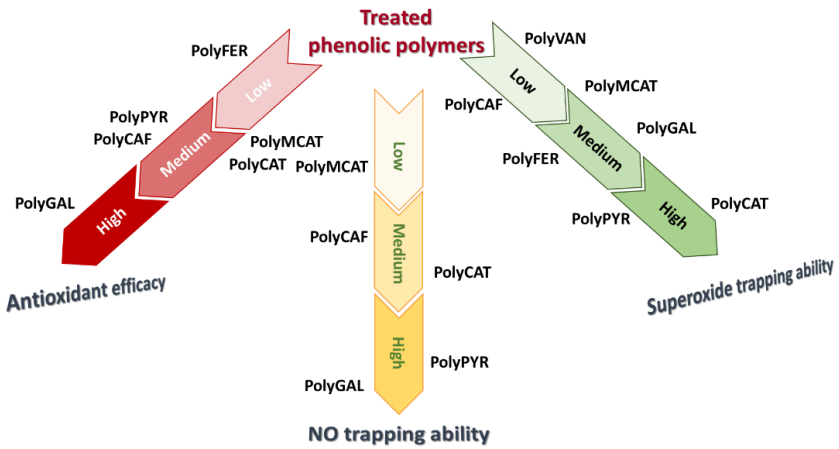

Figure 2.5.2. Overview of the antioxidant and radical-scavenging properties of acid-treated enzymatically synthesized phenolic polymers.

Overall, these results, coupled also with the cost effectiveness of the acid activation protocol, open new perspectives for the exploitation of these materials as functional additives to be used e.g. as functional additives in active packaging or in dermocosmetic formulations.

2.6 Experimental section

Materials and methods

Pomegranates, apples, oranges, bananas, pineapples, tomatoes, and potatoes were purchased at a local supermarket. Grape pomace was kindly provided by Prof. Daniele Naviglio (Department of Chemical Sciences, University of Naples "Federico II", Naples, Italy). Pecan nut shell was provided by Productora de Nuez S.P.R. de R.I. (Hermosillo, Mexico). Chestnut and quebracho tannins were provided by the industrial partner of the PhD project Silvateam (Via Torre, S. Michele Mondovì, Cuneo, Italy).

All solvents and reagents were obtained from commercial sources and used without further purification.

UV-Vis spectra were recorded using a HewlettPackard8453 Agilent spectrophotometer.

HPLC analysis were performed on an instrument equipped with an Agilent G1314A UV-Vis detector, using a Phenomenex Sphereclone octadecylsilane (ODS) column (250 x 4.60 mm, 5 μm) at a flow rate of 1.0 mL/min; a gradient elution was performed with 0.1% formic acid (solvent A)/methanol (solvent B) as follows: 5% B, 0-10 min; from 5 to 80% B, 10-47.5 min; the detection wavelength was set at 254 nm.

ATR-FTIR spectra of agri-food by-products were recorded on a PerkinElmer Spectrum 100 spectrometer equipped with a Universal ATR diamond crystal accessory, and the analysis were performed with an average of 16 scans in the range

4000−450 cm^{-1} (resolution of 4 cm^{-1}). ATR-FTIR spectra of enzymatically synthetized phenolic polymers were recorded on a Nicolet 5700 Thermo Fisher.

EPR measurements were performed using a Bruker Elexys E-500 spectrometer equipped with a superhigh sensitivity probe head. The samples were transferred to flame-sealed glass capillaries, which in turn were coaxially inserted in a standard 4 mm quartz sample tube. Measurements were performed at room temperature. The instrumental settings were as follows: sweep width, 100 G; resolution, 1024 points; modulation amplitude, 1.0 G; scansion time 20.97 s. The amplitude of the field modulation was preventively checked to be low enough to avoid detectable signal overmodulation. The number of scans and microwave power were optimized to avoid microwave saturation of resonance absorption curve. For power saturation experiments, the microwave power was gradually incremented from 0.02 to 164 mW. The g value and the spin density were evaluated by means of an internal standard, Mn^{2+}-doped MgO, prepared by a synthesis protocol reported in the literature.[199] Since sample hydration was not controlled during the measurements, spin density values have to be considered as order of magnitude estimates.[196]

^{1}H NMR spectra were recorded in DMSO-d_6 at 400 or 500 MHz on Bruker or Varian instruments.

Solid-state ^{13}C CP-MAS spectra were collected at 125.77 MHz on a 500 MHz Bruker BioSpin NMR Spectrometer Avance 500, operating at a static field of 11.7 T and equipped with a 4 mm MAS probe, spinning the sample at the magic angle at speeds up to 15 kHz that with the addition of high power ^{1}H decoupling capability allows to decrease or eliminate homo and heteronuclear anisotropies. All the samples were prepared by packing them in zirconia (ZrO_2) rotors, closed with Kel-F caps (50 μL internal volume) and the spinning speed (MAS) was optimized at 12 kHz after some experiments run in the range 4−12 kHz.[187,188]

2.6.1 Preparation of agri-food by-products. The waste part of each agri-food sample was separated from the edible part, rapidly cut into small pieces, and freeze-dried. The lyophilized material was finally shredded using a blender.

2.6.2 Preparation of phenolic polymers. Selected phenols (200–500 mg) were solubilized in ethanol and added to 0.1 M phosphate buffer at pH 6.8 (0.01 M phenol final concentration), containing 1% KCl (ethanol/buffer ratio = 1:4 v/v).[192] HRP (final concentration 2 U/mL) and 30% H_2O_2 (final concentration 0.02 M) were then added in two aliquots, within 1 h of each other. The mixture was kept under magnetic stirring overnight, acidified with 3 M HCl up to pH 3 and kept at 4 ◦C for 24 h. The precipitate was then recovered by centrifugation (7000 rpm, 4 ◦C, 30 min), washed with 0.1 M HCl and lyophilized.

2.6.3 Acid treatment. Fruit and vegetable waste materials or tannin samples (3 g) were treated with 70 mL of 6 M HCl under stirring at 100 ◦C for 1 h.[150,174,179] After cooling at room temperature, the mixture was centrifuged (7000 rpm, 15 min) and the precipitate washed with water until neutrality and freeze dried. Phenolic polymers were treated under the same conditions for 24 h.

2.6.4 Antioxidant assays. DPPH assay:[175,176] To a 0.2 mM ethanolic solution of DPPH, the different agri-food by-product or tannin powders, before and after hydrolytic treatment, were added (final dose 0.05−4.5 mg/mL), and after 10 min under stirring at room temperature the absorbance at 515 nm was measured. In the case of phenolic polymers, 30–400 µL of a 0.33 mg/mL polymer solution in DMSO were added to 2 mL of the DPPH solution and the mixtures were analyzed as above. Trolox was used as a reference antioxidant. Experiments were run in triplicate. **FRAP assay:**[177] To 0.3 M acetate buffer (pH 3.6) containing 1.7 mM $FeCl_3$ and 0.83 mM TPTZ, agri-food by-product and tannin powders, before and after hydrolytic treatment, were added (final dose 0.00625–0.3 mg/mL) and after 10 min under stirring at room temperature the absorbance of the solution at 593 nm was measured. In the case of phenolic polymers, 5–500 µL of a 0.33 mg/mL polymer solution in

DMSO were added to 3.6 mL of the FRAP solution and the mixtures were analyzed as above. Results were expressed as Trolox eqs. Experiments were run in triplicate.

2.6.5 TPC assay.[178] Agri-food by-products or tannins, before and after hydrolytic treatment, were added at a final dose of 0.02−3 mg/mL to a solution consisting of Folin-Ciocalteu reagent, 75 g/L Na_2CO_3, and water in a 1:3:14 v/v/v ratio. After 30 min incubation at 40 ◦C, the absorbance at 765 nm was measured. Gallic acid was used as reference compound. Experiments were run in triplicate.

2.6.6 NO-scavenging assay.[192,200] A 0.33 mg/mL polymer solution in DMSO (600 μL) was added to 6 mL of freshly prepared 0.01 M solution of sodium nitroprusside in 0.2 M phosphate buffer (pH 7.4), and the mixture was taken under vigorous stirring at room temperature. After 2 h, 1 mL of the mixture was added to 2 mL of Griess reagent (0.5% sulfanilamide and 0.05% N-(1-naphthyl)ethylenediamine dihydrochloride in 2.5% phosphoric acid), and the absorbance at 540 nm was measured. Results were expressed as percentage of reduction in the absorbance at 540 nm of a control mixture run in the absence of a sample. Quercetin was used as the reference antioxidant. Experiments were run in triplicate.

2.6.7 Superoxide-scavenging assay.[192,201] A 0.33 mg/mL polymer solution in DMSO (100 μL) was added to 0.05 M ammonium hydrogen carbonate buffer (pH 9.3) containing 0.33 mM EDTA, 0.01 mM nitroblue tetrazolium and 3.3 mM pyrogallol. The mixture was taken under vigorous stirring, and after 5 min, the absorbance at 596 nm was measured. Results were expressed as percentage of reduction in the absorbance at 596 nm of a control mixture run in the absence of a sample. Quercetin was used as the reference antioxidant. Experiments were run in triplicate.

2.6.8 Alkali fusion.[183] 100 mg of KOH, 100 mg of NaOH, and 2 mg of $Na_2S_2O_4$ were melted in a pyrex tube at 240 °C. 20 mg of sample were then added, and the mixture was kept at 240 °C for further 10 min. After cooling to room temperature,

10 mL of a 1% sodium dithionite solution was added. The resulting mixture was taken to pH 3 with 6 M HCl and then extracted for three times with 15 mL of ethyl acetate. The organic layers were anhydrified with sodium sulfate, taken to dryness, dissolved in methanol, and analyzed by HPLC.

2.6.9 Alkaline hydrogen peroxide degradation.[179] 10 mg of each sample were suspended in 1 mL of 1 M NaOH and then 50 µL of 30% H_2O_2 were added. The mixture was kept at room temperature under vigorous stirring for 24 h and then treated with 5% w/v $Na_2S_2O_5$, taken to pH 3 with 6 M HCl, filtered on a 0.45 µm PVDF filter, and analyzed by HPLC.

2.6.10 Acid degradation.[184] 50 mg of sample were placed in a pyrex tube. Then, 5 mL of 4 M HCl were added, and the mixture was vortexed for 1 min and incubated in an oven at 90 ◦C for 24 h. After cooling, the pH was adjusted to 2.5 with 6 M NaOH, and the mixture was centrifuged for 10 min at 5000 rpm. The supernatants were recovered, taken to 10 mL by addition of water, and analyzed by HPLC after filtration on a 0.45 µm PVDF filter. The solid residues were dissolved in 10 mL of DMSO/methanol 1:1 v/v and then analyzed by HPLC as well.

Chapter 3

Microbial fermentation as a strategy to improve the functional properties of agri-food (by)products

3.1 Introduction

Fermentation traditionally represents a low-cost practice to preserve food and increase the bioactivity of plant extracts.[202] For centuries, foods of animal or vegetable origin have been subjected to fermentation processes mediated by bacteria, yeasts, or fungi. This procedure leads to a series of advantages, such as the enrichment of food in vitamins, proteins, amino acids, essential fatty acids, and also phenolic compounds. Furthermore, fermentation may increase food flavour, decrease cooking time, and slow down spoilage processes.

Through the action of different enzymes, in particular amylase, protease and lipase, the microorganisms used in fermentation processes are able to hydrolyze polysaccharides, proteins and lipids into non-toxic products characterized by flavours, aroma and texture, which may attract the consumers.

The microorganisms used in traditional fermentation include lactic acid bacteria, for example *Lactobacillus plantarum*, *Lactobacillus buchneri*, and *Lactobacillus rhamnosus*. Fungal fermentation is another commonly used strategy, with *Aspergillus niger* and *Aspergillus oryzae* as the most employed microorganisms. Yeasts also play a key role in fermentation. They are eukaryotic microorganisms that live in water, soil, air and on plant and fruit surfaces.[203] On a nutritional level, yeasts are not particularly demanding compared to other microorganisms such as lactic acid bacteria.[203] However, their growth is supported by the presence of compounds such as fermentable sugars, amino acids, vitamins, minerals and oxygen. Various types of yeast strains are available, among which *Saccharomyces cerevisiae*

is known to be very effective for conversion of complex sugars to ethanol and other substances. Alcoholic fermentation, in particular, leads to the formation of ethanol and CO_2, including a lowering of pH, and these factors are responsible of the longer shelf life of fermented food.

Alcoholic fermentation takes place in two phases: in the first, the enzyme invertase, deriving from yeast, hydrolyzes complex sugars (mainly disaccharides such as sucrose) into glucose and fructose. During the second phase, ethanol is formed from simple sugars. The glycolysis reaction takes place in the cytoplasm of the organism, in which glucose, diphosphorylated by two molecules of ATP, splits into two molecules of pyruvic acid. The absence of oxygen does not allow the normal Krebs cycle and aerobic cellular respiration, hence pyruvate undergoes decarboxylation, leading to formation of CO_2 and acetaldehyde. The latter is finally reduced to ethanol by NADH (Figure 3.1.1). Fermentation temperature normally varies between 20 and 25 °C, and the process can last from a few days to two weeks.[204] Industrial production of fermented food and beverages leads, however, to the accumulation of a huge amount of biomass, whose disposal represents an environmental and economic problem. Therefore, the search for possible applications of these wastes is attracting considerable interest.

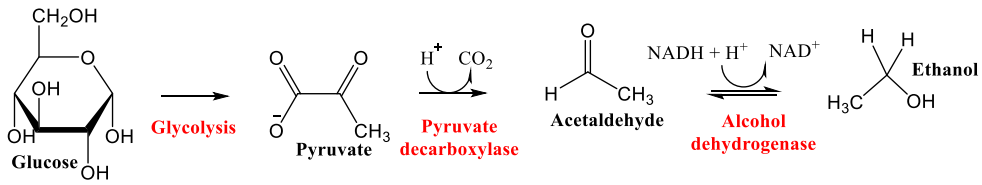

Figure 3.1.1. Alcoholic fermentation process.

Apart from being exploited to improve the nutritional and organoleptic properties as well as the shelf life of foods and beverages, in recent year fermentation, with particular reference to solid-state fermentation,[205] is emerging as a clean technology for agri-food by-products valorization, providing bioactive extracts for application

as food additives or cosmetic ingredients.[206] Indeed, solid state fermentation has been applied to a variety of easily available wastes to get mostly phenolic compounds.[202]

In this context, in the first part of this Chapter the characterization of the main phenolic compounds and antioxidant properties of waste materials deriving from the preparation of fermented fruit distillates are reported, whereas in the second part the results of analogous characterization experiments carried out on pomegranate peel and seeds, spent coffee grounds (SCG) and pecan nut shell subjected to a solid state fermentation treatment with *S. cerevisiae* and *A. niger* are discussed. As far as the first part is concerned, wastes deriving from a local agricultural distillery were analyzed. This company produces distilled beverages from fruits subjected to spontaneous fermentation processes by indigenous yeasts. The distillation process generates high volumes of solid residues, which however could represent an easily available and low cost source of bioactives. In this project, in particular, the solid residues from quince, Cilento fig, nectarine peach and strawberry fermentation and distillation were examined.

3.2 Preparation of extracts from fresh fruits and distillation residues

As previously mentioned, quince, Cilento fig, nectarine peach and strawberry distillation residues were analyzed.

Quinces, are asymmetrical apples of variable size, rich in pectins, in potassium and polyphenolic compounds, in particular flavonoids, procyanidins and hydroxycinnamic acids.[207]

The white Cilento figs also contain high content of phenols, mainly rutin, isoquercetin, chlorogenic acid and caffeoylmalic acid.[208]

Nectarine peaches are a low-calorie source of antioxidants, minerals, and vitamins. In particular, they are rich in vitamins C, A and E, together with xanthophylls (lutein, zeaxanthin and beta-cryptoxanthin). The main phenolic compounds identified in the pulp and peel are chlorogenic acid, catechin, neochlorogenic acid, epicatechin, gallic acid, rutin, quercetin-3-O-galactoside, cyanidin 3-O-β-glucoside (C3G) and cyanidin-3-O-rutinoside.[209]

Strawberry is a variety of fruits of *Fragaria*. Strawberries have a high sugar content, and are an excellent source of vitamin C, flavonoids and anthocyanins.[210]

These samples, together with the corresponding fresh fruits for comparison, were preliminarily filtered and dried, after that, they were finely ground in a blender and subjected to a solid-liquid extraction with water, DMSO, methanol or ethanol.

3.2.1 HPLC analysis of the distillation residue extracts

The distillation residue extracts were preliminarily analyzed by HPLC. Based on the number and amounts of detected compounds, methanol was found to be the best solvent for all the samples examined (see for example Figure 3.2.1.1), therefore in further analysis attention was focused primarily on the methanolic extracts. In particular, each extract was again analyzed by HPLC under previously developed conditions for analysis of phenolic compounds in extracts from plant material.[121] Analysis were carried out using a UV-Vis detector, with wavelength set to 254 nm (generally considered a universal detection wavelength for aromatic compounds), 280 nm (more specific for flavanols and dihydrocalcones), 320 nm (more specific for hydroxycinnamic acids), and 400 nm (specific for flavonols).

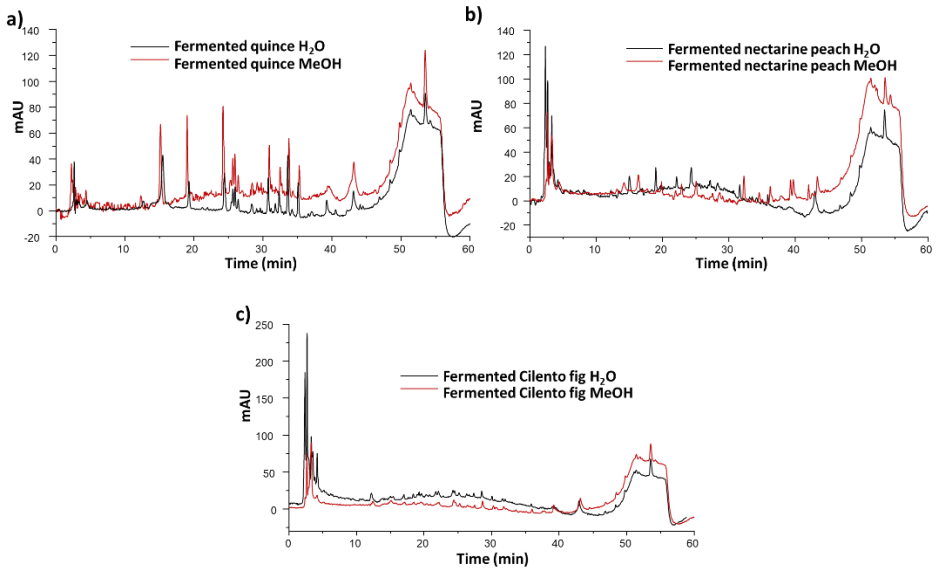

Figure 3.2.1.1. Elutographic profiles of the aqueous (black trace) and methanolic (red trace) extracts obtained from the distillation residue of (a) quince, (b) nectarine peach and (c) Cilento fig. Eluant: 0.1% formic acid (solvent A)/methanol (solvent B): 5% B (0-10 min), from 5 to 80% B (10-47.5 min); detection wavelength = 254 nm.

In Figure 3.2.1.2 the elutographic profiles at 254 nm of the methanolic extracts of fermented and fresh quince are shown. The extracts from the distillation residue showed a series of products eluted at 14, 88 and 90 min which were not found in the starting fresh sample and therefore were clearly associated with the process. The elutographic profiles at different detection wavelengths, showed, in particular, the presence of a single main flavonol in the fermented fruit, eluted at 90 min, which was absent in fresh quince.

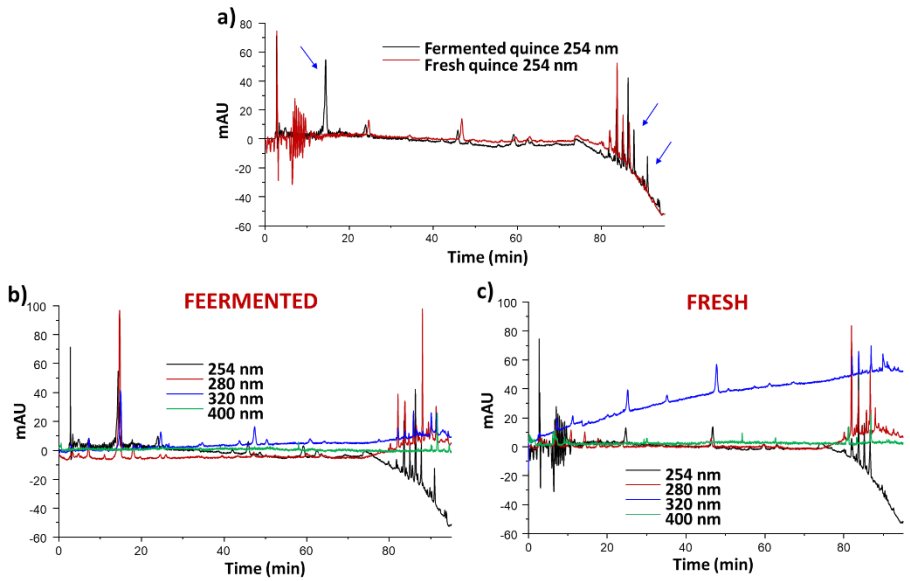

Figure 3.2.1.2. (a) Elutographic profiles of the methanolic extracts from fermented (black trace) and fresh (red trace) quince, recorded at 254 nm. Elutographic profiles of extracts from (b) fermented and (c) fresh quince, recorded at 254 nm (black trace), 280 nm (red trace), 320 nm (blue trace) or 400 nm (green trace). Arrows indicate compounds present only in the extracts from the fermented sample.

HPLC analysis of peach (Figure 3.2.1.3a) and fig (Figure 3.2.1.3b) extracts was found to be less informative, although, also in this case, the fermented materials showed the presence of products eluted at 14 min and 90 min.

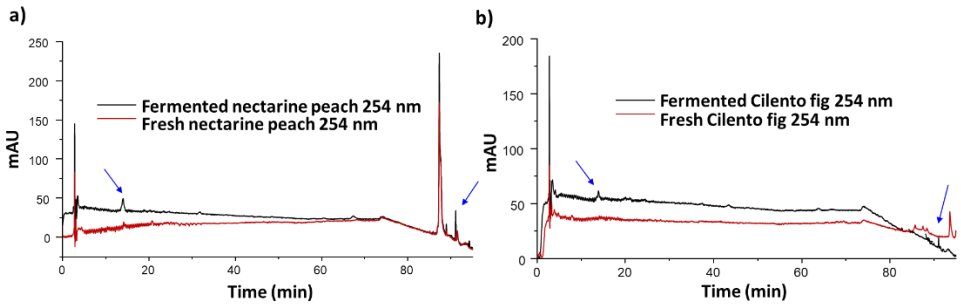

Figure 3.2.1.3. Elutographic profiles of the methanolic extracts from fermented (black trace) and fresh (red trace) (a) nectarine peach and (b) Cilento fig.

Notably, the elutographic profiles of the methanolic extract of the distillation residue of strawberry showed the presence of a single compound eluted at 88 min, which was completely absent in the chromatographic profile of the extract from the fresh fruit (Figure 3.2.1.4).

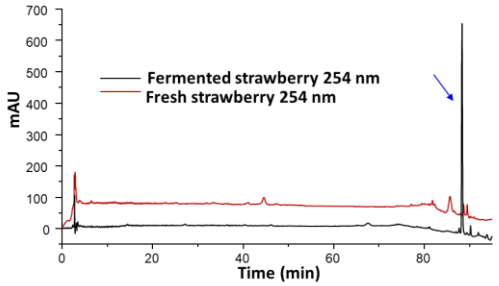

Figure 3.2.1.4. Elutographic profiles of the methanolic extracts of fermented (black trace) and fresh (red trace) strawberry. Arrow indicates the compound present only in the extract from the fermented sample.

3.2.2 Identification of the main phenolic components of the distillation residue extracts

In order to obtain information on the structure of the main phenolic compounds present in the distillation residue extracts, these latter were analyzed by LC-MS, which allowed to identify the peak at 14 min and 90 min present in the fermented quince extract as 3,4-dihydroxybenozic acid (3,4-DHBA) and quercetin, respectively. This hypothesis was confirmed by comparing the elutographic profile of the quince extract with those of pure standards. These compounds were identified also in the methanolic extracts from fermented nectarine peach and Cilento fig.

The compound eluted at 88 min present in the methanolic extract of fermented strawberry was instead identified as EA.

Table 3.2.2.1 shows the extraction yields of the identified phenolic compounds.

Table 3.2.2.1. Extraction yields (in methanol), expressed as weight percentage with respect to the starting material, of the identified phenolic compounds in the distillation residues.

Sample	3,4-DHBA	Quercetin	EA
Fermented nectarine peach	0.13%	0.05%	-
Fermented Cilento fig	0.03%	0.04%	-
Fermented quince	0.31%	0.03%	
Fermented strawberry	-	-	1.85%

3.2.3 Evaluation of the antioxidant properties of the distillation residue

In order to obtain information on the antioxidant properties of the distillation residues, DPPH assay was performed on the solid samples following the "QUENCHER" method.[175,176] Fresh samples were analyzed as well for comparison. Fermented nectarine peach and fig showed EC_{50} values up to 5-fold lower than those of the fresh materials. On the other hand, a decrease in the antioxidant properties was observed for fermented quince and strawberry, exhibiting EC_{50} values about 2-fold and 14-fold higher than those determined for the fresh materials, respectively (Table 3.2.3.1).

Table 3.2.3.1. Antioxidant properties of solid fermented and fresh fruit samples, determined by DPPH assay. Results are expressed as EC_{50} (mg/mL). Reported are the mean ± SD values of at least three experiments.

Sample	Fermented	Fresh
Nectarine peach	2.5 ± 0.1	12.7 ± 0.8
Quince	15.6 ± 1.2	6.4 ± 0.4
Cilento fig	9.4 ± 0.4	41 ± 3
Strawberry	21 ± 2	1.54 ± 0.1

3.3 Effects of solid state fermentation with *S. cerevisiae* and *A. niger* on the phenolic content and antioxidant properties of agri-food by-products

In a second set of experiments, the effects of solid state fermentation with *S. cerevisiae* and *A. niger* on the phenolic content and antioxidant properties of pomegranate peel and seeds, SCG and pecan nut shell were evaluated. The fermented samples were received from the laboratory of Prof. Cristobal Aguilar of Universidad Autónoma de Coahuila in Mexico. The materials were first grounded in a mortar and then extracted with distilled water or DMSO under vigorous magnetic stirring for 1 h, at room temperature. The supernatants, obtained after centrifugation, were then analyzed by HPLC. For comparison the same procedure was applied on unfermented sample from the same source.

3.3.1 HPLC analysis of the extracts

In the case of SCG, the chromatograms of the aqueous fermented extracts were characterized by the presence of peaks at ca. 5, 14, 26 and 31 min, not evident in the case of the starting material. These compounds were particularly abundant in the *S. cerevisiae* fermented sample. On the other hand, fermentation led to a decrease in the species eluted between 24 and 25 min present in the starting material (Figure 3.3.1.1a). Similar results were observed for the DMSO extract, that was characterized by the presence of a main product eluted at 26 min (Figure 3.3.1.1b).

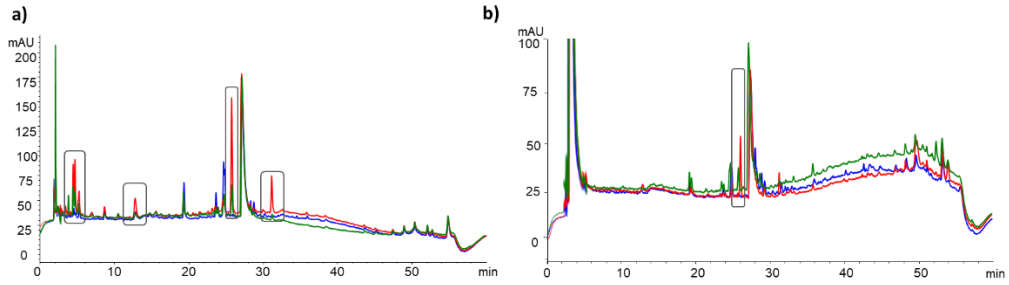

Figure 3.3.1.1. Elutographic profiles of unfermented (blue trace), *S. cerevisiae* fermented (red trace) and *A. niger* fermented (green trace) SCG (a) aqueous and (b) DMSO extracts. Boxes indicate compounds present only in the extract from the fermented samples.

The elutographic profiles of pecan nut shell extracts did not show any product associated with the fermentation process, although, in particular for the aqueous extracts (Figure 3.3.1.2a), a decrease in the compounds eluted at 25 and 40 min was observed following fermentation.

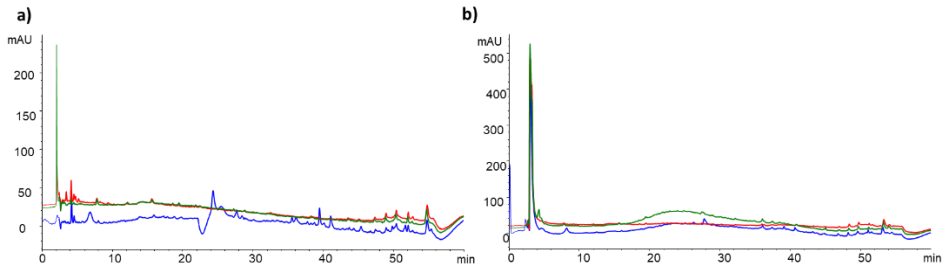

Figure 3.3.1.2. Elutographic profiles of unfermented (blue trace), *S. cerevisiae* fermented (red trace) and *A. niger* fermented (green trace) pecan nut shell (a) aqueous and (b) DMSO pecan nut shell extracts.

Rather more informative were the elutographic profiles of pomegranate waste extracts (Figure 3.3.1.3). In particular, the aqueous extract of the starting material was characterized by the presence of punicalagin as the main product, eluted at 24 min.[174] After fermentation, this compound almost completely disappeared, probably due to hydrolytic processes carried by microorganisms. In accordance with this

hypothesis, the elutographic profiles of the DMSO extracts (Figure 3.3.1.3b) exhibited a single peak at ca. 40 min identified as EA.

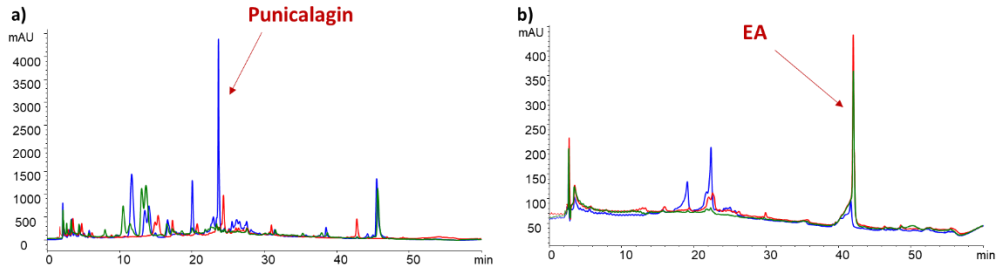

Figure 3.3.1.3. Elutographic profiles of unfermented (blue trace), *S. cerevisiae* fermented (red trace) and *A. niger* fermented (green trace) pomegranate waste (a) aqueous and (b) DMSO extracts.

3.3.2 Evaluation of the antioxidant properties and total phenolic content of the extracts from unfermented and fermented samples

The antioxidant properties of the different extracts were preliminarily evaluated by the DPPH assay. In general, DMSO extracts showed more efficient antioxidant properties than the aqueous ones. As far as the effects of fermentation are concerns, the aqueous extract from fermented SCG showed a remarkable increase in the DPPH reducing ability compared to the extract from the untreated sample, whereas the effects on the DMSO extract were less evident. *A. niger* fermentation was found to be detrimental for pecan nut shell, while *S. cerevisiae* was apparently able to improve the antioxidant properties for the DMSO extract. The same applies to pomegranate waste, as evident by the lower EC_{50} values determined for the extracts prepared by the *S. cerevisiae* fermented sample (Table 3.3.2.1).

Table 3.3.2.1. Antioxidant properties of fermented and unfermented agri-food by-product extracts determined by DPPH assay. Results are expressed as EC_{50} (μL of extract/mL). Reported are the mean ± SD values of at least three experiments.

Sample	Fermented by *S. cerevisiae*	Fermented by *A. niger*	Fresh
SCG (water)	14.5 ± 0.5	18.3 ± 0.4	29.3 ± 0.6
SCG (DMSO)	5.2 ± 0.4	8.8 ± 0.6	5.7 ± 0.2
Pecan nut shell (water)	33 ± 0.2	71.4 ± 3.1	29.3 ± 0.6
Pecan nut shell (DMSO)	2.6 ± 0.1	19 ± 2	9.4 ± 0.8
Pomegranate peel and seeds (water)	0.130 ± 0.002	0.50 ± 0.02	0.19 ± 0.1
Pomegranate peel and seeds (DMSO)	0.17 ± 0.001	0.28 ± 0.01	0.36 ± 0.02

In another series of experiments, the antioxidant properties of the extracts were determined also by the FRAP assay (Table 3.3.2.2). In partial agreement with the DPPH assay results, DMSO extracts exhibited the highest reducing properties for most of the samples. In this case, the most significant effects of bioprocessing were observed for SCG and pomegranate wastes, for which fermentation with *A. niger* led to samples with antioxidant properties up to 3-fold higher in the case of the aqueous extract. Notably, fermentation of pecan nut shell with both microorganisms led to a remarkable worsening of the reducing properties, particularly evident for the DMSO extracts.

Table 3.3.2.2. Antioxidant properties of fermented and unfermented agri-food by-product extracts determined by the FRAP assay. Results are expressed as Trolox eqs (mg of Trolox/mL of extract). Reported are the mean ± SD values of at least three experiments.

Sample	Fermented by *S. cerevisiae*	Fermented by *A. niger*	Fresh
SCG (water)	1.49 ± 0.08	4.0 ± 0.1	1.43 ± 0.01
SCG (DMSO)	1.4 ± 0.1	2.32 ± 0.01	1.6 ± 0.1
Pecan nut shell (water)	0.072 ± 0.004	0.09 ± 0.01	0.104 ± 0.003
Pecan nut shell (DMSO)	0.67 ± 0.02	0.82 ± 0.07	2.7 ± 0.3
Pomegranate peel and seeds (water)	24 ± 1	60 ± 1	19.1 ± 0.3
Pomegranate peel and seeds (DMSO)	48.7 ± 0.7	110 ± 3	146 ± 3

In order to obtain information on the phenolic content responsible for the antioxidant properties observed, in a last series of experiments the total phenolic content of the

extracts was determined by the Folin-Ciocalteu assay. The results (Table 3.3.2.3) confirmed the detrimental effect of fermentation on pecan nut shell, whereas an increase in the TPC values of the DMSO extracts from *A. niger* fermented SCG and pomegranate peel and seeds was observed.

Table 3.3.2.3. Total phenolic content of fermented and unfermented agri-food by-product extracts determined by TPC assay. Results are expressed as gallic acid eqs (mg of gallic acid/mL of extract). Reported are the mean ± SD values of at least three experiments.

Sample	Fermented by *S. cerevisiae*	Fermented by *A. niger*	Fresh
SCG (water)	1.3 ± 0.1	0.72 ± 0.04	1.8 ± 0.2
SCG (DMSO)	1.88 ± 0.01	2.72 ± 0.02	1.734 ± 0.004
Pecan nut shell (water)	0.271 ± 0.004	0.18 ± 0.01	0.809 ± 0.004
Pecan nut shell (DMSO)	0.5 ± 0.1	1.34 ± 0.08	1.718 ± 0.002
Pomegranate peel and seeds (water)	35.3 ± 0.2	36 ± 4	50.4 ± 0.4
Pomegranate peel and seeds (DMSO)	39 ± 2	67 ± 5	43 ± 3

Actually, some discrepancies emerge from the data reported in Tables 3.3.2.1, 3.3.2.2, and 3.3.2.3. For instance, in the case of DPPH assay, fermentation by *S. cerevisiae* exerted a positive effect for the DMSO extract of pecan nut shell, but an opposite trend was observed in the FRAP and TPC assay. The same applies to the aqueous and DMSO extracts of pomegranate.

The lack of correlation between the results may be interpreted considering the differences in the three assays. Indeed, whereas FRAP and TPC assays monitor a pure electron transfer mechanism, DPPH may be classified as a mixed-mode assay, since the radical which may be quenched either *via* a hydrogen atom donation or by direct reduction through an electron transfer mechanism, and the steric accessibility is a major determinant of the DPPH reduction reaction. Moreover, the DPPH assay is performed in alcoholic solvents, whereas FRAP and TPC assays are carried out in acidic and alkaline aqueous media, respectively, hence solubility properties of the compounds to be tested may significantly affect the antioxidant response detected by the three assays.[211,212]

3.3.3 EA recovery from fermented pomegranate wastes

Based on the results of the HPLC analysis reported in paragraph 3.3.1, highlighting the formation of significant amounts of EA in the fermented pomegranate wastes, further experiments were directed to the recovery of this compound. EA is endowed with a plethora of health beneficial properties, including anti-mutagenic and anti-carcinogenic activity,[213] prevention of the onset of cardiovascular diseases, atherosclerosis, and dyslipidemic disorders,[214] and stimulation of wound healing and skin elasticity,[215] therefore the obtainment of EA-rich extracts from plant source represents a very active research area.

At first, pomegranate waste materials, before and after fermentation with *S. cerevisiae* and *A. niger,* were extracted with 7:3 v/v ethanol/water mixture at a 1:16 solid to liquid (s/l) ratio, using an ultrasound microwave system. HPLC analysis of the extracts evidenced an EA content of 4.8 ± 0.6 mg/g (w/w with respect to the starting material) for the unfermented sample. On the other hand, values of 9.0 ± 0.3 mg/g and 46 ± 3 mg/g were found for *A. niger* and *S. cerevisiae* fermented materials, respectively.

To get an insight into the effects of fermentation on the ellagitannins present in the pomegranate wastes under the two conditions investigated, the extracts were subjected to qualitative LC-MS analysis. As expected, punicalagin α and β were found to be the main phenolic components in the fresh sample, together with punicalin β and granatin in lower amounts. As expected, fermentation induced a remarkable consumption of punicalagin and granatin, particularly evident in the *S. cerevisiae* treated sample, coupled to an increase in EA and especially punicalin α (Figure 3.3.3.1).

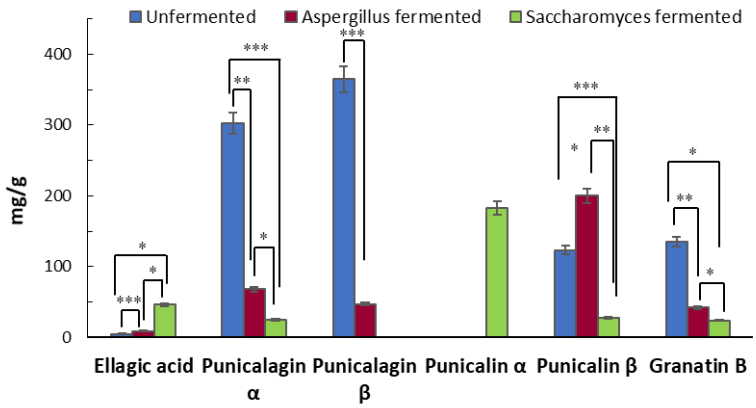

Figure 3.3.3.1. Quantitative analysis of the main ellagitannins identified in the pomegranate waste extracts. Statistical analysis is shown on the bars: * $p < 0.05$; ** $p < 0.01$; *** $p < 0.005$.

Indeed, it is known that hydrolytic cleavage of punicalagin leads to punicalin and hexahydroxydiphenic acid, which is then converted to EA by spontaneous lactonization. The same has been reported for granatin (Scheme 3.3.3.1).

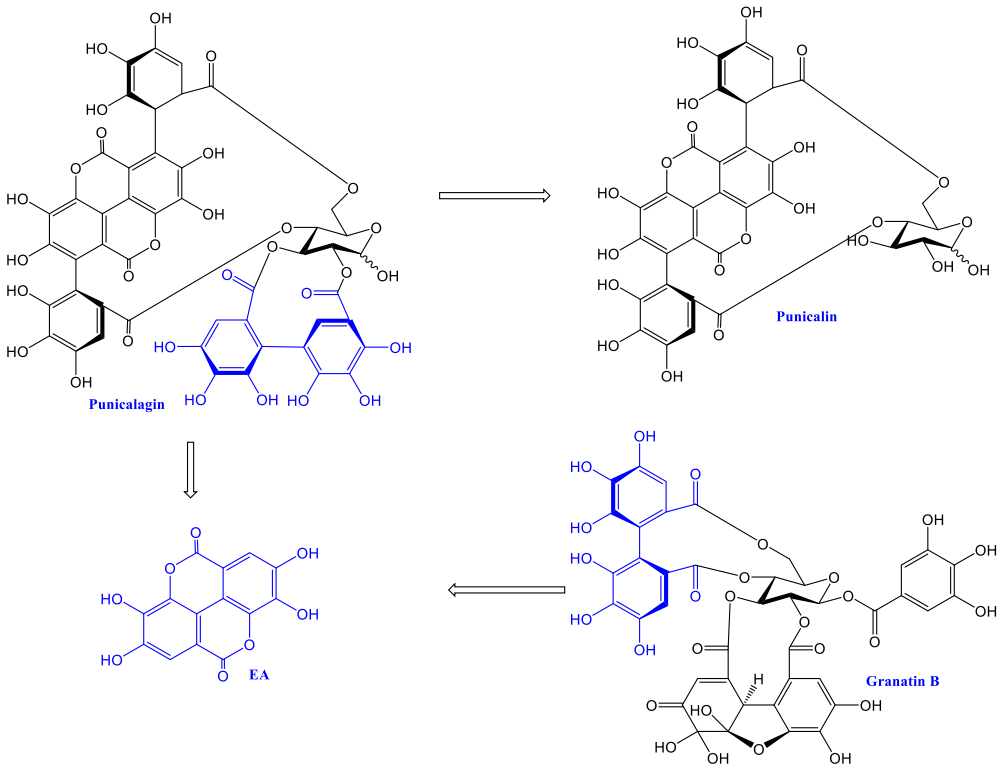

Scheme 3.3.3.1. Structures of the main ellagitannins identified in pomegranate waste extracts and proposed formation pathways of EA.

Based on these data, in further experiments different extraction conditions were investigated on *S. cerevisiae* fermented sample in order to optimize the recovery yields of EA. DMSO was chosen as the extraction solvent due to the relative high solubility of EA in this medium. Using a s/l ratio of 1:10 g/mL under stirring for 1 h, a yield of 21.0 ± 1.2 mg/g yield was obtained. Reiteration of the extraction process up to three times provided an overall yield of 30 ± 1 mg/g. Use of a 1:100 g/mL s/l ratio resulted in an increase of the recovery yield to 40.0 ± 0.2 mg/g, that is a 4% w/w yield, which was comparable to that obtained with the ultrasound microwave assisted extraction described above. Actually, the employment of this methodology was found to be crucial if an ethanol/water mixture is used as the extraction solvent,

since under normal stirring conditions at room temperature the EA extraction yield was only 2 mg/g (0.2% w/w).

A very "clean" elutographic profile was obtained by HPLC analysis of the DMSO extract, showing EA as the sole component (Figure 3.3.3.2).

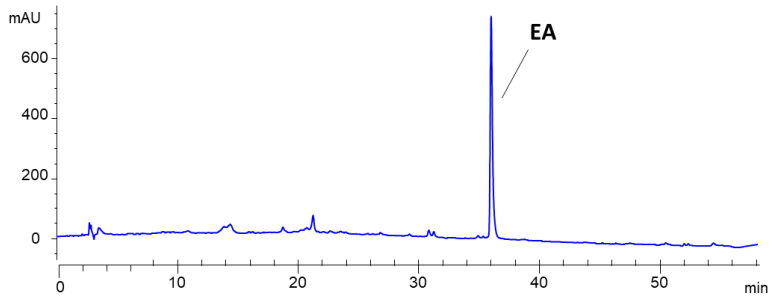

Figure 3.3.3.2. HPLC elution profile of the DMSO extract (1:20 dilution in methanol) of *S. cerevisiae* fermented pomegranate wastes.

3.4 Conclusions

In this Chapter, the changes induced by fermentation processes on the phenolic composition and antioxidant properties of selected agri-food by-products have been reported. In particular, waste materials resulting from the production of distillates from spontaneously fermented quince, Cilento fig, nectarine peaches and strawberries were investigated, together with pecan nut shell, SCG and pomegranate peel and seeds subjected to solid state fermentation with *S. cerevisiae* and *A. niger*.

HPLC analysis of different extracts of the fermented and corresponding unfermented materials highlighted the occurrence of significant structural modifications induced by the microorganisms on the phenolic compounds in most samples, leading in some cases to the formation of compounds endowed with biological properties, in relative high yields. These results open, therefore, new perspectives for the possible valorization of these materials as a source of bioactive compounds, to be used, for example, in the nutraceutical and cosmeceutical sectors.

3.5 Experimental section

Materials and methods

Quince, Cilento fig, nectarine peach and strawberry distillation residues were provided by Berolà (Portico di Caserta, Caserta), together with the corresponding fresh fruits not subjected to fermentation, and stored at -25 ° C. *A. niger* and *S. cerevisiae* fermented materials, together with the corresponding starting agri-food wastes, were provided by Prof. Cristobal N. Aguilar (Bioprocesses and Bioproducts Research Group, Food Research Department, School of Chemistry, Universidad Autónoma de Coahuila, Mexico) and stored at -25 °C.

All solvents and reagents were obtained from commercial sources and used without further purification.

UV-Vis spectra were recorded on a HewlettPackard8453 Agilent spectrophotometer.

HPLC analysis were performed on an instrument equipped with an Agilent G1314A UV-Vis detector, using a Phenomenex Sphereclone ODS column (250 × 4.60 mm, 5 μm) at a flow rate of 1.0 mL/min; the gradient elution was as follows:

- 0.1% formic acid (solvent A)/methanol (solvent B): 5% B, 0-10 min; from 5 to 80% B, 10-47.5 min; the detection wavelength was set at 254 nm (eluant I).

- 0.2% formic acid (solvent A) /methanol (solvent B): 5% B (0-10 min), from 5 to 15% B (10-50 min), 15% B (50-70 min), from 15 to 60% B (70-90 min); the detection wavelengths were set at: 254, 280, 320 e 400 nm (eluant II).

LC-MS analysis were performed in positive ionization mode on an Agilent LC-MS ESI-TOF 1260/6230DA instrument with the following parameters: nebulizer pressure 35 psig; drying gas (nitrogen) 5 L/min, 325 °C; capillary voltage 3500 V; fragmentor voltage 175 V. An Eclipse Plus C18 column (150 × 4.6 mm, 5 μm) was used with the same mobile phases as above, at a flow rate of 0.4 mL/min.

3.5.1 Preparation of extracts from fresh and fermented by-products. After thawing and grinding, 0.3 g of each sample was kept under vigorous magnetic stirring in 3 mL of distilled water, ethanol, methanol or DMSO. After 1 h the mixtures were centrifuged (7000 rpm, 20 min) and the supernatants stored at -25 ° C until further HPLC analysis, using eluant I for *A. niger* and *S. cerevisiae* fermented materials, and both eluant for distillation residues.

In the case of pomegranate peel and seeds, the fresh and fermented materials were also extracted with ethanol/water (7:3 v/v) using a 1:16 (g/mL) s/l ratio. An ultrasound and microwave-assisted extraction was performed using a hybrid technology system Ultrasound/Microwave Cooperative Workstation (Nanjing ATPIO Instruments Manufacture, Nanjing, China). Ultrasound time was set at 20 min (25 KHz) and microwave frequency was set at 2450 MHz (70 ◦C). In other experiments, different extraction procedures were carried out using ethanol, water, or DMSO as solvent at a 1:10 g/mL or 1:100 g/mL ratio. When required, the extraction was repeated three times and the concentration of EA in the combined extracts was determined by HPLC analysis, using eluant I.

3.5.2 Antioxidant assays. DPPH assay:[175,176] To a 0.2 mM ethanolic solution of DPPH, 2-90 µL of extracts from fresh and fermented materials were added, and after 10 min under stirring at room temperature the absorbance of the solution at 515 nm was measured. Trolox was used as a reference antioxidant. Experiments were run in triplicate. **FRAP assay:**[177] To 0.3 M acetate buffer (pH 3.6) containing 1.7 mM FeCl3 and 0.83 mM TPTZ, extracts from fresh and fermented materials (0.02–90 µL) were added, and after 10 min under stirring at room temperature the absorbance of the solution at 593 nm was measured. Results were expressed as Trolox eqs. Experiments were run in triplicate.

3.5.3 TPC assay.[178] Extracts from fresh and fermented materials (0.2–150 µL) were added to a solution consisting of Folin-Ciocalteu reagent, 75 g/L Na_2CO_3, and water in a 1:3:14 v/v/v ratio. After 30 min incubation at 40 ◦C, the absorbance at 765 nm

was measured. Gallic acid was used as reference compound. Experiments were run in triplicate.

Chapter 4

Exploitation of tannins and by-products from tannin industry as functional materials

4.1 Introduction

Tannins are widely distributed in the plant kingdom, and among these compounds, wood tannins, in particular hydrolyzable and condensed tannins obtained from *Castanea sativa* (chestnut) and *Shinopsis lorentzii* (quebracho) wood, respectively, are among the most available worldwide.

As widely mentioned in the Introduction, tannins are currently used in food industry as additives in wine, as food supplements, and in animal feeds due to their biologically relevant properties.[20]

Wood tannins, in particular, have recently described as interesting alternatives to synthetic adhesives in wood industry.[67,69,70] Wood protection properties of tannins, alone or in combination with eco-friendly additives, have been also investigated,[67,72–76] while different studies have evaluated the possibility to use a combination of tannins and furfuryl alcohol for the creation of almost totally biosourced foams and resins.[67] Both hydrolysable and condensed tannins are also able to act as corrosion inhibitors for metals.[67,69,78–80]

In addition, several papers have reported the use of wood tannins for the production of functional films and coatings for a wide range of applications.[81–85] As an example, condensed tannins extracted from radiata pine bark have been assessed as functional additives in acrylic-based resins, providing materials with a high photo-oxidative stability,[216,217] whereas black wattle tannins incorporated at concentrations of 5% and 10% into a novolac resin and then coated on a steel plate provided a significant thermal protection when exposed to a flame.[218]

Tannin extraction from wood, generally performed in hot water, generates high volume of residual biomasses, known as exhausted woods, commonly used in the production of pellets for heating and energy production. Despite the large availability of these wood by-products, their possible exploitation as antioxidant materials has still remained rather unexplored.

In this context, this Chapter is focused on experiments concerning the possible use of hydrolyzable and condensed tannins, hereinafter indicated as CT and QT (chestnut and quebracho tannins, respectively), for the implementation of antioxidant coatings. Furthermore, the antioxidant and functional properties of exhausted woods from tannin industry will be reported. Finally, formulations for dermocosmetic applications incorporating exhausted chestnut wood mud (CWM) were investigated.

This part of the PhD project was carried out in collaboration with "Centro Ricerche per la Chimica Fine S.r.l." of Silvateam S.p.a. (San Michele Mondovì, Cuneo, Italy), who provided tannins, fresh and exhausted woods, and CWM.

4.2 Wood tannin-based antioxidant coatings

Coating represents a promising technology for material functionalization. Although films and coatings are often used as synonyms, they refer to different concepts, purpose, and utilization. Film is a thin layer of a matrix, in which different additives, such as antioxidant compounds, can be incorporated. On the other hand, coatings involve the formation of a film of a specific additive directly on the surface of the matrix without direct incorporation.[219,220] As in the case of functional films, a wide number of antimicrobial and antioxidant compounds can be used.[221] Among these, tannins occupy a prominent role due not only to their remarkable bioactivities, but also to their intrinsic ability to produce functional coatings on a variety of materials. However, a comparative investigation between hydrolyzable and condensed wood

tannins for the implementation of a functional antioxidant coating is still lacking in the literature.

Herein, a simple and versatile dip-coating methodology for the functionalization of nylon filter is reported, involving immersion of the substrate into a tannin solution at room temperature, for 2 h (Figure 4.2.1). The choice of nylon membrane filters as substrates was based on the remarkable affinity of tannins toward polyacrylamide, and on the homogeneous and uniform surface, which make them particularly suitable for coating applications.[222]

In order to find the best conditions for functionalization, different coating conditions, in term of tannin concentrations, use of oxidizing conditions and of metal ions, were investigated. At first, aqueous solution of tannins at different concentrations (0.02, 0.1, and 0.5 mg/mL) were employed. Then, the use of oxidizing conditions was investigated using two different oxidizing systems, that is the enzyme laccase (in water or in phosphate buffer at pH 6.0) and air in 0.05 M carbonate buffer at pH 9.0, which is the medium widely reported in literature for the preparation of polydopamine coatings.[223,224] Finally, the use of iron ions to improve coating formation[225] was evaluated. Indeed, iron(II) ions are commonly employed as in the widespread used iron gall ink and iron-polyphenol coordination has been emerging as a highly promising tool for design and synthesis of functional materials.[226]

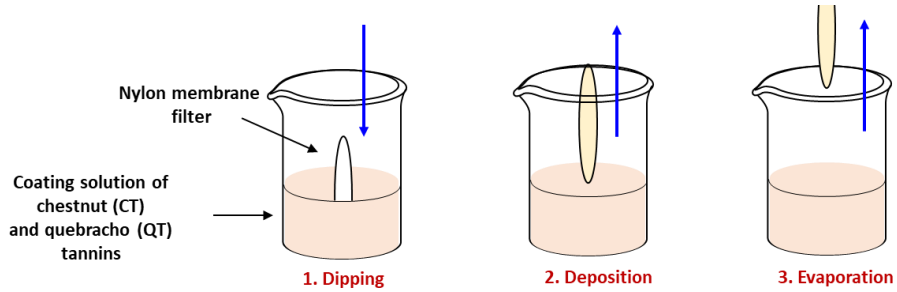

Figure 4.2.1. Schematic representation of the dip coating procedure.

The functionalized nylon filters showed varying colors depending on the kind of tannin and on the coating conditions (Figure 4.2.2).

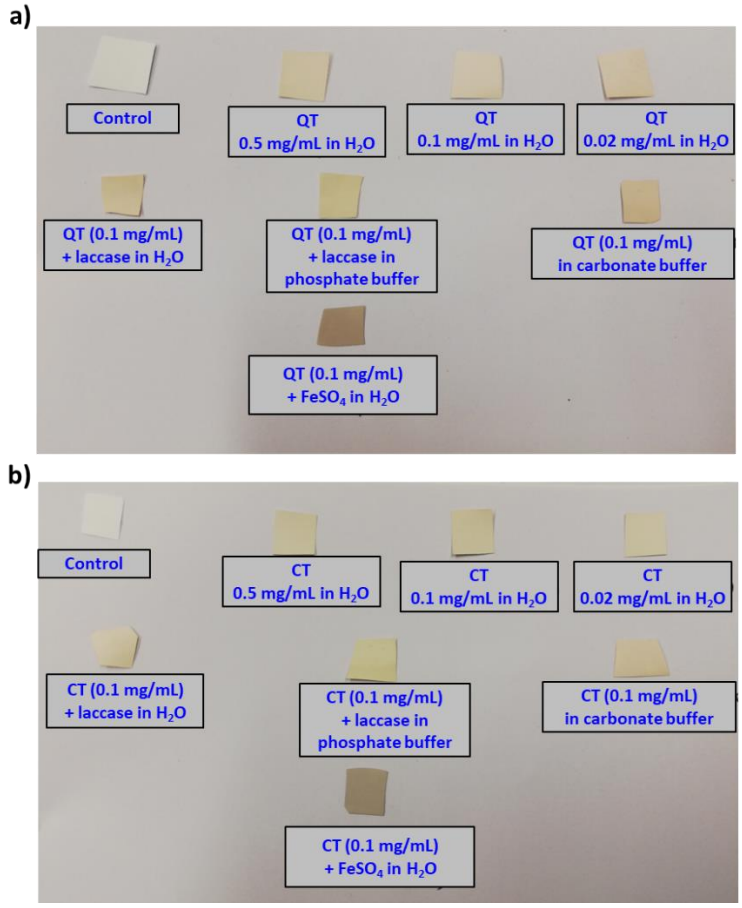

Figure 4.2.2. Nylon membrane filters coated with (a) quebracho tannins (QT) and chestnut tannins (CT).

4.2.1 UV-Vis analysis of the coating solutions

To gain information on the chemical modifications occurring on CT and QT under the different dip coating conditions the UV-Vis spectra of the different solutions were recorded at the beginning and the end of the dip coating procedure. UV-Vis spectra of the starting tannin aqueous solutions showed absorption maxima at 280

nm for QT and at ca. 270 nm for CT. After 2 h, spectra exhibited a very similar shape but a significant decrease in absorbance, which however was not detected in the absence of the nylon filter, demonstrating the occurring of an efficient coating without significant structural modifications of the phenolic compounds (Figure 4.2.1.1a,b). UV-Vis analysis of the solutions prepared using oxidizing agents, recorded at 2 h, showed the development of a chromophore in the visible region for both tannins, probably due to the formation of oxidation products. Different chromophoric species were instead detected in the presence of iron ions, as particularly evident in the case of CT (Figure 4.2.1.1c,d).

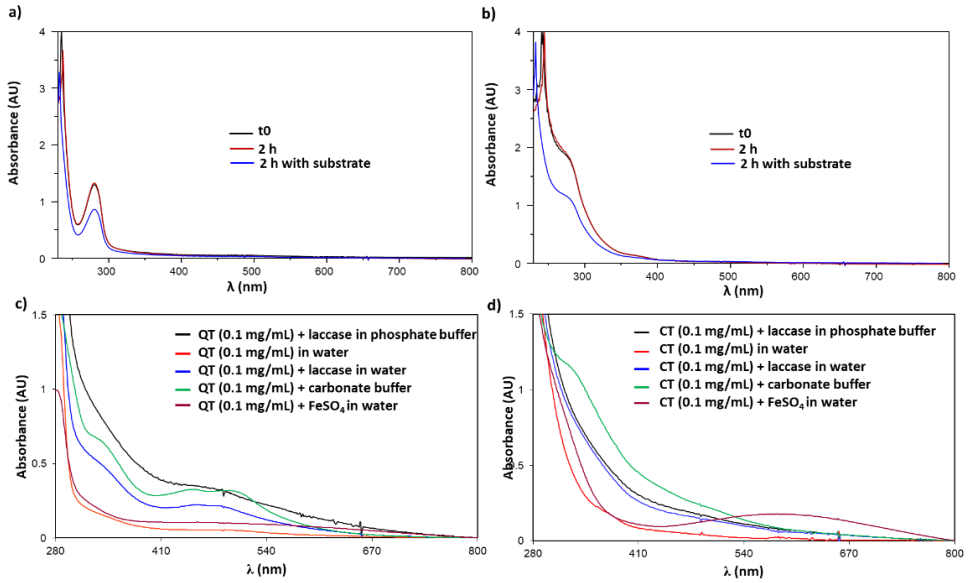

Figure 4.2.1.1. UV-Vis spectra of (a) QT and (b) CT aqueous solutions before and after addition of the nylon filter and UV-Vis spectra of the different dip coating solutions of (c) QT and (d) CT at 2 h.

The amounts of tannins adhered to the nylon membrane filter under the different coating conditions were also evaluated and the results are reported in Table 4.2.1.1. The highest amounts of deposited tannins were achieved with the 0.5 mg/mL solutions. On the other hand, the use of oxidizing conditions, particularly alkaline

carbonate buffer, led to deposition of lower amounts of material, while in the presence of iron ions the turbidity of the solutions did not allow determination of deposited tannin amount.

Table 4.2.1.1. Amounts of tannin adhered to the nylon membrane filter under the different coating conditions. Reported are the mean ± SD values of at least three experiments.

Sample	mg of tannins adsorbed/mg sample (after 2 h)
QT (0.5 mg/mL) in H_2O	0.28 ± 0.01
QT (0.1 mg/mL) in H_2O	0.031 ± 0.001
QT (0.02 mg/mL) in H_2O	0.0061 ± 0.0003
QT (0.1 mg/mL) + laccase in H_2O	0.031 ± 0.002
QT (0.1 mg/mL) + laccase in phosphate buffer pH 6.0	0.021 0.001
QT (0.1 mg/mL) in carbonate buffer pH 9.0	0.021 ± 0.001
CT (0.5 mg/mL) in H_2O	0.26 ± 0.01
CT (0.1 mg/mL) in H_2O	0.042 ± 0.002
CT (0.02 mg/mL) in H_2O	0.041 ± 0.002
CT (0.1 mg/mL) + laccase in H_2O	0.041 ± 0.002
CT (0.1 mg/mL) + laccase in phosphate buffer pH 6.0	0.032 ± 0.002
CT (0.1 mg/mL) in carbonate buffer pH 9.0	0.011 ± 0.001

4.2.2 Evaluation of the antioxidant properties of the tannin-coated substrates

The antioxidant properties of the coated substrates were initially evaluated by the DPPH assay. The percentage of DPPH reduction was evaluated at 10 min and 2.5 h and, as evident from Table 4.2.2.1, a progressive increase in DPPH reduction was observed over time. Generally, higher DPPH reducing properties were determined for QT-coated membrane filters under the different conditions, with respect to CT-coated substrates. Notably, these data are in disagreement with the DPPH reducing ability of CT and QT, since the first exhibit more efficient antioxidant properties, as demonstrated in the Chapter 2.

Solutions of tannins at higher concentrations provided materials endowed with higher DPPH reducing activity, in line with the amounts of adhered tannins (Table 4.2.1.1). As expected, oxidizing conditions provided substrates with lower reducing capacities, particularly in the case of CT. On the other hand, the presence of iron ions had a positive effect on the CT-coated membranes.

Table 4.2.2.1. DPPH reduction at different times by the tannin-coated nylon membrane filters. Reported are the mean ± SD values of at least three experiments.

Sample	DPPH reduced (%) (after 10 min)	DPPH reduced (%) (after 2.5 h)
QT (0.5 mg/mL) in H_2O	85 ± 6	81 ± 3
QT (0.1 mg/mL) in H_2O	83 ± 4	81 ± 2
QT (0.02 mg/mL) in H_2O	56 ± 3	83 ± 4
QT (0.1 mg/mL) + laccase in H_2O	79 ± 4	84 ± 5
QT (0.1 mg/mL) + laccase in phosphate buffer (pH 6.0)	61 ± 3	85 ± 6
QT (0.1 mg/mL) in carbonate buffer (pH 9.0)	41 ± 2	67 ± 4
QT (0.1 mg/mL) + $FeSO_4$ in H_2O	76 ± 4	86 ± 6
CT (0.5 mg/mL) in H_2O	56 ± 3	86 ± 6
CT (0.1 mg/mL) in H_2O	23 ± 1	75 ± 3
CT (0.02 mg/mL) in H_2O	28 ± 1	56 ± 3
CT (0.1 mg/mL) + laccase in H_2O	25 ± 1	61 ± 3
CT (0.1 mg/mL) + laccase in phosphate buffer (pH 6.0)	25 ± 1	65 ± 4
CT (0.1 mg/mL) in carbonate buffer (pH 9.0)	7 ± 1	33 ± 2
CT (0.1 mg/mL) + $FeSO_4$ in H_2O	40 ± 2	82 ± 4

In another series of experiments, in order to understand if the antioxidant activity was due to the release of tannins in solution, washing experiments were carried out in ethanol, under the same conditions used in the DPPH assay. The UV-Vis spectra of the solutions recorded after 2.5 h indicated a release of variable amounts of

tannins depending on the coating conditions, without qualitative differences among the solubilized species (Figure 4.2.2.1).

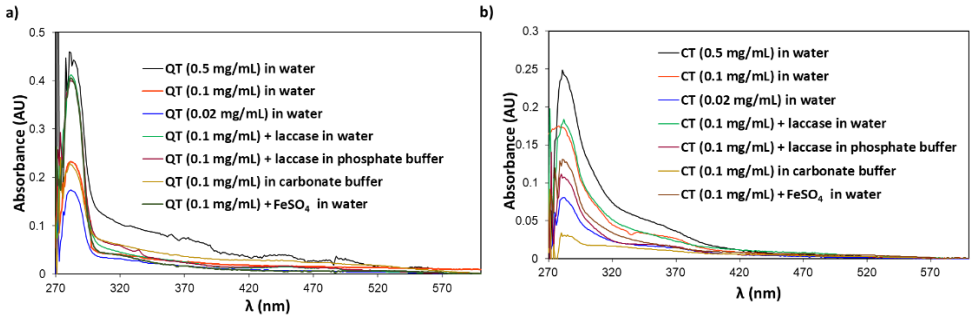

Figure 4.2.2.1. UV-Vis spectra of released (a) QT and (b) CT, after washing in ethanol for 2.5 h.

Therefore, in subsequent experiments the DPPH assay was repeated on the coated filters after washing with ethanol, showing indeed lower antioxidant capacities by the washed substrates, particularly in the case of coatings carried out in water. However, a relatively high antioxidant activity was still retained, particularly in the case of QT-coated filters. When oxidizing conditions (laccase or alkaline pH) were employed, the coatings were found to be more robust, especially in the case of QT, since washing showed less significant effects (Figure 4.2.2.2).

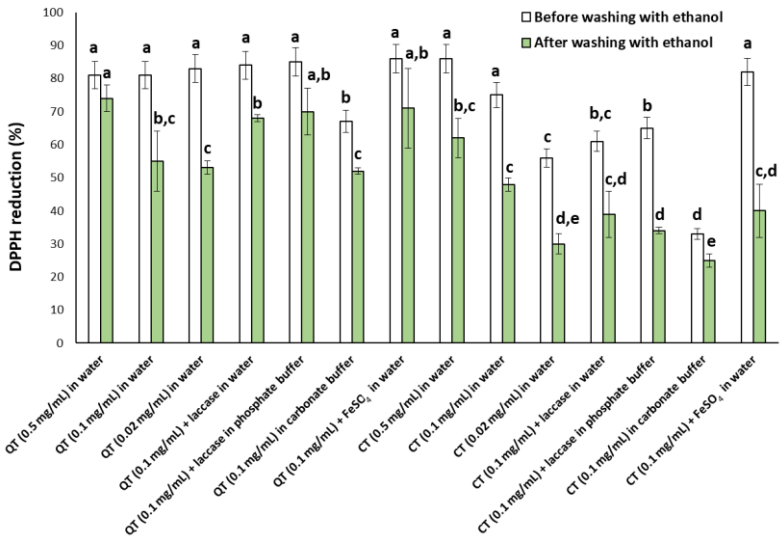

Figure 4.2.2.2. DPPH reduction at 2.5 h before and after washing of the coated substrates with ethanol. Values without a common letter are significantly different ($p < 0.05$).

Finally, the antioxidant properties of the coated nylon membrane filters were evaluated by the FRAP assay. The experiments were performed directly on filters preliminarily washed with the assay medium, although in this case no significant release of the coating tannins was observed. The Trolox eqs determined for each coated substrate are reported in Table 4.2.2.2 and Figure 4.2.2.3. Compared to the DPPH assay, the differences between the CT- and QT-functionalized substrates were less significant.

Table 4.2.2.2 Trolox eqs determined at different times for the tannin-coated nylon membrane filters in the FRAP assay. Reported are the mean ± SD values of at least three experiments.

Sample	nmol Trolox/mg filter (after 10 min)	nmol Trolox/mg filter (after 2.5 h)
QT (0.5 mg/mL) in H_2O	6.9 ± 0.7	32 ± 3
QT (0.1 mg/mL) in H_2O	5.8 ± 0.6	29 ± 3
QT (0.02 mg/mL) in H_2O	5.5 ± 0.5	25 ± 2
QT (0.1 mg/mL) + laccase in H_2O	4.8 ± 0.5	26 ± 3
QT (0.1 mg/mL) + laccase in phosphate buffer (pH 6.0)	11 ± 1	26 ± 3
QT (0.1 mg/mL) in carbonate buffer (pH 9.0)	5.2 ± 0.5	25 ± 2
QT (0.1 mg/mL) + $FeSO_4$ in H_2O	5.8 ± 0.6	28 ± 3
CT (0.5 mg/mL) in H_2O	10 ± 1	35 ± 4
CT (0.1 mg/mL) in H_2O	9 ± 1	33 ± 3
CT (0.02 mg/mL) in H_2O	6.1 ±0.7	22 ± 2
CT (0.1 mg/mL) + laccase in H_2O	4.9 ± 0.5	25 ± 3
CT (0.1 mg/mL) + laccase in phosphate buffer (pH 6.0)	4.2 ± 0.4	21 ± 2
CT (0.1 mg/mL) in carbonate buffer (pH 9.0)	3.1 ±0.3	12 ± 1
CT (0.1 mg/mL) + $FeSO_4$ in H_2O	5.9 ±0.6	26 ± 3

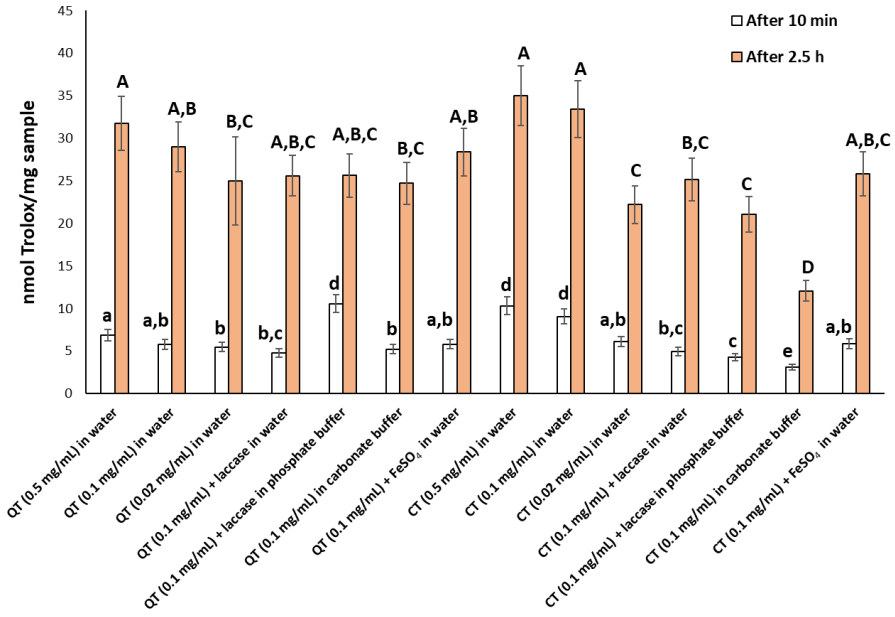

Figure 4.2.2.3 Trolox eqs determined at 10 min and 2.5 h for the tannin-coated nylon membrane filters in the FRAP assay. Reported are the mean ± SD values of at least three experiments. Values in a series without common letters are significantly different ($p < 0.05$).

4.2.3 Assessment of tannin structural modifications under the dip coating conditions by UV-Vis analysis

With the aim to better understand the chemical modifications occurring on tannins during the coating process, a series of additives were added to the solutions at 2 h reaction time before UV-Vis analysis. When oxidizing conditions were employed, the addition of reducing agents, such as sodium borohydride, caused the disappearance of the visible chromophore (Figure 4.2.3.1a-d), demonstrating the formation of oxidation products under these conditions. On the other hand, the visible chromophore generated in the presence of iron ions was not affected by the addition of sodium borohydride (Figure 4.2.3.1e,f) and was probably due to the formation of a stable tannin/iron complex, as demonstrated by the slightly loss of the chromophore even after addition of the strong chelating agent EDTA. To what

extent the chemical transformations observed are relevant to the different antioxidant properties exhibited by the tannin-coated nylon filters is an issue that will be defined in future studies.

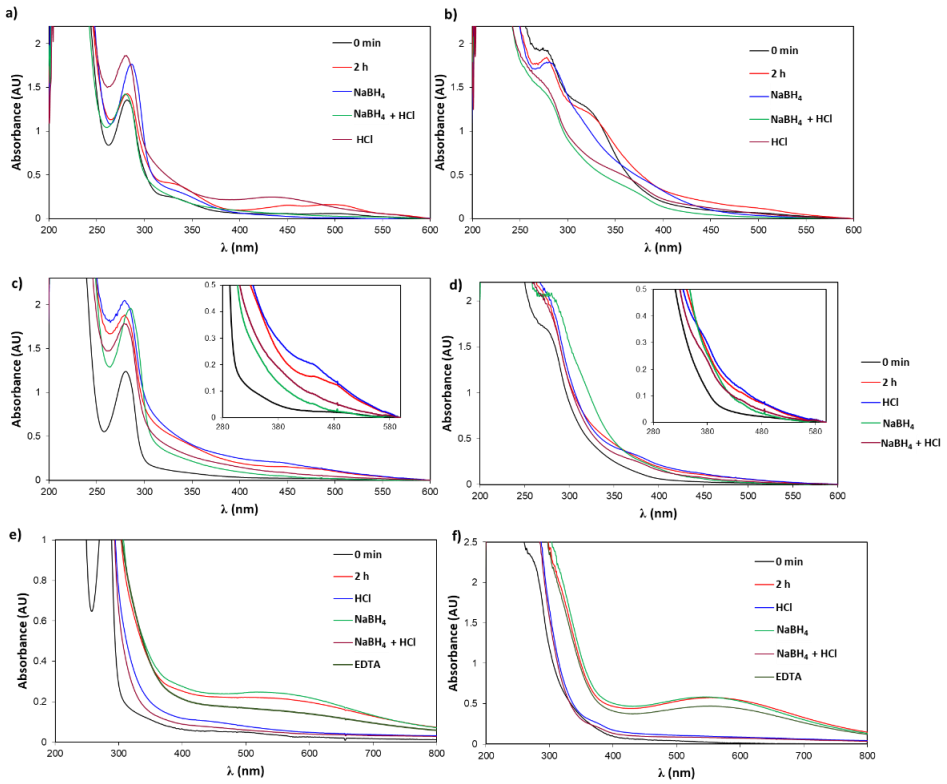

Figure 4.2.3.1. UV-Vis spectra before and after addition of different additives to (a) QT and (b) CT solutions in 0.1 M carbonate buffer (pH 9.0); (c) QT and (d) CT solutions in 0.05 M phosphate buffer (pH 6.0) containing laccase and (e) QT and (f) CT solutions in water containing $FeSO_4$.

4.3 Characterization of the functional properties of exhausted woods

4.3.1 Antioxidant properties

The exhausted biomasses generated during the tannin industrial extraction were initially evaluated in term of antioxidant properties, in comparison with fresh woods and tannins.

As reported in Table 4.3.1.1, the lowest DPPH-reducing properties among the waste materials were exhibited by chestnut wood fiber (CWF), produced from steamed exhausted chestnut wood, with an EC_{50} value of 0.054 mg/mL. Quebracho and chestnut exhausted wood also exhibited EC_{50} values lower than those reported for other agri-food by-products (see Chapter 2). Of course, as expected, more efficient antioxidant properties were exhibited by tannins and fresh wood samples, still containing the active molecules.

FRAP assay (Table 4.3.1.1) showed less encouraging results than the DPPH assay, probably due to the lower solubility of the samples in the aqueous medium used for the FRAP assay, with only chestnut tannins showing a satisfactory reducing power.

The Folin-Ciocalteu assay allowed to determine, as expected, a TPC value particularly high only for pure quebracho and chestnut tannins, although CWF showed a TPC value comparable to those obtained for fresh chestnut wood and remarkable higher than those measured for exhausted woods.

As previously mentioned, the antioxidant assays were performed on solid samples, therefore, differences in the antioxidant properties may be likely interpreted considering the different solubility of the sample in the assay media.

Table 4.3.1.1. Antioxidant properties and TPC values of exhausted and fresh woods. Reported are the mean ± SD values of at least three experiments.

Sample	EC_{50} (mg/mL) (DPPH assay)	Trolox Eqs (FRAP assay)	mg of gallic acid/g of sample (Folin-Ciocalteu assay)
CWF	0.054 ± 0.003	0.17 ± 0.01	151 ± 17
Exhausted chestnut wood	0.436 ± 0.003	0.06 ± 0.01	51 ± 3
Fresh chestnut wood	0.128 ± 0.003	0.19 ± 0.01	153 ± 9
CT	0.019 ± 0.002	1.2 ± 0.1	457 ± 59
Exhausted quebracho wood	1.14 ± 0.04	0.051 ± 0.005	40 ± 1
Fresh quebracho wood	0.099 ± 0.001	0.08 ± 0.01	194 ± 8
QT	0.026 ± 0.002	0.47 ± 0.03	550 ± 99

The different wood samples were characterized also for their ability to act as superoxide scavengers. Tannins and fresh woods showed the highest trapping ability. Despite CWF and exhausted chestnut woods were found to be characterized by different phenolic content (Table 4.3.1.1), they exhibited a scavenging activity very similar and almost comparable to that of the fresh samples (Figure 4.3.1.1), confirming the complex mechanisms of scavenging assays which did not allow the correlation between antioxidant and trapping properties.

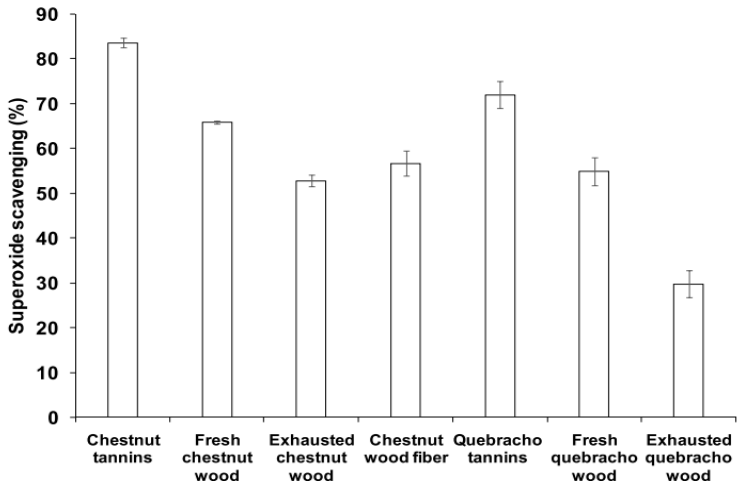

Figure 4.3.1.1. Superoxide scavenging activity of tannins and fresh and exhausted woods. Reported are the mean ± SD values of at least three experiments.

4.3.2 Effects of the acid hydrolytic treatment on exhausted woods

In a second series of experiments, exhausted woods were subjected to the hydrolytic treatment described in Chapter 2, and then evaluated for their antioxidant properties by the DPPH and FRAP assays. Only CWF showed a 2-fold increase in Trolox eqs after hydrolysis, whereas no significant changes in the Fe^{3+}-reducing properties was observed for exhausted chestnut and quebracho woods (Figure 4.3.2.1). On the other hand, the hydrolytic processing led to an activation of all the samples in the DPPH assay (Figure 4.3.2.1a).

No significant improvement in the scavenging ability was detected in exhausted woods subjected to the hydrolytic treatment (data not shown).

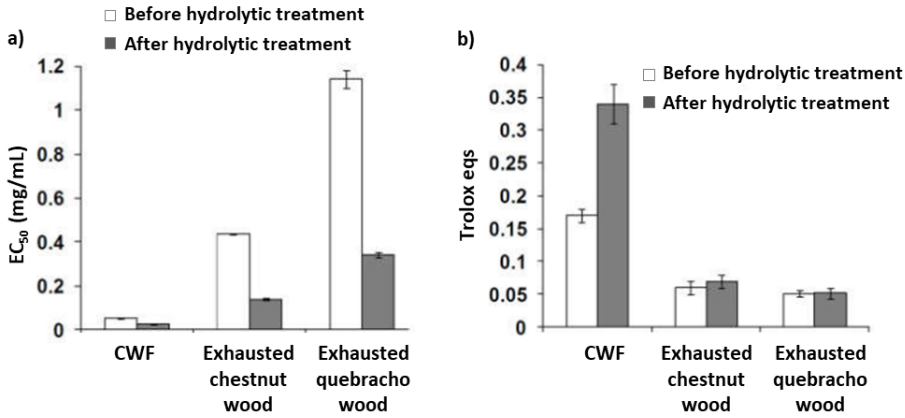

Figure 4.3.2.1. Antioxidant properties of exhausted wood samples, before and after acid hydrolytic treatment. (a) DPPH assay; (b) FRAP assay. Reported are the mean ± SD values of at least three experiments.

To obtain information on the structural modification induced by the acid treatment, the wood by-products before and after hydrolysis were extracted in DMSO and the obtained solutions analyzed by UV-Vis spectroscopy and HPLC after proper dilution in methanol. After hydrolysis, an increase in the absorption was observed in CWF and exhausted chestnut wood, in agreement with what reported for the

hydrolyzable tannins CT in Chapter 2 (Figure 2.3.2.1.2a). On the other hand, in the case of exhausted quebracho wood, the acid treatment did not influence the UV-Vis properties of the DMSO-extractable fraction (Figure 4.3.2.2).

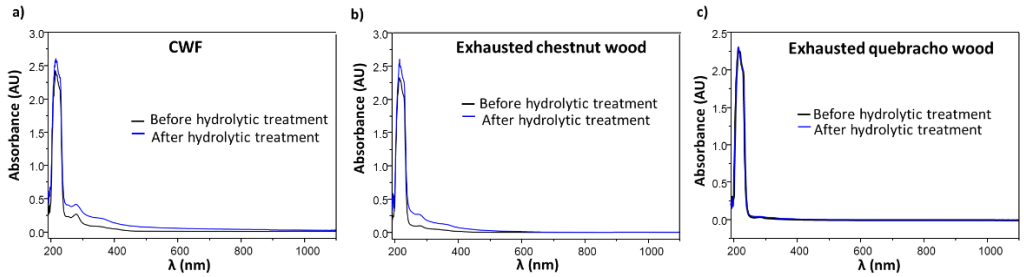

Figure 4.3.2.2. UV-Vis spectra of the DMSO-soluble fractions of wood by-products, before and after hydrolytic treatment.

In Figure 4.3.2.3 the HPLC profile of the DMSO soluble fraction of CWF is reported. After hydrolysis, an increase in the amount of EA was observed, in agreement again with data reported for CT and pomegranate waste (Figure 2.3.2.1.2b and Figure 2.3.2.1.3). Less significant results were obtained from exhausted woods (not shown).

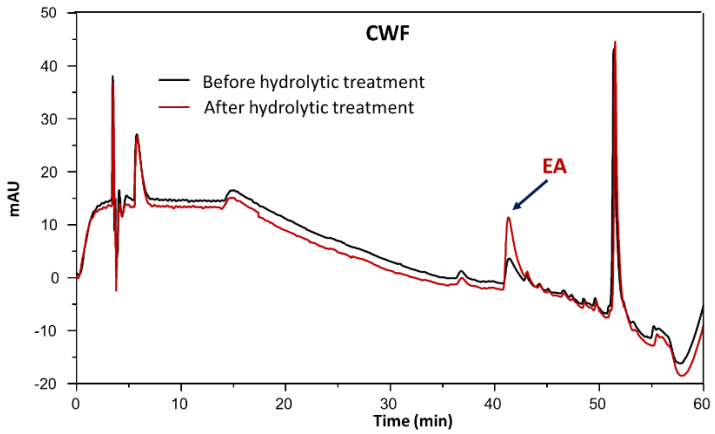

Figure 4.3.2.3. HPLC profiles of the DMSO-soluble fractions of CWF before and after hydrolytic activation.

4.3.3 Pollutant adsorption properties of exhausted woods

Forest industry waste materials have been recently studied as dye and heavy metals adsorbents. These materials are available in large quantities and due to their low-cost and physico-chemical features, can be used as sorbents. Wood derived by-products contain various organic compounds, among which lignin, in particular, has been reported to be able to bind dyes and metals through different mechanisms.[227–229] Therefore, in a further series of experiments the adsorption capacity of the exhausted woods was evaluated against methylene blue (MB), as a model organic dye, nitric oxide (NO) and nitrogen dioxide (NO_2), that is pollutants commonly found in smoke and exhaust gases, and cadmium ions (Cd^{2+}), as a model of toxic heavy metals.

As shown in Table 4.3.3.1, when a 5 mg/L solution of dye was used, CWF was able to totally adsorb MB. Good results were obtained also for both exhausted chestnut and quebracho woods, that showed adsorption properties very similar to those observed with the fresh wood samples. Increasing the concentration of MB up to 25 mg/L, a 20%–30% dye removal was still observed. Experiments carried out on hydrolyzed samples did not show significant increase in the adsorption properties (Figure 4.3.3.1a).

Table 4.3.3.1. Pollutant adsorption properties of exhausted woods. Reported are the mean ± SD values of at least three experiments.

Sample	MB adsorption (%)	NO_x scavenging (%)
CWF	100	32 ± 5
Exhausted chestnut wood	73 ± 3	23 ± 1
Fresh chestnut wood	79 ± 1	38 ± 1
Exhausted quebracho wood	77 ± 1	79 ± 1
Fresh quebracho wood	77 ± 2	86 ± 5

Notably, UV-Vis analysis of the samples at the concentration used in the assay (0.2 mg/mL) and in the assay medium (water), showed a very low solubility of CWF and

exhausted woods, a promising feature for the exploitation of these materials for wastewater purification (Figure 4.3.3.1b).

The samples were also characterized for their capability to act as NO_x scavenger: notably, exhausted quebracho wood was found to be able to exert a ca. 80% scavenging, a value significantly higher than that observed for chestnut woods. This is likely the result of the higher trapping efficiency toward nitric oxides of condensed tannins with respect to hydrolyzable tannins, ascribable to presence of the nucleophile resorcinol moiety.[230] In any case, exhausted woods were only slightly less potent than fresh woods as NOx scavengers, pointing to components other than low molecular weight tannins as major determinants of this property.

Finally, the ability of the different wood samples to remove heavy metals from aqueous solutions was investigated using Cd^{2+} as model ions. As shown in Figure 4.3.3.1c, CWF was the most active among the waste materials, and an increase in heavy metal removal capacity was observed after the acid hydrolytic treatment for all the samples examined.

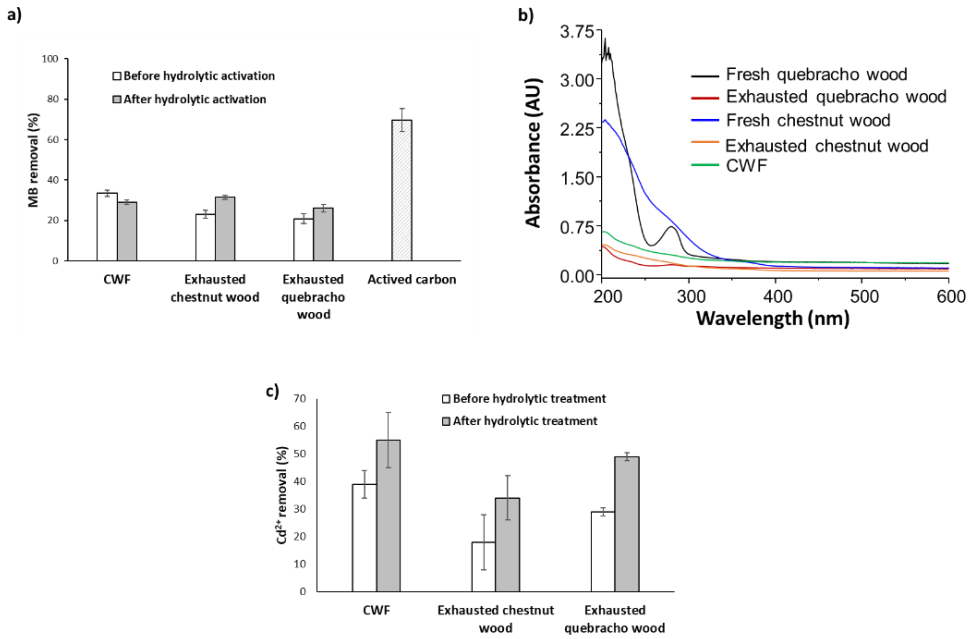

Figure 4.3.3.1. (a) MB adsorption properties of exhausted woods, before and after hydrolytic treatment (25 mg/L MB starting concentration). (b) UV-Vis spectra of wood samples in water (0.2 mg/mL). (c) Cd^{2+} removal capability of exhausted woods before and after hydrolytic treatment.

4.4 CWM as source of EA for dermocosmetic applications

Chestnut wood mud (CWM) represents another important tannin industry by-product, deriving from exhausted chestnut wood further to a natural fermentation process. This material contains high amounts of EA as the results of hydrolytic processes occurring on residual ellagitannins which are not recovered during the tannin extraction process in hot water, and could therefore represent a valuable source of this polyphenol endowed with remarkable biological properties, including antioxidant, anti-inflammatory, antimicrobial, antidiabetic, antiviral, and anticancer activities.[231]

The use of EA in cosmetic field, in particular, has been widely described. Several studies have indeed reported the potential use of EA for the prevention or treatment of skin disorders. For example, EA was found to be effective against contact dermatitis,[232] in wound bandaging,[233] or as photoprotective and antiaging agent.[234,235] Furthermore, EA is considered to be a useful molecule in the treatment of skin pigmentation disorder, such as hyperpigmentation, melasma and other dyschromia.[236–238]

Despite the remarkable properties of this molecule, its use is actually limited by the low permeability and low solubility in aqueous solvents. To overcome these drawbacks, different strategies have been proposed, including chemical derivatization or encapsulation in controlled release formulations.[239–241] In this context, liposomes, spherical bilayer vesicles formed by dispersion of polar lipids in aqueous solvents, recently have been largely utilized as a drug delivery vehicle for administration of nutrients and pharmaceutical drugs in biomedical, food and agricultural industries.[240]

In this scenario, the development of novel formulations for dermocosmetic applications based on the incorporation of CWM into liposomes was carried out. The antioxidant properties as well as the protective effects against UVA-induced oxidative photodamage in cellular assays were evaluated. In addition, the controlled-release profile of EA under simulated physiological conditions was investigated by UV-Vis spectroscopy and HPLC analysis.

4.4.1 CWM processing and extraction

CWM was first dried in an oven at 35 °C for one week and then grounded in a common blender, after that the powder was passed through sieves to obtain two different fractions indicated as CWM-A and CWM-B, with particle sizes of 100 and 32 μm, respectively.

In order to quantify the amount of EA contained in the two samples, these latter were dissolved in DMSO and analyzed by HPLC and UV-Vis spectroscopy. As an example, data for CWM-A are shown in Figure 4.4.1.1. The UV-Vis spectrum was characterized by broad maximum at ca. 360 nm, as expected for EA.[242] In agreement with this observation, HPLC analysis showed a main peak eluted at ca. 38 min, identified as EA by comparison with an authentic standard.

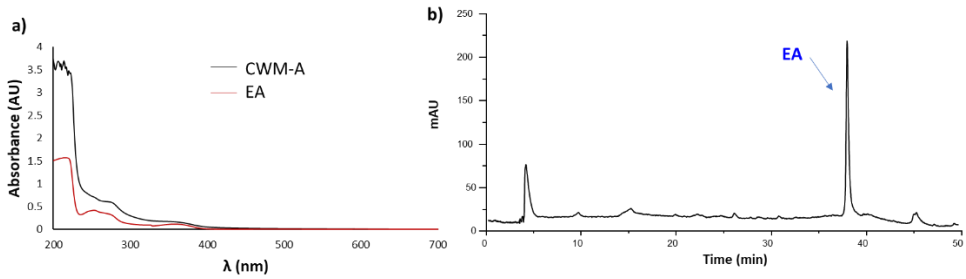

Figure 4.4.1.1. (a) UV-Vis spectrum (recorded at 0.02 mg/mL) and (b) HPLC profile (recorded at 1 mg/mL) of CWM-A.

The content of EA in the two samples are reported in Table 4.4.1.1.

Table 4.4.1.1. EA content (% w/w) in CWM samples as determined by HPLC analysis.

Sample	EA content (%)
CWM-A	6
CWM-B	5

Based on these encouraging results, the CWM samples were incorporated into liposomes (in collaboration with Dr. Caddeo of University of Cagliari) and characterized for their antioxidant, photoprotective and controlled release properties.

4.4.2 Antioxidant properties of liposome-incorporated CWM samples

The antioxidant properties of CWM samples before and after incorporation into liposomes were investigated by DPPH and FRAP assay. Notably, as reported in

Table 4.4.2.1., incorporation into liposomes induced a decrease in the EC_{50} values determined in the DPPH assay with respect to the solid sample, and a similar improvement of the reducing properties was observed in the FRAP assay. Liposomes alone were not found to exhibit significant antioxidant properties. These results clearly suggested a larger availability of the antioxidant compounds present in CMW, such as EA, further to incorporation into the liposome formulation.

Table 4.4.2.1. Antioxidant properties of CWM samples. Reported are the mean ± SD values of at least three experiments.

	DPPH assay EC_{50} (mg/mL)	**FRAP assay (mg of Trolox/mg of sample)**
Liposomes	-	0.00015 ± 0.00002
CWM-A/liposomes	0.0389 ± 0.0005	0.364 ± 0.061
CWM-B/liposomes	0.0375 ± 0.0004	0.393 ± 0.042
Solid CWM-A	0.103 ± 0.001	0.047 ± 0.002

4.4.3 Release of EA from liposome-incorporated CWM samples

The release of CWM and EA from the liposome-incorporated samples was followed by UV-Vis spectroscopy and HPLC over 5 weeks in PBS at 37 °C. No significant release of EA or other phenolic compounds was observed in the case of CWM-A, whereas promising results were obtained with liposome-incorporated CWM-B. Indeed, as showed in Figure 4.4.3.1a, the release of CWM, determined by UV-Vis analysis at 280 nm, linearly increased over time and reached values around 25% after 37 days of incubation. On the other hand, a complete release of EA, as determined by HPLC analysis, was observed (Figure 4.4.3.1b).

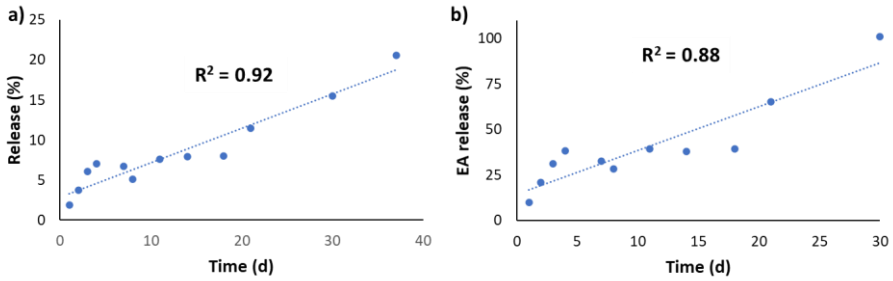

Figure 4.4.3.1. Kinetics of release of (a) CWM, determined by UV-Vis analysis, and (b) EA, determined by HPLC analysis, from liposome-incorporated CWM-B sample.

4.4.4 Evaluation of the antioxidant properties of the released fractions

In further experiments, the antioxidant properties of the released fractions from liposome-incorporated CWM were evaluated. In particular, aliquots of the incubation medium were periodically withdrawn and the Fe^{3+}-reducing properties were evaluated spectrophotometrically by the FRAP assay (Figure 4.4.4.1). As expected, the reducing power increases over time on account of the progressive release of the antioxidant compounds from the liposomes. It was not possible to perform the DPPH assay, due to the interference of released materials with the assay medium.

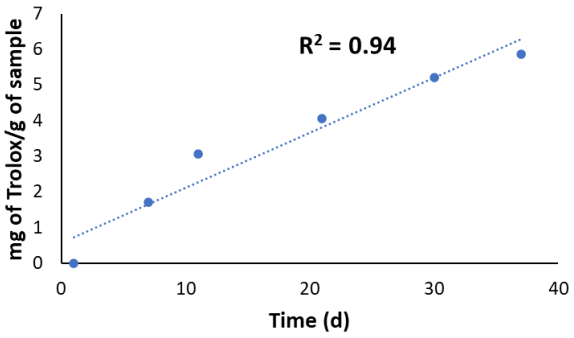

Figure 4.4.4.1. Results of the FRAP assay on liposome-incorporated CWM-B sample over time.

4.4.5 Preliminary evaluation of the photoprotective properties of liposome-incorporated samples in cellular models

In order to assess the possible use of liposome-incorporated CWM for cosmetic applications, its biocompatibility was tested on immortalized human keratinocytes (HaCaT) by the research group of Prof. Daria Monti (Department of Chemical Sciences, University of Naples "Federico II"). The samples were found to be not toxic (data not shown), therefore the protective effect against photoinduced oxidative stress was subsequently assessed. In particular, irradiation with UVA was chosen as a source of stress as this has been shown to induce many side effects on human skin,[243] and reactive oxygen species (ROS) production was evaluated by the dichlorofluorescein (DCF) assay. As shown in Figure 4.4.5.1a, DCF fluorescence was significantly increased after UVA irradiation. Interestingly, when the cells were preincubated with liposome-incorporated CWM-B, but not CWM-A, prior to UVA exposure, ROS production significantly decreased, reaching almost the levels observed in non- irradiated cells. Similar results were obtained with EA at concentration comparable to that present in the CWM-B sample (Figure 4.4.5.1b), suggesting that this compound could be the main responsible for the observed activity. As expected, no photoprotective properties were exhibited by liposomes alone (Figure 4.4.5.1b).

These data confirmed the potential of CWM-B as an active ingredient in cosmetic formulations.

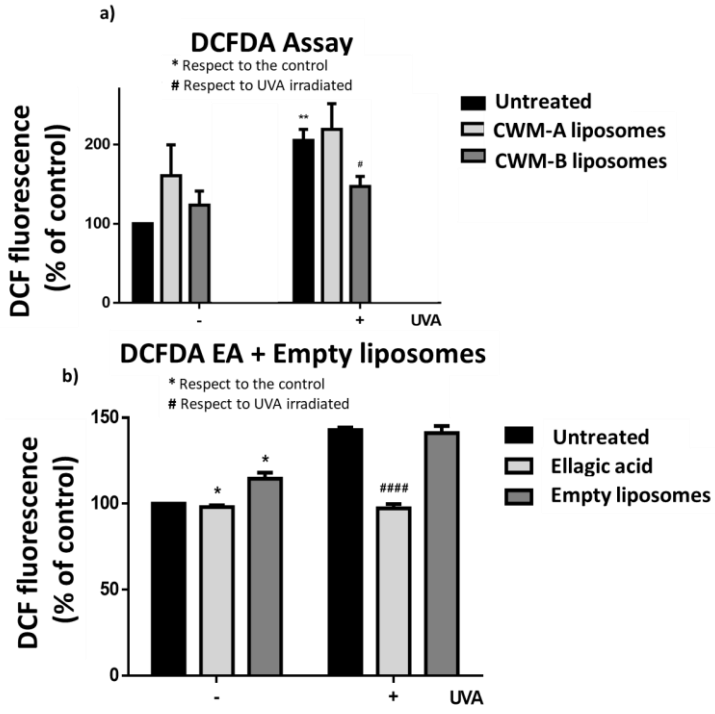

Figure 4.4.5.1. Analysis of the effects on intracellular ROS levels of a) liposome-incorporated CWM and b) EA on UVA-stressed HaCaT cells, determined by the DCF assay.

4.5 Conclusion

In this Chapter, the attention was focused on tannin and by-products of the tannin industry. At first, a comparative evaluation of the antioxidant properties of nylon membrane filters coated with hydrolyzable and condensed tannins from chestnut and quebracho wood, respectively, was carried out. The results of this study demonstrated that coating with 0.5 mg/mL tannins provided the best adsorption, resistance to washing-out and electron-donating capacity. Furthermore, the slight superior ability of condensed tannins to form functional, robust, and more resistant to washing-out coatings was also demonstrated. Secondly, the residual biomasses derived from wood tannins extraction, known as exhausted woods, were characterized in term of antioxidant and other functional properties, which were

found to be particularly promising for the chestnut wood fiber (CWF) sample. Finally, liposome-based formulations were demonstrated to be very effective for the controlled release of antioxidant and photoprotective compounds, mainly EA, from a fermented exhausted chestnut wood sample.

4.6 Experimental section

Materials and methods

Exhausted and fresh chestnut (from *Castanea sativa*) and quebracho (from *Schinopsis lorentzii*) woods, CWM, CWF, as well as chestnut and quebracho tannins, were provided by the industrial partner of this PhD project (Silvateam, S. Michele Mondovì, Cuneo, Italy). Tannins were obtained by extraction of wood chips in autoclaves with water, at 120 °C, under pressure; the tannin powder was eventually obtained by spray-drying. CWF was obtained from exhausted chestnut wood after drying in oven overnight at 60 °C and milling to obtain <250 μm particles.

Whatman® Nylon membrane filters (0.45 μm pore size, 47 mm diameter) were purchased from Sigma-Aldrich (Milan, Italy).

The enzyme laccase was provided by Prof. Giardina of the Department of Chemical Sciences of University of Naples "Federico II".[244]

Liposome-incorporated sample were provided by Dr. Carla Caddeo of University of Cagliari.

The evaluation of the photoprotective properties of liposome-incorporated samples in cellular models was carried out by Prof. Daria Monti of the Department of Chemical Sciences, University of Naples "Federico II".

All solvents and reagents were obtained from commercial sources and used without further purification.

UV-Vis spectra were recorded using a HewlettPackard 8453 Agilent spectrophotometer.

HPLC analysis were performed with an Agilent instrument equipped with a UV-Vis detector; a Phenomenex Sphereclone ODS column (250 x 4.60 mm, 5 μm) was used, at a flow rate of 1.0 mL/min. A gradient elution using 0.1% formic acid in water (solvent A) and methanol (solvent B) was performed as follows: 5% B, 0-10 min; from 5 to 80% B, 10-57.5 min. The detection wavelength was set at 254 nm.

Metal analysis was carried out on an inductively coupled plasma mass spectrometry (ICP-MS) instrument Aurora M90 model by Bruker.

4.6.1 Coating procedure. Functionalization of nylon membrane filters was performed using the following solutions for each tannin:

• Water solutions of tannins at 0.02, 0.1 and 0.5 mg/mL concentrations, prepared dissolving 7.5 mg in 15, 75 and 375 mL of distilled water;

• 0.1 mg/mL of tannins (prepared dissolving 3.0 mg in 30 mL) in distilled water containing 300 μL of a 1.7 U/mL laccase solution;

• 0.1 mg/mL of tannins (prepared dissolving 3.0 mg in 30 mL) in 0.05 M phosphate buffer (pH 6.0) containing 300 μL of a 1.7 U/mL laccase solution;

• 0.1 mg/mL of tannins (prepared dissolving 3.0 mg in 30 mL) in distilled water containing 3.5 mg of $FeSO_4$;

• 0.1 mg/mL of tannins (prepared dissolving 7.5 mg in 75 mL) in 0.05 M carbonate buffer (pH 9.0).

The nylon filters were dipped in the solutions and kept under magnetic stirring for 2 h, after that they were abundantly washed with distilled water and allowed to air dry. When required the mixtures were periodically analyzed by UV-Vis spectroscopy.

In another series of experiments, after the 2 h incubation the following additives were added to each solution and the mixtures were analyzed by UV-Vis spectroscopy:

• 6 M HCl until pH 2;

• $NaBH_4$ followed or not by acidification with 6 M HCl;

• EDTA sodium salt.

4.6.2 Quantification of tannin deposition. 8 mg of nylon membrane filters were dipped in 8 mL of the solutions described above. The mixtures were kept under magnetic stirring at room temperature and after 2 h the UV-Vis spectra of the solutions were recorded. The amount of tannin deposited on the nylon filter was evaluated by determining the decrease in absorbance at 280 nm for QT and 270 nm for CT in comparison to control solutions not containing the filters.

4.6.3 Antioxidant properties of coated nylon membrane filters: **DPPH assay.** 5 mg of coated nylon filters were added to 5 mL of a 200 μM ethanolic solution of DPPH.[175,176] The samples were kept at room temperature and absorbance at 515 nm was measured after 10 min and 2.5 h. The assay was carried out on the filters as such or previously washed with ethanol. Experiments were run in triplicate. **FRAP assay.**[177] 5 mg of coated nylon filters, previously washed with 0.3 M acetate buffer, were added to 2 mL of FRAP solution (1.7 mM $FeCl_3$ and 0.83 mM TPTZ in 0.3 M acetate buffer (pH 3.6) at 10:1:1 v/v/v ratio).[177] The mixtures were kept at room temperature and absorbance at 593 nm was measured after 10 min and 2.5 h. Experiments were run in triplicate.

4.6.4 Hydrolytic treatment. Exhausted woods (3 g) were treated with 70 mL of 6 M HCl under stirring qt 100 ◦C for 24 h.[150,174,179] After cooling at room temperature, the mixture was centrifuged (7000 rpm, 15 min) and the precipitate washed with water until neutrality and freeze dried.

4.6.5 Antioxidant properties of exhausted woods. DPPH assay: To a 0.2 mM ethanolic solution of DPPH, the different wood samples (before and after hydrolytic treatment) or tannin powders were added (final dose 0.03−1.5 mg/mL), and after 10 min under stirring at room temperature, the absorbance at 515 nm was measured.[175,176] **FRAP assay:** To 0.3 M acetate buffer (pH 3.6) containing 1.7 mM $FeCl_3$ and 0.83 mM TPTZ, the different wood samples (before and after hydrolytic treatment) or tannin powders were added (final dose 0.00625–0.3 mg/mL) and after 10 min under stirring at room temperature the absorbance of the solution at 593 nm was measured.[177] Results were expressed as Trolox eqs. Experiments were run in triplicate.

4.6.6 TPC assay. Tannins powders, exhausted and fresh woods were added to a solution consisting of Folin-Ciocalteu reagent, 75 g/L Na_2CO_3, and water in a 1:3:14 v/v/v ratio. After 30 min incubation at 40 ◦C, the absorbance at 765 nm was measured. Gallic acid was used as reference compound. Experiments were run in triplicate.[178]

4.6.7 NOx scavenging assay. A solution of sodium nitrite (1 M) in water was added to 10% sulfuric acid over 10 min.[245] The developed red orange gas (0.2–0.6 mL) was withdrawn with a syringe and conveyed through a tip containing 5 mg of wood sample into 3 mL of Griess reagent (0.5% sulfanilamide and 0.05% N-(1-naphthyl)ethylenediamine dihydrochloride in 1.25% phosphoric acid) and the absorbance at 540 nm was measured. Experiments were run in triplicate.

4.6.8 Superoxide-scavenging assay.[150] Wood or tannin powders (final dose 0.0625 mg/mL) were added to 0.05 M ammonium hydrogen carbonate buffer (pH 9.3) containing 0.4 mM EDTA and 12 μM nitroblue tetrazolium, followed by a 20 mM pyrogallol solution in 0.05 mM HCl (3.3 mM final pyrogallol concentration). The mixture was vigorously stirred for 5 min, after that absorbance at 596 nm was measured. Results were expressed as percentage of reduction of the absorbance at

596 nm of a control mixture run in the absence of sample. Experiments were run in triplicate.

4.6.9 MB adsorption assay.[246] Adsorption experiments were performed at room temperature by adding wood samples (0.2 mg/mL) to a 5 or 25 mg/L aqueous solution of MB. The mixtures were taken under stirring and after 30 min the absorbance at 654 nm was measured. Activated carbon was used as reference material. Experiments were run in triplicate.

4.6.10 Cd^{2+} adsorption.[247] A 1.5 mM stock solution of the heavy metal was prepared by dissolving 10 mg of cadmium carbonate in 39 mL of 0.1 M HCl. Prior to the adsorption experiments a 1.5 mg/mL suspension of each wood sample in 0.01 M phosphate buffer (pH 7.0) was obtained by homogenization in a Tenbroeck glass-to-glass homogenizer for 4 min. 0.7 mL of the wood suspensions and 0.1 mL of the metal solution were added to 10 mL of 0.01 M phosphate buffer at pH 7.0. After 2 h, the mixtures were filtered through a 0.45 μm nylon membrane, acidified by addition of 69% nitric acid (1:100 v/v), properly diluted with 1% nitric acid, and analyzed by ICP-MS. A calibration curve was built with cadmium solutions at five different concentrations. For each binding experiment a blank experiment was planned in which the metal ion was added in the phosphate buffer and incubated for 2 h without addition of the wood sample. Experiments were run in triplicate.

4.6.11 Antioxidant properties of CWM samples and liposome-incorporated CWM samples: DPPH assay.[175,176] Samples (final dose 0.0067–0.15 mg/mL) were added to 3 mL of a 0.2 mM ethanolic solution of DPPH, and after 10 min under stirring at room temperature the absorbance at 515 nm was measured. Experiments were run in triplicate. **FRAP assay**.[177] Samples were added (final dose 0.00167–0.1 mg/mL) to 3 mL of 0.3 M acetate buffer (pH 3.6) containing 1.7 mM $FeCl_3$ and 0.83 mM TPTZ, and after 10 min under stirring at room temperature the absorbance of

the solutions at 593 nm was measured. Results were expressed as Trolox eqs. Experiments were run in triplicate.

4.6.12 Release experiments from liposome-incorporated CWM. Each liposome-incorporated CWM sample (3 g) was placed in a dialysis membrane (MWCO 100-500D) and dialyzed against 30 mL of 1x PBS at pH 7.4. The samples were kept at 37 °C in a water bath. 0.5 mL of release medium was periodically withdrawn and replaced with an equal volume of corresponding fresh media and UV-vis spectra were recorded. Each experiment was run in triplicate.

4.6.13 Antioxidant properties of released fractions from liposome-incorporated CWM samples: FRAP assay.[177] The FRAP reagent was prepared by mixing 0.3 M acetate buffer (pH 3.6), 10 mM TPTZ in 40 mM HCl, and 20 mM ferric chloride in water, in a 10:1:1 v/v/v ratio. To 2 mL of this solution, aliquots (150 µL) of the released fractions form liposome-incorporated CWM were added. After 10 minutes under stirring, the mixtures were centrifugated (3 min at 5000 rpm) and the absorbance at 593 nm was measured.

Chapter 5

Exploitation of deep eutectic solvents for the recovery of antioxidant compounds from agri-food by-products

5.1 Introduction

Extraction of phenolic compounds from agri-food by-products is generally performed by solid-liquid extraction techniques,[248] which however typically involve long extraction times, high costs, and the use of organic solvents characterized by intrinsic drawbacks, such as low boiling points, flammability, toxicity, and non-biodegradability.[249] Therefore, the search for green solvents exhibiting good extraction properties, but also low-costs and minimal environmental impact, is attracting increasing attention.[250]

Recently, deep eutectic solvents (DES) have been widely reported as eco-friendly and biocompatible solvents for the extraction of phenolic compounds from agri-food by-products.[251,252] DES are easily prepared by mixing, at a suitable temperature, a hydrogen bond acceptor (HBA) and a hydrogen bond donor (HBD), and compared to common organic solvent are generally low cost, biodegradable and biocompatible.[252–254]

DES can be described by the general formula Cat^+X^-zY, where Cat^+ is typically ammonium, sulfonium, or phosphonium, X^- is a Lewis base, usually a halide, Y is a Lewis or Brønsted acid, that forms a "complex" with X^-, and z is the number of Y molecules that interact with the anion.[255] The resulting mixture is characterized by a melting point lower than that of individual constituents.

Choline chloride (ChCl), a cheap and non-toxic salt, is the most popular HBA used for DES preparation, while urea, ethylene glycol, glycerol, but also alcohols, amino acids, carboxylic acids and sugars can be used as HBD.[256–258]

The physicochemical properties of DES, such as freezing point, conductivity, density, viscosity, and polarity, normally depend on their composition, therefore it is possible to modulate them by modifying the HBD and HBA components.

In this Chapter, the use of DES for phenolic compounds extraction from chestnut wood fiber (CWF) is described. Indeed, as reported in Chapter 4, CWF was found to be a material endowed with good antioxidant properties, but the possibility to practically exploit it as a source of high value compounds has remained unexplored, despite the many advantages offered by this material, such as the large availability throughout the year and the cleanness of the manufacturing process. In particular, three different environmentally friendly extraction protocols of CWF phenolic compounds were designed and optimized. The approach employed included a first screening of different DES to select the best one to extract low molecular weight phenolic compounds (mainly EA). Then, an optimization of the extraction conditions was performed. Harsher DES-based extraction conditions were also tested for recovery of lignin, and finally, a sequential two-step DES-based extraction protocol was developed, selectively affording an EA-enriched and an EA-free, lignin-enriched sample. Part of this work was carried out during a six-month stage at "Centro Ricerche per la Chimica Fine S.r.l." of Silvateam S.p.a. (San Michele Mondovì, Cuneo, Italy).

In the second part of this Chapter, the possibility to exploit the developed protocol for the recovery of lignin from other agri-food by-products such as shells of edible buts, is reported.

5.2 DESs screening for extraction of antioxidant compounds from CWF

Twenty-five DESs were prepared as reported in Table 5.2.1. All the solvents were transparent and stable over the whole period of use. At first, extraction was carried out at 40 °C for 60 min with a 66.7 g/Kg s/l ratio. Due to the high viscosity, DES were used as 70% w/w aqueous solution, in order to allow a higher mass transfer rates and, consequently, higher extraction yields.[259–261] Hydration of the solvent may have an important impact on the eutectic mixture system.[262] Actually, several research papers aimed at investigating the molecular behaviour of various DES-water systems have demonstrated that the eutectic mixture system is preserved by addition of water up to 50% w/w, whereas higher percentages of water led to a disruption of the DES structure, with a consequent transition from a water-in-DES to a DES-in-water mixture and further to an aqueous solution of hydrated DES components.[263] On this basis, a 30% w/w water content in the eutectic mixture was used.[259]

The different extracts were analyzed by the Folin-Ciocalteu, DPPH, and FRAP assays, in comparison with extracts prepared under the same conditions using water, methanol, and ethanol as conventional solvents. As evident from Figure 5.2.1a, all the DES extracts showed TPC values higher than that obtained with water (red line). Moreover, several solvents led to TPC values higher than that obtained with methanol (black line), and in particular ChCl:UREA, ChCl:TA2, LA:GLU and ChCl:GLY3 proved to be more efficient even than ethanol (green line).

Table 5.2.1. DESs prepared and used in the present study.

DES components	mol/mol ratio	Preparation conditions	Abbreviation
Lactic acid/Sodium acetate	3:1	30 min, 60 °C	LA:SA3
Lactic acid/Sodium acetate	5:1	30 min, 60 °C	LA:SA5
Glycerol/Sodium acetate	3:1	2 h, 70 °C	GLY:SA3
Glycerol/Sodium acetate	5:1	2 h, 70 °C	GLY:SA5
Glycerol/Na-K tartrate/H_2O	5:1:3	40 min, 70 °C	GLY:TAR3
Glycerol/Na-K tartrate/H_2O	5:1:4	40 min, 70 °C	GLY:TAR4
ChCl/Glycerol	1:1	30 min, 60 °C	ChCl:GLY1
ChCl/Glycerol	1:2	30 min, 60 °C	ChCl:GLY2
ChCl/Glycerol	1:3	30 min, 60 °C	ChCl:GLY3
ChCl/Glycerol	1:4	30 min, 60 °C	ChCl:GLY4
ChCl/Ethylene glycol	1:2	30 min, 60 °C	ChCl:EG2
ChCl/Ethylene glycol	1:3	30 min, 60 °C	ChCl:EG3
ChCl/Ethylene glycol	1:4	30 min, 60 °C	ChCl:EG4
ChCl/Lactic acid	1:2	30 min, 60 °C	ChCl:LA2
ChCl/Lactic acid	1:9	30 min, 60 °C	ChCl:LA9
ChCl/Tartaric acid	1:1	6 h, 90°C	ChCl:TA1
ChCl/Tartaric acid	2:1	6 h, 90°C	ChCl:TA2
ChCl/Glycolic acid	1:3	20 min, 70 °C	ChCl:GLA
ChCl/Oxalic acid dihydrate	1:1	20 min, 70 °C	ChCl:OXA
ChCl/Urea	1:2	30 min, 70 °C	ChCl:UREA
ChCl/Malic acid	1.5:1	> 8 h, 80 °C	ChCl:MA
ChCl/Maleic acid	1:1	2 h, 80 °C	ChCl:MAL
ChCl/Malonic acid	1:1	1 h, 80 °C	ChCl:MALO
Lactic acid/Glucose	5:1	2 h, 80 °C	LA:GLU
Lactic acid/Fructose	5:1	30 min, 80 °C	LA:FRU

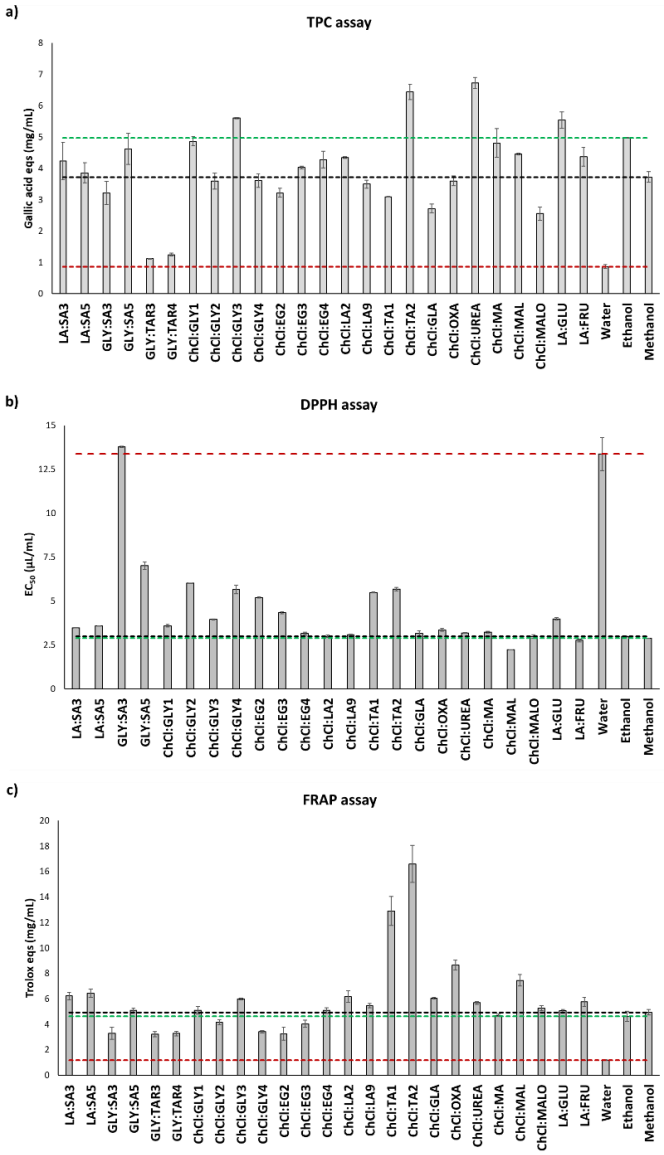

Figure 5.2.1. (a) TPC, (b) DPPH, and (c) FRAP assay results for CWF extracts obtained with selected DESs (66.7 g/Kg solid-to-solvent ratio, 40°C, 60 min, 30% w/w H_2O). Reported are the mean ± SD values of at least three experiments.

In the DPPH assay (Figure 5.2.1b), again DESs extracts showed EC_{50} values lower than that obtained with water (red line), although the results appeared to be less encouraging than those obtained from the Folin-Ciocalteu assay, since all extracts

exhibited EC_{50} values higher or similar than those obtained for methanol (green line) and ethanol (black line) extracts. More interesting results were obtained in the FRAP assay (Figure 5.2.1c), as ChCl-tartaric acid based DESs ChCl:TA1 and ChCl:TA2 extracts showed reducing properties 2.6- and 3.3-fold higher than that exhibited by the ethanol or methanol extracts, respectively. Differences in the results of the three assays may be interpreted considering that these latter are based on different reaction mechanisms and are performed in different media.[194,264]

By making a compromise between the results of the Folin-Ciocalteu, DPPH, and FRAP assays, ChCl:TA2 was selected as the most promising DES for the recovery of antioxidant phenolic compounds from CWF. Further experiments were therefore directed to the optimization of the extraction conditions using this solvent.

5.2.1 Optimization of the extraction conditions for the recovery of antioxidant compounds from CWF using ChCl:TA2

The effects of different parameters, such as s/l ratio, extraction time, temperature and water content on the TPC of the ChCl:TA2 extract were sequentially evaluated. At first, s/l ratio of 100, 66.7, 50 and 33.3 g/Kg values were used, keeping the other operating conditions fixed (60 min, 40 °C, and 30% w/w water content). Higher s/l ratios were not analyzed, because the high viscosity of the mixture made it impossible to separate the supernatant from the residual solid. By increasing s/l ratio, a linear increase (R^2=0.97) in the TPC value was observed, indicating that no solvent saturation occurred (Figure 5.2.1.1a). Based on these results, a 100 g/Kg was chosen as the optimal s/l ratio.

Extraction times between 60 and 180 min were then investigated (Figure 5.2.1.1b), keeping fixed the other operating conditions (100 g/Kg s/l, 40°C, 30% w/w water content). Although no statistically significant differences were observed, the highest TPC value was obtained after 90 min extraction, which was therefore selected as the optimal time. Actually, a slight decrease in the TPC value was observed by

prolonging to extraction time up to 180 min, likely as a consequence of the onset of chemical modifications processes.

Temperature is known to affect DES viscosity and compound solubility. In this case, an increase of the extraction temperature from 40 °C to 50 °C, led to an improvement of the phenolic compound extraction yield, whereas at higher temperatures a decrease of TPC was observed, probably due again to phenolic compound oxidation/degradation. On this basis, 50 °C was selected as optimal extraction temperature (Figure 5.2.1.1c).

In a last series of experiments, water content in the DES was varied from 20% to 50% w/w. It was not possible to use a lower water content due to the high viscosity of the DES as stated also above. TPC values linearly decreased with increasing water content (R^2 = 0.99) (Figure 5.2.1.1d), therefore 20% w/w was chosen as optimal parameter.

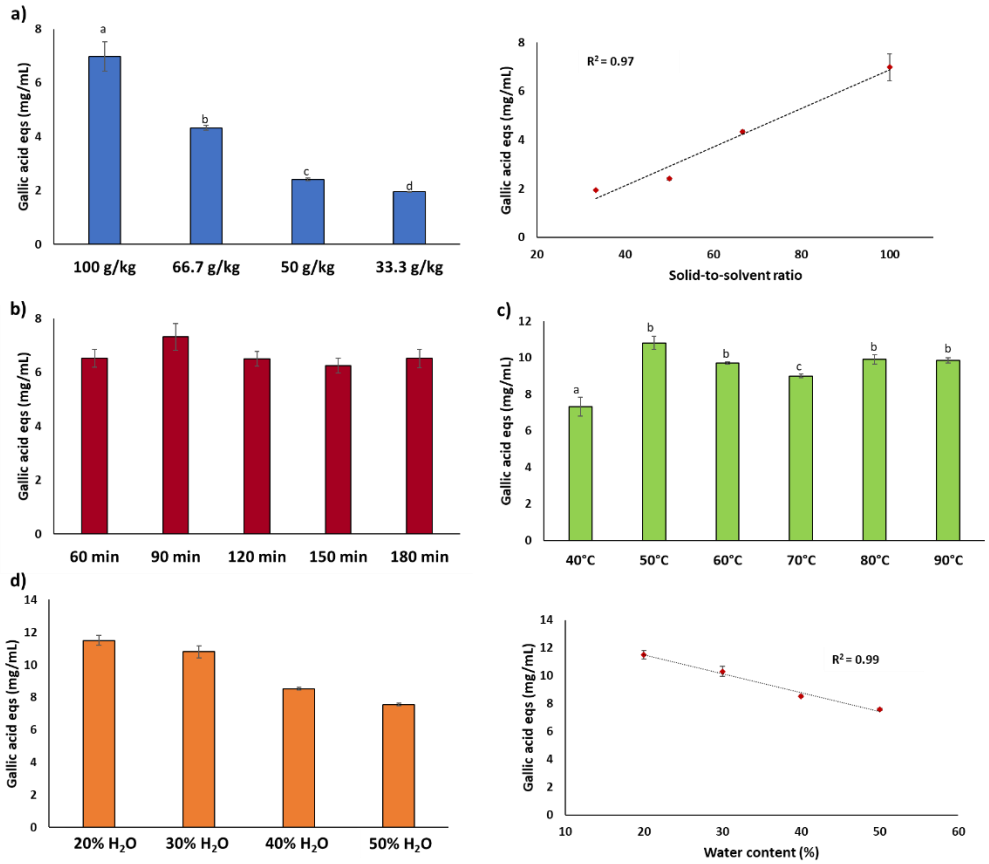

Figure 5.2.1.1. TPC assay results for CWF extracts obtained with ChCl:TA2 at (a) different s/l ratio, (b) different extraction times, (c) different extraction temperatures, and (d) different water content. Reported are the mean ± SD values of at least three experiments. Values without a common letter are significantly different ($p < 0.05$).

To further optimize the extraction protocol for the recovery of antioxidant compounds from CWF, a response surface methodology was also employed, in collaboration with the research group of Prof. Lavecchia from the Department of Chemical Engineering, Materials and Environment of Sapienza University of Rome. This analysis led to the following considerations:

(a) under the conditions tested, the recovery of antioxidants was influenced by temperature (T), s/l ratio (R) and percentage of added water (W);
(b) the extraction yield was affected linearly by T and W, whereas the effect of R involved both a linear and a quadratic term;
(c) T and W had a positive effect on antioxidant recovery and the contribution of the latter was greater;
(d) all the interaction coefficients were not significant, indicating that each factor exerted its effect independently of the others.

The reduced model was used to optimize the extraction conditions. Maximization of the response variable was performed numerically using the gradient descent method. The extraction time (E), which was found to be not significant under the conditions of the study, was set to its center-point value (90 min). The following results were obtained: T = 70 °C; R = 40 g/kg; W = 50% w/w. The corresponding extraction yield (y = g of gallic acid eqs per 100 g of the starting material) was 23.17 g/100 g.

Finally, a validation of the model was carried out by performing new experiments under the optimum conditions and in two points inside and outside the factorial region of the central composite design (CCD). Table 5.2.1.1. evidenced that the experimentally determined values (y_{exp}) were very close to the model predictions (y_{pred}) and all included in their 95%-prediction intervals (PI 95%), demonstrating the good predictive ability of the model and the effectiveness of the optimization procedure.

Table 5.2.1.1. Results of validation experiments.

Point	E (min)	T (°C)	R (g/Kg)	W (% w/w)	y_{exp} (g/100g)	y_{pred} (g/100g)	PI 95% (g/100g)
Optimum	90	70	40	50	25.76	23.17	19.12–27.22
Internal	90	60	50	35	17.09	16.13	12.25–20.01
External	90	45	90	25	8.98	7.64	3.21–12.07

The experimental conditions optimized by the CCD model (90 min, 70°C, 40 g/Kg s/l ratio, and 50% w/w of water) provided a total phenolic compound extraction

yield of 25.8 g/100 g of starting CWF, which was about 1.6-fold higher than that determined for the extract deriving from the protocol optimized using independent variables (15.7 g/100 g of starting CWF). The extracts obtained with the two optimizing protocols were analyzed by UV-Vis spectroscopy and HPLC after proper dilution. The UV-Vis spectrum (Figure 5.2.1.2) showed for both samples a broad maximum at 340-370 nm, suggestive of the presence of EA.[242] This hypothesis was confirmed by HPLC analysis, showing a main peak eluted at ca. 35 min, identified as EA by comparison of the chromatographic properties with those of an authentic standard. Notably, EA yields of 3.3% w/w and 0.16% w/w with respect to starting CWF were determined for the independent variables- and CCD-optimized extraction, respectively. This could be a consequence of the higher water content adopted in the CCD-optimized protocol (50% w/w vs 20% w/w in the case of the independent variables-optimized protocol), limiting the extractability of water insoluble compounds like EA. On this basis, further experiments were carried out on the extract obtained using the independent variables-optimized protocol.

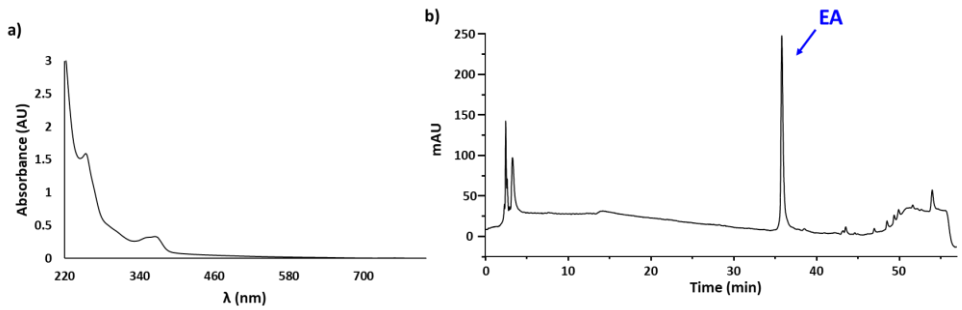

Figure 5.2.1.2. (a) UV-Vis spectrum and (b) HPLC profile of the ChCl:TA2 CWF extract (0.33 mg/mL in methanol, starting from 5 mg/mL solution in DMSO).

5.2.2. Characterization of the antioxidant properties of the ChCl:TA2 CWF extract

Folin-Ciocalteu, DPPH and FRAP assays were then performed on the CWF extract obtained under the optimized conditions (100 g/kg s/l ratio, 50°C, 90 min, 20%

water content) in comparison to those obtained using water, ethanol, and methanol. The TPC content of ChCl:TA2 extract was found to be ca. 7-fold higher than that obtained with water and ca. 2-fold higher than those obtained with ethanol and methanol (Figure 5.2.2.1a). In the DPPH assay, the DES extract exhibited EC_{50} value almost 5-fold lower than that of the water extract and comparable to that of methanol extract (Figure 5.2.2.1b). FRAP assay showed a similar trend, with the ChCl:TA2 extract exhibiting a number of Trolox eqs 4.8, 2.3 and 1.8-fold higher than those determined for the water, ethanol, and methanol extract, respectively (Figure 5.2.2.1c), demonstrating the high efficiency of the ChCl:TA2 DES in extracting CWF phenolic compounds.

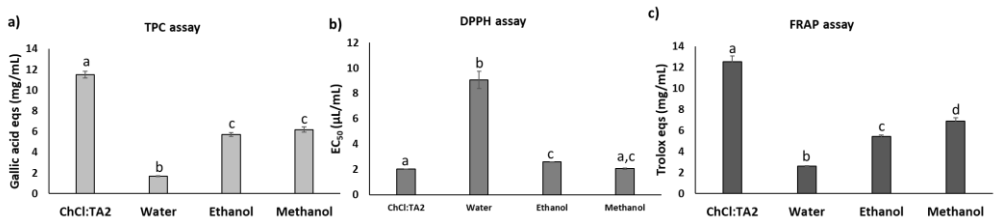

Figure 5.2.2.1. (a) TPC, (b) DPPH and (c) FRAP assay results for CWF extracts under optimized experimental conditions. Reported are the mean ± SD values of at least three experiments. Values without a common letter are significantly different ($p < 0.05$).

As reported above, EA was identified as the main low molecular weight phenolic component in the ChCl:TA2 CWF extract, with a yield of 3.3% w/w with respect to starting CWF and ca. 12% w/w with respect to the solubilized material. Notably, this yield was comparable to that obtained with DMSO, chosen as a reference extraction solvent for this polyphenol,[265] and remarkable higher than those obtained with water (ca. 0.03%) and methanol (ca. 0.6%) under the same extraction conditions.

5.3 CWF lignin extraction with DESs under harsher experimental conditions

In addition to EA, CWF contains also lignin, which could account in part for the remaining 88% w/w of the ChCl:TA2 extract. However, several attempts to recover solid lignin from this extract, for example by precipitation in acidic water,[266] failed. Therefore, in further experiments harsher extraction conditions were investigated, as reported for other biomasses.[267,268] In particular, higher extraction temperatures (120 °C) and longer extraction times (8 h) were adopted, maintaining the same s/l ratio and water content. For comparison, the efficacy of ChCl:LA2 was also tested, having this latter being reported to exhibit a strong selective dissolving ability toward lignin.[269,270] Under these conditions, a dark brown liquid was obtained and subjected to two different precipitation protocols, involving addition of 0.01 M HCl or of an acetone/water solution.[269] After precipitation, a brown solid was obtained in 10% w/w yield for both DES and for both precipitation protocols.

The obtained samples were then analyzed for their antioxidant properties and TPC, in comparison to starting CWF and pure EA.

As shown in Table 5.3.1, all the samples exhibited at least 4.5-fold stronger antioxidant properties and 2.5-fold higher TPC than the starting CWF. The ChCl:TA2 samples were found to be on average 1.3-fold more active than those recovered with ChCl:LA2, whereas no significant effect of the precipitation protocol was observed.

Table 5.3.1. Antioxidant properties of samples recovered from CWF by harsh treatment. Reported are the mean ± SD values of at least three experiments. Values in the same column without a common italic letter (a-d) are significantly different ($p < 0.05$).

Sample	EC_{50} (mg/mL) (DPPH assay)	Trolox eqs (mg of Trolox/mg of sample) (FRAP assay)	Gallic acid eqs (mg of gallic acid/mg of sample) (TPC Assay)
ChCl:TA2 (+ 0.01 M HCl)	0.018 ± 0.001^{a}	0.52 ± 0.02^{a}	1.0 ± 0.1^{a}
ChCl:TA2 (+ acetone/water)	0.0193 ± 0.0001^{a}	0.50 ± 0.05^{a}	1.01 ± 0.06^{a}
ChCl:LA2 (+ 0.01 M HCl)	0.0237 ± 0.0009^{b}	0.35 ± 0.01^{b}	0.72 ± 0.04^{b}
ChCl:LA2 (+ acetone/water)	0.0244 ± 0.0001^{b}	0.38 ± 0.01^{b}	0.73 ± 0.01^{b}
EA	0.0051 ± 0.0004^{c}	1.04 ± 0.02^{c}	2.5 ± 0.1^{c}
CWF	0.11 ± 0.01^{d}	0.037 ± 0.007^{d}	0.281 ± 0.004^{d}

5.3.1 Structural characterization of lignin recovered by treatment of CWF with DES under harsh conditions

To gain information on the phenolic composition of the recovered solid samples, these were dissolved in DMSO and analyzed by UV-Vis spectroscopy and HPLC. As an example, here are reported the data for the ChCl:TA2 and ChCl:LA2 samples obtained after precipitation induced by acetone/water. The UV-Vis spectra showed an absorption maximum at around 367 nm (Figure 5.3.1.1a), and HPLC analysis (Figure 5.3.1.1b) showed a single peak at around 35 min, suggesting, again, the presence of EA. Quantitative analysis demonstrated a content of EA of about 27 ± 3% w/w and 16 ± 2% w/w for the ChCl:TA2 and ChCl:LA2 sample, respectively, in agreement with the more efficient antioxidant properties determined for the ChCl:TA2. However, based on a comparison between the data for pure EA and CWF-derived samples, it could be concluded that the antioxidant properties of the recovered samples cannot be attributed exclusively to EA, but also to non-chromatographable phenolic species, such as lignin.

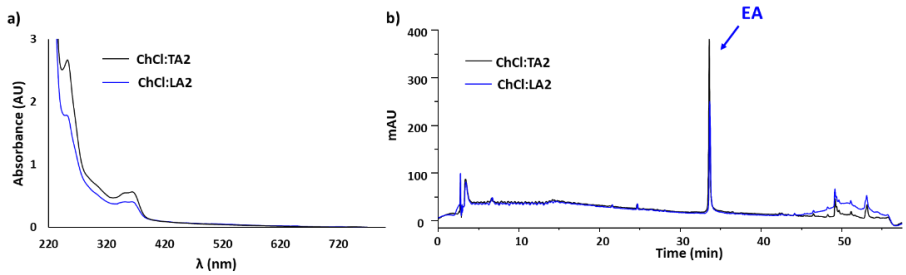

Figure 5.3.1.1. (a) UV-Vis spectra (recorded at 0.1 mg/mL in methanol) and (b) HPLC profiles (recorded at 0.25 mg/mL) of the recovered solids from CWF treatment with ChCl:TA2 and ChCl:LA2 under harsh conditions, followed by addition of 7:3 v/v acetone/water mixture.

Additional information on the phenolic components of the CWF extracts was provided by ^{1}H NMR spectra recorded in DMSO-d_6 (Figure 5.3.1.2). For both samples, a singlet at 7.48 ppm due to EA was observed.[271] Furthermore, the spectra showed a very broad signal in the region 6.0-7.4 ppm, indicative of the presence of a heterogeneous phenolic polymer such as lignin.[272] As expected, this signal was particularly evident in the spectrum of the ChCl:LA2 sample. Notably, a progressive sedimentation of a brown solid was observed in the NMR tubes over time, probably due to a slow lignin precipitation. Therefore, the precipitates were then recovered by centrifugation, lyophilized, and then redissolved in DMSO. The ^{1}H NMR spectra of the precipitates, recorded after immediate dissolution in DMSO-d6, showed the disappearance of the typical signal of EA.

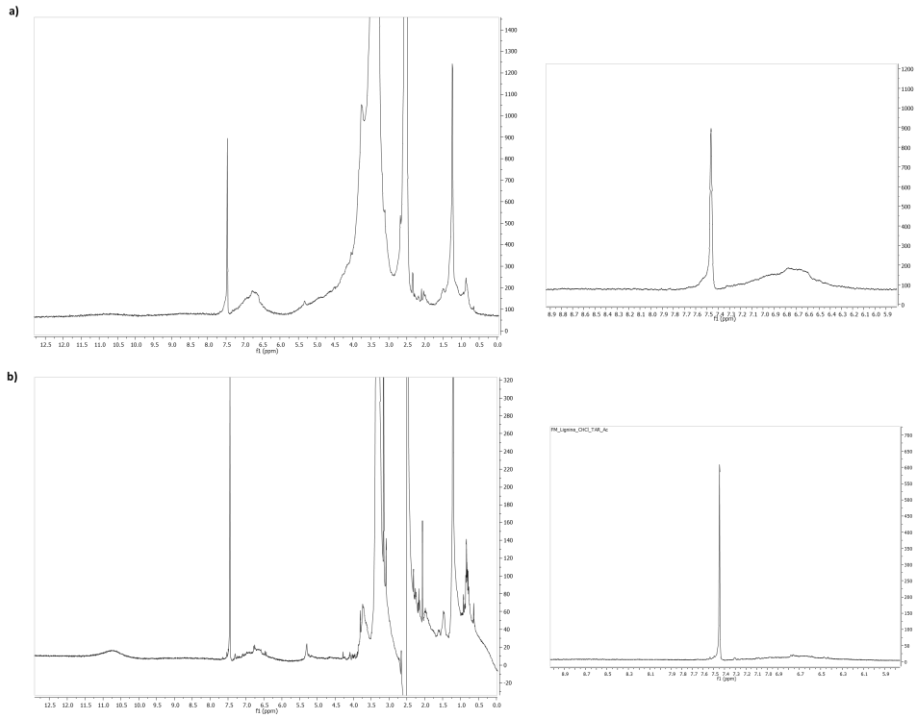

Figure 5.3.1.2. ^{1}H NMR spectra (DMSO-d_6) of solid samples recovered from CWF by treatment with (a) ChCl:LA2 and (b) ChCl:TA2 under harsh conditions, followed by addition of 7:3 v/v acetone/water mixture.

The DMSO washing procedure was therefore exploited to confirm the presence of lignin in the CWF extracts obtained under the harsh experimental conditions. First, ATR-FTIR spectra of the ChCl:TA2 sample before (black trace) and after (red trace) washing with DMSO, as well as that of pure EA (blue trace), were recorded and are showed in Figure 5.3.1.3. In particular, the spectrum of the starting ChCl:TA2 sample was almost superimposable to that of EA, particularly in the 1700-500 cm^{-1} region, whereas in the 2950–2850 cm^{-1} region two sharp peaks, typically associated to the C−H stretching vibration of lignins, were present.[150] After washing with DMSO, no traces of EA were found in the DMSO-washed sample, which was instead still characterized by the two sharp peaks due to lignin. Similar results were

obtained for the ChCl:LA2 sample, although in this case the signals in the 2950–2850 cm^{-1} region were found to be more intense as expected (Figure 5.3.1.3c).

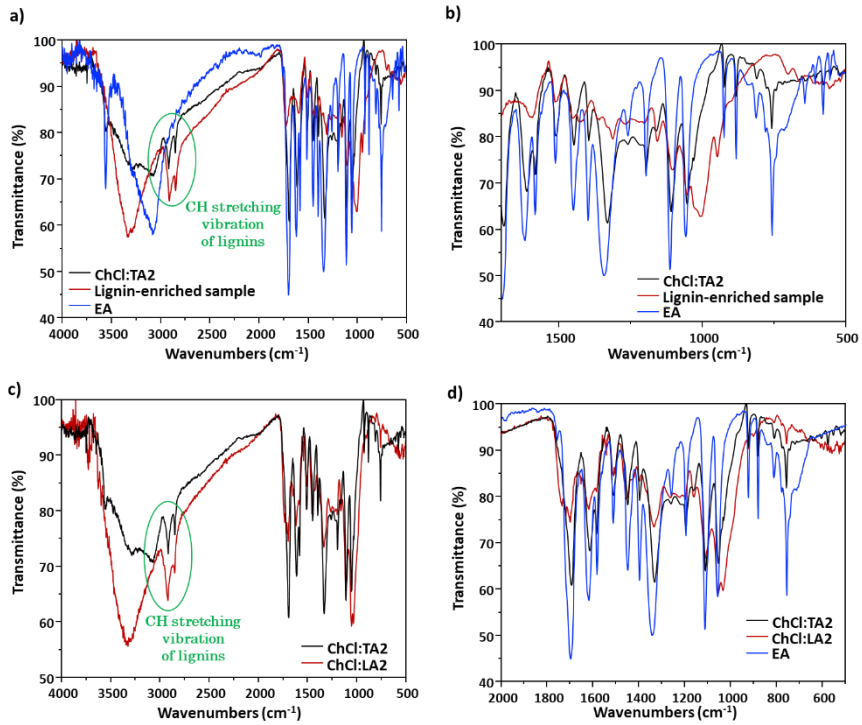

Figure 5.3.1.3. ATR-FTIR spectra of (a) samples recovered by CWF treatment with ChCl:TA2 before (black trace) and after (red trace) washing with DMSO and of pure EA (blue trace). (b) Expanded plots (1700-500 cm^{-1} region). (c) ATR-FTIR spectra of the samples recovered by CWF treatment with ChCl:TA2 (black trace) and ChCl:LA2 (red trace). (d) Expanded plots (2000-500 cm^{-1} region).

The ChCl:LA2 samples were also characterized by EPR spectroscopy (Figure 5.3.1.4). The EPR spectrum of the untreated CWF sample showed a singlet at a g value of 2.0036, as previously reported for other wood-derived lignin-rich samples.[273] This signal was quite broad (ΔB = 5.7 G) and was characterized by a ca. 50% Gaussian contribution to the lineshape, as expected for a chemically heterogeneous material. On the other hand, the spectrum of the sample recovered

from ChCl:LA2 extraction was slightly narrower (ΔB = 4.0 G) and, at the same time, the Gaussian contribution to the lineshape decreased, suggesting that the extraction procedure enriched the sample in selected components, hence reducing its heterogeneity. The observed g value also changed, decreasing to 2.0031, in line with previous data, indicating a lower g value for lignins treated with acidic solutions.[274]

Interestingly, the spin density of the ChCl:LA2 sample decreased by one order of magnitude with respect to the pristine CWF sample. This quite unexpected result is in line with the fact that components other than lignin, such as EA, were extracted in the DES. On the other hand, after washing with DMSO the sample exhibited a higher weight normalized intensity, in agreement with an enrichment in the lignin component. Normalized power saturation curves (Figure 5.3.1.4b) confirmed a lower degree of variety of the free-radical population in the DES-recovered samples.

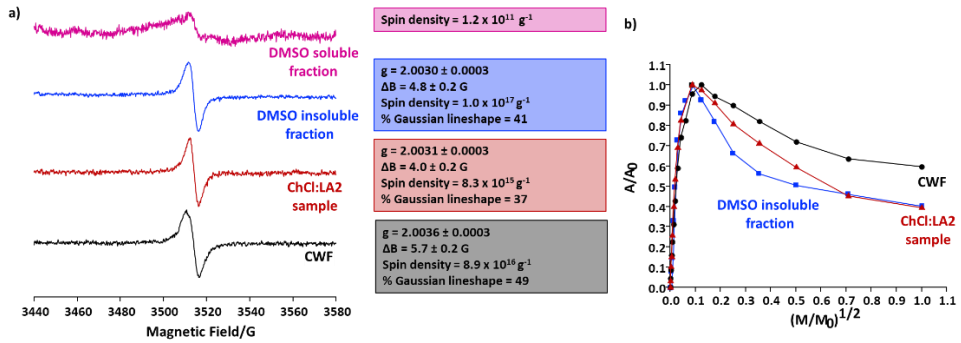

Figure 5.3.1.4. (a) Solid state EPR spectra and (b) power saturation profiles of CWF at different purification stages.

DMSO-washed ChCl:LA2 sample was finally analyzed by the DPPH assay, that evidenced an EC_{50} value about 30-fold higher than that obtained for the starting sample, indicating that DMSO washing removed not only EA but also other low molecular weight lignin components endowed with potent antioxidant properties. This was confirmed by the EPR spectrum of the DMSO soluble fraction (Figure 5.3.1.4a), which showed a weak but clearly detectable signal attributable to lignin

related species (EA is EPR silent). On this basis, an *ad hoc* treatment aimed to selectively obtain an EA- and a lignin-enriched sample from CWF was finally designed.

5.4 Sequential two-step DES-based treatment of CWF

Firstly, a mild treatment of CWF with ChCl:TA2 was performed using the optimized "mild" conditions initially developed (100 g/Kg s/l, 50 °C, 90 min, 20% w/w of water). The extract was then treated with a 1% KCl aqueous solution in order to exploit a salting-out effect for the recovery of a light brown solid sample (indicated as mild treatment sample, MTS) in ca. 7.5% w/w yield with respect to starting CWF. Subsequently, the residual, undissolved CWF was treated with ChCl:LA2 under the harsh conditions described above (120 °C, 8 h), and the dark brown liquid thus obtained was treated as well 1% KCl or 0.01 M HCl to give a fine brown precipitate (harsh treatment sample, HTS). in comparable yields (ca. 5% w/w yield with respect to starting CWF).

The antioxidant properties as well as the TPC of MTS and HTS are reported in Table 5.4.1.

MTS exhibited the highest antioxidant properties, whereas HTS was found to be 50% less active in the DPPH assay. In any case, all the samples exhibited strong antioxidant properties and a higher TPC than the starting CWF (Table 5.3.1).

Table 5.4.1. Antioxidant properties of HTS and MTS recovered by a sequential two-step DES-based treatment of CWF. Reported are the mean ± SD values of at least three experiments. Values in the same column without a common italic letter (a-c) are significantly different ($p < 0.05$).

Sample	EC_{50} (mg/mL) (DPPH assay)	Trolox eqs (mg of Trolox/mg of sample) (FRAP assay)	Gallic acid eqs (mg of gallic acid/mg of sample) (TPC Assay)
MTS	0.024 ± 0.001^{a}	0.42 ± 0.02^{a}	1.23 ± 0.06^{a}
HTS (1% KCl)	0.0468 ± 0.0001^{b}	0.19 ± 0.01^{b}	1.05 ± 0.01^{b}
HTS (0.01 M HCl)	0.0545 ± 0.0002^{c}	0.16 ± 0.01^{b}	1.01 ± 0.02^{b}

As expected, the UV-Vis spectrum and the chromatographic profile of MTS (Figure 5.4.1) showed an absorption maximum at 367 nm and a single peak eluted at ca. 35 min, respectively, indicative of the presence of EA. Quantitative analysis indicated an EA content of 31 ± 4% w/w. On the other hand, HTS contained only 0.4% w/w EA, highlighting the selectivity of the two-step treatment to provide both an EA-rich sample and an EA-free, lignin-rich sample. Based on the EA content and on the antioxidant properties of standard EA reported in Table 5.3.1, it can be concluded again that the antioxidant properties of MTS are due not only to the high content of EA but also to the presence different non-chromatographable phenolic compounds.

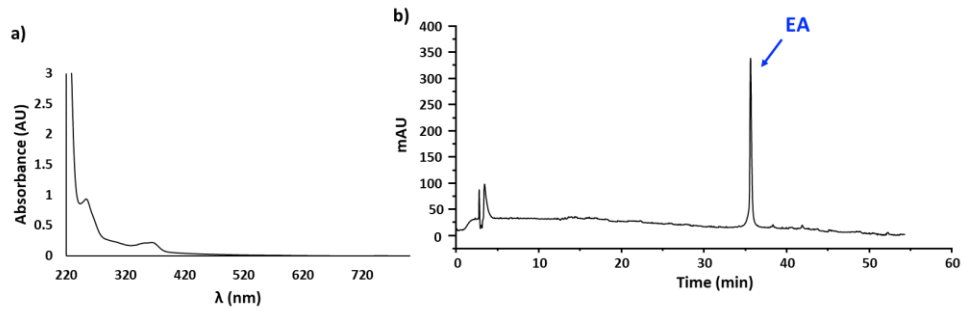

Figure 5.4.1. (a) UV-Vis spectrum (recorded at 0.015 mg/mL in methanol, stating from a 5 mg/mL DMSO solution) and (b) HPLC profile of MTS (recorded at 0.3 mg/mL in methanol, stating from a 5 mg/mL DMSO solution).

5.4.1 Characterization of the main phenolic components of MTS and HTS

The characterization of the main phenolic components (other than EA) present in MTS and HTS was performed by ATR-FTIR and EPR analysis. The ATR-FTIR spectrum of MTS (Figure 5.4.1.1) was, as expected, almost superimposable to that of pure EA, although the two sharp peaks in the 2950–2850 cm^{-1} region associated to the C−H stretching vibration of lignins[150] were also present. On the other hand, HTS did not showed the peculiar signals of EA in the 1700-500 cm^{-1} region, in agreement with the remarkable low content determined by HPLC analysis.

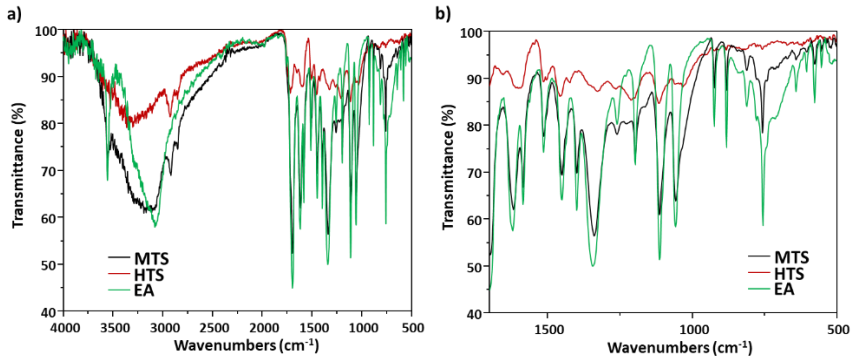

Figure 5.4.1.1. (a) ATR-FTIR spectra of MTS (black trace), HTS (red trace) and standard EA (green trace). (b) Expanded plot in the region 1700-500 cm^{-1}.

EPR analysis (Figure 5.4.1.2) confirmed the efficacy of the two-step treatment in providing a lignin fraction with good purity (HTS), as evident from the relatively high spin density and the low ΔB values, indicating, together with the power saturation profile, a homogenous free radical population. Interestingly, despite the high content of EA, MTS showed a well-detectable EPR signal too, likely due to low-molecular weight lignins extracted during the initial mild treatment, in agreement with the presence of the signals at 2950–2850 cm^{-1} in the ATR-FTIR spectrum.

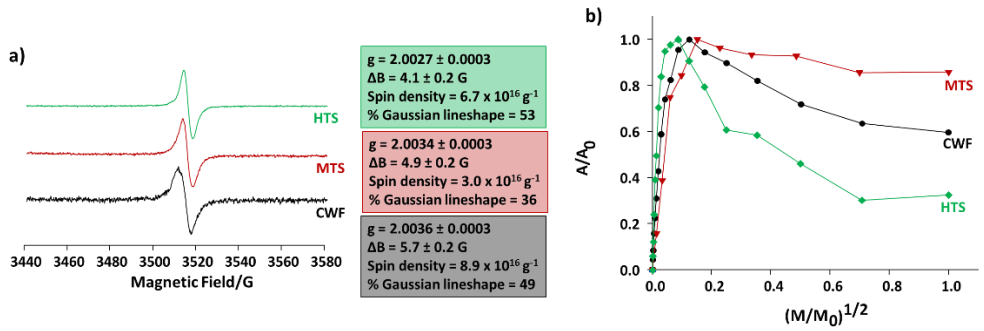

Figure 5.4.1.2. (a) Solid state EPR spectra and (b) power saturation profiles of starting CWF (black trace), MTS (red trace) and HTS (green trace).

To further characterize HTS, alkaline hydrogen peroxide and acid degradation were performed. The HPLC profile of the alkaline hydrogen peroxide degradation mixture of HTS showed, among others, two main peaks eluted at 25.0 and 26.7 min which were identified as vanillic and syringic acid, respectively (Figure 5.4.1.3a), based on a comparison of the chromatographic properties with those of authentic standards. These data are indicative of the presence of syringyl and guaiacyl units in HTS, in agreement with the results of structural analysis of lignin in chestnut wood performed by pyrolysis.[275] On the other hand, no detectable amounts of EA were observed in the HPLC profile of the supernatant from the acid degradation mixture (Figure 5.4.1.3b), ruling out the presence of significant amounts of residual hydrolyzable chestnut tannins in HTS.

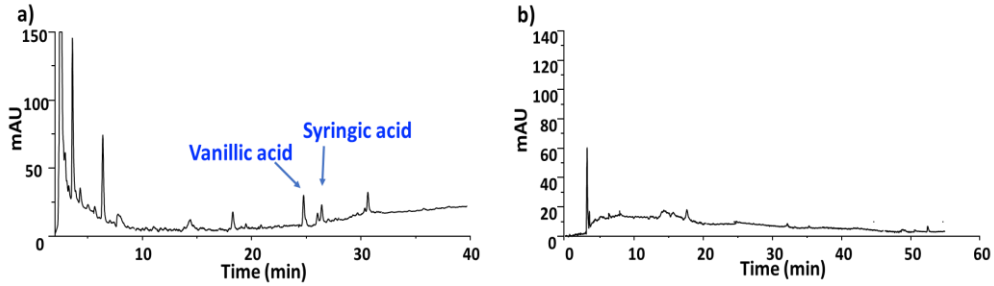

Figure 5.4.1.3. HPLC profiles of the chemical degradation mixtures of HTS. (a) Alkaline hydrogen peroxide degradation mixture. (b) Supernatant from the acid degradation mixture.

5.5 DES-based lignin extraction from edible nut shells

Based on the results reported in the previous paragraphs, the possibility to exploit the ChCl:LA2 developed protocol for the recovery of lignin from other agri-food by-products, such as edible nut shells, was assessed. In particular, pistachio, chestnut, pecan, hazelnut and peanut shells were selected.

At first, the different nut shells were roughly grinded with a blender and then homogeneously pulverized with a ball mill (15 min, 50 oscillations/s). A ball mill is a type of grinder which works on the principle of impact and attrition: size reduction is done by impact of the balls drop from near the top of the shells. Shells pulverization was found to be crucial in order to decrease the particles size, increasing the surface extension and thus making the extraction process more efficient.

The samples were then extracted by using ChCl:LA2 under the harsh experimental conditions (100 g/kg s/l ratio, 120 °C, 20% w/w of water) previously described, for 24 h. As indicated in the Paragraph 5.3, lignin was recovered by precipitation with 0.01 M HCl and subsequent centrifugation and lyophilization. In Table 5.5.1 the extraction yields obtained from the different shells are reported, pointing to pecan nut shells as the best sample in term of solid lignin recovery yield. On the other hand, peanuts exhibited the lowest yields.

Table 5.5.1. Lignin extraction yields obtained from different shells.

Shells	Yields (%)
Pistachio	27
Chestnut	19
Pecan	33
Hazelnut	25
Peanut	19

5.5.1 Antioxidant properties of nut shells lignins

The recovered lignins, as well as the starting materials, were characterized in term of antioxidant properties. The results are reported in Figure 5.5.1.1a. In the DPPH assay, among the starting materials the lowest EC_{50} values were determined for pecan nut shells and chestnut shells, which showed EC_{50} values of about 0.1 mg/mL, whereas pistachio shells exhibited an EC_{50} value ca. 66 times higher.

Regarding the antioxidant properties of lignins, chestnut pecan nut shells samples showed again the most promising results, with a 4-fold and 1.3-fold EC_{50} values reduction with respect to the starting materials. Peanut and hazelnut lignins also showed a significant decrease in the DPPH-reducing capability, with EC_{50} values about 6- and 9-fold lower than that determined for the starting by-products, respectively. Pistachio lignin showed an EC_{50} value up to 55-fold lower than that observed for the pistachio waste and represented the material with the most significant improvement in the antioxidant properties.

A similar trend was observed in the FRAP assay. Chestnut shells and pecan nut shells were found to be the most active among the waste materials, while hazelnut, pistachio and peanuts were characterized by a lower number of Trolox eqs. In contrast with the DPPH assay, chestnut shells lignin showed a comparable activity to that of the starting by-product, while pecan shells lignin exhibited a worsening of the reducing properties of about 3 times. In the case of the other three samples, peanut, hazelnut and pistachio lignins showed a number of Trolox eqs 2-, 3- and 3-fold higher than the starting wastes, in that order (Figure 5.5.1.1b).

In order to obtain information on the main constituents responsible for the antioxidant properties observed, in a last series of experiments the TPC was determined for each by-product and the corresponding lignin. Chestnut and pecan nut shells exhibited the highest phenolic content compared to the other wastes, as

expected based on the results of the DPPH and FRAP assays. All the lignin samples exhibited an increase in TPC (Figure 5.5.1.1c).

Notably, in the case of pecan nut shell lignin, despite the sample showed only a slight increase in the DPPH-reducing ability and a worsening in the ferric-reducing properties, a remarkable increase in the number of gallic acid eqs (up to 10-fold) with respect to the starting material, was observed. These differences are likely a consequence of the different solubility of the sample in the strongly alkaline medium used for the TPC assay compared to the reaction media used in the DPPH and the FRAP assays.

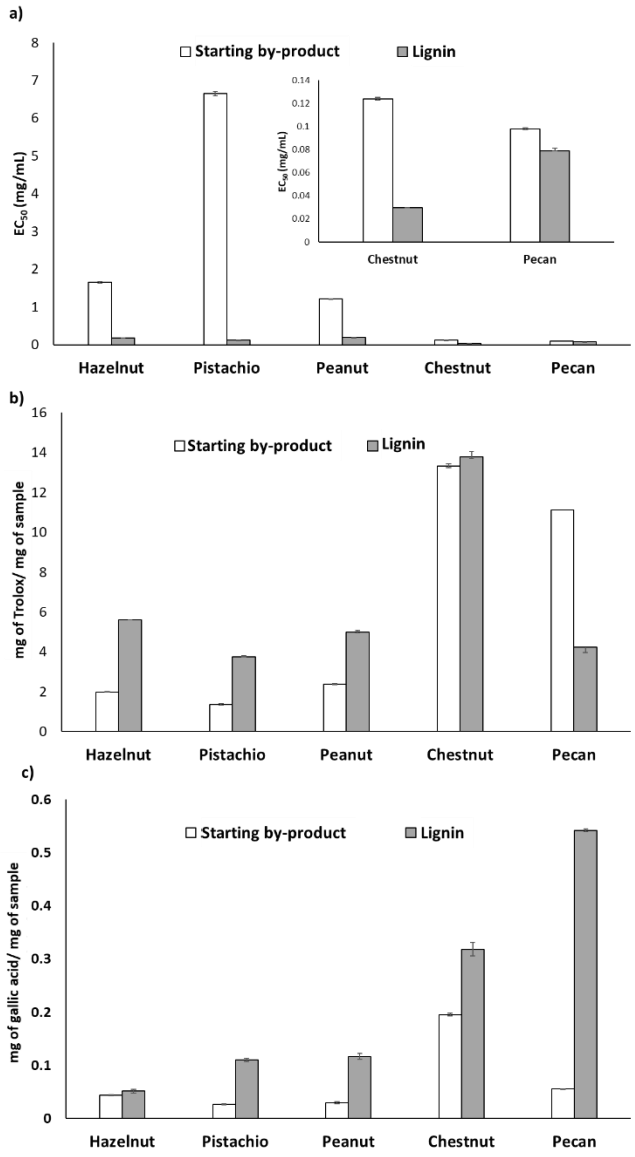

Figure 5.5.1.1. Antioxidant properties and TPC of selected nut shells and lignin thereof. (a) DPPH assay; (b) FRAP assay; (c) TPC assay. Reported are the mean ± SD values of at least three experiments.

5.5.2 Structural characterization of nut shell-derived lignins

To gain further information on the nature of the DES-recovered lignins, the DMSO-soluble fractions of the different extracted materials were analyzed by HPLC after proper dilution in methanol. Most of the elutographic profiles did not show the presence of detectable species, suggesting the absence of low molecular weight, chromatographable phenolic compounds in the lignin samples. Only in the case of the chestnut shell-derived sample a main peak at around 36 min was detected, due to the presence of EA (in ca. 2% w/w yield, with respect to the starting material) (Figure 5.5.2.1).

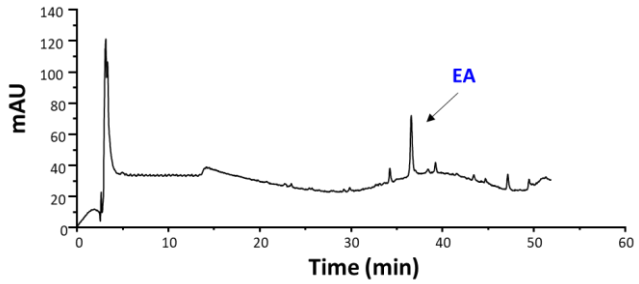

Figure 5.5.2.1. HPLC profile of the DMSO soluble fraction of chestnut shell lignin.

To gain an insight into the structural features of the recovered, in subsequent experiments an ATR-FTIR analysis was carried out. As an example, the ATR-FTIR spectra of pistachio shells and extracted lignin are reported in Figure 5.5.2.2, showing the presence of the signals at around 2950–2850 cm^{-1}, typically associated to the C−H stretching vibration of lignins.[150] In particular, a marked decrease in the signal at around 1000 cm^{-1}, associated to C–O–C skeletal vibration of in polysaccharides was observed in the lignin sample,[276] probably due to the removal of this component from the starting material further to DES-based treatment.

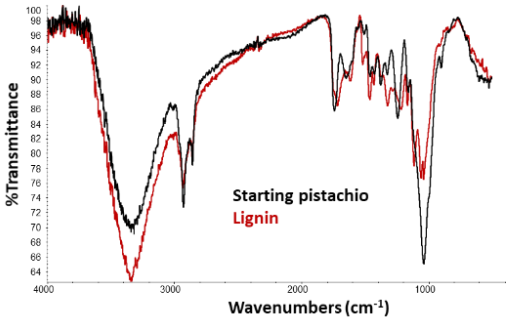

Figure 5.5.2.2. ATR-FTIR spectra of pistachio waste (black line) and lignin (red line).

To rule out the presence of condensed tannins in the extracted samples, since it is well known that these compounds are other important phenolic constituents of nut shells,[277,278] vanillin-HCl assay was performed. The highest catechin eqs values were observed for chestnut and pecan nut shells (Figure 5.5.2.3), with the other samples exhibiting a significant lower or even a zero content of condensed tannins. In any case, no condensed tannins were found in the extracted lignins.

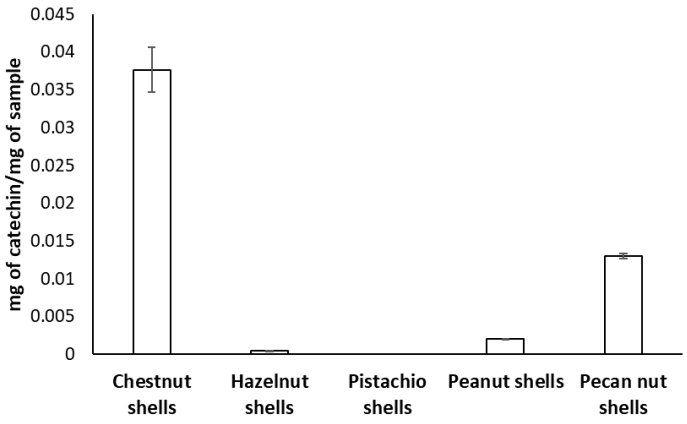

Figure 5.5.2.3. Condensed tannins content in the selected nut by-products determined by vanillin-HCl assay. Reported are the mean ± SD values of at least three experiments.

Finally, alkaline hydrogen peroxide was performed on all the shell samples. As an example, the HPLC profile of the alkaline hydrogen peroxide degradation mixture of pistachio shell-derived lignin showed, among others, two main peaks eluted at 25.0

and 26.7 min which were identified, as in the case of CWF, as vanillic and syringic acid, respectively (Figure 5.5.2.4).

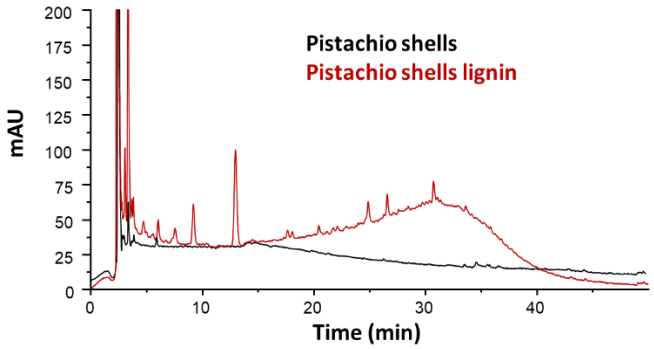

Figure 5.5.2.4. HPLC elution profiles alkaline hydrogen peroxide degradation mixture of pistachio by-product and lignin thereof.

5.6 Conclusions

In this Chapter, a straightforward, low-cost, and smart green protocol has been described based for the selective recovery of value-added phenolic compounds from CWF. In particular, an *ad hoc* two step treatment was carried out, involving a first mild step, in which the extraction was carried out with ChCl:TA2, affording EA in high yields, and a harsh step on residual CWF, in which ChCl:LA2 allowed to obtain an extract containing mainly a structurally homogeneous guaiacyl-syringyl lignin, as demonstrated by EPR and chemical degradation analysis. Both extracts were characterized by a high TPC and potent antioxidant properties.

The harsh treatment was then preliminarily applied to the extraction of lignin-rich materials from nut by-products. The developed protocol could therefore be exploited for the valorization also of other agri-food by-products for the selective recovery of both low- and high-molecular weight phenolic compounds for application as antioxidant additives in the biomedical, food and/or cosmetic sector.

5.7 Experimental section

Materials and methods

CWF was obtained from exhausted chestnut wood after drying in an oven overnight at 60 °C followed by milling to obtain <250 μm particles and was provided by Silvateam (S. Michele Mondovì, Cuneo, Italy).

Pistachios, chestnuts, pecan nuts, hazelnuts and peanuts were purchased in a local supermarket. The nut shells were grinded with a blender and then homogeneously pulverized with a ball mill (15 min, 50 oscillations/s) before extraction.

All solvents and reagents were obtained from commercial sources and used without further purification.

UV-Vis spectra were recorded using a HewlettPackard 8453 Agilent spectrophotometer.

ATR-FTIR spectra were recorded on a Nicolet 5700 Thermo Fisher Scientific instrument. Spectra were recorded as an average of 128 scans in the range 4000−450 cm^{-1} (resolution of 4 cm^{-1}).

^{1}H NMR spectra were recorded in DMSO-d_6 at 400 MHz on a Bruker instrument.

EPR measurements were performed using a Bruker Elexys E-500 spectrometer equipped with a superhigh sensitivity probe head. The samples were transferred to flame-sealed glass capillaries, which in turn were coaxially inserted in a standard 4 mm quartz sample tube. Measurements were performed at room temperature. The instrumental settings were as follows: sweep width, 140 G; resolution, 1024 points; modulation amplitude, 1.0 G; conversion time 20.5 ms; time constant 10.24 ms. The amplitude of the field modulation was preventively checked to be low enough to avoid detectable signal overmodulation. The number of scans and microwave power

were optimized to avoid microwave saturation of resonance absorption curve. For power saturation experiments, the microwave power was gradually incremented from 0.001 to 127 mW. The g value and the spin density were evaluated by means of an internal standard, Mn^{2+}-doped MgO, prepared by a synthesis protocol reported in the literature.[199] The EPR spectra of the DMSO soluble samples (20 µL in a flame-sealed glass capillary) were acquired at a microwave power equal to 7.93 mW, which was preventively checked to be a non-saturating condition. For these measurements, a TEMPO solution in DMSO (10^{-5} mol/kg) was used as an external standard in order to estimate the sample spin density.

HPLC analysis were performed with an Agilent instrument equipped with a UV-Vis detector; a Phenomenex Sphereclone ODS column (250 x 4.60 mm, 5 µm) was used, at a flow rate of 1.0 mL/min. A gradient elution using 0.1% formic acid in water (solvent A) and methanol (solvent B) was performed as follows: 5% B, 0-10 min; from 5 to 80% B, 10-57.5 min. The detection wavelength was set at 254 nm.

5.7.1 DES preparation. Twenty-five different DES were prepared as reported.[257] Briefly, different HBA and HBD were mixed at appropriate ratios and heated under stirring at proper temperatures until a homogeneous liquid was formed. All the solvents were stored at ambient temperature. No crystal precipitation was observed over the period of use.

5.7.2 DES screening for extraction of antioxidant compounds from CWF 0.2 g of CWF was added at 66.7 g/Kg s/l ratio to the different solvents containing 30% w/w of water. After stirring for 60 min at 40 °C, the mixtures were centrifuged at 5000 rpm for 10 min. Extracts were diluted 1:5 v/v in methanol before further analysis. Control experiments were performed using water, ethanol, or methanol as conventional solvents, under the same conditions.

5.7.3 Optimization of the extraction conditions using independent variables. Treatment of CWF with 2:1 mol/mol ChCl:TA2 was repeated by sequentially varying the s/l ratio (33.3-200 g/Kg), the extraction time (60-180 min), the extraction temperature (40-90 °C), and the percentage of water (20-50% w/w).

5.7.4 Experimental design for optimization of extraction conditions. A central composite design (CCD) was used to investigate the effects of extraction time, temperature, s/l ratio, and the percentage of added water on the recovery of antioxidants from CWF. The CCD consisted of a full two-level factorial design (24 points), eight axial points at a distance ±α from the central point and six replicates of the central point. The value of α was taken as $(2^4)^{1/4} = 2$, to ensure the orthogonality and rotatability of the design. Factor levels were chosen based on the results of preliminary experiments and literature studies.

The yield of antioxidant extraction, expressed as g of gallic acid eqs per 100 g of the starting material, was taken as the response variable. Overall, the experimental design consisted of 30 runs (Table 5.7.4.1), which were performed in random order to minimize the effects of uncontrolled factors.

The statistical design and analysis of experiments were performed using the Design-Expert® software (version 7.0.0, Stat-Ease, Inc., Minneapolis, MN, USA).

Table 5.7.4.1. Experimental design layout and observed response (y = g of gallic acid eqs per 100 g of the starting material). SO is the standard order of experiments and RO is the run order.

SO	RO	Factor level				Response y
		E (min)	T (°C)	R (g/Kg)	W (% w/w)	(g/100g)
1	10	60	50	40	30	13.12
2	2	120	50	40	30	13.98
3	26	60	70	40	30	18.13
4	6	120	70	40	30	21.90
5	20	60	50	80	30	9.40
6	12	120	50	80	30	10.16
7	30	60	70	80	30	11.99
8	13	120	70	80	30	14.97
9	7	60	50	40	50	19.37
10	21	120	50	40	50	18.72
11	9	60	70	40	50	25.07
12	29	120	70	40	50	20.74
13	23	60	50	80	50	16.64
14	16	120	50	80	50	16.62
15	19	60	70	80	50	16.89
16	8	120	70	80	50	18.36
17	1	30	60	60	40	15.53
18	3	150	60	60	40	16.64
19	24	90	40	60	40	15.31
20	17	90	80	60	40	20.08
21	18	90	60	20	40	23.89
22	5	90	60	100	40	13.22
23	27	90	60	60	20	10.41
24	4	90	60	60	60	20.89
25	14	90	60	60	40	13.72
26	15	90	60	60	40	15.78
27	11	90	60	60	40	11.66
28	22	90	60	60	40	18.35
29	28	90	60	60	40	16.11
30	25	90	60	60	40	18.00

5.7.5 Lignin recovery with DES under harsh conditions.[267,268] 2 g of CWF was added to 20 g of ChCl:TA2, or ChCl:LA2 containing 20% w/w water, and the mixture was taken under stirring for 8 h at 120 °C. After cooling, 15 mL of ethanol were added, and the suspension was vacuum filtered. Subsequently, the solid residue was washed twice with 50 mL of ethanol. The liquid phases collected from initial

filtration and washing of the solid were combined and taken to a rotary evaporator to remove the organic solvent. Then, two different protocols were applied to precipitate lignin: a) The dark brown liquid was poured into 200 mL of 7:3 v/v acetone/water and stirred for 2 h; acetone was then removed in a rotary evaporator at 60 °C, after that water was added until precipitation of a brown solid was observed; the precipitate was collected by filtration, washed three times with 1:9 v/v ethanol/water, and lyophilized to give 200 mg of a brown powder (10% w/w yield with respect to starting CWF). b) The dark brown liquid was poured into 130 mL of 0.01 M HCl and the precipitated solid was collected as above (203 mg, 10% w/w yield with respect to starting CWF).

When required, the brown powder obtained was suspended in DMSO (10 mg/mL) and after 72 h the mixture was centrifuged (7000 rpm, 15 min): the supernatant was collected and stored until further analysis, whereas the precipitate was washed three times with 0.01 M HCl and recovered by lyophilization (44-52% w/w).

In the case of nut by-products, the lignin extraction was carried out adding 10 g of each by-product to 100 g of ChCl:LA2 containing 20% w/w water, and the mixture was taken under stirring for 24 h at 120 °C. After cooling, the sample was centrifuged at 7000 rpm for 15 min. The residual solid was washed three times with 100 mL of ethanol, which was then removed in a rotary evaporator at 60 °C. The supernatant obtained from the first centrifugation was added to 1 L of 0.01 M HCl (pH 2). The formed precipitate was then centrifuged (7000 rpm, 10 min, 4 °C), washed twice with 0.01 M HCl, once with water and eventually recovered by lyophilization.

5.7.6 Sequential two-step DES-based treatment of CWF. 1 g of CWF was added to 10 g of ChCl:TA2 containing 20% w/w water, and the mixture was taken under stirring in a pyrex glass bottle at 50 °C for 90 min (mild treatment). Then, the residual solid was separated from the supernatant by centrifugation (7000 rpm, 20

min), and the latter was poured into 100 mL of 1% KCl aqueous solution and kept at room temperature for 4 h. The precipitate that separated was recovered by centrifugation (7000 rpm, 20 min, 4 °C), washed three times with 1% KCl and lyophilized to give 75 mg of sample (mild treatment sample (MTS), 7.5% or 28% w/w yield with respect to starting CWF or dissolved CWF, respectively). The residual solid was instead added to 10 g of ChCl:LA2 containing 20% w/w water, and the mixture was taken under stirring in a pyrex glass bottle at 120 °C for 8 h. The dark brown liquids collected by subsequent centrifugation (7000 rpm, 20 min, 4°C) were poured into 100 mL of 1% KCl aqueous solution or 0.01 M HCl and kept at 4°C for 24 h. The formed precipitates were then recovered by centrifugation (7000 rpm, 20 min, 4°C), washed three times with 1% KCl or 0.01 M HCl and lyophilized (harsh treatment sample (HTS), 50 mg, ca. 5% or 10% w/w yield with respect to starting CWF or dissolved CWF for both precipitation protocols).

5.7.7 Folin-Ciocalteu assay.[178] Diluted CWF extracts (10–200 μL) were added to 2.1 mL of water followed by 0.15 mL of Folin-Ciocalteu's reagent and 0.45 mL of a 75 g/L Na_2CO_3 solution. After 30 min incubation at 40 °C, absorbance at 765 nm was measured. For solid samples, these were added at final doses of 0.0025-0.8 mg/mL to the same solutions as above. Gallic acid was used as reference compound. Experiments were run in triplicate.

5.7.8 Antioxidant assays: DPPH assay.[175,176] Diluted CWF extracts (15-375 μL) were added to 3 mL of a 0.2 mM ethanolic solution of DPPH, and after 10 min under stirring at room temperature the absorbance at 515 nm was measured. In the case of solid samples, these were added at 0.0025-0.9 mg/mL to the DPPH solution and the mixtures were analyzed as above. Trolox was used as a reference antioxidant. Experiments were run in triplicate. **FRAP assay**.[177] To 3 mL of 0.3 M acetate buffer (pH 3.6) containing 1.7 mM $FeCl_3$ and 0.83 mM TPTZ, 0.75-30 μL of diluted extracts were added, and after 10 min under stirring at room temperature the absorbance of the solutions at 593 nm was measured. In the case of the solid

samples, these were added at final doses of 0.000625-0.4 mg/mL to the FRAP solution and the mixtures were analyzed as above. Results were expressed as Trolox eqs. Experiments were run in triplicate.

5.7.9 Alkaline hydrogen peroxide degradation.[179] 10 mg of sample were suspended in 1 M NaOH (1 mL), and 50 µL of 30% H_2O_2 was added. The mixture was kept at room temperature under vigorous stirring and after 24 h treated with 5% $Na_2S_2O_5$ in water, taken to pH 3 with 6 M HCl, filtered on a 0.45 µm PVDF filter, and analyzed by HPLC.

5.7.10 Acid degradation.[184] 50 mg of sample were treated in a pyrex tube with 5 mL of 4 M HCl at 90 ◦C for 24 h. The mixtures were then allowed to cool to room temperature, taken to pH 2.5 by addition of 6 M NaOH, and centrifuged (7000 rpm, 10 min). The supernatants were recovered, taken to 10 mL by addition of water, and analyzed by HPLC after filtration on a 0.45 µm PVDF filter. The solid residues were dissolved in 10 mL of DMSO/methanol 1:1 v/v and analyzed by HPLC as well.

5.7.11 Vanillin-HCl Assay.[279] Nuts by-products and lignin solutions in DMSO were added (final dose 0.0625–2 mg/mL) to 1 mL of a 1% w/vanillin solution in methanol. 1 mL of 9 M HCl was added, and the mixture was incubated at 30 °C for 10 min. Finally, the absorbance at 500 nm was measured. Catechin was used as reference compound. Experiments were run in triplicate.

Chapter 6

Agri-food wastes as sustainable functional additives in food packaging and antibacterial devices

6.1 Introduction

As previously mentioned, in recent years, agri-food by-product valorization has received great attention in a green and circular economy perspective. In this context, the production of value-added compounds endowed with health promoting and other functional properties from agri-food by-products to be used in different fields, provides several economic, social, and environmental benefits, therefore in the last decade many studies have been aimed at the production of sustainable food additives, nutraceuticals, pharmaceuticals, and cosmeceuticals from these sources.[112,280] In particular, the incorporation of agri-food waste materials in polymeric films, to be used, for example, in the food related applications or for preparation of antimicrobial functional devices has received considerable attention.[280,281]

Regarding food applications, oxidation and microbial spoilage are the main causes of deterioration of foods along the different stages of the supply chain, that is production, transport, processing, storage, and marketing,[282] and of course cause negative effects on food quality, including a decrease of the nutritional properties as well as changes in color, taste and odor. Furthermore, the presence of pathogenic microorganisms increases the risk of foodborne diseases.[282] These processes are of course directly related to food losses and therefore significantly affect waste production and economy.

A strategy to protect food against external contamination, physical damage, light, microorganisms, humidity, and chemical degradation, is the use of active food

packaging, that allows to preserve food quality and shelf-life, thus minimizing food losses and wastage. Active packaging is not only a real physical barrier to protect food and act as a selective barrier to gases, but is also able to delay or prevent microbiological spoilage and oxidative degradation processes.[282,283]

Despite their widespread use and usefulness, packaging materials are actually one of the major sources of waste. EUROSTAT reported that in EU, packaging produced approximately 77.7 million tons of wastes in 2018, with paper and cardboard generating about 41% of total packaging waste (31.8 million tons), followed by plastics (19%, 14.8 million tons) and glass (14.5 million tons).[284] Among synthetic plastics, polyvinylchloride (PVC), polyethylene terephthalate (PET), polypropylene (PP), polyethylene (PE), polyamide (PA) and polystyrene (PS) are the most commonly used.[285] These polymers are characterized by excellent mechanical and barrier properties. They are soft, light, transparent and cost-effective, which make them particularly preferred among packaging materials.[282] However, the use of synthetic polymers is becoming more and more limited, because of their non-recyclable and/or non-biodegradable nature. Therefore, the development and utilization of alternative bio-based and biodegradable materials deriving from biopolymers, is increasingly attracting attention.

Biopolymers can be classified into four categories:[282,283]

- Biomass-derived polymers, directly extracted from biomass, including polysaccharides (starches, lignocellulosic products, pectins, gums), lipids and proteins (casein, whey proteins, collagen/gelatin, zein, soy, and gluten);
- Polymers produced by microbial metabolism, e.g polyhydroxylalkanoates (PHAs), including poly(hydroxybutyrate) (PHB) and poly(3-hydroxybutyrate-co-3-hydroxyvalerate) (PHBV);
- Polymers chemically synthesized using monomers obtained from agricultural resources, e.g. poly(lactic acid) (PLA);

- Polymers obtained by chemical synthesis from fossil resources (aliphatic co-polyesters, aromatic co-polyesters) e.g. poly(ε-caprolactone) (PCL), poly(esteramides) (PEA), aliphatic co-polyesters (e.g., PBSA) and aromatic co-polyesters (e.g., PBAT).

Biopolymers are generally inexpensive, non-toxic, and resistant to mechanical damage; moreover, they may show excellent water vapor permeability properties (that makes them particularly interesting in the fresh product packaging) and good film-forming abilities, acting as barrier against odors and aromas but also against fats and oils migration,.[280,286] and, above all, they are biodegradable. Most of them can in fact be degraded by naturally-occurring organisms, producing environmental-friendly by-products.[287] Therefore, the use of biopolymers in food packaging systems may allow the reduction of environmental impacts and waste generation. On the other hand, when compared to synthetic polymers, biopolymers show some drawbacks, such as fragility, low flexibility and low heat distortion temperature.[287] Recently, biopolymers have been also used in a variety of biomedical applications, due to their biocompatibility and specific biological properties. As an example, chitosan show excellent antimicrobial properties, and chitosan-based films have therefore been recently used not only in food packaging, but also in biomedical fields, as antimicrobial devices for healthcare applications.[288]

As stated above, in active packaging systems the polymeric film does not play the sole role of container or barrier, but it interacts with food to extend shelf-life and improve its quality. In this context, with the aim of improving also biopolymer-based film performance, in recent years the use of agri-food by-product-derived phenolic compounds as functional additives have become increasingly attractive,[289–294] since they may provide antioxidant properties, antimicrobial activity, improved mechanical properties, and improved food quality. In addition. The incorporation of natural bioactive compounds represents an alternative to minimize the use of preservative chemical additives. Actually, proliferation of pathogenic bacteria

represents an important issue not only in food, but also for human health, hence phenol-rich agricultural and food industry by-products are an attractive source of natural and sustainable additives to be used also in biomedical applications. As an example, antibacterial devices composed of biopolymers added with agri-food wastes and nanomaterials with broad antibacterial activity (for example silver nanoparticles, here indicated as AgNPs) have been recently widely described.[295,296]

6.2 Pecan nut shell as a functional polyphenol source for active packaging

As previously reported, pecan (*Carya illinoinensis*) nuts are a major agricultural product in states such as Mexico and United States, where the highest production (more than 90%) is concentrated, followed by South Africa and Australia. However, their use is recently spreading also in other country, in particular in China. Since about 50% w/w of the fruit is not edible,[297] pecan nut production and processing generates high volumes of wastes, constituted mainly of nut shells. Pecan nut shells contain mainly fiber (cellulose, hemicellulose) and high amounts of antioxidant phenolic polymers, like lignin and condensed tannins.[298] Recently, the incorporation of a phenol-rich pecan nut shell hydroalcoholic extract (PNSE) into PE and PLA films has been reported. In particular, PNSE was found to act as a polymer thermal and photochemical stabilizer, both in an oxygen-depleted environment and in the presence of oxygen during polymer service life.[277] In another work, fractionation of pecan nut shells provided two components, a fibrous polysaccharide and an acid insoluble lignin fraction, which when incorporated as fillers in PLA-based biocomposites were found to be able to reinforce the polymer and control its aging.[299] Inclusion of PNSE in octenyl succinate starch films has been described too, providing films with improved water resistance and UV-light barrier properties.[300]

On this basis, in this Chapter the attention will be focused on the use of pecan nut shell as a low-cost, safe, and sustainable additive for the preparation of polymeric

films to be used in food packaging. In particular, the functional properties of the PNSE-containing PE and PLA films were assessed. Furthermore, the water-soluble constituents of PNSE were incorporated into whey protein (WP) films. Indeed, functionalization of milk whey proteins (WP)-based films with natural antioxidant and/or antimicrobial additives has been recently received considerable attention, prompted by the increasing need for full green approaches to novel functional materials.[301]

In particular, the investigations carried out in the frame of these studies were directed to:

a. Characterization of the functional properties of PNSE;
b. Preparation, morphological and mechanical characterization of PNSE-functionalized PE, PLA and WP films;
c. Evaluation of the possible exploitation of the PNS-functionalized films in the food packaging sector.

This part of the PhD project was carried out in collaboration with Professor Andreas Schieber of the Institute of Nutritional and Food Sciences, University of Bonn (Bonn, Germany), as envisaged by the PON Ricerca e Innovazione 2014-2020, Azione I.1 “Dottorati Innovativi con caratterizzazione Industriale”) PhD project.

6.2.1 Characterization of the functional properties of PNSE

6.2.1.1 Characterization of the main phenolic components of PNSE

In a first series of experiments, the phenolic composition of PNSE was investigated by spectroscopic (UV-Vis and EPR analysis) and chromatographic (HPLC) techniques. Furthermore, chemical degradation treatments commonly used for the qualitative and quantitative analysis of phenolic polymers, such as thiolysis, phloroglucinolysis, and alkali fusion, were carried out.

The UV-Vis spectrum of PNSE showed the presence of an absorption maximum at 278 nm, with a shoulder at around 300 nm (Figure 6.2.1.1.1a). As reported in Chapter 2, these spectrum features may be related to the presence of phenolic compounds such as condensed tannins. This hypothesis was in part confirmed by EPR analysis. The EPR spectrum of PNSE showed indeed a typical signal of a phenolic polymer at a g value of 2.0035 ± 0.0002 (Figure 6.2.1.1.1b). A spin density of 5.4 ± 0.5 × 10^{14} spin/g and a relatively large ΔB value of 5.1 ± 0.2 G was found, probably related to a low extent of π-electron conjugation across the phenolic polymer moieties. The Lorentian lineshape percentage was found to be about 75%. Moreover, the normalized power saturation profile (Figure 6.2.1.1.1c) showed only a slope change in a monotonously increasing trend, suggesting a high molecular heterogeneity in the paramagnetic centers, in line with the hypothesis of the presence of condensed tannins in the samples.

The DMSO-soluble fraction of PNSE was analyzed by HPLC, after proper dilution in methanol. However, the chromatographic profile showed very low amounts of chromatographically defined compounds.

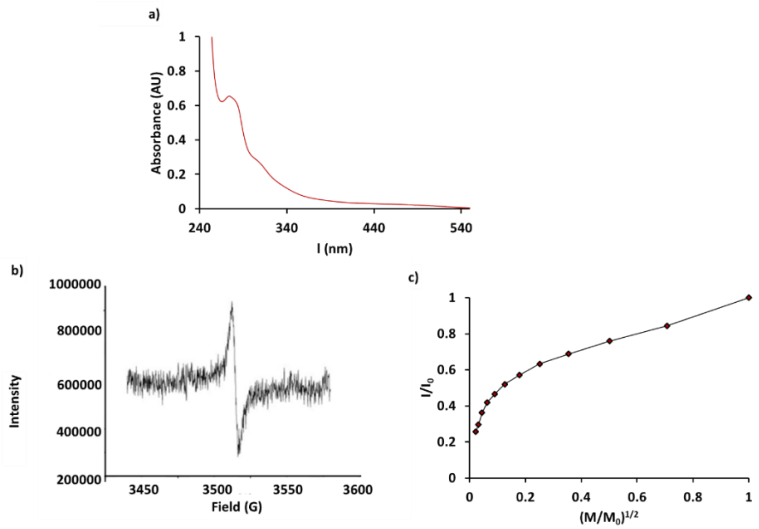

Figure 6.2.1.1.1. (a) UV-Vis spectrum of a 0.2 mg/mL PNSE solution in methanol; (b) EPR spectrum and (c) EPR power saturation profile of PNSE.

To gain further information about the nature of its phenolic components, PNSE was subjected to chemical degradation treatments. As previously described, alkali fusion is commonly employed to analyze insoluble and complex phenolic polymers and is based on the identification of low-molecular weight markers derived from oxidative degradation of the polymer.[183] On the other hand, thiolysis and phloroglucinolysis are acid-catalyzed depolymerization protocols carried out in the presence of a strong nucleophile, and are used as a validated approach for the characterization of condensed tannins.[302,303] In the case of PNSE, the chromatographic profiles of degradation mixtures showed (epi)gallocatechin, (epi)catechin and hydroxybenzoic acids as the main cleavage products (Figure 6.2.1.1.2),). In particular, phloroglucinolysis experiments revealed a rather high mean degree of polymerization (mDP) value (Table 6.2.1.1.1) and (epi)gallocatechin as the most abundant terminal and extension unit, suggestive of prodelphinidin-type tannins.

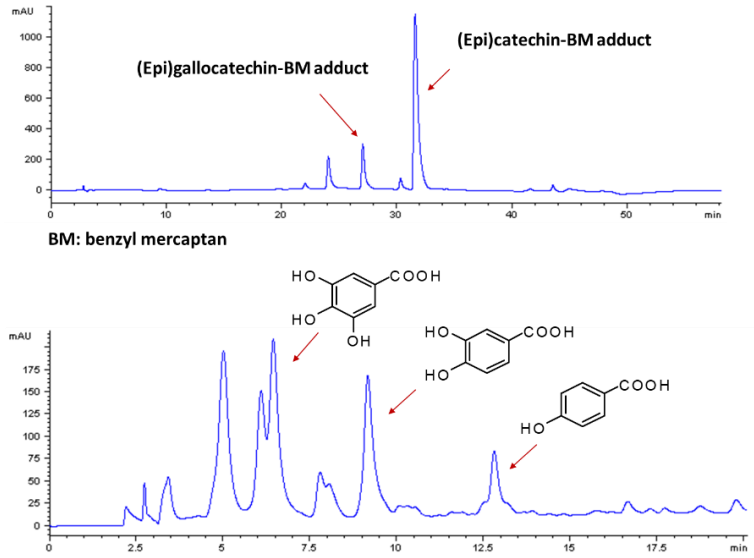

Figure 6.2.1.1.2. HPLC profiles and identified compounds of (a) thiolysis mixture and (b) alkali fusion mixture of PNSE.

Table 6.2.1.1.1. Composition of proanthocyanidins in PNSE determined by phloroglucinolysis degradation experiments. Calculated mean degree of polymerization (mDP) is 20.1.

Compound	Composition of terminal units (%)	Composition of extension units (%)
Catechin	33.4	6.0
Epicatechin	0	15.8
(Epi)gallocatechin	53.3	77.4
Epicatechin gallate	1.5	0.2
(Epi)gallocatechin gallate	3.1	0.3
(Epi)afzelechin	8.2	0.2
A-type dimers	0	0.1

6.2.1.2 Evaluation of the antioxidant properties of PNSE

The antioxidant properties of PNSE were investigated by DPPH and FRAP assays. The DPPH assay indicated an EC_{50} value of 4.00 ± 0.01 µg/mL, 1.5-fold lower than that observed with the standard antioxidant Trolox (6.00 ± 0.02 µg/mL), demonstrating very efficient antioxidant properties of this material in organic solvents. On the other hand, a value of only 0.18 ± 0.01 Trolox eqs was measured in the FRAP assay, probably due to a lower PNSE solubility in the aqueous assay medium.

6.2.1.3 Evaluation of PNSE cellular biocompatibility

Before evaluating the food relevant functional properties of PNSE, its biocompatibility was demonstrated by the 3-(4,5-dimethyl-2-thiazolyl)-2,5-diphenyl-2H-tetrazolium bromide (MTT) reduction assay on HepG2 cells, which are widely used to study the toxicity and the chemopreventive potential of antioxidant compounds.[304] PNSE did not show significant toxic effects over a time of 72 h at concentrations up to 50 µg/mL (Figure 6.2.1.3.1), which can be considered a possible concentration for the use of extracts as food additive.[150]

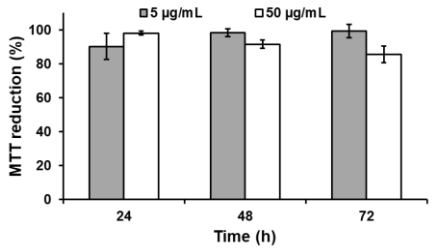

Figure 6.2.1.3.1. Effect of PNSE on HepG2 cell viability determined by MTT assay at different times. Reported are the mean ± SD values of at least three experiments.

6.2.1.4 Enzymatic browning inhibition properties of PNSE

In another series of experiments, the inhibitory properties of PNSE toward mushroom tyrosinase were investigated, using L-DOPA or L-tyrosine as the substrate. Indeed, tyrosinase belongs to the enzyme class of polyphenol oxidases, which play a critical role in the oxidative deterioration of food products, particularly fruit and vegetables. PNSE showed IC_{50} values of 55 ± 6 and 70 ± 16 µg/mL for the catecholase and cresolase activity of the enzyme (Figure 6.2.1.4.1), respectively, which were only slightly lower than that obtained for kojic acid, generally used as a reference compound in this assay.[23] Based on the promising results obtained against mushroom tyrosinase, the enzymatic browning inhibition properties of PNSE in apple smoothies were evaluated. Apples were blended in the presence of a 0.085% PNSE solution, and the additive was found to be able to significant inhibit the onset of browning of about 40% after 3 h (Figure 6.2.1.4.2).

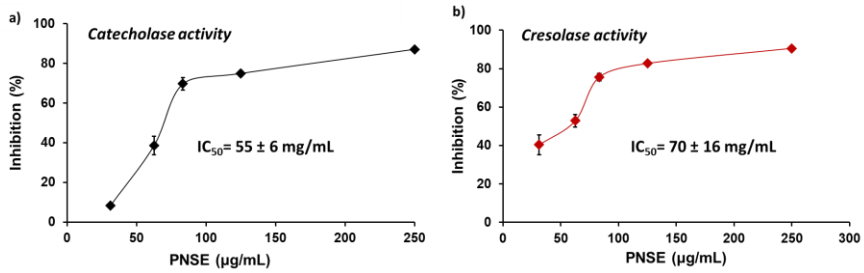

Figure 6.2.1.4.1. Inhibition activity of PNSE against mushroom tyrosinase using L-DOPA (catecholase activity) or L-tyrosine (cresolase activity) as substrate.

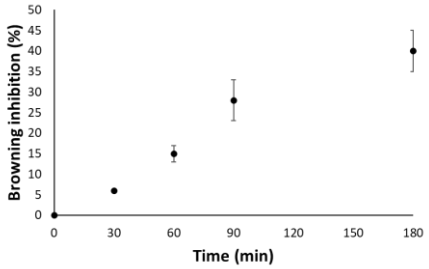

Figure 6.2.1.4.2. Effects of PNSE on the enzymatic browning of apple smoothies. Reported are the mean ± SD values of at least three experiments.

6.2.1.5 Anthocyanin stabilization capacity of PNSE

In a final set of experiments, the effect of PNSE on anthocyanin stability was determined. Anthocyanins are commonly used as food additives for their capability to impart specific colour and for their health-beneficial properties. However, the use of anthocyanins is limited by the high susceptibility to degradation, with consequent colour loss, depending, among other, on light, pH, and temperature.[305–307] Different studies have demonstrated the capability of phenolic compounds to inhibit anthocyanin degradation due to their ability to form non-covalent complexes with these compounds through π-stacking interactions.[308,309] Therefore, the ability of PNSE to stabilize anthocyanins at high temperature, that is under accelerated storage conditions,[310] was evaluated. Notably, a significant increase in the heat stability of anthocyanins was observed in presence of PNSE even at a concentration as low as 0.02 mg/mL (Figure 6.2.1.5.1a), at which no stabilizing effect was observed with well-known anthocyanin stabilizers, such as ferulic and chlorogenic acids (Figure 6.2.1.5.1b).[311,312] Further experiments were carried out using a commercial bilberry juice, and the results showed again a stabilizing activity of PNSE with a dose-dependent effects, leading to an almost 50% lower decrease in anthocyanin content at 2 mg/mL (Figure 6.2.1.5.1c).

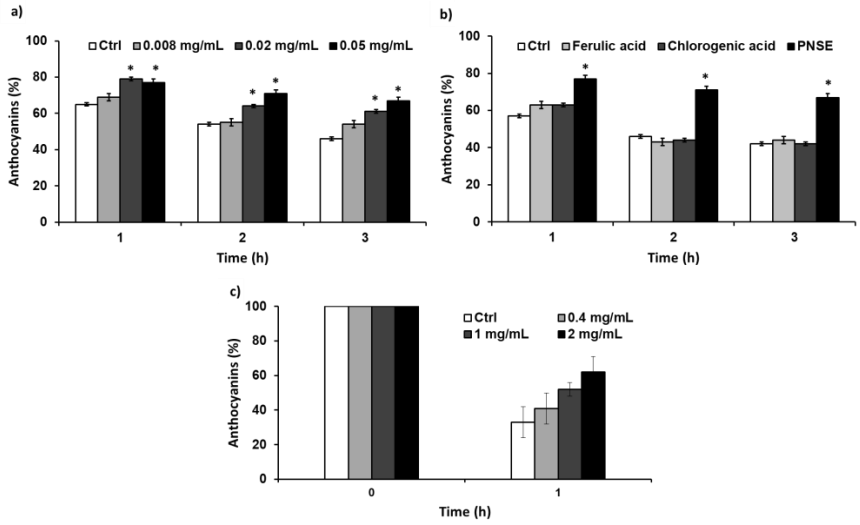

Figure 6.2.1.5.1. Effect on a red wine-anthocyanin solution stability at 90 °C of (a) PNSE at different doses, (b) in comparison with references phenolic compounds (all at 0.05 mg/mL). (c) Effect of PNSE on anthocyanin stability at 90 °C in a bilberry juice. *$p < 0.05$ compared to control. Reported are the mean ± SD values of at least three experiments.

6.2.1.6 Preparation and antimicrobial activity evaluation of a PNSE-water soluble fraction

In a second series of experiments aimed at the preparation of functionalized WP films, an aqueous solution of PNSE was prepared, given the need to work in water dictated by the protein nature of the polymeric matrix. In particular, a 30 mg/mL water solution of PNSE was prepared, which was found to be stable at room temperature at least over 1 week as determined by UV–vis analyses, indicating no variation in its absorption spectra. This solution was then preliminarily investigated for its antimicrobial activity and was found to induce a complete growth inhibition against food relevant pathogens such as *Salmonella enterica subsp. enterica ser. Typhimurium* (ATCC® 14028) (MIC_{100}= 7.5 mg/mL) and *Enterococcus faecalis* (ATCC® 29212) (MIC_{100}= 1.85 mg/mL).

6.2.2 Assessment of the possible exploitation of PNS-functionalized films in the food packaging sector

Prompted by its interesting properties, the possibility to use PNSE as a functional additive for active packaging was evaluated, after incorporation in PE, PLA and WP films.

While PE is one of the most industrially used synthetic polymers, PLA is one of the most studied biopolymers. It is a biodegradable aliphatic polyester, which can be produced by fermentation of renewable sources such as corn, cassava, potato and sugarcane.[313] As far as applications in the food sector are concerned, PLA possesses:[314]

- Transparency;
- Selective permeability against carbon dioxide compared to oxygen;
- Good mechanical, fat and oil and water resistance;
- Low melting temperatures, that make it easily processable.

In addition it may act as an ultraviolet light barrier, is biocompatible, biodegradable over period of months, and recyclable, since it can be hydrolyzed back to lactic acid under mild and environmentally friendly conditions.[314]

On the other hand, WP are another largely available biomass for film production. The world production of whey is estimated to be around 180 million tons/year, and WP represent about 15–20% of the total milk proteins. The main fractions of WP are β-lactoglobulin and α-lactalbumin, that possess exceptional film forming abilities, leading to transparent, flexible, colourless, and odourless materials. Furthermore, they show good oil/gas barrier properties at relatively low humidity. However, WP-based films are characterized by poor water barrier properties due to their hydrophilicity.[315]

At first, PE and PLA films containing PNSE at different doses, were prepared in collaboration with the Institute for Polymers, Composites and Biomaterials (IPCB-

CNR) of Pozzuoli (Naples) in Italy, by extrusion and solvent-casting techniques.[277] In the case of WP films, a film forming solution, containing glycerol, WP and the water solution of PNSE was prepared as previously reported.[316,317] WP-based films were then produced using the solvent casting technique.[316]

6.2.2.1 Evaluation of the antioxidant properties of PE and PLA films containing PNSE

PLA and PE films containing PNSE at different doses were then tested for their antioxidant properties. In the case of extruded films, PNSE was incorporated at 1, 2 and 3% w/w. In the DPPH assay, the functionalized films showed significant antioxidant properties in a dose-dependent manner, particularly evident in the case of PLA containing PNSE at 3% w/w, that induced a DPPH reduction higher than 80% after 1 week, while, under the same conditions, PE was able to decrease DPPH solution absorbance only up to 30% (Figure 6.2.2.1.1a,b) (the obtained data were corrected for the spontaneous decay over time of DPPH). On the other hand, solvent-cast PLA films containing PNSE at 3% and 10% w/w showed remarkably higher antioxidant properties compared to those obtained by extrusion. The 10% w/w PNSE containing PLA film, in particular, was found to be able to induce a 60% reduction of DPPH after only 30 min (Figure 6.2.2.1.2a), and both films, at 3 and 10% w/w loading, completely reduced DPPH after 1 day. It was not possible to prepare PE films by solvent casting, due to its extremely low solubility in most solvents.

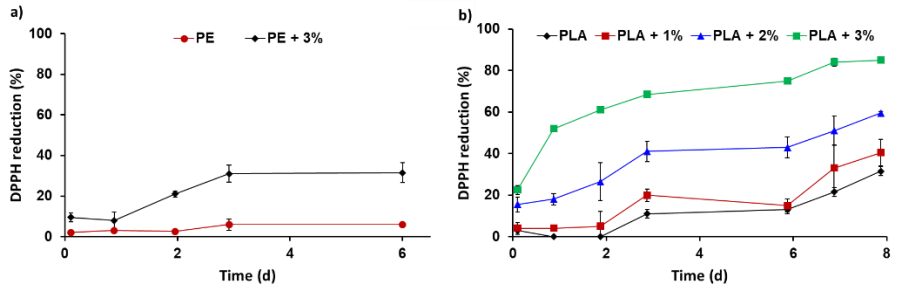

Figure 6.2.2.1.1. Antioxidant properties determined by DPPH assay of extruded (a) PE and (b) PLA films, containing PNSE at different doses. Reported are the mean ± SD values of at least three experiments.

Due to their promising reducing properties against DPPH compared to extruded films, the antioxidant activity of the solvent-cast PLA films was also evaluated by the FRAP assay (Figure 6.2.2.1.2b). Trolox equivalent values of 0.78×10^{-3} and 1.26×10^{-3} were exhibited by the films incorporated with 3% and 10% w/w of PNSE, respectively, after 96 h.

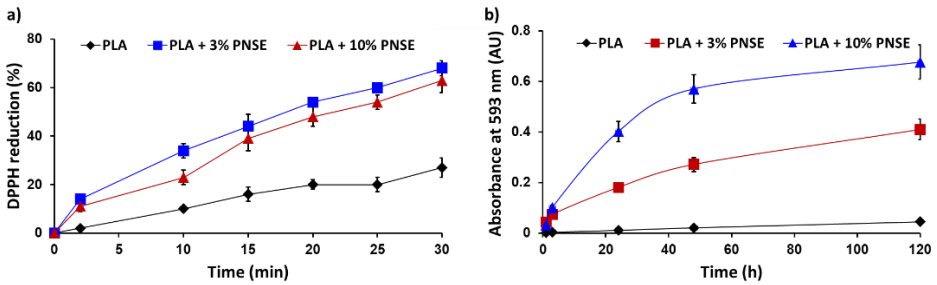

Figure 6.2.2.1.2. Antioxidant properties of solvent-cast PLA films containing PNSE determined by (a) DPPH and (b) FRAP assays. Reported are the mean ± SD values of at least three experiments.

In order to interpret the different results obtained from the two functionalized polymers in the two assays, release experiments were carried out in the antioxidant assay media (ethanol, in the case of DPPH assay, and sodium acetate at pH = 3.6, in

the case of FRAP assay). Extruded films did not release PNSE in ethanol, reflecting the low antioxidant properties observed in the DPPH assay, while solvent-cast films released almost all the incorporated PNSE, thus showing a higher antioxidant power (Figure 6.2.2.1.3). On the other hand, in acidic aqueous media, solvent-cast PLA films did not release PNSE, probably due to its low solubility in water.

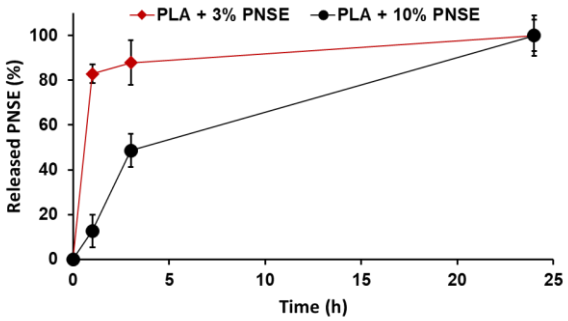

Figure 6.2.2.1.3. Release of PNSE from solvent casting-prepared PLA films in the DPPH assay medium. Reported are the mean ± SD values of at least three experiments.

6.2.2.2 Enzymatic browning inhibition properties of solvent-cast PLA films containing PNSE.

PNSE-functionalized PLA films were also investigated for their capability to act as inhibitors of enzymatic browning in apple smoothies. As shown in Figure 6.2.2.2.1a,b, PLA alone or incorporated with 3% w/w PNSE did not exert any effect on enzymatic browning, while in the presence of 10% w/w PNSE a 30% inhibition was observed, highlighting the ability of PNSE to delay enzymatic browning processes even when incorporated in PLA films.

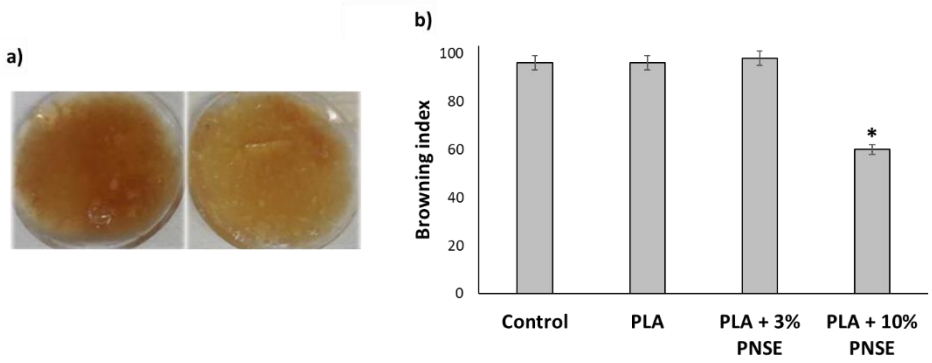

Figure 6.2.2.2.1. (a) Effects on apple smoothies enzymatic browning of solvent-cast neat PLA film (left) and PLA film containing 10% w/w PNSE (right), (b) browning index calculated after 3 h. *$p < 0.05$ compared to control.

6.2.2.3 Evaluation of the antioxidant properties of WP films containing PNSE

As for PE and PLA films, the antioxidant properties of the WP films containing PNSE were also evaluated. DPPH assay did not indicate any reducing properties for the PNSE-functionalized films. On the contrary, interesting results were obtained in the FRAP assay (Figure 6.2.2.3.1a), which allowed to determine for the functionalized film a Trolox equivalent value 2.4 times higher than that of the control film after 4 h (0.6 ± 0.1 μg/mg *vs* 0.27 ± 0.02 μg/mg). This result again highlighted the ability of PNSE to impart significant antioxidant properties to the film, although the film alone also showed slight reducing properties, likely due to the capability of some WP amino acids to act as electron donors.[318] The marked differences between the results obtained in the DPPH and FRAP assays can be interpreted on the basis of the higher affinity of the protein-based films for the aqueous medium used in the second assay compared to the organic solvent in which the DPPH assay was performed. To verify if the antioxidant properties of the WP/PNSE film were associated to a release of PNSE, as in the case of solvent-cast PLA films, release experiments were performed in the FRAP medium. The solution was periodically analyzed by UV–vis spectroscopy in comparison with a solution of

the control film. The results shown in Figure 6.2.2.3.1b indicated a significant release of WP (λ_{max} 286 nm) from the control film. Notably, a remarkable lower absorption was observed in the case of the PNSE-functionalized film (Figure 6.2.2.3.1b), suggesting a kind of waterproofing action of PNSE preventing protein leaching. Indeed, assuming that the absorption at 280 nm is due to WP, the lower absorption observed in the case of WP/PNSE compared to WP (0.24 *vs* 0.92, respectively) (Figure 6.2.2.3.1b) could indicate a lower release of WP in the solution, thus confirming that the tannin components in PNSE, that are known to strongly interact with proteins,[319] contribute to reinforce the WP film structure.

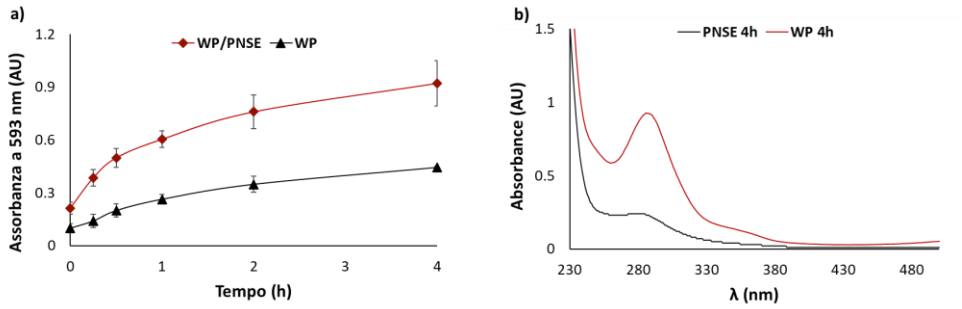

Figure 6.2.2.3.1. (a) Antioxidant properties of the WP and WP/PNSE films determined by FRAP assay. (b) Comparison of the spectra of the WP and WP/PNSE film solutions in 0.3 M acetate buffer (pH 3.6) after4 h. Reported are the mean ± SD values of at least three experiments.

6.2.2.4 Evaluation of the antimicrobial activity of WP films containing PNSE

The antimicrobial effects of WP-based films were tested on *Salmonella enterica subsp. enterica ser. Typhimurium* (ATCC® 14028) and on *Enterococcus faecalis* (ATCC® 29212). The results showed that bacterial cell growth was inhibited only in the presence of PNSE and only in the area in direct contact with the film (Figure 6.2.2.4.1). Since the additive was not released by the film (see above), it can act as microbial growth inhibitor only on bacterial cells at direct contact with the film.

These data would therefore suggest the PNSE could be suitable to be applied in the control and prevention of bacterial contaminations in food.

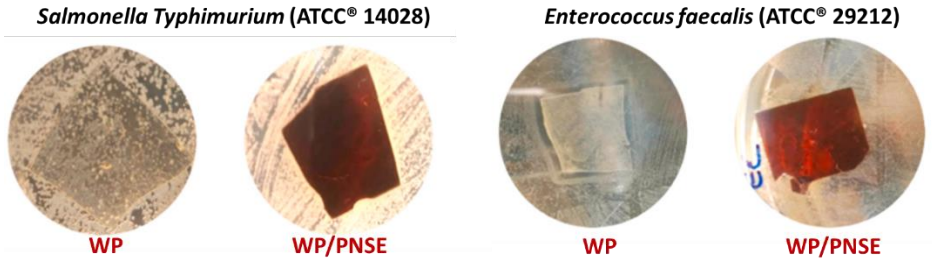

Figure 6.2.2.4.1. Antimicrobial activity of WP films containing PNSE evaluated against *Salmonella enterica subsp. enterica ser. Typhimurium* ATCC® 14028 and *Enterococcus faecalis* ATCC® 29212.

6.2.3 Morphological and mechanical characterization of PNSE-functionalized PE, PLA and WP films

6.2.3.1 Morphological characterization of PE and PLA films containing PNSE

Extruded PE and PLA films containing PNSE at 3% w/w were initially characterized by SEM, which revealed the presence of submicrometer-sized PNSE particles (indicated by arrows) well distributed in PE, while in the case of PLA films particle agglomerates could be observed (Figure 6.2.3.1.1a). In light of this findings, the poor antioxidant properties of extruded films observed in the DPPH assay could be due to the efficient PNSE particle embedding in the polymeric matrix.[320,321] Indeed, in the extrusion technique, the high temperatures melt the polymer, and the mechanical shear due to screw rotation allows for comminution of the additive and efficient blending with the polymer matrix. The subsequent roll calendaring process results in the formation of a thin film in which the additive is finely dispersed. On the other hand, the solvent-cast PLA films were prepared without mechanical shear and the film formation is based on the slow solvent evaporation. This process could cause the polymer to settle on the bottom of the container, while the extract remains

on the top, leading to a coating layer rather than a real incorporation. This layer measured about 30 µm on the film surface (Figure 6.2.3.1.1b). Therefore, in this case PNSE is expected to diffuse in the assay media, thus resulting in higher antioxidant properties.

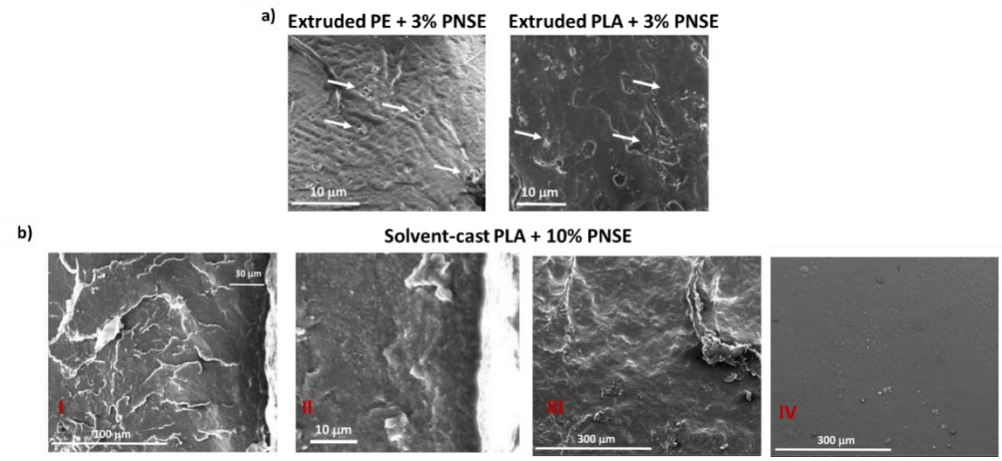

Figure 6.2.3.1.1. (a) SEM images of cross-sections of extruded PE + 3% PNSE (left) and PLA + 3% PNSE (right) films. (b) SEM images of cross-section (I and II), top surface (PNSE-rich) (III), and bottom surface (PLA-rich) (IV) of solvent-cast PLA + 10% PNSE films.

6.2.3.2 Mechanical characterization of PLA films containing PNSE

In view of the promising antioxidant properties of the solvent-cast PLA, only the films prepared under this process were further investigated and characterized. In particular, ATR-FTIR analysis, mechanical characterization (in term of strain at break, modulus and stress at break) and oxygen permeability experiments were carried out. The incorporation of PNSE in PLA films provided a fairly homogeneous dark red coloration (Figure 6.2.3.2.1).

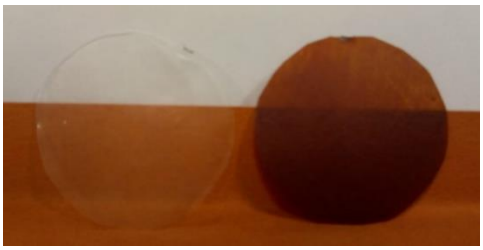

Figure 6.2.3.2.1. Digital photo of solvent-cast neat PLA film (left) and PLA film containing 10% w/w PNSE (right).

The ATR-FTIR spectrum of the PNSE-containing PLA film (Figure 6.2.3.2.2) showed the appearance of signals at 3300 cm^{-1} due to the phenol O−H stretching, at 1613 cm^{-1} due to the presence of aromatic C=C, and 1538 and 1515 cm^{-1}, associated to in-plane bending of phenyl C−H bonds.[277,322] On the other hand, the presence of PNSE did not affect the absorption frequency of the PLA carbonyl groups, as evident by the unmodified signal at 1750 cm^{-1}, indicating the absence of significant interactions between the polymer and the additive (Figure 6.2.3.2.2).

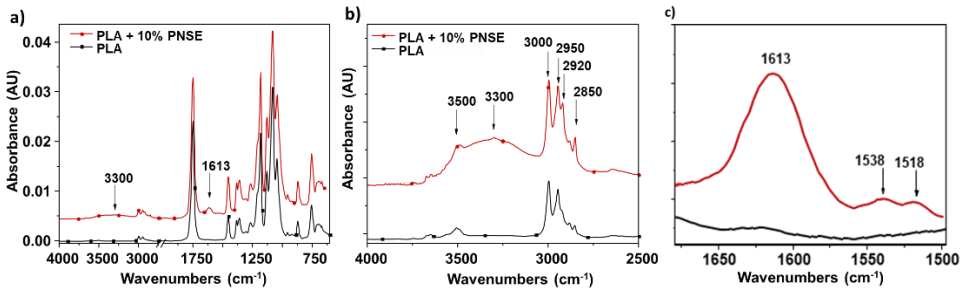

Figure 6.2.3.2.2. (a) FTIR-ATR spectra and enlargement of the (b) 4000-2500 cm^{-1} and (c) 1700-1500 cm^{-1} region of solvent-cast PLA and PLA + 10% PNSE films.

The mechanical properties of the solvent-cast films were measured by tensile tests. Strain and stress at break, and elastic modulus values of PLA and PLA+10% PNSE are shown in Table 6.2.3.2.1. PNSE slightly affected the strain at break value of PLA, which decreased from 41% to 32%, probably due to the presence of PNSE aggregates, formed during solvent casting process (evident also in the SEM images)

(Figure 6.2.3.2.3), which are able to accelerate cracks.[277] PNSE slightly affected also the modulus and stress at break, as reported for other natural additives or fillers.[277,322,323] In another set of experiments, oxygen transmission rate (OTR) experiments showed that the incorporation of PNSE did not significantly affect the oxygen permeability property of the film.

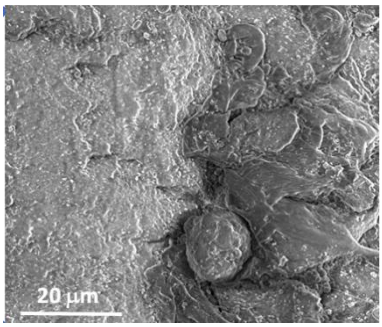

Figure 6.2.3.2.3. (a) SEM images of cross-section solvent-cast PLA films containing 10% of PNSE.

Table 6.2.3.2.1. Mechanical properties of solvent cast PLA films. Reported are the mean ± SD values of at least three experiments. Starred values in the same column are significantly different ($p < 0.05$).

	Strain at break (%)	**Modulus (MPa)**	**Stress at break (MPa)**
PLA	41 ± 20	1414 ± 411	25 ± 2*
PLA + 10% PNSE	32 ± 18	1454 ± 220	20 ± 2*

6.2.3.3 Mechanical characterization of WP films containing PNSE

The incorporation of PNSE in WP films provided homogeneous red films (Figure 6.2.3.3.1a). The mechanical properties determined for the films are reported in Figure 6.2.3.3.1b. Film thickness increased significantly ($p < 0.05$) in the presence of the extract. The PNSE-films were also found to be less flexible, as evident from the elongation at break and Young's modulus values. However, a significant increase in tensile strength was observed, probably due to the interaction between the amino groups of the polymer and phenolic compounds present in the extract.[324]

Interesting results were obtained for the water vapor, CO_2 and O_2 permeability of the film functionalized with PNSE. In contrast to what observed with PLA films, the barrier properties of WP films were found to be significantly higher ($p < 0.05$) compared to the unfunctionalized films (Figure 6.2.3.3.1c). These results are very important for a potential use of these materials in the food sector.

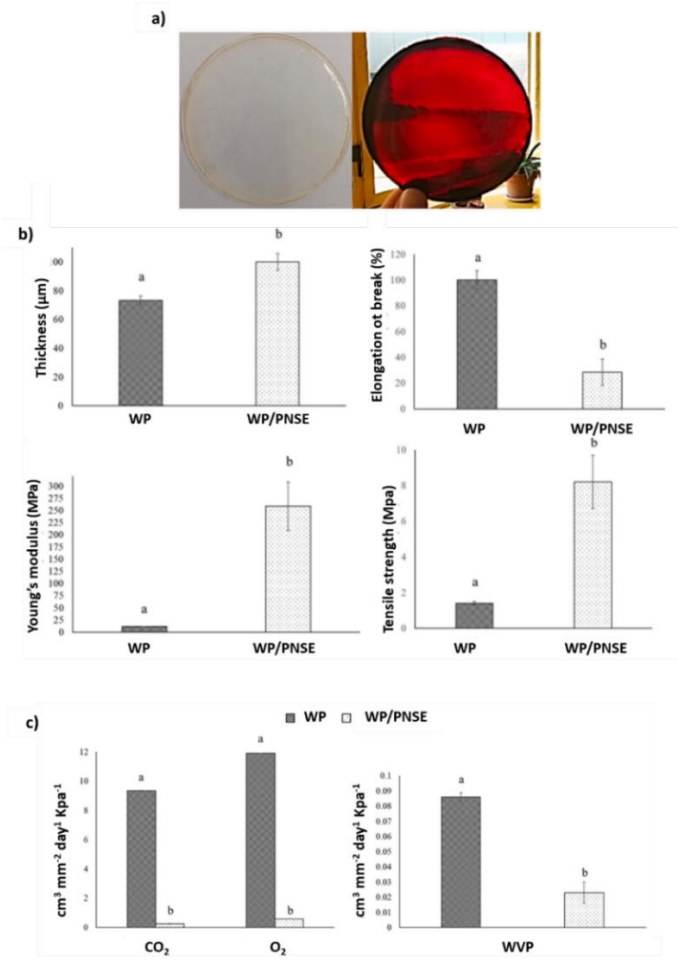

Figure 6.2.3.3.1. (a) Digital photos of neat WP film (left) and WP/PNSE film (right). (b) Effect of PNSE on the mechanical properties of WP-based films. (c) Barrier properties of WP-based films. Reported are the mean ± SD values of at least three experiments. Different letters indicate significant differences between the values reported in the same plot ($p < 0.05$).

6.3 SCG as a polyphenol-rich additive for the development of antibacterial devices

As previously reported, coffee is one of the most consumed beverages in the world and is responsible for the production of huge amounts of wastes, among which SCG. Given the high content of organic compounds, SCG represent a considerable pollution hazard when discarded in the environment. On the other hand, the high content of phenolic content makes SCG one of the most important agricultural by-product endowed with potent antioxidant properties which have prompted their use as a source of natural and sustainable additives for functionalization of materials for biomedical, technological, and food-related applications.[325] In particular, SCG has been also employed as reducing agents for the preparation of silver nanoparticles (AgNP),[326] which are particularly interesting for their bactericidal, antifungal and antitumor properties,[327] which have stimulated their exploitation for the functionalization of natural polymers and other materials[328,329] for the development of antimicrobial devices. As reported in Chapter 2, the antioxidant properties of SCG may be significantly improved by acid hydrolysis, and the hydrolyzed spent coffee grounds thus obtained, indicated as HSCG, were found to efficiently improve the thermal and photo-oxidative stability of polyethylene films and delayed lipid peroxidation when incorporated in fish and soybean oils.[150] Furthermore, the possible use of HSCG as a food supplement was also described, based on the antioxidant and prebiotic activity exhibited in a simulated gastrointestinal digestion/fermentation model.[181] In this context, in this paragraph the attention will be focused on the possible use of HSCG to induce the formation AgNPs for their incorporation in chitosan films, with the aim to develop new antimicrobial and antioxidant devices.

Specifically, the study was directed to:

d. Optimization of the reaction conditions of the synthesis of AgNP-HSCG;
e. Morphological and functional characterization of AgNP-HSCG;

f. Preparation of chitosan films containing AgNP-HSCG;
g. Morphological and functional characterization of chitosan films containing AgNP-HSCG.

6.3.1 Preparation, morphological and functional characterization of AgNP-HSCG

6.3.1.1 Optimization of AgNP-HSCG preparation conditions

In order to optimize the NPs preparation protocol, the effects of a series of parameters, such as solvent, reaction time, HSCG concentration, and silver ion concentration, were evaluated. At first, typical experiments were carried out using 8 or 40 mg of HSCG (final dose 0.2 or 1% w/w), added to 4 mL of a 2, 10 or 50 mM $AgNO_3$ solution in water. The suspension was kept under stirring at different temperatures (room temperature, 60 °C, 80 °C or 120 °C) for different times (30 min, 1 h, 3 h, 24 h, 72 h or 10 d).

Other experiments were also carried out under the following conditions:

- in ethanol, for 24 h, with 10 mM $AgNO_3$ and 1% HSCG;
- in the presence of 0.1 M KOH for 24 h with 2 mM $AgNO_3$ and 1% HSCG.

Control samples were prepared in the absence of $AgNO_3$.

At the end of incubation, the solid materials were recovered by centrifugation, then were extensively washed with water and lyophilized. X-ray diffraction (XRD) analysis revealed the presence, along with Ag(0), of also an AgCl crystalline phase in all the samples, likely due to the presence of residual chloride ions in the HSCG sample deriving from the hydrolytic activation treatment, which involves the use of concentrated HCl.[150] After several experiments, it was found that the parameter which significantly affected AgCl precipitation, and hence incorporation in the final material, was the reaction temperature. The best results were obtained at 120 °C, under which conditions a 6 ± 2 % w/w Ag(0) incorporation, with no traces of AgCl,

was obtained after only 3 h (Figure 6.3.1.1.1). Based on these results, incubation of 1% HSCG with 10 mM $AgNO_3$ at 120 °C for 3 h was chosen as the optimal condition for AgNP-HSCG preparation.

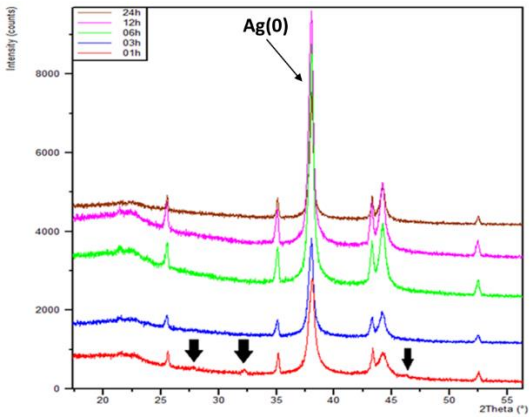

Figure 6.3.1.1.1. XRD profiles of 1% HSCG incubated with 10 mM $AgNO_3$ at 120 °C for different times (1-24 h). Arrows indicate diffraction peaks due to AgCl.

6.3.1.2 Morphological characterization of AgNP-HSCG

The AgNP-HSCG obtained under the optimal settings were then characterized by TEM, that showed a prevalence of particles with a spherical shape and a diameter size ranging from 15 to 25 nm with the tendency to form clusters of about 200 nm (Figure 6.3.1.2.1a).[330,331] These data were confirmed by DLS analysis that evidenced a bimodal particles distribution, with two distinct peaks at 21 and 255 nm (Figure 6.3.1.2.1b). The volume size distribution showed that, on a mass basis, the majority of the sample consisted of small particles around 21 nm with a 9:1 ratio of small particles to aggregates. UV-Vis analysis of the resuspended material did not reveal the broad plasma resonance peak around 450 nm typically attributed to AgNPs,[330] likely suggesting efficient embedding and stabilization of reduced silver in the organic material.

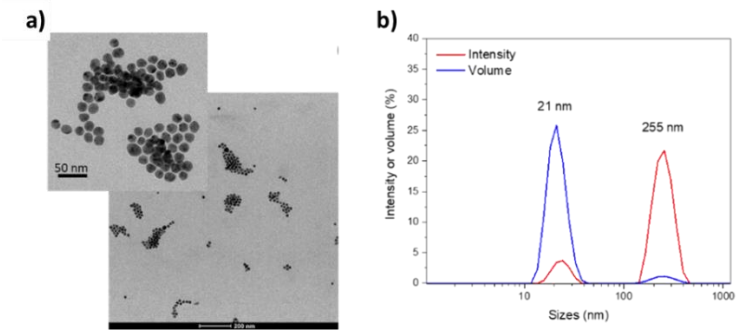

Figure 6.3.1.2.1. (a) TEM images and (b) DLS analysis of 1% HSCG incubated with 10 mM $AgNO_3$ at 120 °C for 3 h (AgNP-HSCG).

6.3.1.3 Functional characterization of AgNP-HSCG

At first, the antioxidant properties of AgNP-HSCG were evaluated with respect to untreated HSCG. In both DPPH and FRAP assays, AgNP-HSCG exhibited antioxidant properties only 20% lower than HSCG, suggesting that only a limited portion of the phenolic moieties (mainly lignin) of HSCG is involved in the silver ion reduction process. AgNP-HSCG also showed significantly higher antimicrobial activity with respect to AgNP-SCG analysed in other studies.[332] AgNP-HSCG was particularly active against Gram-negative bacteria *E. coli* ATCC25922 and *P. aeruginosa* ATCC27853, with minimal inhibitory concentration (MIC) values about 4-fold lower compared to that obtained against the Gram-positive bacterium *S. aureus* ATCC29213 (Table 6.3.1.3.1), and a minimal bactericidal concentration (MBC) value comparable to MIC against *P. aeruginosa*.

Table 6.3.1.3.1. MIC and MBC values of AgNP-HSCG expressed as µg/mL of the whole material (AgNP/HSCG) or silver (Ag(0)).

Strain	MIC (µg/mL) (AgNP-HSCG/Ag (0))	MBC (µg/mL) (AgNP-HSCG/Ag(0))
S. aureus ATCC29213	250/15	>1000/>60
E. coli ATCC25922	62/3.7	1000/60
P. aeruginosa ATCC27853	62/3.7	62/3.7

6.3.1.4 Preparation, morphological and mechanical characterization of chitosan films functionalized with AgNP-HSCG

Due to the promising antioxidant and antimicrobial properties, AgNP-HSCG were incorporated at 0.3, 0.6 and 2.0% w/w of AgNP in chitosan films (indicated as CH0.3, CH0.6 and CH2.0) and characterized in comparison with control chitosan films (CH0).

Chitosan is a linear polysaccharide composed of D-glucosamine (deacetylated unit) and N-acetyl-D-glucosamine (acetylated unit). It is produced by deacetylation of chitin, the structural element of the crustacean exoskeleton.[333] This polymer is characterized by natural antimicrobial activity, which promoted its application in different fields.[288,334] Chitosan shows high solubility in acetic acid and hydrochloric acid, and good film forming ability.. Chitosan-based films are flexible and durable to extension. Moreover, they are biodegradable and biocompatible, that make them suitable for e.g. biomedical applications.[288] Despite the high number of advantages, chitosan films are susceptible to humidity and are not appropriate for some applications due to their solubility in slightly acidic aqueous media.[288]

Addition of AgNP-HSCG provided differently coloured films, depending on additive concentration (Figure 6.3.1.4.1a). The films were characterized by SEM and ATR-FTIR spectroscopy. SEM images of pure chitosan film CH0 showed a smooth surface and a homogeneous and compact structure with very small cavities, due to the incorporation of air bubbles during the casting process (Figure 6.3.1.4.1b).

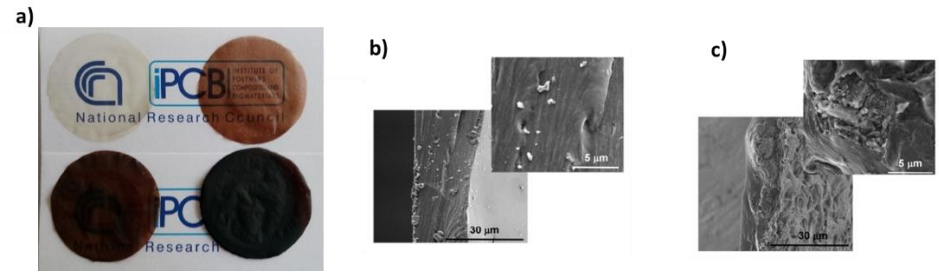

Figure 6.3.1.4.1. (a) Digital photos (from left to right and from top to bottom CH0, CH0.3, CH0.6 and CH2.0) and SEM images of cross-sections of: (b) CH0 and (c) CH2.0.

On the other hand, CH2.0 (Figure 6.3.1.4.1c) showed a rough surface, with HSCG aggregates embedded into the polymer matrix. AgNP were dispersed within the polymer matrix, with no evidence of particle lumps. ATR-FTIR analysis (Figure 6.3.1.4.2) showed, in the case of functionalized films, the presence of a shoulder at 1740-1710 cm^{-1} characteristic of hemicellulose acetyl groups and carboxylic acids, as well as a band at 1300-1200 cm^{-1}, related to C-O and C-H vibrations.[150,181] Furthermore, a shift of the anti-symmetrical stretching of the C-O-C bridge[335] from 1152 to 1154 cm^{-1} was also present, probably due to a reduction of the interactions between chitosan chains caused by AgNP-HSCG.

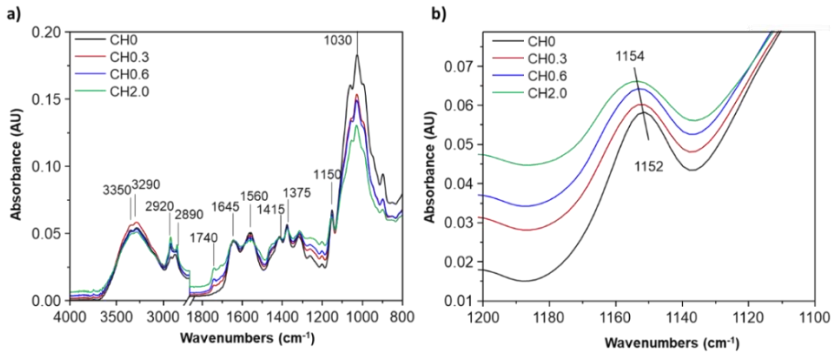

Figure 6.3.1.4.2. (a) FTIR-ATR spectra of the neat and incorporated chitosan films and (b) enlargement of the 1152 cm^{-1} absorption peak.

A significant increase of thickness was observed after incorporation of AgNP-HSCG, as expected based on literature evidence.[296,336] The stability of the films to moisture was also determined by swelling experiments. The swelling index, measured at 31 days, showed a decrease by increasing the AgNP-HSCG content. For pure chitosan, the swelling capacity cannot be determined because after 31 d the film appeared to be partly disrupted and massively blemished by microorganisms (Table 6.3.1.4.1) These results are in accordance with the hypothesis that the presence of AgNP-HSCG reduced the hydrophilicity of the film and protected it against biotic degradation, improving the long-term water stability. AgNP-HSCG also increased water vapour permeability (WVP) of chitosan, but not significantly affected the mechanical properties (Table 6.3.1.4.1). Actually, in the case of CH2.0, AgNP-HSCG had a negative effect on ductility due to the formation of aggregates acting as defects in the chitosan matrix, as evident from SEM images (Figure 6.3.1.4.1).

Table 6.3.1.4.1. Mechanical characterization of chitosan-based films. Reported are the mean ± SD values of at least three experiments.

	Thickness (µm)	**SI_{31d} (%)**	**WVP (g/m h Pa) × 10^{-12}**	**Strain at break (%)**	**Modulus (MPa)**	**Stress at break (MPa)**
CH0	34 ± 7	Not detected	1.34 ± 0.03	22 ± 12	1202 ± 279	23 ± 13
CH0.3	51 ± 18	301 ± 25	5.89 ± 0.07	27 ± 5	1093 ± 470	27 ± 13
CH0.6	47 ± 7	210 ± 18	3.35 ± 0.07	28 ± 4	1578 ± 212	30 ± 12
CH2.0	55 ± 4	178 ± 19	4.12 ± 0.08	19.1 ± 0.5	1333 ± 30	29.0 ± 0.8

6.3.1.5 Functional characterization of chitosan films containing AgNP-HSCG

The antioxidant properties of the chitosan films were evaluated by DPPH and FRAP assay. In the first case, functionalized chitosan films led to only 20% DPPH reduction after 6 h in the case of CH0.6 and CH2.0 (Figure 6.3.1.5.1a). On the other hand, efficient AgNP-HSCG dose-dependent reducing properties were determined in the FRAP assay, with CH2.0 exhibiting a Trolox equivalent values of 1.47×10^{-3} at 60 min (Figure 6.3.1.5.1b). The higher response of the films observed in the

FRAP assay was probably due to the higher affinity of chitosan for acidic aqueous media, compared to that for organic solvents, such as ethanol, used in the DPPH assay.

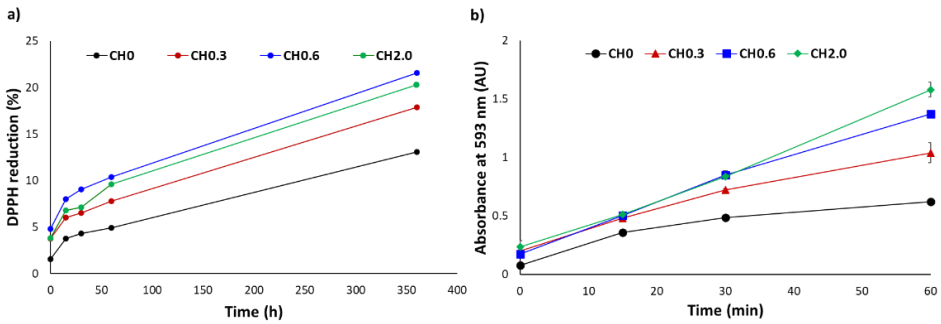

Figure 6.3.1.5.1. Antioxidant properties of chitosan/AgNP-HSCG films determined by (a) DPPH and (b) FRAP assays. Reported are the mean ± SD values of at least three experiments.

Functionalized films were also characterized for their antimicrobial activity and showed MIC values, expressed as AgNP concentration in the chitosan films, of 0.3% w/w for both Gram-negative and Gram-positive bacteria (Table 6.3.1.5.1). As far as MBC is concerned, the most promising values were found against Gram-negative bacterial strains, as expected on the basis of antimicrobial activity of AgNP-HSCG.

Table 6.3.1.5.1. Antimicrobial activity of composite films with different AgNP percentages (0.3%, 0.6%, 2%).

Strain	MIC (% AgNP)	MBC (% AgNP)
S. aureus ATCC29213	0.3	0.6
E. coli ATCC25922	0.3	0.3
P. aeruginosa ATCC27853	0.3	0.3

The antimicrobial activity of chitosan films was also evaluated by a modified agar diffusion assay. Inhibition zones were obtained even with the lowest amount of AgNP (Figure 6.3.1.5.2) while no effects were observed with control films (CH0).

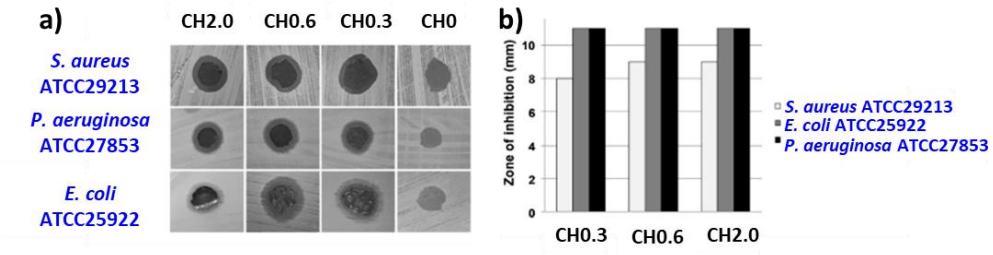

Figure 6.3.1.5.2. Antimicrobial activity of the composite films measured by the disk diffusion method. (a) Inhibition zones images. (b) Diameters of inhibition zones. Reported are the mean ± SD values of at least three experiments.

6.4 Conclusions

In this Chapter, the possible exploitation of two different agri-food by-products, pecan nut shells and SCG, as low-cost sources of polyphenols to be exploited in active packaging and in antimicrobial devices was investigated. Regarding pecan nut shells, a hydroalcoholic extract, indicated as PNSE was prepared and tested for their functional properties. PNSE, containing condensed tannins as the amin phenolic components, showed high antioxidant, enzymatic browning inhibition, and antimicrobial activities. Based on these promising properties, the extract was incorporated into PLA and WP films for food packaging applications. PLA films exhibited good antioxidant and enzymatic browning inhibition properties both in organic and in aqueous solvents. In particular, the low amounts of PNSE released from the films when taken in aqueous media would suggest their applications to water-rich foods. On the other hand, the more substantial migration observed in organic solvents would warrant even higher oxidative stability in the case of low water content foodstuffs, such as oils, butters, and sauces, also in the light of literature data indicating very low toxicity of PNSE in animal models. The incorporation of a water solution of PNSE in WP films produced a sustainable material endowed with good antioxidant and remarkable antimicrobial properties against the food pathogen *Enterococcus faecalis* and *Salmonella enterica subsp.*

enterica ser. Typhimurium. Other important results presented in this Chapter concern the preparation of AgNPs based on the use of hydrolyzed SCG as reducing agent. Generation of AgNPs was induced by redox interactions between Ag^+ ions and reducing units in the activated SGC, most likely surface-exposed phenolic moieties from the lignin component. The prepared AgNP-HSCG, were incorporated in chitosan films, providing materials endowed with high antioxidant and antimicrobial activity, particularly against Gram negative bacteria.

6.5 Experimental section

Materials and methods

1 g of pecan nut shells was treated twice with 10 mL of ethanol/water (6:4 v/v) for 30 min in an ultrasonic bath at room temperature. The mixture was then centrifuged for 20 min at 7763 g, the supernatant was filtered on Whatman paper No. 2 (GE Healthcare) and ethanol was removed in a rotary evaporator. The residual solution was then lyophilized to give PNSE as a red powder in 15 % w/w yield.[277]

For the preparation of the water solution of PNSE, 0.5 g of PNSE were added to 10 mL of water. The suspension was taken in an ultrasonic bath for 30 min and then centrifuged at 7000 rpm for 30 min. The supernatant was removed, and the precipitate was dried by lyophilization and weighted to determine by difference the amount of material which had gone into solution. PNSE concentration in the supernatant was found to be 30 mg/mL.

Anthocyanins were kindly provided by Prof. A. Schieber (Institute of Nutritional and Food Sciences, Molecular Food Technology, University of Bonn, Bonn, Germany). Red Delicious apples and bilberry juice (> 40% fruit content) were purchased from local shops. WP were purchased from Bioline (London UK).

HSCG were prepared from espresso SCG collected from a local coffee shop.[150] In particular, 3 g of SCG were treated with 70 mL of 6 M HCl under stirring at 100 °C,

overnight. After cooling at room temperature, the mixture was centrifuged (7000 rpm, 4 °C, 30 min) and the precipitate washed with water until neutrality and lyophilized to give a black powder with a yield of ca. 31%.

All solvents and reagents were obtained from commercial sources and used without further purification.

UV-Vis spectra were recorded using a HewlettPackard8453 Agilent spectrophotometer.

HPLC analysis was performed on an instrument equipped with an Agilent G1314A UV-Vis detector, using a Phenomenex Sphereclone ODS column (250 x 4.60 mm, 5 µm) at a flow rate of 1.0 mL/min; a gradient elution was performed with 0.1% formic acid (solvent A)/methanol (solvent B) as follows: 5% B, 0-10 min; from 5 to 80% B, 10-47.5 min; the detection wavelength was set at 254 nm.

LC-MS analyses were performed in positive ionization mode on an Agilent LC-MS ESI-TOF 1260/6230DA instrument with the following parameters: nebulizer pressure 35 psig; drying gas (nitrogen) 5 L/min, 325 °C; capillary voltage 3500 V; fragmentor voltage 175 V. An Eclipse Plus C18 column (150 × 4.6 mm, 5 □m) was used with the same mobile phase as above, at a flow rate of 0.4 mL/min.

UHPLC-ESI-MS analysis were performed with a Waters Acquity i-Class instrument equipped with a binary pump, an autosampler (cooled to 10 °C, injecting 5 µL), a column oven (40 °C), and a diode-array detector. The column was a Nucleoshell Phenyl-Hexyl (2.0 × 150 mm, 2.7 µm, Macherey-Nagel). Eluant A was 0.1% formic acid in water and eluant B was 0.1% formic acid in acetonitrile. A gradient elution program at a flow rate of 0.4 mL/min was used as follows: 1% B, 0-3 min; from 1 to 20% B, 3-22 min; from 20 to 100% B, 22-23 min; 100 %B, 23-25 min. The mass spectrometer was a LTQ-XL ion trap system (Thermo Fisher Scientific) operating under the following detection conditions: sheath gas (N_2), 52 arbitrary units; aux gas (N_2), 1 unit; sweep gas (N_2), 1 unit; ion spray voltage, 5 kV; capillary temperature,

300 °C; capillary voltage, 35 V; collision energy, 35 V. The mean degree of polymerization (mDP) was calculated according to equation below:

$$mDP = \frac{\sum area\ all\ adducts + (\sum area\ dimeric\ adducts \cdot 2) + (\sum area\ trimeric\ adducts \cdot 3 + \sum area\ terminal\ units}{\sum area\ terminal\ units}$$

FTIR-ATR spectra were recorded n a PerkinElmer Spectrum 100 spectrometer equipped with a Universal ATR diamond crystal accessory, and the analysis were performed with an average of 16 scans in the range 4000−450 cm^{-1} (resolution of 4 cm^{-1}).

EPR measurements were performed using an X-band (9 GHz) Bruker Elexys E-500 spectrometer equipped with a super-high sensitivity probe head. PNSE was introduced in a flame-sealed glass capillary coaxially inserted in a standard 4 mm quartz sample tube. Measurements were carried out at room temperature, with the following settings: sweep width, 140 G; resolution, 1024 points; modulation frequency, 100 kHz; modulation amplitude, 1.0 G, receiver gain, 60 dB. The amplitude of the field modulation was preventively checked to be low enough to avoid detectable signal overmodulation. A microwave power of ~0.6 mW was used to avoid microwave saturation of resonance absorption curve. To improve the signal-to-noise ratio 16 scans were accumulated. For power saturation experiments, the microwave intensity was gradually increased from 0.004 to 127 mW. The g value and the spin density were determined using Mn^{2+}-doped MgO as an internal standard.[192] Spin density values must considered as order of magnitude estimates, since sample hydration was not controlled.

SEM was performed using a FEI Quanta 200 FEG SEM in high vacuum mode. Samples were first mounted onto SEM stubs by means of carbon adhesive disks and sputter coated with a Au–Pd alloy layer of 18.0 ± 0.2 nm, using a MED 020 Bal-Tec AG coater in the case of incorporated PLA films and 15 nm thick Au-Pd layer in the case of AgNP-HSCG chitosan films.

Bright field TEM analysis was performed on a FEI Tecnai G12 Spirit Twin (LaB6 source) at 120 kV acceleration voltage. TEM images were collected on a FEI Eagle 4k CCD camera. Analyses were performed on the supernatant obtained after settling of a water suspension of the material treated for 30 min in an ultrasound bath at room temperature.

XRD analysis was performed with a X'Pert Pro diffractometer, equipped with a PIXCel 1D detector, under CuKα radiation. Powder spectra were collected under ambient conditions in the range 5-80 °2θ, with a step size of 0.013 °2θ and counting time of 20 seconds per step. The 8 PANalytical High-Score package, equipped with the ICDD PDF 2 database, was used to identify the crystalline phases in the samples. The amount of AgNP in the samples was evaluated by the RIR/Rietveld method:[337] a weighted amount (10% w/w) of corundum (NIST Standard Reference Material 676a) was added to each sample, the mixture was carefully homogenized, and the diffraction spectrum was acquired. Then, a quantitative analysis was performed using the MAUD software,[338] obtaining the relative mass percentage of corundum, Ag, and AgCl if present. The results were rescaled accounting for the actual amount of corundum, obtaining the absolute weight percentage of each phase as the mean value from three different samples. The structural information of each phase was acquired from the Crystallography Open Database (Crystallography Open Database, 2020).

6.5.1 Phloroglucinolysis.[303] 5 mg of PNSE were dissolved in 1 mL of methanol. One aliquot was used as the control to assess the content of free flavanols. Another aliquot of 100 µL was evaporated to dryness under nitrogen and subsequently, 100 µL of a reaction solution constituted of ascorbic acid (10 mg/mL) and phloroglucinol (50 mg/mL) in 0.1 M methanolic HCl were added. The mixture was kept under stirring in a water bath at 50 °C. After 20 min, the reaction was quenched by adding 500 µL aqueous sodium acetate (40 mM), filtered and analyzed by UHPLC- ESI-MS.

6.5.2 Thiolysis.[302] 8 mg of PNSE were treated with 2 mL of methanol, 20 µL of 37% HCl and 50 µL of benzyl mercaptan (BM) at 40 °C under stirring. After 1 h the mixture was diluted in 5 mL of methanol/water 1:1 v/v, and directly analyzed by HPLC and LC-MS.

6.5.3 Alkali fusion.[183] 100 mg of KOH, 100 mg of NaOH, and 2 mg of Na_2S2O_4 were melted in a pyrex tube at 240 °C. 20 mg of PNSE were then added, and the mixture was kept at 240 °C for further 10 min. After cooling to room temperature, 10 mL of a 1% sodium dithionite solution was added. The resulting mixture was taken to pH 3 with acetic acid and then extracted for three times with 15 mL of ethyl acetate. The organic layers were anhydrified on sodium sulfate, taken to dryness, dissolved in methanol, and analyzed by HPLC and LC-MS.

6.5.4 Antioxidant properties of PNSE: **DPPH assay.**[175] 20 µL of a 0.1-1 mg/mL PNSE solution in DMSO were added to 2 mL of a 200 µM ethanolic solution of DPPH. After 10 min under stirring at room temperature, the absorbance at 515 nm was measured. Trolox was used as reference antioxidant. Each experiment was run in triplicate. **FRAP assay**.[177] 20 µL of a 0.05-0.5 mg/mL PNSE solution in DMSO were added to 2 mL of a FRAP solution containing 1.7 mM $FeCl_3$ and 0.83 mM TPTZ in 0.3 M acetate buffer (pH 3.6). The mixture was stirred for 10 min at room temperature, after that the absorbance at 593 nm was measured. Each experiment was run in triplicate. Results were expressed as Trolox eqs.

6.5.5 Cell viability assays. The cytotoxic effects of PNSE on human hepatocarcinoma (HepG2) cells were evaluated using the MTT assay. Cells were plated on 96-well plates at a density of 5×10^3 per well in 100 µL of medium and incubated at 37 °C with 5% CO_2. The medium was then replaced with 100 µL of fresh media containing PNSE at 5-50 µg/mL and cells were incubated at 37 °C with 5% CO_2. After 24-72 h incubation at 37 °C, the medium containing PNSE was withdrawn, and fresh medium (100 µL) containing 10% MTT was added to each well, after that, cells were incubated in darkness at 37 °C for 4 h. Cell survival was

reported as the relative absorbance, with respect to control, of blue formazan measured at 570 nm with a Synergy Multi Plate Reader.

6.5.6 Enzymatic browning inhibition properties of PNSE. **Mushroom tyrosinase inhibition assay**.[339,340] 10 μL of a PNSE solution in DMSO were incubated at room temperature in 2 mL (0.02-0.25 mg/mL PNSE final concentration) of 50 mM phosphate buffer (pH 6.8) containing 20 U/mL of mushroom tyrosinase. After 10 min, 20 μL of a 100 mM $_{L}$-DOPA or $_{L}$-tyrosine solution in 0.6 M HCl were added (1 mM final concentration), and the absorbance at 475 nm was measured after other 10 min. **Apple smoothie browning inhibition assay**. Red Delicious apples were rapidly cut in small pieces after removing the peel, and ca. 50 g were finely blended with a domestic mixer in the presence of a 0.085% PNSE solution (prepared by dissolving 100 mg PNSE in 15 mL of DMSO followed by addition of 100 mL of double-distilled water) and transferred on a watch glass. Blank smoothie samples were prepared in the absence of PNSE. Changes in color were periodically analyzed with a Chroma Meter CR-400/410 (Konica Minolta) colorimeter (three different measurements were taken during the same experiments and three different experiments were performed). The browning index (BI) was calculated as follows:

$$Browning\ index\ (BI) = \frac{100(\mathrm{x} - 0.31)}{0.17}$$

$$x = \frac{\alpha * +1.75\mathrm{L} *}{5.645L * + \alpha * -3.012b *}$$

Kojic acid and ascorbic acid were used as reference compounds. In other experiments smoothies prepared by blending 50 g of apple pulp in 100 mL of double-distilled water were rapidly transferred on a watch glass and immediately covered with solvent-cast PLA films, neat or containing PNSE. The changes in color were periodically analyzed with a colorimeter as above. Uncovered smoothies were used as blank samples.

6.5.7 Anthocyanin stabilization properties of PNSE.[310] 0.1 mg/mL of red wine anthocyanins were dissolved in 5 mL of 0.3 M acetate buffer (pH 3.6). 40-250 µL of 1 mg/mL PNSE solution in DMSO were added (corresponding to 0.008-0.05 mg/mL final concentration of PNSE in the anthocyanin solution). The mixtures were taken at 90 °C and periodically analyzed by measuring the absorbance at 521 nm at 1 h intervals. Control mixtures containing the same amount of DMSO (without extracts) and unheated samples were analyzed in the same way. In another series of experiments, PNSE (2-10 mg) was added to 5 mL of bilberry juice, and the mixtures were taken at 90 °C and periodically analyzed as described above, after a 1:40 v/v dilution in 0.3 M acetate buffer (pH 3.6).

6.5.8 Antimicrobial activity of PNSE: the antimicrobial activity was investigated by the microbroth dilutions assay,[341] performed in Difco Nutrient Broth (Becton-Dickenson, Franklin Lakes, NJ, USA) using a bacterial inoculum of 2×10^6 CFU/mL and testing increasing concentrations of PNSE (0− 15 mg/mL).

6.5.9 Preparation of PE and PLA films containing PNSE. In the case of extruded PE and PLA films, PNSE was mixed with PE or PLA powder at 1, 2, or 3% w/w (g of PNSE/g of polymer). Then, the powder mixture was extruded with a flat die single-screw extruder, and films with an average thickness of 70 ± 10 µm were obtained by calendering.[277] In the case of solvent-cast PLA films, a suitable amount of PNSE was dissolved in 50 mL of a chloroform:methanol (8:2 v/v) solution by sonication over 30 min. Then, 2 g of PLA pellets were added, and the mixture was stirred for 120 min at 80 ºC using a magnetic heater-stirrer. The resulting solution was transferred to a 12 cm-diameter Petri dish, and the solvent allowed to slowly evaporate for 2 d to obtain films of 180 ± 10 µm thickness. The solvent casting technique was not applicable to PE due to its extremely low solubility in most solvents.

6.5.10 Preparation of WP films containing a water solution of PNSE. A film forming solution (FFS) was firstly prepared by dissolution of 500 mg of WP in 25

mL of distilled water. Subsequently 60% w/w (with respect to proteins) of glycerol was added. Then, 8 mL of PNSE solution in water, containing 240 mg of PNSE, was added and the pH was brought to 12 by using 0.1 M NaOH. The films were prepared by casting method: the FFSs were poured in 9 cm diameter Petri dishes and then allowed to dry at 25 ◦C (45 % relative humidity (RH)) for 24 h. The obtained films were cut into 1 × 8 cm strips and kept at 25 ◦C, with RH of 50 %, for 24 h in a glass chamber containing saturated $Mg(NO_3)_2$ before being tested.

6.5.11 Film mechanical properties characterization. In the case of PLA films, tensile tests were performed at 23 ± 2 °C and 45 ± 5% RH using a dynamometer (Instron 5564) equipped with a 1 kN load cell, at 5 mm min^{-1} clamp displacement rate. Before testing, the dumbbell-shaped specimens were conditioned at 25 °C and 50% RH for 48 h. At least 10 specimens were tested for each formulation. OTR was measured by using a ExtraSolution $PermeO_2$ instrument working in a gas/membrane/gas configuration, using a measuring surface of 50 mm, at 50% RH, 23 ± 1 °C, and 1 atm of pressure difference (ΔP) across the membrane. The test was ended when the collected data reached an OTR accuracy within 0.5%.

In the case of WP incorporated films, the thickness was measured in 6 different points with a micrometer (Electronic digital micrometer - Metrocontrol srl, Casoria Italy - sensitivity 0.001 mm), while the tensile strength (TS), elongation at break (EB) and Young's modulus (YM) were obtained on 5 strips of each sample by means of Instron Universal Testing Instrument model No. 5543A (Instron Engineering Corp., Norwood, MA, USA) using 5 cm gage length, 1 kN load and 5 mm/min speed. The measurement of film gas permeability towards CO_2, H_2O vapor and O_2 was carried out in triplicate at 25 ◦C and 50 % RH, using the MultiPerm permeabilimeter (Extra Solution s.r.l., Pisa, Italy). Aluminium masks were used with the aim of reducing the area of the film tested to 5 cm^2.

6.5.12 Antioxidant Properties of PE, PLA and WP films. **DPPH assay**: 2-10 sections of PE or PLA (both extruded or solvent-cast) films of 1 cm^2 total surface

area (corresponding to ca. 20-100 mg of material) were added in a vial containing 20 mL of a 55 μM ethanolic solution of DPPH. In the case of WP films, 1 cm^2 film section (corresponding to 28 mg of material) was added to 10 mL of a 50 or 200 μM ethanolic solution of DPPH, and the absorbance at 515 nm was periodically analyzed over 4 h. Blank samples without the films were also prepared. Each experiment was performed in triplicate. **FRAP assay**: In the case of PE and PLA films, 5 film sections of 1 cm^2 total surface area (corresponding to ca. 50 mg of material) were introduced in a vial containing 20 mL of a FRAP solution prepared as described above and allowed to sit for 4 d at room temperature. In the case of WP films, 1 cm^2 film section (corresponding to 28 mg of material) was added to 10 mL of FRAP solution. The absorbance of each solution at 593 nm was periodically analyzed. Blank samples without the films were also prepared. Each experiment was performed in triplicate. Results were expressed as Trolox eqs.

In separate experiments the release of PNSE from the films in the assay media was evaluated. PE or PLA (both extruded or solvent-cast) film sections of 1 cm^2 total surface area (corresponding to ca. 50 mg of material) were introduced in a vial containing 20 mL of ethanol or FRAP solution. In the case of WP films, 1 cm^2 film section (corresponding to 28 mg of material) was added to 10 mL of FRAP solution. UV-Vis spectra of each solution were periodically recorded. Experiments were run in triplicate. The amount of PNSE released was determined by means of a calibration curve obtained with 0.05-0.2 mg/mL PNSE solutions in the same solvents.

6.5.13 AgNP-HSCG preparation. 8 or 40 mg of HSCG (final dose 0.2 or 1% w/w) were added to 4 mL of a 2, 10 or 50 mM $AgNO_3$ solution in water, and the suspension was kept under stirring at room temperature, 60 °C, 80 °C or 120 °C. After 30 min, 1 h, 3 h, 24 h, 72 h or 10 d the mixture was centrifuged (7000 rpm, 15 min) and the solid washed three times with water, lyophilized and analyzed

In other experiments the reaction was run:

i. in ethanol, for 24 h, with 10 mM $AgNO_3$ and 1% HSCG;
ii. in the presence of 0.1 M KOH for 24 h with 2 mM $AgNO_3$ and 1% HSCG.

After optimization of the experimental conditions, 1 g of HSCG was suspended in 100 mL of a 10 mM $AgNO_3$ solution in water. The suspension was kept under stirring at 120 °C, and after 3 h the mixture was centrifuged (7000 rpm, 30 min) and the solid repeatedly washed with water, lyophilized and obtained as a black powder (560 mg).

6.5.14 Antioxidant properties of HSCG and AgNP-HSCG. **DPPH assay.** 5, 10 or 15 mg of HSCG or AgNP-HSCG were added to 50 mL of a 200 μM DPPH ethanolic solution. After vigorous stirring at room temperature for 10 min, the absorbance at 515 nm was measured. Experiments were run in triplicate. **FRAP assay**. 5, 8 or 12 mg of HSCG or AgNP-HSCG were added to 166 mL of FRAP solution, prepared as described above. After vigorous stirring at room temperature for 10 min, the absorbance at 593 nm was measured. Experiments were run in triplicate.

6.5.15 Preparation of chitosan films containing AgNP-HSCG. Chitosan solution was prepared by dissolving 3 g of chitosan powder in 300 mL of 3% v/v aqueous acetic acid solution, under stirring at 70 °C. After cooling, 0.6 g of glycerol were added. Composite films were prepared by adding 0.010, 0.020 or 0.067 g of AgNP-HSCG to 20 mL of chitosan, corresponding to 0.3, 0.6 and 2.0% w/w AgNP with respect to chitosan. The resulting suspensions were sonicated in an ultrasound bath for 10 min, then the solution was left to evaporate at room temperature.

6.5.16 Mechanical characterization of chitosan films containing AgNP-HSCG. Swelling measurements were carried out by weighting each sample before and after exposure to 100% RH. First, the dry sample was weighed, and the value recorded as Wd. Then, it was transferred into a chamber saturated with water moisture. The

sample was periodically recovered, weighed, and the value recorded as Ws. The swelling index (SI) was calculated as below:

$$SI = \frac{(\mathrm{Ws} - \mathrm{Wd})}{Wd}$$

WVP of chitosan films was determined according to ASTM E96 standard method. The samples, with exposed area of 6.54 cm^2, were sealed over a circular opening of three 25 cm^2 aluminium permeability cups (BYK-Gardner) filled with distilled water. The cups were weighed, then kept in oven at 25 °C under 50% RH. The weight change of each cup was periodically measured to determine the water vapor transmission rate (WVTR), from which WVP was obtained multiplying WVTR by the film thickness and dividing by the partial pressure of water across the film (1584. 6 Pa). The latter was obtained multiplying the difference in fractional RH across the film (0.5) by the saturation vapor pressure at 25 °C (3169.2 Pa). Mechanical properties were determined using a Instron model 5564 dynamometer equipped with a 1 kN load cell in tensile mode at 25 ± 2 °C, 50 ± 5% RH, and 5 mm min^{-1} clamp separation rate. Prior to the test, the dumbbell-shaped specimens were conditioned at 25 °C and 50% RH for 48 h. Young's Modulus, stress and strain at break were calculated from the experimental stress-strain curves.

6.5.17 Antioxidant properties of chitosan films containing AgNP-HSCG. **DPPH assay.** Film sections of ca. 1 cm^2 total surface area (corresponding to 15 mg of material) were deposited on the bottom of a vial containing 3 mL of a 55 μM ethanolic solution of DPPH. A blank sample without the films was also prepared. The absorbance of each solution at 515 nm was periodically analyzed. Experiments were run in triplicate. **FRAP Assay**. Film sections of ca. 1 cm^2 total surface area (corresponding to 15 mg of material) were deposited on the bottom of a vial containing 3 mL of a FRAP solution prepared as described above. A blank sample without the films was also prepared. The absorbance of each solution at 593 nm was

periodically analyzed. Results were expressed as Trolox eqs. Experiments were run in triplicate.

6.5.18 Antimicrobial activity of chitosan films containing AgNP-HSCG. The antimicrobial activity of HSCG and AgNP-HSCG was tested against three different pathogenic bacteria, Gram-negative (*E. coli* ATCC25922 and *P. aeruginosa* ATCC27853) and Gram-positive (*S. aureus* ATCC29213) bacteria. MIC was evaluated by the broth microdilution method.[342] Briefly, a fresh culture on Tryptic Soy Agar (TSA) was suspended in Tryptic Soy Broth (TSB) at a turbidity equivalent to that of 0.5 McFarland standard, and diluted 1:100 with TSB. 500 µL of each isolate were added into a 24-well polystyrene flat-bottomed microtiter plate (BD Falcon, Mississauga, Ontario Canada). The sample was added to bacterial suspensions in each well at a final concentration ranging from 0 to 1 mg/mL. Growth control wells contained only bacteria in TSB. The plates were incubated for 24 h at 37 °C. The cells suspension turbidity was quantified by microtiter plate reader (Tecan, Milan, Italy) at 595 nm. Absorbance was proportional to bacterial growth. MBC was defined as the concentration that caused $\geq 3 \times \log_{10}$ reduction in colony count from the starting inoculum plated on Muller Hinton II agar compared to the positive control, incubated for 24 h at 37 °C.[343,344] Each experiment was performed in triplicate in three independent experiments. The antimicrobial activity of chitosan films was evaluated by a modified agar diffusion assay and microplate growth inhibition assay. The film samples were punched to make disks of 6 mm in diameter. In the modified agar diffusion assay (disk test), 100 mL of each bacterial suspension in Mueller Hinton II broth with a turbidity of 0.5 McFarland were spread out on Muller Hinton II agar plates, and the film disks were added by swabbing in three directions. The plates were examined for possible clear zones and after incubation at 37 °C for 24 h the inhibition zone diameters were measured. In the growth inhibition assay, bacterial suspensions adjusted to McFarland 0.5 and diluted 1:100 with TSB were added into a 24-well microtiter plates. Film disks were placed on the plates inoculated with the bacterial cultures and incubated at 37 °C for 24 h.

MIC and MBC were determined. Each experiment was performed in triplicate in three independent experiments.

Chapter 7

Agri-food by-product extracts as lipid peroxidation and enzymatic browning inhibitors

7.1 Introduction

Lipid peroxidation is the oxidation reaction of fats, responsible for the rancidity of foods at high lipid content. This process can occur as a result of exposure to oxygen, light, or heat, and can also be induced by metals (such as iron). Lipid peroxidation leads not only to the formation of hydroperoxides and peroxides, but also of carbonyl compounds, particularly aldehydes, which are responsible for the characteristic fried or rancid smell and of the alteration of the nutritional and organoleptic properties of the food. In addition, due to their marked reactivity toward a variety of biomolecules, these compounds may also induce carcinogenic effects.

The compounds most susceptible to lipid peroxidation are polyunsaturated fatty acids (PUFA), due to the presence of the carbon-carbon double bonds. Indeed, the susceptibility to oxidation increases with the degree of unsaturation. Vegetable oils are therefore more subjected to the rancidity process than saturated fats of animal origin.

Enzymatic browning is another issue of great concern in the food preservation sector. This process induces a gradual change of colour of food products to brown or dark brown over time and involves the action of polyphenol oxidases (PPO). Enzymatic browning occurs mainly in fruit and vegetable products during harvesting, transport, storage and processing.[345] Mechanical actions such as peeling, cutting, slicing and shredding or any strong temperature variations during storage can cause physical damage to tissues, and as a result, PPO and phenolic compounds

are released and exposed to the oxygen, giving rise to oxidation reactions which transform the phenolic compounds into the corresponding quinones. The latter are highly reactive species that can undergo polymerization reactions, leading to the formation of dark pigments.[345]

Among the PPO capable of catalyzing enzymatic browning reactions, a principal role is played by tyrosinase. The latter, widely distributed in microorganisms, animals, and plants, is an enzyme containing two copper ions in the active site, which can catalyze two distinct reactions:

• Oxidation of monophenols to *o*-diphenols (cresolase or monophenolase activity);

• Oxidation of *o*-diphenols to the corresponding *o*-quinones (catecholase or diphenolase activity).

On this basis, identification of active compounds capable of inhibiting tyrosinase and lipid peroxidation has becoming increasingly important for the food industry, and there is a constant search for inhibitors from natural sources with no harmful side effects. In this context, in this Chapter the inhibition ability of extracts prepared from selected agri-food waste materials, rich in phenolic compounds, against lipid peroxidation and enzymatic browning will be reported.

Specific aims of the research work described in this Chapter included:

1. Preparation of selected agri-food by-product extracts;
2. Evaluation of lipid peroxidation inhibition activity;
3. Evaluation of enzymatic browning inhibition activity

7.2 Extraction of agri-food by-products

The first part of the work was aimed at optimizing the extraction process from selected agri-food wastes. In the initial extraction procedure, 0.5 g of each waste material (apple, grape pomace, orange and SCG) were extracted using water or

ethanol/water 6:4 v/v at a 100 mg/mL s/l ratio. The mixtures were kept under magnetic stirring for 30 min at room temperature and then centrifuged for 15 minutes. In the case of water extracts, the supernatants were recovered by lyophilisation, whereas, in the case of the hydroalcoholic extracts, ethanol was first removed in a rotavapor, before proceeding with lyophilization. As shown in Table 7.2.1, the aqueous and hydroalcoholic extracts were obtained in quite similar yields. Moreover, all waste materials, with the exception of grape pomace, exhibited very low extraction yields. To improve these latter, in another series of experiments the extraction was carried out using an ultrasonic bath or undergoing the solid residues from the first extraction to a further extraction treatment with fresh solvent, under the same conditions. Using this last procedure, the extraction yields were found to be significantly higher, especially in the case of aqueous apple waste and SCG extracts (Table 7.2.1).

Table 7.2.1. Yields of aqueous and hydroalcoholic extracts obtained from the selected agri-food by-products, referred to the dry weight of the starting material. Reported are the mean of two experiments.

Sample	Yield (%) without ultrasound	Yield (%) with ultrasound
SCG (water)	5	12
SCG (ethanol/water)	6	9
Grape pomace (water)	48	61
Grape pomace (ethanol/water)	44	63
Apple peel (water)	10	35
Apple peel (ethanol/water)	18	21
Orange peel (water)	12	23
Orange peel (ethanol/water)	12	15

7.2.1 Evaluation of the lipid oxidation inhibition properties

7.2.1.1 Accelerated thermal aging of oil samples

In order to evaluate the ability of the aqueous and hydroalcoholic extracts to inhibit lipid peroxidation process, soybean oil and cod liver oil, rich in polyunsaturated fatty acids, and therefore more susceptible to peroxidation, were selected. Indeed,

soybean oil is characterized by high concentration of linoleic acid (ca. 58%) and α-linolenic acid (4-10%), while cod liver oil is rich in omega-3 fatty acids, in particular eicosapentaenoic and docosahexaenoic acids, particularly sensitive to oxidation following exposure to air, light, heat and metal ions.

The inhibitory activity was first evaluated by the ferrous oxidation-xylenol orange (FOX) assay, based on the oxidation reaction of Fe^{2+} to Fe^{3+} induced by the hydroperoxides and on the ability of Fe^{3+} to form a complex with xylenol orange characterized by an intense blue-purple colour, with a maximum absorption at 560 nm.[150,346]

In a first series of experiments, 300 mg of soybean and cod liver oil samples were subjected to accelerated aging at 60 °C,[347] in the presence and absence of 45 mg of agri-food extracts. The inhibition properties of the extracts were determined after a 7-day period in the case of soybean oil and 48 hours in the case of cod liver oil, given its higher susceptibility to oxidation. These times were selected at optimal based on control experiments run in the absence of extracts.

The data reported in Figure 7.2.1.1.1a showed low inhibitory effects (<30%) for both aqueous and hydroalcoholic apple peel, orange peel and grape pomace extracts. On the contrary, SCG extracts were found to be able to completely inhibit the peroxidation process at the tested concentration. Similar results were obtained using soybean oil (Figure 7.2.1.1.1b).

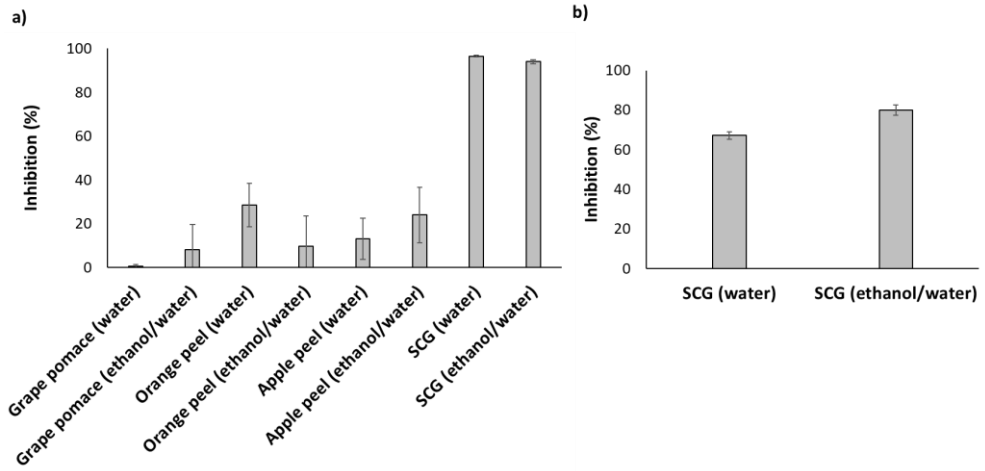

Figure 7.2.1.1.1. Inhibition properties of agri-food extracts on thermally induced lipid peroxidation in (a) cod liver and (b) soybean oil samples. Reported are the mean ± SD values of at least three experiments.

In a further series of experiments, the dose-dependence of the lipid peroxidation inhibition for the SCG extracts was investigated. As evidenced in Figure 7.2.1.1.2a, the extracts tested on cod liver oil showed a dose-dependent behaviour and similar results were obtained on soybean oil, confirming the efficacy, in particular, of the hydroalcoholic extract (Figure 7.2.1.1.2b).

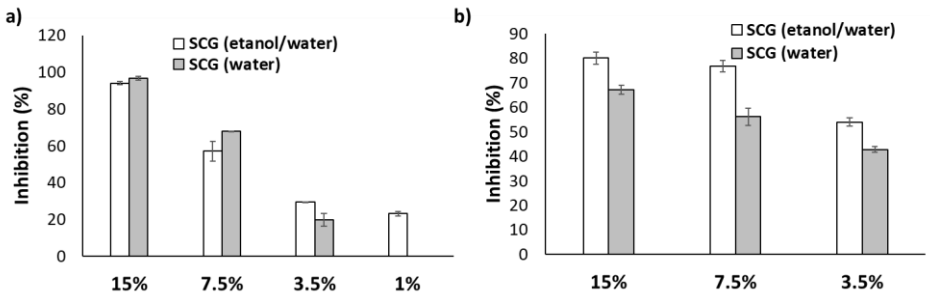

Figure 7.2.1.1.2. Dose-dependence experiments of SCG extracts on thermally induced lipid peroxidation in (a) cod liver and (b) soybean oil samples. Reported are the mean ± SD values of at least three experiments.

In a last series of experiments, the antioxidant properties of SCG extracts were compared to those of reference antioxidants such as BHA, BHT, ferulic acid, gallic acid and Trolox. All samples were tested at 7.5% w/w dose. As shown in Figures 7.2.1.1.3, the SCG extracts exhibited an activity comparable or superior to that observed for BHA and ferulic acid.

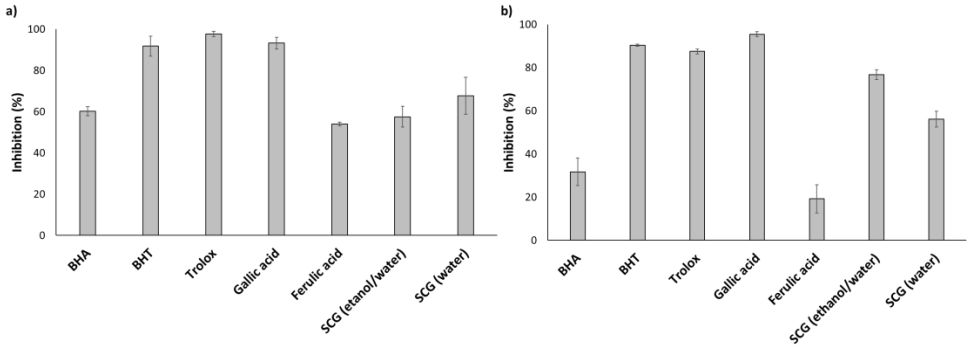

Figure 7.2.1.1.3. Inhibition properties of SCG extracts and reference antioxidants on thermally induced lipid peroxidation in (a) cod liver and (b) soybean oil samples. Reported are the mean ± SD values of at least three experiments.

7.2.1.2 Accelerated iron-induced aging of oil samples

The thiobarbituric acid reactive substances (TBARS) assay was used to monitor the ability of the extracts to inhibit the iron-induced peroxidation on cod liver oil. Reaction of carbonyl compounds, in particular of malondialdehyde, generated by the decomposition of lipid peroxidation products with thiobarbituric acid leads to the formation of a highly conjugated adduct, characterized by an absorption maximum at 532 nm. In particular, 10 mg of oil and 5 mg of each extract were homogenized in a TRIS buffer at pH 5.0 and then subjected to oxidation by adding Fe^{2+} ions. After 3 h, the mixtures were analyzed spectrophotometrically by measuring the absorbance at 532 nm.[150] Again, SCG extracts showed the best inhibitory activity on the lipid peroxidation process (Figure 7.2.1.2.1a).

Also for this assay, dose-dependence experiments on SCG extracts showed an increasing inhibitory effect with increasing dose (Figure 7.2.1.2.1b). Finally, a comparison with reference antioxidants showed the superior activity of the hydroalcoholic extract of SCG with respect to all the selected standards (Figure 7.2.1.2.1c).

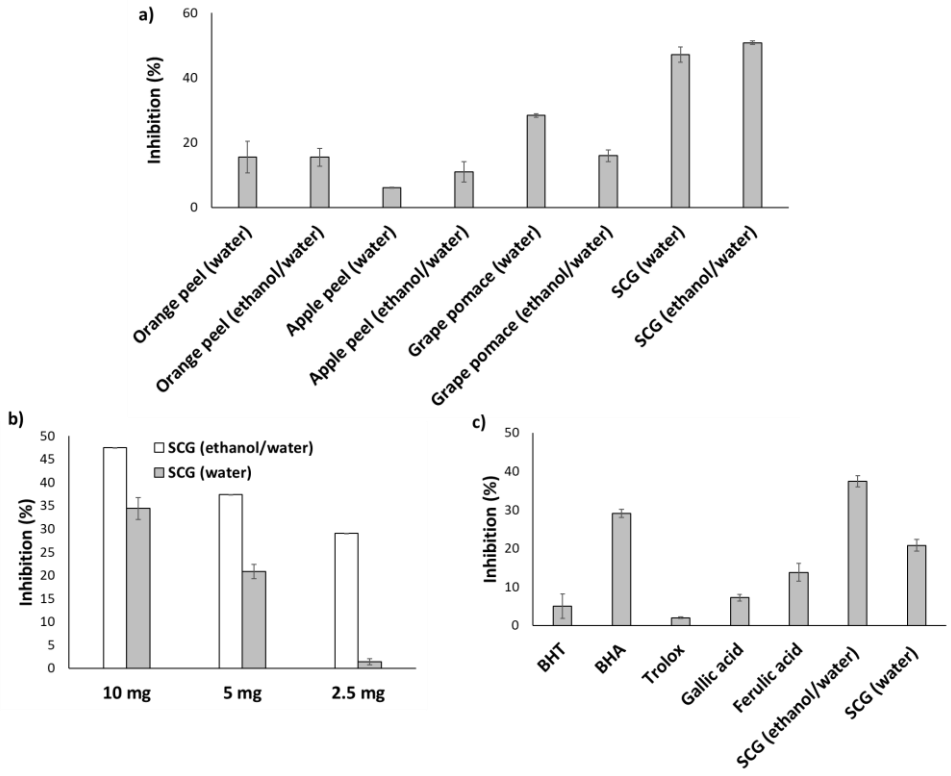

Figure 7.2.1.2.1. (a) Inhibition properties of SCG extracts and (c) reference antioxidants (5mg) on iron-induced lipid peroxidation and (b) dose-dependence experiments on cod liver samples. Reported are the mean ± SD values of at least three experiments.

7.2.2 Evaluation of browning inhibition properties

7.2.2.1 Tyrosinase inhibition properties of selected agri-food by-products

The tyrosinase inhibition properties of the aqueous and hydroalcoholic extracts of the different agri-food by-products were initially investigated using mushroom

tyrosinase and L-DOPA as substrate. Tyrosinase is a polyphenol oxidase playing a critical role in the oxidative deterioration of food products, particularly fruit and vegetables. Tyrosinase inhibition is important also for cosmetic purposes because this enzyme catalyzes the key steps of human melanogenesis, and overproduction of melanin is associated with several pigmentary disorders. The assay was based on the detection of dopachrome formation (λ_{max} = 475 nm), following oxidative cyclization of dopaquinone, resulting from the tyrosinase-induced oxidation of the substrate, in the presence and absence of the inhibitor.

Each extract was incubated at different concentrations in 50 mM phosphate buffer (pH 6.8) in the presence of mushroom tyrosinase (20 U/mL) at room temperature. After 10 min L-DOPA was added and after further 10 minutes, the absorbance at 475 nm was measured. The inhibitory capacity was expressed as IC_{50}, which is the concentration of inhibitor at which a 50% inhibition of the enzyme activity occurs.

Control experiments carried out in the absence of L-DOPA allowed to rule out the possible contributions to browning of tyrosinase substrates present in the extracts (e.g. caffeic acid and derivatives in the case of SCG).

As reported in Figure 7.2.2.1.1, promising results were obtained with the hydroalcoholic grape pomace and SCG extracts, which exhibited IC_{50} < 1 mg/mL. In particular, hydroalcoholic grape pomace extract showed an IC_{50} values only ca. 3-fold higher than that observed for ascorbic acid, used as a reference compound. On the other hand, no inhibition was observed in the case of orange and apple waste extracts.

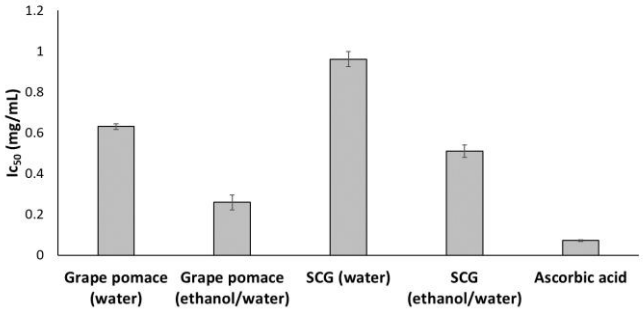

Figure 7.2.2.1.1. IC_{50} values determined for selected agri-food extracts in the mushroom tyrosinase inhibition assay. Reported are the mean ± SD values of at least three experiments.

In another set of experiments, the importance of the pre-incubation of the extracts with the enzyme on the observed inhibition effects were evaluated. In particular, mushroom tyrosinase was incubated without the extract for 10 minutes in phosphate buffer at pH 6.8. Subsequently, each sample was added at a concentration corresponding to the IC_{50} value, immediately followed by $_L$-DOPA. After 10 minutes the absorbance at 475 nm was measured. As shown in Figure 7.2.2.1.2, SCG extracts still induced an approx. 50% inhibition, thus ruling out a significant role of the pre-incubation with the enzyme in the observed effects. On the other hand, a lower efficacy of grape pomace extracts was evident without pre-incubation.

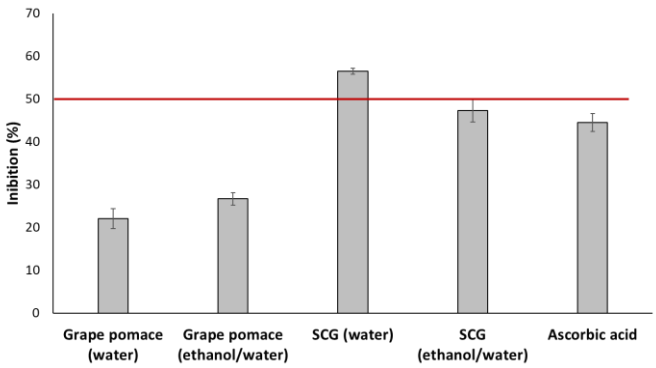

Figure 7.2.2.1.2. Inhibition percentage obtained for the selected extracts without pre-incubation with the enzyme. Reported are the mean ± SD values of at least three experiments. Each extract was tested at the IC_{50} previously determined.

7.3 Conclusions

Lipid peroxidation process, both induced by metal ions or high temperatures, can significantly affect the nutritional and organoleptic properties of foods stored in metal containers or during production, transport, processing, storage, and marketing of lipid-rich foods.

Enzymatic browning processes is another undesirable event which may occur in fruits and vegetables during storage and/or processing.

It has been widely demonstrated that phenolic compounds are able to delay lipid peroxidation in oils or fats and can also act as inhibitors of tyrosinase, the enzyme responsible for enzymatic browning processes. On this basis, in recent years, great attention has been focused on the use of agri-food by-products as sustainable and low-cost sources of phenolic compounds endowed with antioxidant and enzymatic browning inhibition properties.

In this context, as described in this Chapter, extracts prepared from different agri-food waste materials were analyzed for their inhibition activities in lipid peroxidation and enzymatic browning inhibition model assays. The most promising properties were exhibited by the SCG extracts, which were found to be very effective as lipid peroxidation inhibitor in cod liver and soybean oil samples, and the hydroalcoholic grape pomace extract, that showed very promising enzymatic browning inhibition properties, with an IC_{50} values against tyrosinase only 3-fold higher than that observed for the reference compound ascorbic acid.

Although still preliminary, since further experiments are needed to fully characterize the mechanisms and the major determinants of the lipid peroxidation and tyrosinase inhibition properties of the different extracts, the results showed in this Chapter open new perspectives for the functional use of agri-food wastes in food-related application.

7.4 Experimental section

Materials and methods

Apples and oranges were purchased at a local supermarket. SCG was collected from a local coffee shop. Grape pomace was kindly provided by Dr. Daniele Naviglio (Department of Chemical Sciences, University of Naples "Federico II", Italy).

All solvents and reagents were obtained from commercial sources and used without further purification.

UV-Vis spectra were recorded using a HewlettPackard8453 Agilent spectrophotometer.

7.4.1 Extracts preparation. 1.5 g of SCG, orange peel, apple peel or grape pomace were finely grounded in a home blender and then extracted with 15 mL of water or ethanol/water 6:4 v/v, in an ultrasonic bath for 30 min, at room temperature. The mixture was then centrifuged (7000 rpm) for 15 min, the supernatant was recovered, and the solid residue was subjected to a new extraction under the same conditions described above. The combined supernatants, after removing ethanol in a rotavapor when necessary, were subjected to freeze-drying and then kept in a vacuum desiccator for 24 h, to remove traces of residual solvent.

7.4.2 FOX assay.[150,346] 45 mg of each extract were deposited on the bottom of a flask containing 300 mg of soybean or cod liver oils and incubated at 60 °C. Control samples without extracts were also incubated. The hydroperoxide contents of the oil samples were determined after 7 days of incubation with soybean oil and 48 hours with cod liver oil. A total of 10 mg of the oil samples were withdrawn and dissolved in 3 mL of chloroform, and 90 µL of each solution was mixed with 2 mL of reagent mixture containing 0.11 mM xylenol orange, 0.25 mM ammonium iron(II) sulfate hexahydrate, and 25 mM H_2SO_4 in methanol containing 3.88 mM BHA. After 30 min incubation in the dark at room temperature, absorbance at 560 nm was

measured. Experiments were run in triplicate. In other experiments the reaction was carried out by varying the extract amounts (3-25 mg) or by using reference antioxidants (15 mg).

7.4.3 TBARS assay.[150] Cod liver oil (10 mg) was suspended in 1 mL of a buffer solution (0.05 M TRIS, 0.15 M KCl, 1% Triton X-100, pH 5.0) and taken under stirring for 5 min in the presence or absence of extracts (5 mg). A total of 100 µL of 1 mM iron(II) chloride tetrahydrate was added, and the mixtures were taken under vigorous stirring at room temperature. After 3 h, TBARS were quantified as follows: 100 µL of 2% BHT in ethanol was added to all the mixtures to stop the oxidation process, followed by addition of 1 mL of TBA reagent (15% w/v trichloroacetic acid and 0.375% w/v TBA in 0.25 M HCl). The reaction mixtures were taken under stirring at 80 °C for 15 min, and the samples were centrifuged at 2000 rpm for 10 min. The absorbance of the supernatant was then measured at 532 nm. Experiments were run in triplicate. In other experiments the reaction was carried out by varying the quantity of extract (2.5-10 mg) or by using reference antioxidants (5 mg).

7.4.4 Mushroom tyrosinase inhibition assay.[340] Stock solutions of the different samples (25 mg/mL) were prepared in DMSO and 1-200 µL of each solution was incubated at room temperature with mushroom tyrosinase (20 U/mL) in 2 mL of 50 mM phosphate buffer (pH 6.8). After 10 minutes, 20 µL of a 100 mM solution of $_{L}$-DOPA, dissolved in 0.6 M HCl (final concentration 1 mM), were added and the course of the reaction was followed by measuring the absorbance at 475 nm after additional 10 minutes. In control experiments the reaction was carried out in the absence of the sample or in the presence of ascorbic acid as positive control. When required, the extracts were added 10 min after the addition of tyrosinase, followed immediately by the addition of the $_{L}$-DOPA solution.

Chapter 8

Development of synthetic strategies for the preparation of anthocyanin metabolites

8.1 Introduction

As reported in the Introduction, anthocyanins, belonging to the class of flavonoids, form the largest class of natural water-soluble pigments which, dependently on different factors, among all pH, can appear red, purple, or blue. Anthocyanins are abundantly present in fruit and vegetables, mainly in glycoside form, and play important roles also from a nutritional point of view.

Although more than 500 different anthocyanins have been identified, deriving from different hydroxylation, methoxylation and glycosylation patterns, as well as different substituents on the sugar moiety, only six are the most commonly anthocyanidins found in plants: cyanidin, delphinidin, pelargonidin, peonidin, malvidin and petunidin, with a distribution of 50%, 12%, 12%, 12%, 7% and 7%, in that order (Figure 8.1.1).[348]

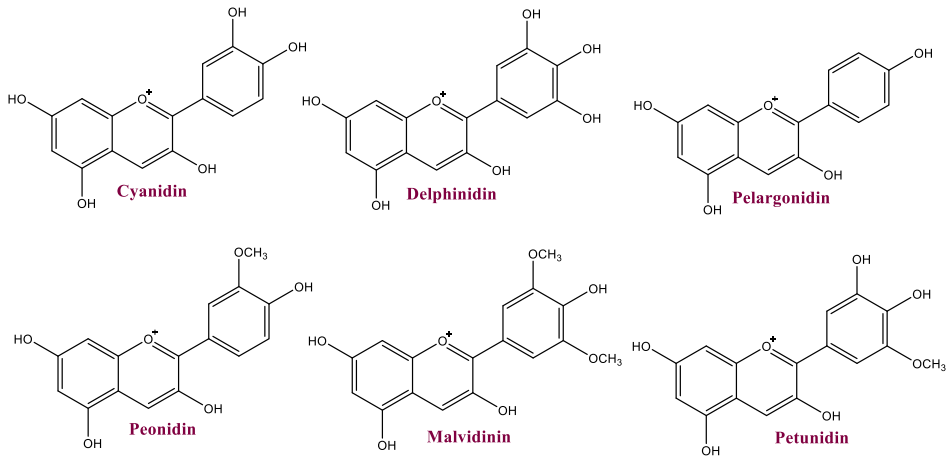

Figure 8.1.1. Main naturally occurring anthocyanidins.

Anthocyanidins are known for their poor stability, closely related to a series of factors, such as light, temperature, pH, metal ions and oxygen.[349] In particular, in aqueous solution, pH variations induce severe structural modifications and rearrangements. In acidic solutions (pH 1-3), anthocyanins are stable and present mainly as the flavylium cation; an increasing of pH leads to the conversion of the flavylium cation into the quinoidal base (pH 6-7) or into the colorless hemichetal, which can undergo ring opening, giving rise to a pale yellow chalcone (pH 6). Chalcone can also undergo chemical degradation, producing phenolic acids.[35] As previously mentioned, the pH is also responsible for the colour variations of anthocyanidins, which in acidic conditions appear red, at neutral pH tend to a purple colour, while at alkaline pH, they appear blue (Figure 8.1.2).

Anthocyanins are characterized by a wide number of beneficial biological properties on human health. First of all, they show remarkable antioxidant activity, and are able to act as radical species scavengers. Moreover, cyanidin, delphinidin and petunidin glycosides are also able to act as metal chelators. Anthocyanins are also able to positively affect blood and lymphatic microcirculation, contribute to maintaining good liver health, protect the skin from UV rays, strengthen the immune system, as well as prevent cardiovascular, inflammatory and neoplastic diseases.[350] Recently, protective effects of anthocyanins against neurodegenerative diseases, including Alzheimer's, Parkinson's diseases and amyotrophic lateral sclerosis have been reported.[351] Anthocyanins were also found to be able to inhibit cancer cell proliferation,[352] and act as antidiabetic agents, especially against type II diabetes mellitus.[353]

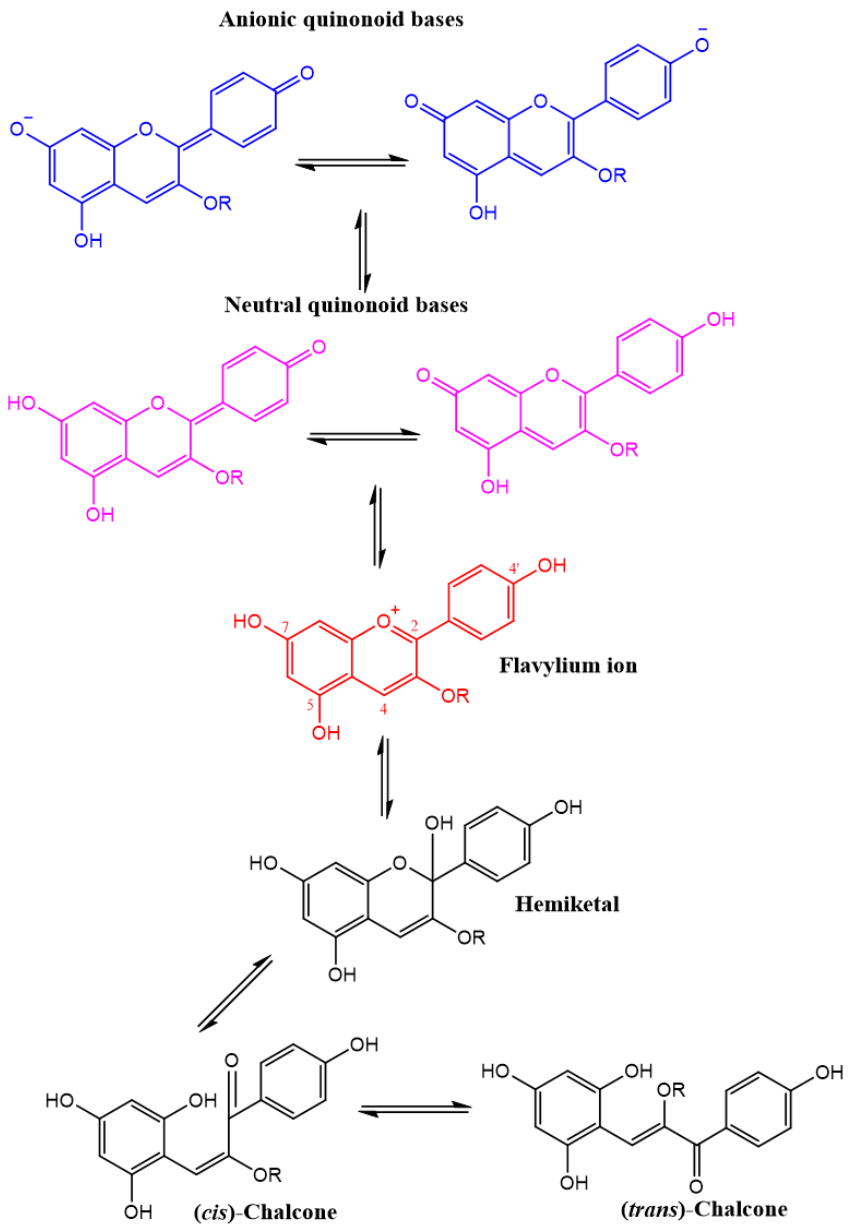

Figure 8.1.2. Acid-base equilibrium of anthocyanins and corresponding colour variations. Adapted from Ref.[308]

Anthocyanins are regularly assumed through the diet, being abundantly present in vegetables, cereals, fruit, and fruit-derived products, such as wines, juices, and jams.

The richest sources of anthocyanins are berries belonging to the *Vitaceae* and *Rosaceae* families, and to the *Ribes* and *Vaccinium* genera. In these food sources, anthocyanin concentrations can reach several hundred milligrams *per* 100 g of fresh weight. However, anthocyanins are known for their poor bioavailability, which is estimated in ranges from 2% to less than 1%, with only traces detected in the target organs or in the bloodstream. Actually, the bioavailability of anthocyanins is significantly underestimated, due to the presystemic metabolism of these pigments.[354] For example, a study carried out on humans has shown that the consumption of 500 mg of isotopically labelled cyanidin 3-O-β-glucoside (C3G) may lead to a relative bioavailability of around 12%.[355,356] For these reasons, it is crucial to acquire knowledge about anthocyanin bioprocessing after their intake.

Anthocyanins are metabolized throughout the gastrointestinal tract, starting from the oral cavity, where the food matrix is ground and mixed with saliva and other food components. Saliva, which is at pH = 7, determines the partial formation of the hemiketal and the opening of the C ring.[357] Subsequently, in the stomach, characterized by an acidic pH (~ 1), anthocyanins are stable in the form of flavylium cation, and are easily released from the denatured food matrix.[358] Some studies in rats and humans have shown that anthocyanins reach the plasma very quickly, within 10 min to 30 min of their oral intake, which led to the conclusion that they are efficiently absorbed by the gastric epithelium.[358] However, the main absorption site of anthocyanins is the small intestine, at which level the anthocyanins are close to neutral or mildly alkaline (pH 7.5–8.0), and their stability is reduced and converted to hemiketal and chalcone. Anthocyanins can be transported within the enterocytes through both active and passive transport. In the first case, the anthocyanins are transported intact, in the glycoside form, by the glucose transport systems, after which deglycosylation by cytosolic β-glucosidase can occur. In the second case, since anthocyanin are highly water soluble and are very large molecules, they are initially deglycosylated to the aglycone in the intestinal lumen by β-glucosidase or in epithelial cell membranes by lactase-phlorizin hydrolase,

producing aglycones, which are more hydrophobic and smaller than the glycosides and can easily infiltrate the epithelial layer passively.[359]

Before entering the bloodstream, anthocyanins can undergo metabolic transformations that increase their hydrophilicity and facilitate their elimination from the body through bile and urine. Not absorbed anthocyanins are eliminated through the faeces.

Anthocyanins are substrates for several enzymes located in the small intestine and colon, and in the liver (hydrolyzing and conjugating enzymes, phase I and phase II, respectively).[360] Before conjugation, anthocyanins can undergo degradation to phenolic acids and aldehydes, in processes that can also involve the intestinal microbiota at the level of the colon. In this process, the cleavage of the sugar moiety is the first step, followed by the hydrolysis of the O-glycoside bond, for ring opening. Depending on the substituents attached to the B ring, different products can be formed.[361] Cyanidin is degraded to protocatechuic acid, malvidin to syringic acid, peonidin to vanillic acid, delphinidin to gallic acid and pelargonidin to 4-hydroxybenzoic acid.[354,361] After the fission of ring C, ring A gives rise to phenylacetaldehyde and benzaldehydes.[361]

Phase I metabolism plays an important role in the availability of anthocyanins. Despite between 30% and 40% of C3G was found as protocatechuic acid in human plasma,[362] also the methylated derivative peonidin 3-glucoside was detected 15 seconds after administration. Pelargonidin 3-glucoside is metabolized in humans into pelargonidin 3-glucuronide, pelargonidine-3-glucoside-glucuronide and is degradated in 4-hydroxybenzoic acid.[354] Delphinidin-3-glucoside, petunidin-3-glucoside and malvidin-3-glucoside were found in the blood in their native forms after ingestion, while the glucuronidated forms were identified as the main metabolites in urine.[363]

The study of phase II metabolism of anthocyanins has attracted considerable interest, too, due to the remarkable bioactivity of methylated, sulfated and/or glucuronidated derivatives.[364] However, the commercial availability of phase II metabolites is very limited, therefore the development of protocols for the synthesis of standard reference substances is of paramount importance. Several approaches have been reported to synthesize phase II metabolites of flavonoids in general. Among these, the use of enzymes appears to be of particular interest, because not only ensures good regioselectivity, but also generally requires mild reaction conditions, fundamental in case of unstable molecules such as anthocyanins. For example, methylated, sulfated and glucuronidated derivatives of cyanidin and C3G have been obtained using porcine liver enzymes.[365] Specifically, methylation has been mediated by catechol-O-methyltransferase (COMT) enzyme, leading to the formation of the methylated derivative in the 3' position, that is peonidin-3-O-glucoside. Glucuronidation has been carried out via glucuronosyltransferase (UGT), leading to the formation of three different monoglucuronidated forms of C3G and a glucuronidated cyanidin, for which, however, it was not possible to predict the glucuronidation position.[365] In the same study, the presence of sulfated metabolites of C3G, obtained by action of sulfotransferases (SULT), has been also highlighted, although even in this case it was not possible to identify the sulfation site.[365]

Despite the promising results, enzymatic processes are not feasible on a large scale, and for this purpose, a chemical synthesis could be more promising. In this context, flavonoids methylation has been described with the use of dimethyl sulfate (DMS)[366] or methyl iodide.[367] Several O-alkyl derivatives of naringenin, including mono-, di- and trimethylated derivatives, have been synthesized using anhydrous potassium carbonate and various alkyl iodides.[368]

Regarding anthocyanins, sulfation of cyanidin and C3G has been carried out using a SO_3-triethylamine complex,[369] while a variety of methylated derivatives (in particular three monomethylated derivatives, three dimethylated derivatives, three

trimethylated derivatives and one tetramethylated derivative) of C3G have been observed by reaction with dimethyl carbonate.[370] In both cases, however, a series of limitations were encountered, including the instability of the sulfate groups under acidic conditions and at high temperatures and complex purification procedures, which have allowed the isolation of the derivatives in very small quantities.

In this context, in the present Chapter the results of preliminary experiments aimed at the development of synthetic methodologies for the preparation of anthocyanin metabolites are reported. In particular, three different protocols have been developed for the preparation of sulfated, methylated and glucuronidated derivatives of C3G.

This part of the thesis work was carried out in collaboration with Prof. Andreas Schieber and Dr. Maike Passon of the Institute of Nutritional and Food Science of the University of Bonn, who provided the starting anthocyanin and carried out the LC-MS analysis of the reaction mixtures. Part of the work was also directed to the investigation of different food products as sources of C3G.

8.2 Synthesis of anthocyanin metabolites

8.2.1 Sulfation reactions

For the preparation of C3G sulfated derivatives SO_3-pyridine complex (SO_3-Py) was used as sulfating agent (Figure 8.2.1.1). This reagent is able to effectively react with phenolic groups of natural compounds, including flavonoids, although in the case of C3G, non-phenolic hydroxyl groups of the glucose unit are also present, which could be sulfated as well.

Figure 8.2.1.1. General scheme of OH group sulfation reaction using SO_3-Py complex as sulfating agent.

In a first series of experiments, the reaction was carried out at C3G concentration of 20 mM in dry N,N-dimethylformamide (DMF), at room temperature, in the presence of 8 molar eqs of SO_3-Py. After 10 min, the mixture was diluted 1:20 v/v with a 0.6 M HCl solution and analyzed by HPLC, which showed no consumption of C3G.

After several attempts, interesting results were obtained by carrying out the reaction at 45 °C, in the presence of 5 molar eqs of SO_3-Py. The HPLC profile of the reaction mixture after 10 min highlighted the formation of a single main product (indicated as A in Figure 8.2.1.2a) characterized by a lower retention time than the starting C3G, as expected for a more polar, sulfated derivative.

In order to obtain a higher consumption of the starting compound, higher temperature (e.g. 70 °C) were investigated, leading however to similar results.

A significant C3G consumption, as well as the formation of apparently stable products, was observed running the reaction at 45 °C with 5 molar eqs of SO_3-Py, followed by addition of further 5 molar eqs after 10 min. The chromatogram showed in this case an almost complete consumption of C3G, accompanied by the formation of a series of products, probably characterized by a higher sulfation degree (B-G) (Figure 8.2.1.2b). This hypothesis was confirmed by LC-MS analysis, which effectively highlighted the presence of monosulfated derivatives in the "Sulfate 1" mixture, while different mono- and disulfated derivatives were found to be present in the “Sulfate 2” mixture (Figure 8.2.1.3). These products are currently being purified for a full spectroscopic characterization.

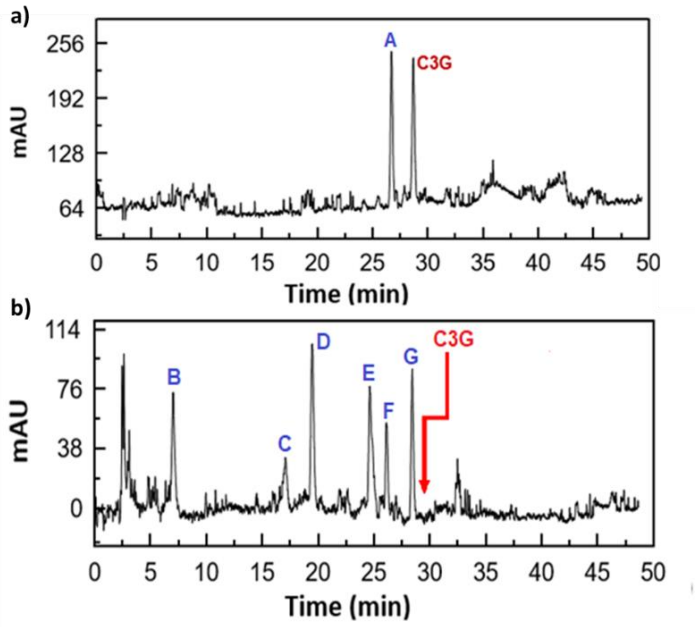

Figure 8.2.1.2. HPLC profile of the reaction mixture of C3G with (a) SO_3-Py (5 molar eqs), carried out at 45 ° C for 10 min (indicated as "Sulfate 1" in Figure 8.2.1.3), and (b) SO_3-Py (5 + 5 molar eqs), carried out at 45 ° C for 10 min + 10 min (indicated as "Sulfate 2" in Figure 8.2.1.3). Eluant I: 0% B, 10 min; 0% to 3% B, 10-15 min; from 3% to 25% B, 15-60 min, detection wavelength = 523 nm.

Sample	Compound	Formula	Retention Time [min]	Observed m/z	Mass Error [ppm]	Mass Error [mDa]	Observed CCS (Å2)	Observed drift (ms)
Sulfate 1	Cyanidin-3-glucoside	$C_{21}H_{21}O_{11}$	15,48	449,1077	-0,2	-0,1	201,67	6,88
	Cyanidinglucoside monosulfate 10	$C_{21}H_{20}O_{14}S$	16,59	529,0644	0,5	0,3	213,08	7,34
	Cyanidinglucoside monosulfate 11	$C_{21}H_{20}O_{14}S$	17,33	529,0646	0,9	0,5	215,36	7,43
Sulfate 2	Cyanidinglucoside monosulfate 10	$C_{21}H_{20}O_{14}S$	16,61	529,0654	2,5	1,3	213,53	7,36
	Cyanidinglucoside monosulfate 11	$C_{21}H_{20}O_{14}S$	17,32	529,0653	2,1	1,1	215,51	7,43
	Cyanidinglucoside disulfate		17,39	609,0217	1,3	0,8	223,84	7,76
	Cyanidinglucoside disulfate		18,38	609,0215	0,9	0,5	222,20	7,69

Figure 8.2.1.3. Results of the LC-MS analysis of C3G sulfation mixtures.

8.2.2 Methylation reactions

Methylation of C3G was initially carried out using iodomethane as methylating agent, which, however, did not lead to a significant consumption of the starting product, even at long reaction times (up to 24 h) and high temperatures (up to 45 °C) (Figure 8.2.2.1).

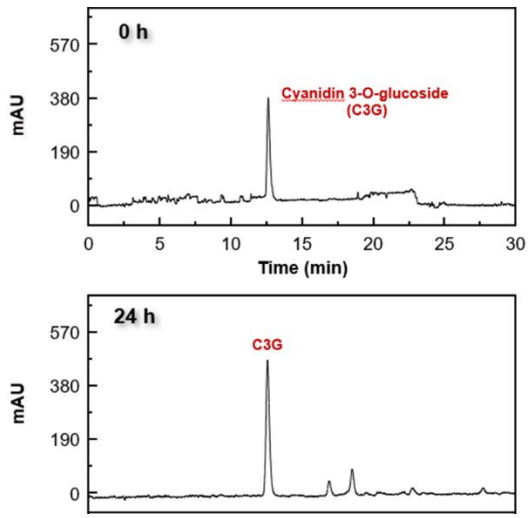

Figure 8.2.2.1. HPLC profile of the reaction mixture of C3G with iodomethane and K_2CO_3, carried out at 45 ° C for 24 h. Eluant II: from 3% to 25% B, 0-45 min; 25% to 30% B, 45-50 min; 30% to 80% B, 50-55 min.

Subsequently, a procedure reported in literature, based on the use of DMS for the preparation of O-methylated derivatives of quercetin, was adopted.[366] DMS is often used as methylating agent of nucleophilic functional groups such as phenols, amines and thiols, and is able to transfer methyl groups via a bimolecular nucleophilic substitution reaction (SN_2). The reaction was carried out in the presence of K_2CO_3 as a base, in order to deprotonate the phenolic groups and thus make them more nucleophilic (Figure 8.2.2.2).

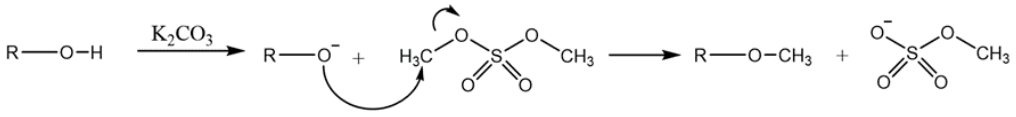

Figure 8.2.2.2. General scheme of OH group methylation reaction using DMS as methylating agent.

In a first series of experiments the reaction was carried out with 120 mM C3G in dry DMF, in the presence of 400 mM K_2CO_3 and 45 molar eqs of DMS. The mixture was kept under magnetic stirring at 45 °C and periodically analyzed by HPLC after 1:30 v/v dilution in 0.6 M HCl. As evident from the HPLC profiles shown in Figure 8.2.2.3, a progressive consumption of C3G was observed, accompanied by the formation of different products, some of which eluted at higher retention times than C3G, as expected for methylated products. However, other products at lower retention times, and hence more polar, were also detectable. Indeed, the use of DMS as methylating agent could lead to the formation of secondary sulfated products, as reported in literature.[371]

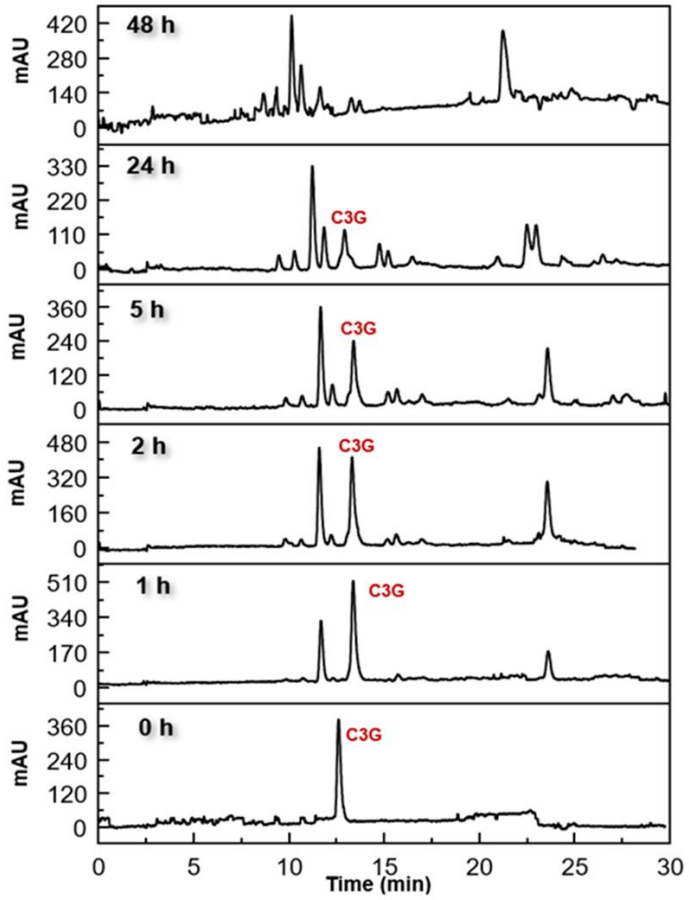

Figure 8.2.2.3. HPLC profiles of the methylation mixture of C3G with DMS and K_2CO_3 at 45 °C, at different times. Eluant II: from 3% to 25% B, 0-45 min; 25% to 30% B, 45-50 min; 30% to 80% B, 50-55 min, detection wavelength = 523 nm.

This hypothesis was confirmed by HPLC analysis of the reaction mixture run under the same gradient conditions used for the analysis of the sulfation mixtures (Figure 8.2.2.4a) and by LC-MS analysis (Figure 8.2.2.4b), which confirmed the presence of mono- and disulfated derivatives of C3G.

In any case, the LC-MS analysis confirmed the occurrence of the methylation reaction of C3G, since two dimethylated derivatives were detected. A similar pattern of products was obtained by carrying out the reaction at room temperature or at

60°C, but in this last condition the products were formed faster. Although the formation of sulfation products could seem a drawback, it could actually allow the isolation of the methylated and sulfated derivatives from a single reaction mixture. This possibility is currently under investigation.

It must be considered that only methylation at the B-ring of anthocyanins is biologically relevant, especially at C3'-OH, to mimic COMT activity,[372] so further structural characterization of the methylated derivatives is required, particularly in this case.

a)

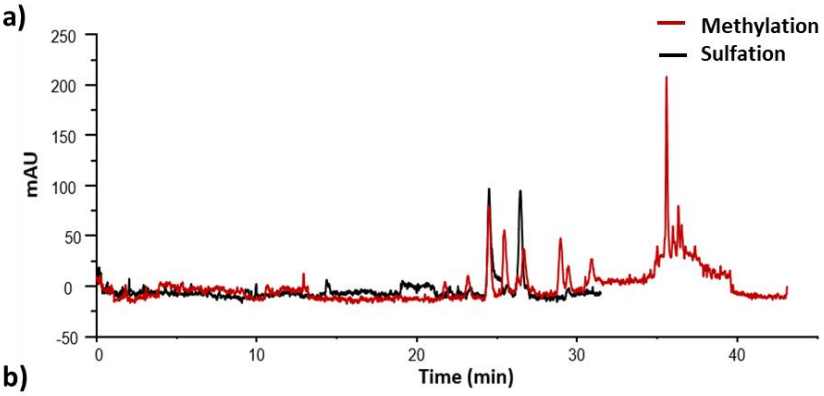

b)

Sample	Compound	Formula	Retention Time [min]	Observed *m/z*	Mass Error [ppm]	Mass Error [mDa]	Observed CCS (Å^2)	Observed drift (ms)
Methylated	**Cyanidin-3-glucoside**	$C_{21}H_{21}O_{11}$	**15,50**	**449,1077**	**-0,4**	**-0,2**	**201,88**	**6,89**
	Cyanidinglucoside monosulfate 10		16,59	529,0647	1,1	0,6	213,21	7,34
	Cyanidinglucoside dimethylated 1		**17,30**	**477,1025**	**0,8**	**0,4**	**206,75**	**7,09**
	Cyanidinglucoside monosulfate 11		17,33	529,0644	0,5	0,3	215,68	7,44
	Cyanidinglucoside disulfate		17,40	609,022	1,7	1	223,79	7,75
	Cyanidinglucoside monosulfate 12		18,04	529,0641	0	0	212,58	7,32
	Cyanidinglucoside disulfate		18,39	609,021	0,2	0,1	222,09	7,69
	Cyanidinglucoside dimethylated 2		**19,58**	**477,1026**	**1,2**	**0,6**	**205,19**	**7,03**

Figure 8.2.2.4. (a) Comparison between the HPLC profiles of C3G methylation (in red) and sulfation (black) mixtures, obtained under the elution conditions used for the analysis of the sulfation mixtures. (b) Results of the LC-MS analysis of the C3G methylation mixture.

8.2.3 Glucuronidation reactions

For the synthesis of C3G glucuronidated derivatives, a procedure reported in literature was used as reference,[373] based on the use of 1-bromo-2,3,4-tri-O-acetyl-α-acid methyl ester of D-glucuronic acid in the presence of Ag_2O and $CaSO_4$. This reagent is able to mediate the transfer of glucuronic acid units on nucleophilic OH groups. However, under the conditions described above, the anthocyanin underwent rapid degradation with the formation of a dark precipitate, presumably due to the presence of silver oxide. The conditions previously developed for the methylation reaction were therefore adopted, and C3G was reacted with the 1-bromo-2,3,4-tri-O-acetyl-α-D-glucuronic acid methyl ester in the presence of K_2CO_3. Under these conditions, the deacetylation and hydrolysis of the ester functionality in the product should also be promoted (Figure 8.2.3.1).[374]

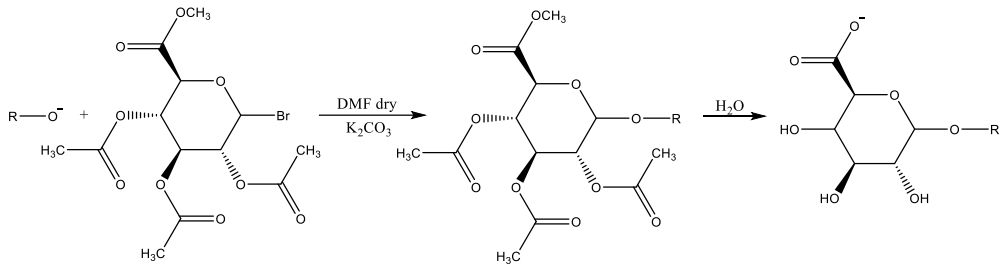

Figure 8.2.3.1. General scheme of glucuronidation of hydroxyl groups by reaction with the methyl ester of 1-bromo-2,3,4-tri-O-acetyl-α-D-glucuronic acid.

In particular, the reaction was carried with 40 mM C3G in dry DMF, in the presence of 4 molar eqs of the glucuronic acid derivative and 140 mM K_2CO_3. The mixture was kept under magnetic stirring at room temperature and periodically analyzed by HPLC. However, under these conditions, the formation of significant amounts of any product was not observed even at long times. Similar results were obtained using 8 molar eqs of glucuronidating agent, at 45 °C. By further forcing the reaction conditions (16 molar eqs of glucuronidating agent, 70 ° C) it was finally possible to observe, after 4 h, a complete consumption of the starting C3G and the formation of

two main products (A and B, Figure 8.2.3.2). LC-MS analysis of this reaction mixture is currently underway.

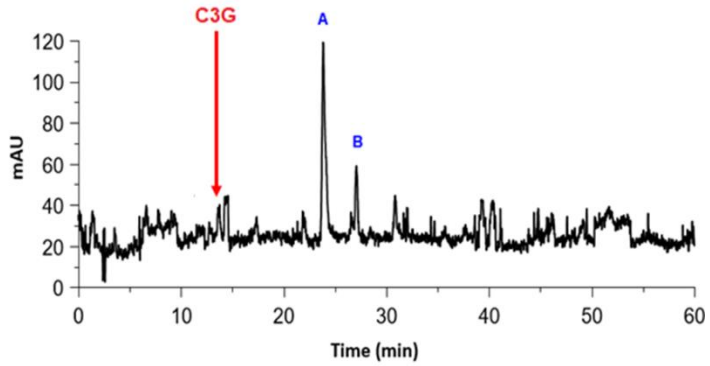

Figure 8.2.3.2. HPLC profile of the reaction mixture of C3G with the methyl ester of 1-bromo-2,3,4-tri-O-acetyl-α-D-glucuronic acid (16 molar eqs) at 70 °C after 4 h. Eluant II: from 3% to 25% B, 0-45 min; 25% to 30% B, 45-50 min; 30% to 80% B, 50-55 min, detection wavelength = 523 nm.

8.3 Conclusions

In this Chapter, the development of different methodologies for the synthesis of cyanidin 3-O-glucoside metabolites was described.

Although the results are still very preliminary, and only a complete spectroscopic characterization of the products will allow to identify which hydroxyl functionalities of C3G have undergone derivatization, this is the first systematic study aimed at the development of simple reaction conditions based on the use of inexpensive reagents for the hemisynthesis of metabolites of a highly reactive and unstable compound such as C3G. In the future, these synthetic strategies could probably be applied on a larger scale, starting also from other anthocyanins and the corresponding anthocyanidins, thus providing a quick and easy way to obtain reference compounds that can be used not only to identify and quantify the metabolites of these pigments in biological fluids, but also to test their biological properties.

8.4 Experimental section

Materials and methods

Cyanidin 3-O-β-glucoside (C3G) was provided by Dr. Maike Passon (Institute of Nutritional and Food Science, University of Bonn). Grape pomace was provided by Dr. Daniele Naviglio (Department of Chemical Sciences of the University of Naples "Federico II"). Red cabbage, blackberries, blueberries, and black currants were bought at a local supermarket.

All solvents and reagents were obtained from commercial sources and used without further purification.

HPLC analysis were performed on an ODS column, 250 mm x 4.6 mm, with particles of 5 μm diameter (Sphereclone, Phenomenex). The detection was carried out at 523 nm using a mixture of water/acetonitrile/formic acid 87:3:10 v/v/v (solvent A) and acetonitrile (solvent B) as eluant, at a flow rate of 1.0 mL/min under different gradient conditions:

i) 0% B, 10 min; 0% to 3% B, 10-15 min; from 3% to 25% B, 15-60 min (sulfation reactions, eluant I);

ii) from 3% to 25% B, 0-45 min; 25% to 30% B, 45-50 min; 30% to 80% B, 50-55 min (methylation and glucuronidation reactions and analysis of extracts from natural sources, eluant II).

8.4.1 Sulfation reaction. To 1.5 mg of C3G (0.003 mmol), dissolved in 150 μL of dry DMF, 4 mg of SO_3-Py (0.025 mmol, 8 molar eqs) were added. The mixture was kept under magnetic stirring at room temperature and periodically analyzed by HPLC after dilution 1:20 v/v with a 0.6 M HCl solution.

In other experiments the reaction was carried out: i) in the presence of 5 molar eqs of SO_3-Py, at 45 °C; ii) in the presence of 5 molar eqs of SO_3-Py for 10 min at 45

°C, with the addition of further 5 molar eqs of SO_3-Py; iii) in the presence of 3 or 4 molar eqs of SO_3-Py, at 70 °C. All mixtures were periodically analyzed by HPLC.

8.4.2 Methylation reaction. To 3.0 mg of C3G (0.006 mmol), dissolved in 50 µL of dry DMF, 25 µL of DMS (0.26 mmol, 44 molar eqs) were added followed by 2.8 mg of K_2CO_3 (0.020 mmol). The mixture was kept under magnetic stirring at a temperature of 45 °C and periodically analyzed by HPLC after 1:30 v/v dilution with a 0.6 M HCl solution.

In other experiments the reaction was carried out: i) at room temperature; ii) at 60 °C. All mixtures were periodically analyzed by HPLC

8.4.3 Glucuronidation reaction. To 2.0 mg of C3G (0.004 mmol), dissolved in 100 µl of dry DMF, 6.5 mg of 1-bromo-2,3,4-tri-O-acetyl-α-D-glucuronic acid methyl ester (0.016 mmol, 4 molar eqs) and 2 mg of K_2CO_3 (0.014 mmol) were added. The mixture was kept under magnetic stirring at room temperature and periodically analyzed by HPLC after 1:20 v/v dilution in 0.6 M HCl.

In other experiments, the reaction was carried out: i) in the presence of 8 molar eqs of the methyl ester of 1-bromo-2,3,4-tri-O-acetyl-α-D-glucuronic acid, at 45 °C or 70 °C; ii) in the presence of 16 molar eqs of the methyl ester of 1-bromo-2,3,4-tri-O-acetyl-α-D-glucuronic acid, at 70 °C. All mixtures were periodically analyzed by HPLC.

Chapter 9

Preparation of a new red pigment from oxidative coupling of chlorogenic acid and tryptophan to be used as a food colorant

9.1 Introduction

Color is a fundamental feature of foods and drink and can play an important role in the market success of a product. The coloring of foods dates back to ancient times.[375] Egyptian writings describe the coloring of drugs, while Romans one describe the coloring of wine.[376] Historically, saffron, paprika, turmeric, and various flowers represented the most popular food coloring substances.[375] In the 19th century, during industrial development, the requirement for food colorants significantly grew, in order to improve the appearance of food and drink products and makes them more attractive for the consumers. The high consumer demand brought to the development of a series of synthetic food colorants easier to produce compared to natural ones.

Nowadays, despite the safety of synthetic colorants is extensively evaluated and strictly regulated, food industry increasingly requires alternatives for the replacement of artificial colorants with those derived from natural sources. However, natural pigments are generally characterized by a high number of limitations for food coloring compared to synthetic colorants. Most of them are sensitive to heat, light, oxygen, pH or presence of proteins and metal ions in the food matrix, resulting in color loss or alteration.

A remarkable example is the poor stability of anthocyanins to light, heat, oxygen, and pH, which has limited in part their use as natural food pigments, although

several stabilization strategies such as copigmentation, encapsulation, use of additives have been developed to improve their use. Therefore, the search for novel natural compound-based food dyes with high stability is becoming increasingly attractive.

In this context, a procedure for the preparation of green benzacridine pigments by reaction of chlorogenic acid (CGA) with lysine, glycine or protein-rich food matrices such as chicken egg albumen, have been recently reported.[377] These pigments were found to be able to impart intense green color to food samples and exhibited a satisfactory thermal stability, without exerting significant toxicity on Caco-2 and HepG2 cell lines.[377]

Interestingly, a systematic investigation of the reactivity of CGA with the 20 proteinogenic amino acids under alkaline conditions, revealed the formation of a peculiar intense red color when tryptophan (TRP) was used,[378] therefore this reaction could be highly attractive for the preparation of a red food dye.

On this basis, in this Chapter the preparation and structural characterization of a new red pigment deriving from oxidative coupling of CGA and TRP and the assessment of its potential as food colorant is described.

9.2 Preparation and characterization of the CGA-TRP pigment

9.2.1 Pigment preparation

In a first series of experiments, an optimization of the reaction conditions for the red pigment preparation was carried out. The reaction was initially carried out at pH 9 with both CGA and TRP at 14 mM and, as expected, an intense red color developed after few hours. In accordance with this observation, UV-Vis spectrum of the

reaction mixture, recorded at 24 h, exhibited an absorption maximum at ca. 540 nm, whose intensity was significantly higher when the reaction was run in the presence of 5 molar eqs of TRP and by prolonging the reaction time up to 64 h (Figure 9.2.1.1a).

On this basis, a preparative-scale reaction was carried out on 0.65 g of CGA with 5 molar eqs of TRP, and after 64 h the pH was adjusted to 1 to stop the reaction. At acidic pH, the immediate precipitation of the red pigment was observed, which was collected by centrifugation and lyophilization. UV-Vis spectrum confirmed the complete precipitation of the pigment since no significant absorption at 540 nm was detected in the supernatant. HPLC and LC-MS analysis of the pigment re-dissolved in alkaline medium evidenced the absence of residual CGA, but the presence of significant amounts (88% w/w) of TRP, partially co-precipitated during acidification of the reaction mixture. On this basis, the pigment was purified by gel filtration on Sephadex G-10 column as previously reported for the green benzacridines from CGA and lysine/glycine.[377] The combined pigment-containing fractions were then acidified, leading to the precipitation of the pigment as a red powder (Figure 9.2.1.1b). HPLC analysis showed the presence of only 5% w/w residual TRP in the purified pigment.

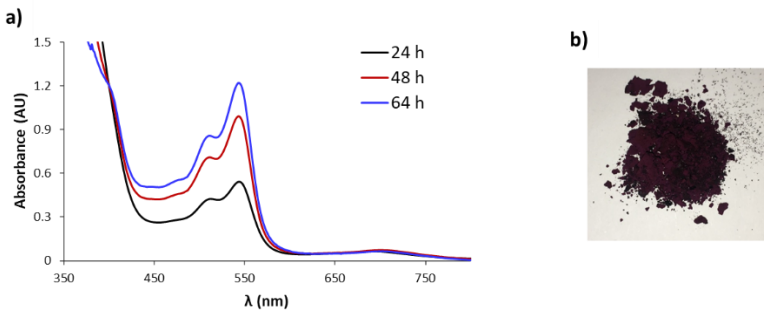

Figure 9.2.1.1. (a) UV-Vis absorption spectrum of the reaction mixture (1:100 v/v dilution in water) of CGA (14 mM) and TRP (70 mM) at pH 9 at different times (b) Digital photo of the red powder.

9.2.2 Structure characterization of the CGA-TRP pigment

The gel filtration purified CGA-TRP pigment was firstly characterized by UV-Vis analysis, which showed absorption maxima in visible region, at 542 and 546 nm, and in the UV region, at ca. 340 e 400 nm (Figure 9.2.2.1a).

HPLC analysis with UV-Vis detection at 254 nm showed the presence of a main group of products eluted between 8 and 12 min, present also in the profile obtained setting the detection wavelength at 578 nm (Figure 9.2.2.1b). LC-MS analysis (Figure 9.2.2.1c,d) showed a similar pattern of products, all exhibiting the same molecular ion peak at m/z 840, probably due to the presence of different isomers, which could suggest acyl migration on the quinic acid moiety at the slightly alkaline pHs of the reaction medium as previously reported.[377,378]

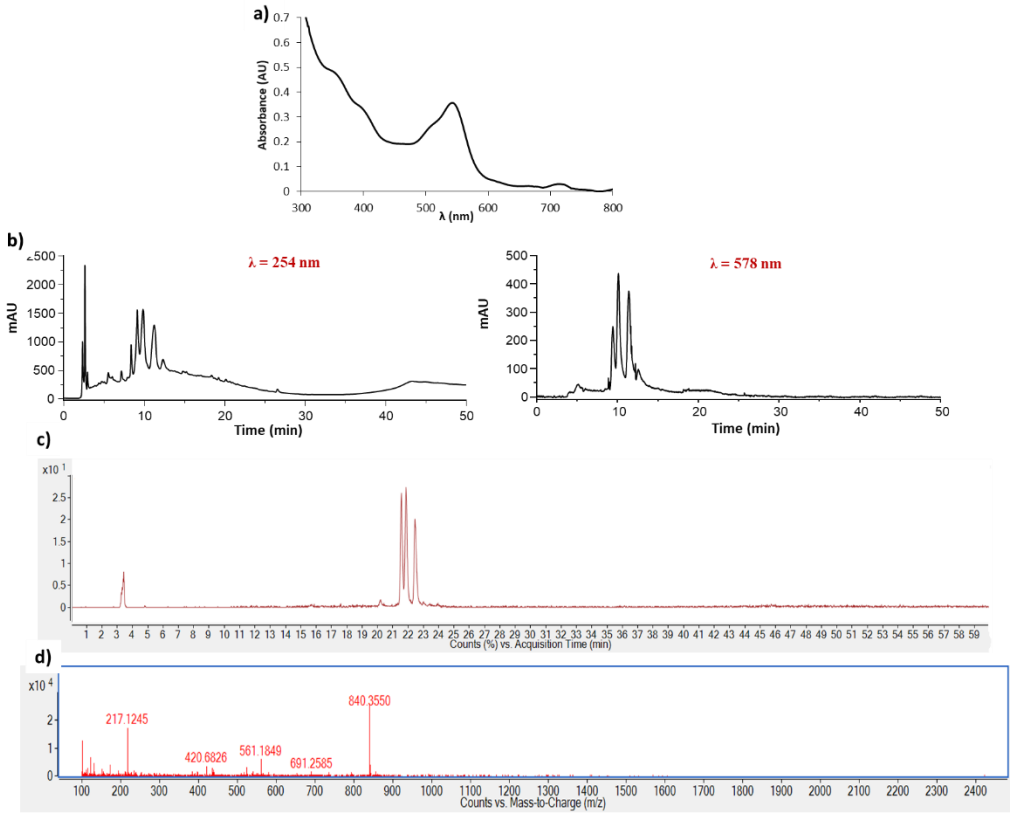

Figure 9.2.2.1. CGA-TRP pigment characterization: (a) UV-Vis spectrum, (b) HPLC elution profiles at λ = 254 nm (left) and 578 nm (right) (eluant: 0.1% formic acid with acetonitrile from 20% to 80% in 40 min, flow rate of 1 mL/min), (c) Extracted ion current (EIC) profile (m/z 840) and (e) MS spectrum of the products eluted at 21-23 min (eluant: 0.1% formic acid with acetonitrile from 20% to 80% in 40 min, flow rate of 0.4 mL/min).

In subsequent experiments, further purification was carried out by semipreparative HPLC, that allowed to collect fractions eluting at around 29 min exhibiting absorption maxima at 540 nm and 280 nm characterized by a 1:1 ratio in the UV-Vis intensity (Figure 9.2.2.2a). HPLC profile of the purified fractions under analytical conditions showed a single peak eluted at ca. 12 min with detection at 578 nm (Figure 9.2.2.2b), for which a pseudomolecular ion peak at m/z 476 $[M+Na]^+$ in the

positive ion mode and m/z 452 $[M-H]^-$ in the negative ion mode was determined by MS analysis (Figure 9.2.2.2c).

On this basis, it can be concluded that the species eluted between 8-12 min of the CGA-TRP pigment are constituted by a major component with a molecular weight of 453 Dalton (CGA-TRP/A) and a minor one responsible for the cluster of peaks characterized by pseudomolecular ion peaks at m/z 840 in the MS spectrum (CGA-TRP/B), which was preferentially revealed by LC-MS but obtained in insufficient amounts for NMR analysis.

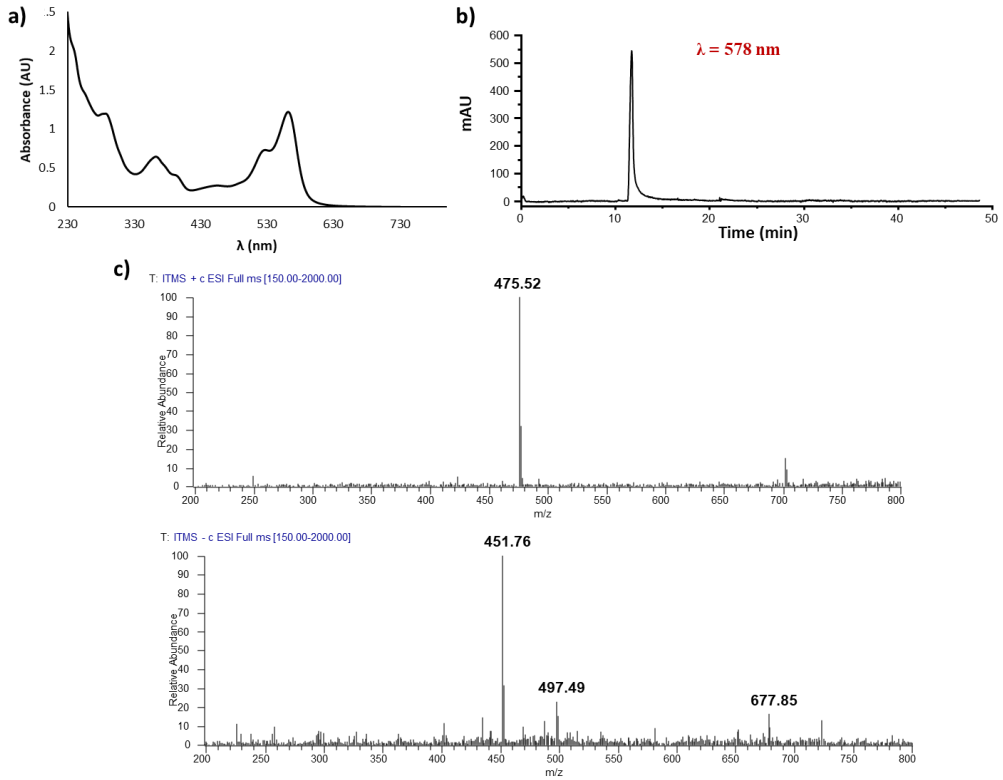

Figure 9.2.2.2. (a) UV–vis spectrum, (b) HPLC profile at λ = 578 nm and (c) ESI/MS spectrum in positive (top) and negative (bottom) modes of the product eluted at 11.8 min.

NMR analysis of CGA-TRP/A (Figure 9.2.2.3-9.2.2.5) allowed definition of the structure shown in Figure 9.2.2.6. Diagnostic for structural characterization proved i) the lack of the signals of the quinic acid moiety; ii) the presence of signals for a single TRP alanyl side chain; iii) complete sets of protons for two indole systems, one of which markedly low-field shifted; iv) a highly shielded proton at 6.81 ppm showing one bond correlation with a carbon at 99.8 ppm; v) a highly deshielded proton at 9.73 ppm correlating with a carbon at 136.5 ppm; vi) four D_2O exchangeable protons.

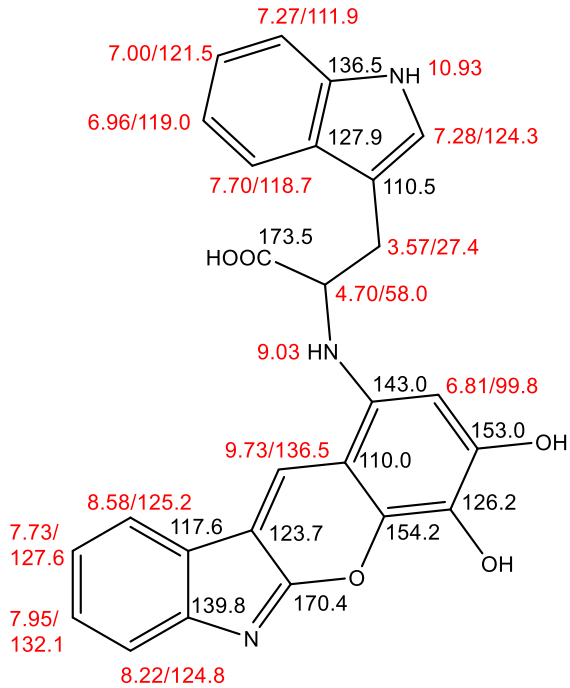

Figure 9.2.2.3. Proposed structure and complete proton and carbon resonance assignment for CGA-TRP/A.

The peculiar structure of compound CGA-TRP/A would derive from a relatively complex sequence of events triggered by oxidation of CGA in the presence of excess TRP leading eventually to loss of the side chain of one TRP moiety as well as

partial loss of the propenoate moiety of chlorogenic acid. Nucleophilic addition of the side chain amino group of TRP to CGA *o*-quinone leading to adduct **I** may likely represent the initial step of the reaction route to CGA-TRP/A (path A). Subsequent oxidative fission of CGA at the benzylic position could be due to the addition of hydrogen peroxide generated by catechol oxidation, followed by a carbonyl forming reaction, as previously described.[379] Subsequent steps would include: i) nucleophilic addition of the 3-position of TRP indole moiety onto the resulting benzaldehyde **II** and ii) concomitant or subsequent ring closure further to the attack to the imine function by an hydroxylated position generated by addition of H_2O to a quinonoid intermediate under the slightly alkaline conditions of the reaction. Finally, a sequence of elimination steps would lead to the highly conjugated system CGA-TRP/A. This system exhibits a cyanine-type push-pull chromophore similar to that of betacyanin pigments and responsible for the observed red color. The formation of the isomeric products with m/z 840 could be associated to a different reaction pathway, starting from the adduct **I** *via* a mechanism previously reported for the reaction of CGA with amino acids in alkaline medium, leading to a benzacridine ring system.[378,380,381] In accord with the proposed formation mechanism, by replacing TRP with its N-acetyl ethyl ester derivative, indole-3-acetic acid or tryptamine, no red chromophore formation was observed.

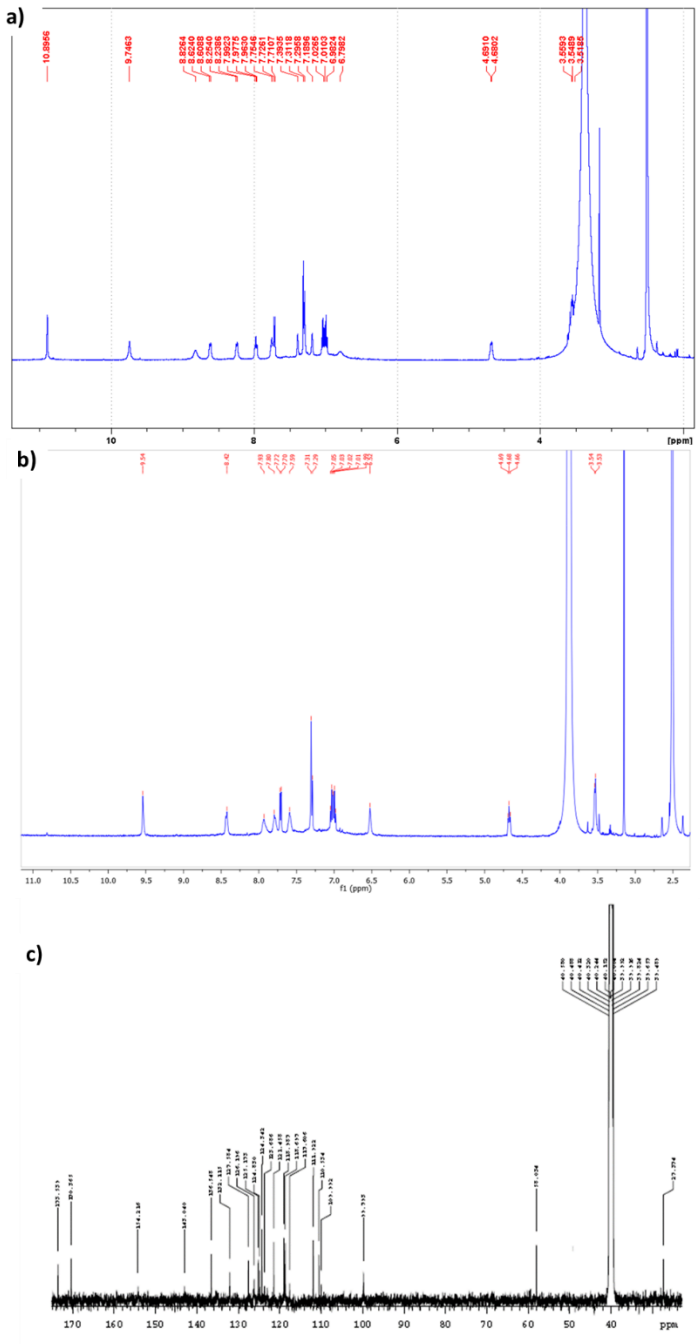

Figure 9.2.2.4. ^{1}H NMR spectrum of CGA-TRP/A in (a) DMSO-d_6 and (b) DMSO-d6 + 20% of D_2O. (c) $_{13}C$ NMR spectrum of CGA-TRP/A in DMSO-d6.

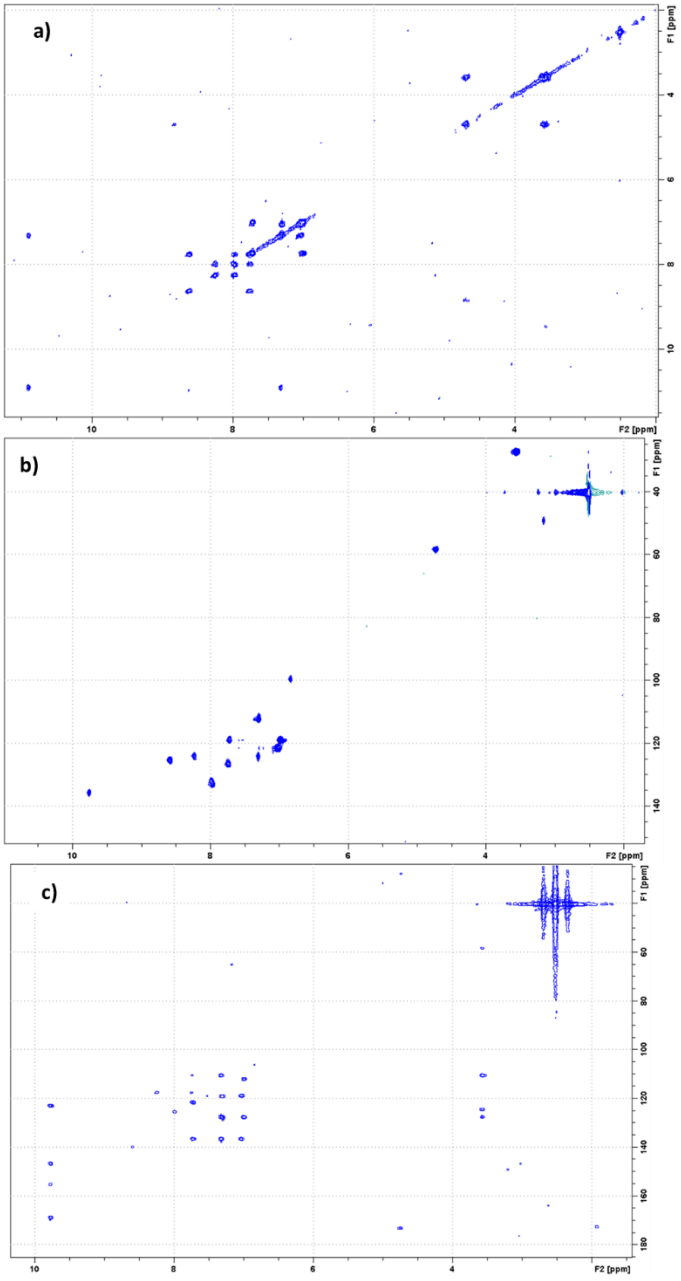

Figure 9.2.2.5. (a) $^{1}H,^{1}H$ COSY, (b) $^{1}H,^{13}C$ HSQC and (c) $^{1}H,^{13}C$ HMBC spectra of CGA-TRP/A in DMSO-d6.

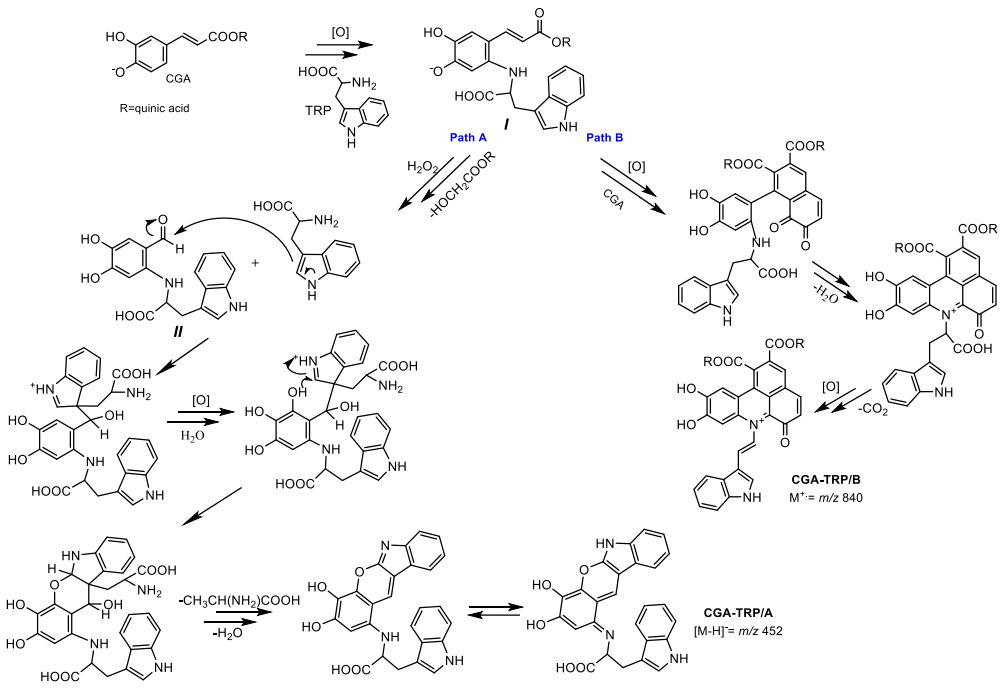

Figure 9.2.2.6. Proposed formation pathways of CGA-TRP/A and CGA-TPR/B.

9.2.3 Functional characterization of CGA-TRP pigment

In further experiments, pH and thermal stability of CGA-TRP pigment were evaluated in comparison with red wine anthocyanins and commercial betanin. As evidenced in Figure 9.2.3.1a, moving from pH 1-4 to pH 5-12, only a ca. 30 nm shift (from 578 to 546 nm) in the absorption maximum was observed, probably due to protonation of the imine type functionality of CGA-TRP/A at low pH, allowing for a more extensive electron delocalization. On the contrary, and as expected, pH impact was more marked on anthocyanins under the same conditions, whereas betanin was characterized by a relatively stability in the pH range 1-10 but underwent significant degradation at pH 12 (Figure 9.2.3.1b,c). In the future, the estimation of pK_a and a computational analysis could be carried out to go deeper into the spectral properties and their pH dependence.

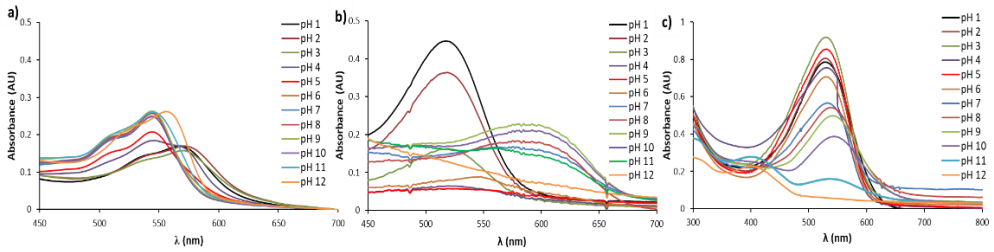

Figure 9.2.3.1. UV-Vis absorption spectra of (a) CGA-TRP pigment (0.018 mg/mL solution), (b) red wine anthocyanins (0.018 mg/mL solution) and (c) betanin (2.5 mg/mL solution), in 0.1 M phosphate buffer at pH 1.0-12.0.

In another series of experiments, the thermal stability of CGA-TRP pigment, red wine anthocyanins and betanin solutions was evaluated at pH 3.6 or 7.0. The pigment solutions were taken in an oven at 90°C and periodically analyzed by UV-Vis spectroscopy.[382] The results shown in Figure 9.2.3.2 indicated a ca. 30% abatement after 1 h of the absorption of the anthocyanin solution, while a complete abatement was observed for betanin after 1 h. On the other hand, CGA-TRP pigment was found to be stable over at least 3 h, with only a 5% absorbance decrease after 1 h. A greater degradation of red wine anthocyanins and betanin was observed at pH 7.0, while CGA-TRP pigment was found again to be stable.

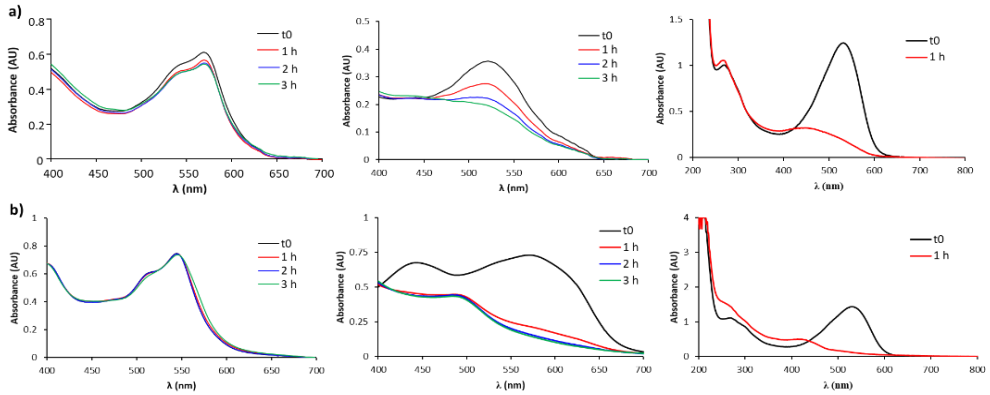

Figure 9.2.3.2. (a) UV–vis absorption spectra of CGA-TRP pigment (left), red wine anthocyanins (middle) and betanin (right) at different times in 0.3 M acetate buffer at pH 3.6 and (b) in 0.1 M phosphate buffer pH 7.0 (pigment concentration = 0.018 mg/mL for CGA-TRP and anthocyanin pigments, and 2.5 mg/mL for betanin).

The possible application of CGA-TRP pigment as a food dye was assessed in several food matrices. Due to the insolubility of the pigment in food matrices whose preparations did not involve a heating step, pre-dissolution in DMSO was needed. The coloring ability of CGA-TRP pigment is shown in Figure 9.2.3.3.

Figure 9.2.3.3. Coloring ability of CGA-TRP pigment in white yogurt (0.007% w/w pigment added as a DMSO solution), gelatin (0.01% w/w pigment), ice cream (0.01% w/w pigment added as a DMSO solution) and popsicle (0.01% w/w pigment), in this order.

To overcome the insolubility limitation, in further experiments the sodium salt of the pigment was prepared and used. A 1% aqueous solution of sodium salt showed extinction coefficient of 244 ± 2, that is a quite high value when compared with other natural red pigments like betanin. The sodium salt of CGA-TRP pigment was

directly added to the food matrix as a powder, leading to satisfactory colorations even when 0.01 % w/w of the pigment was used (Figure 9.2.3.4).

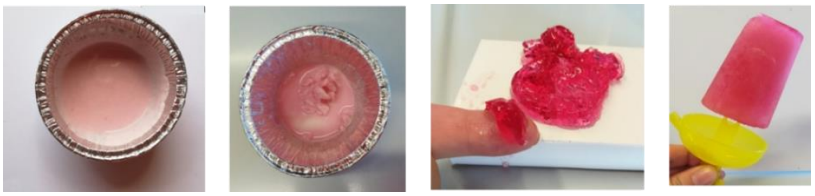

Figure 9.2.3.4. Coloring ability of sodium salt of CGA-TRP pigment (0.01 %w/w) in white yogurt, ice cream, gelatin, and popsicle.

9.2.4 Cytotoxicity of the CGA-TRP pigment

Cytotoxicity of the sodium salt of CGA-TRP pigment was evaluated on human hepatic cells (HepG2) and colonic cells (Caco-2 and CCD-18Co) after exposure to 0–200 µg/mL of the pigment for 24 h.[383] The treatment did not affect cell viability of both cell line, as reported in Table 9.2.5.1, indicating that the concentrations used to obtain an intense red color (100 µg/g), did not exert cytotoxicity.

Table 9.2.5.1. Cytotoxicity of the sodium salt of CGA-TRP pigment. Reported are the mean ± SD values of at least three experiments. Values are means ± SD of 8-14 data. Means in a column without a common letter differ, $P< 0.05$.

	Viable cells (%)		
	CCD-18Co	**Caco-2**	**HepG2**
Control	100.1 ± 5.47[a]	104.4 ± 9.7[a]	100.4 ± 10.1[a]
10 µg/mL	98.5 ± 6.4[a]	103.5 ± 7.1[a]	102.0 ± 10.9[a]
25 µg/mL	99.1 ± 9.3[a]	103.5 ± 9.0[a]	107.6 ± 9.1[a]
50 µg/mL	110.8 ± 8.2[a]	97.9 ± 7.2[a]	100.9 ± 9.5[a]
100 µg/mL	107.4 ± 6.7[a]	96.7 ± 7.9[a]	89.2 ± 10.2[a]
200 µg/mL	105.2 ± 8.8[a]	93.7 ± 5.0[a]	91.7 ± 11.3[a]

9.3 Conclusions

In this last Chapter, an easy preparation protocol of a red pigment by oxidative coupling of CGA with TRP has been reported. The reaction led to the formation of a cyanine-type chromophore integrated in a benzochromeno[2,3-b]indole scaffold,

responsible for its red color. The CGA-TRP pigment showed remarkable stability under different pHs conditions, and at temperatures up to 90°C both in acidic and neutral environment. Its sodium salt showed satisfactory water solubility and an extinction coefficient 5-20 times higher than that of commonly used natural red dyes. These features allowed to lower the use doses up to 0.01% w/w. Moreover, the pigment showed very low toxicity even at high concentrations needed to reach intense red colorations. CGA-TRP pigment and its sodium salt were found to be able to impart a natural red color to food products ranging from milk based, lipophilic ones to high hydrophilic matrices. This pigment could therefore represent a prototype of compounds derived from natural products for use in food applications.

9.4 Experimental section

Materials and methods

All solvents and reagents were obtained from commercial sources and used without further purification.

Red wine anthocyanins were kindly provided by Dr. Fabian Weber (Institute of Nutritional and Food Sciences, Molecular Food Technology, University of Bonn, Germany). Food products were purchased from a local market.

UV-Vis absorption spectra were recorded on a Hewlett Packard 8453 Agilent instrument.

HPLC analyses were performed on an Agilent instrument equipped with a UV-Vis detector (λ = 254 and 578 nm) using a Phenomenex Sphereclone C18 column (250 × 4.6 mm, 5 μm). 0.1% formic acid with acetonitrile from 20% to 80% in 40 min was used as the eluant, at a flow rate of 1 mL/min. Semipreparative HPLC fractionation was run on a Phenomenex Sphereclone C18 column (250 × 10 mm, 5 μm) (Castel Maggiore, Bologna, Italy) using the same gradient at a flow rate of 2 mL/min.

LC-MS analyses were run on an Agilent LC-MS ESI-TOF 1260/6230DA (instrument operating in positive ionization mode in the following conditions: nebulizer pressure 35 psig; drying gas (nitrogen) 5 L/min, 325 °C; capillary voltage 3500 V; fragmentor voltage 175 V). An Eclipse Plus C18 column, 150 × 4.6 mm, 5 μm at a flow rate of 0.4 mL/min was used, using the same eluant as above. Direct infusion in mass spectrometry (LCQ Fleet Thermofisher) was performed in positive and negative electrospray modes. The heater temperature was set at 100 °C, the gas flow rate was 20 (arb) and the capillary temperature was 275 °C. For positive mode the capillary voltage was 10 V, the tube lens voltage was 120 V, and the spray voltage was 5.5 kV. For negative mode the capillary voltage was -42 V, the tube lens voltage was -65.6 V, and the spray voltage was 4.5 kV. The monitored mass range was m/z 200–800.

^{1}H NMR (400 MHz or 500 MHz) and ^{13}C NMR (100 MHz or 126 MHz) spectra were recorded on Bruker Avance III-400 (Milan, Italy) or INOVA 500 (Palo Alto, CA, USA) spectrometers at room temperature. The proton couplings were evidenced by ^{1}H,^{1}H COSY experiments. Proton-detected heteronuclear correlations were measured using a gradient heteronuclear single-quantum coherence (HSQC), optimized for $^{1}J_{HC}$ = 155 Hz, a gradient heteronuclear multiple bond coherence (HMBC), optimized for $^{n}J_{HC}$ = 8 Hz.

9.4.1 Reaction of CGA and TRP. The reaction was carried out according to previously reported procedures.[377] Aqueous solutions of TRP (28-140 mM) and CGA (28 mM) were mixed at a 1:1 v/v ratio. The pH of the solution was adjusted to 9 with 0.1 M NaOH at the beginning of the reaction and after 10 and 30 min. The mixture was left under vigorous stirring and periodically analyzed by UV-Vis spectroscopy and LC-MS at 24 h intervals after 1:100 v/v dilution in water. In other experiments the reaction was run by replacing TRP with N-acetyl ethyl ester TRP, indole-3-acetic acid and tryptamine.

9.4.2 Preparation and characterization of the CGA-TRP pigment. 0.65 g of CGA were reacted with TRP (1.88 g, 5 molar eqs) under the reaction conditions described above. After 64 h, the reaction mixture was acidified to pH 1 with 3 M HCl. The red precipitate was then collected by centrifugation (7000 rpm, 15 min) and lyophilization (ca. 0.99 g). The pigment was re-dissolved in the minimum amount of 0.1 M NaOH and purified on a Sephadex G-10 column (60 ×2.5 cm) using water as eluant. 20 mL fractions were collected and analyzed spectrophotometrically after 1:100 v/v dilution in water. Those showing an absorption maximum at ca. 540 nm were combined, acidified to pH 1 and the precipitate collected by centrifugation and lyophilization, to give ca. 0.24 g (37% w/w yield with respect to CGA) of a red solid. The amount of residual TRP was evaluated by HPLC analysis with detection at 254 nm against a calibration curve obtained with solutions of TRP in a suitable concentration range. For NMR analysis the pigment purified by gel filtration was further fractionated by semipreparative HPLC under the conditions described above. Fractions eluted at around 29 min exhibiting a 1:1 ratio of absorptions at 280 nm and at 550 nm in the UV-Vis spectrum were collected and acidified, and the precipitate collected by centrifugation and lyophilization. The residue was characterized by NMR and MS analysis.

ESI(+): m/z 475.52 ($[M+Na]^+$), ESI(-): m/z 451.76 ($[M-H]^-$)

^{1}H NMR (DMSO-d6) δ (ppm): 3.57 (m), 4.70 (m), 6.81 (bs), 6.96 (t, J = 7.2 Hz), 7.00 (t, J = 7.0 Hz), 7.18 (s), 7.27 (d, J = 7.0 Hz), 7.28 (s), 7.40 (s), 7.70 (d, J = 7.2 Hz), 7.73 (t, d, J = 7.1 Hz), 7.95 (t, J = 7.9 Hz), 8.22 (d, J = 7.9 Hz), 8.58 (d, J = 7.1 Hz), 9.03 (bs), 9.73 (s), 10.93 (s).

^{13}C NMR (DMSO-d6) δ (ppm): 27.4, 58.0, 99.8, 110.0, 110.5, 111.9, 118.7, 119.0, 121.5, 124.3, 124.8, 125.2, 126.2, 127.6, 132.1,136.5, 170.4, 173.5.

9.4.3 Evaluation of the pH stability of the CGA-TRP pigment. 5 mg of the pigment were dissolved in 1.7 mL of 0.06 M NaOH, diluted 1:100 v/v in 0.1 M

phosphate buffer at pH 1-12, and analyzed by UV-Vis spectroscopy. The same procedure was applied to red wine anthocyanins (3 mg/mL in water) or commercial betanin (red beet extract diluted with dextrin) (250 mg/mL in water).

9.4.4 Evaluation of the thermal stability of the CGA-TRP pigment. 5 mg of pigment were dissolved in 1.7 mL 0.06 M NaOH and added to 50 mL of 0.3 M acetate buffer (pH 3.6) or 0.1 M phosphate buffer (pH 7.0). 5 mL of each mixture were taken at 90 °C and hourly analyzed by UV-Vis spectroscopy. Same experiments were carried out on red wine anthocyanins (0.1 mg/mL) and commercial betanin (8.5 mg/mL).

9.4.5 Preparation of the CGA-TRP pigment sodium salt. 30 mg of pigment were suspended in 3 mL of water and 0.1 M NaOH was slowly added until complete solubilization. The sodium salt was recovered by lyophilization and analyzed by UV-Vis spectroscopy for the determination of the extinction coefficient.

9.4.6 Food coloring with CGA-TRP pigment and its sodium salt. *Yogurt*: 2-4 mg of CGA-TRP pigment or its sodium salt were added as such or after dissolution in the minimum amount of DMSO or water, respectively, to 30 g of white yogurt. *Ice cream:* 2-4 mg of CGA-TRP pigment or its sodium salt were added as such or after dissolution in the minimum amount of DMSO or water, respectively, to 15-30 g of frozen milk; the mixture was then blended until the desired consistency was achieved. *Popsicle***:** 4-8 mg of CGA-TRP pigment or its sodium salt were added to 40 mL of water containing 12 g of sucrose; the mixture was heated in a water bath until complete dissolution and then left to freeze in a popsicle mold. *Gelatin***:** 2-4 mg of CGA-TRP pigment or its sodium salt were added to 20 mL of water containing 6 g of sucrose; the suspension was first heated in a water bath until complete dissolution, subsequently 2.5 g of isinglass were added and finally the mixture was left to cool at 4 °C.

9.4.7 Cytotoxicity evaluation. Cell viability was determined by the crystal violet assay in two human cancer cell lines (colonic Caco-2 cells and hepatic HepG2 cells) and in a normal colon cell line (CCD-18Co, kindly provided by Dr. Mª Dolores del Castillo, Instituto de Investigación en Ciencias de la Alimentación, Madrid). Cells were cultured in DMEM-F12 supplemented with 10% fetal bovine serum (FBS) and 50 mg/L of each of the following antibiotics: gentamicin, penicillin, and streptomycin. Cell lines were maintained at 37 ºC in a humidified atmosphere of 5% CO_2. Cells were plated (10^4 cells per well) in 96-well plates for the crystal violet assay and the next day treated for 24 h with different concentrations of the sodium salt of CGA-TRP pigment (10-200 µg/mL) diluted in serum-free culture medium. Then, cells were washed with PBS and incubated with crystal violet (0.2% in ethanol) for 20 min. Plates were rinsed with water, allowed to dry, and 1% SDS was added. The absorbance of each well was measured using a microplate reader at 570 nm (Bio-Tek, Winooski, VT, USA).

List of abbreviations

4-HBA 4-hydroxybenzoic acid
3,4-DHBA 3,4-dihydroyxbenzoic acid
BHA Butylated hydroxyanisole
BHT Butylated hydroxytoluene
C3G Cyanidin 3-O-β-glucoside
CCD Central composite design
CGA Chlorogenic acid
ChCl Choline chloride
CP-MAS Cross-polarization magic angle spinning
CS Coffee silverskin
CT Chestnut tannins
CWF Chestnut wood fiber
CWM Chestnut wood mud
DCF Dichlorofluorescein
DMF Dimethylformamide
DMS Dimethyl sulfate
DPPH 2,2-diphenyl-1-picrylhydrazyl
EA Ellagic acid
EDTA Ethylenediaminetetraacetic acid
EPR Electron paramagnetic resonance
Eqs Equivalents
FBS Fetal bovine serum
FFS Film forming solution
FOX Ferrous oxidation-xylenol orange
FRAP Ferric Reducing/Antioxidant Power
HBA Hydrogen bond acceptor
HBD Hydrogen bond donor
HRP Horseradish peroxidase
HSCG Hydrolyzed spent coffee ground
HTS Harsh treatment sample
ICP-MS Inductively coupled plasma mass spectrometry
L-DOPA 3,4-dihydroxy-L-phenylalanine
MB Methylene blue
MBC Minimal bactericidal concentration
MIC Minimal inhibitory concentration

MTS Mild treatment sample
MTT 3-(4,5-dimethyl-2-thiazolyl)-2,5-diphenyl-2H-tetrazolium bromide
NMR Solid state nuclear magnetic resonance
ODS Octadecylsilane
OTR Oxygen transmission rate
PE Polyethylene
PLA Poly(lactic acid)
PNSE Pecan nut shell hydroalcoholic extract
PolyCAME Poly(caffeic acid methyl ester)
PVDF Polyvinylidene Fluoride
QT Quebracho tannins
RH Relative humidity
RO Run order
ROS Reactive oxygen species
SCG Spent coffee ground
SEM Scanning electron microscopy
SI Swelling index
s/l Solid to liquid ratio
SO Standard order
TBA Thiobarbituric acid
TBARS Thiobarbituric acid reactive substances
TEM Transmission electron microscopy
TEMPO 2,2,6,6-Tetramethylpiperidinyloxy
TPC Total phenol content
TPTZ 2,4,6-tris(2-pyridyl)-s-triazine
Tris Tris (hydroxymethyl) aminomethane
Trolox 6-hydroxy-2,5,7,8-tetramethylchroman-2-carboxylic acid
TRP Tryptophan
TSA Tryptic Soy Agar
TSB Tryptic Soy Broth
WP Whey protein
WVP Water vapour permeability
WVTR Water vapor transmission rate
XRD X-ray diffraction

References

1. S. Osorio, J. G. Vallarino "From central to specialized metabolism: an overview of some secondary compounds derived from the primary metabolism for their role in conferring nutritional and organoleptic characteristics to fruit" *Front. Plant Sci.*, 10 (2019), 835.

2. A. Hussein, R. A. Hussein, A. A. El-anssary "Plants secondary metabolites: the key drivers of the pharmacological actions of medicinal plants" in *Herbal Medicine* (2018), 11–30.

3. R. Amorati, L. Valgimigli "Advantages and limitations of common testing methods for antioxidants" *Free Radic. Res.,* 49 (2015), 633–649.

4. E. Birben, U. M. Sahiner, C. Sackesen, S. Erzurum, O. Kalayci "Oxidative stress and antioxidant defense" *World Allergy Organ. J.,* 5 (2012) 9–19.

5. R. Kaur, J. Kaur, J. Mahajan, R. Kumar, A. Arora "Oxidative stress - implications, source and its prevention" *Environ. Sci. Pollut. Res. Int.,* 21 (2014) 1599–1613.

6. V. I. Lushchak "Free radicals, reactive oxygen species, oxidative stress and its classification" *Chem. Biol. Interact.,* 224 (2014), 164–175.

7. A. Martinez-Gomez, I. Caballero, C. A. Blanco "Phenols and melanoidins as natural antioxidants in structure, reactivity and antioxidant activity" *Biomolecules,* 10 (2020), 400.

8. I. Liguore, G. Russo, F. Curcio, G. Bulli, L. Aran, D. Della-Morte, G. Gargiulo, G. Testa, F. Cacciatore, D. Bonaduce, P. Abete "Oxidative stress, aging, and diseases" *Clin. Interv. Aging,* 13 (2018), 757–772.

9. M. d'Ischia, A. Napolitano, P. Manini, L. Panzella "Secondary targets of nitrite-derived reactive nitrogen species: nitrosation/nitration pathways, antioxidant defense mechanisms and toxicological implications" *Chem. Res. Toxicol.,* 24 (2011), 2071–2092.

10. R. Mishra, S. S. Bisht "Antioxidants and their charecterization" *J. Pharm. Res.,* 4 (2011) 2744–2746.

11. N. Balasundram, K. Sundram, S. Samman "Phenolic compounds in plants and agri-industrial by-products: antioxidant activity, occurrence, and potential uses" *Food Chem.,* 99 (2006), 191–203.

12. F. Shahidi, P. Ambigaipalan "Phenolics and polyphenolics in food, beverages and spices: antioxidant activity and health effects - a review" *J. Funct. Foods,* 18 (2015), 820–897.

13. L. T. N. Ha "Phenolic compounds and health benefites" *Vietnam J. Agri. Sci.,* 14 (2016), 1107–1118.

14. M. Magalhães, B. Manadas, T. Efferth, C. Cabral "Chemoprevention and therapeutic

role of essential oils and phenolic compounds: modeling tumor microenvironment in glioblastoma" *Pharmacol. Res.,* 169 (2021), 105638.

15. M.-T. Huang, T. Ferraro "Phenolic compounds in food and cancer prevention" in *Phenolic Compounds in Food and Their Effects on Health II* (1992), 8–34.

16. F. K. Ofosu, E. B.-M. Daliri, F. Elahi, R. Chelliah, B.-H. Lee, D.-H. Oh "New insights on the use of polyphenols as natural preservatives and their emerging safety concerns" *Front. Sustain. Food Syst.,* 4 (2020), 525810.

17. S. Martillanes, J. Rocha-Pimienta, M. Cabrera-Bañegil, D. Martín-Vertedor, J. Delgado-Adámez "Application of phenolic compounds for food preservation: food additive and active packaging" in *Phenolic Compounds - Biological Activity* (2017), 39–58.

18. L. B. Chibane, P. Degraeve, H. Ferhout, J. Bouajila, N. Oulahal "Plant antimicrobial polyphenols as potential natural food preservatives" *J. Sci. Food Agric.,* 99 (2019) 1457–1474.

19. A. Soto-Vaca, A. Gutierrez, J. N. Losso, Z. Xu, J. W. Finley "Evolution of phenolic compounds from color and flavor problems to health benefits" *J. Agric. Food Chem,.* 60 (2012), 6658–6677.

20. L. Panzella, A. Napolitano "Natural phenol polymers: recent advances in food and health applications" *Antioxidants,* 6 (2017), 30.

21. L. Panzella, A. Napolitano "Condensed tannins, a viable solution to meet the need for sustainable and effective multifunctionality in food packaging: structure, sources, and properties" *J. Agric. Food Chem.,* 70 (2022), 751–758.

22. D. J de Lima Cherubim, C. V. Buzanello Martins, L. O. Fariña, R. A. da Silva de Lucca "Polyphenols as natural antioxidants in cosmetics applications" *J. Cosmet. Dermatol.,* 19 (2020), 33–37.

23. L. Panzella, A. Napolitano "Natural and bioinspired phenolic compounds as tyrosinase inhibitors for the treatment of skin hyperpigmentation: recent advances" *Cosmetics,* 6 (2019), 57.

24. J. Saiz-Poseu, J. Sedó, B. García, C. Benaiges, T. Parella, R. Alibés, J. Hernando, F. Busqué, D. Ruiz-Molina "Versatile nanostructured materials *via* direct reaction of functionalized catechols" *Adv. Mater.* 25 (2013), 2066–2070.

25. J. Guo, T. Suma, J. J. Richardson, H. Ejima "Modular assembly of biomaterials using polyphenols as building blocks" *ACS Biomater. Sci. Eng.,* 5 (2019), 5578–5596.

26. M. A. Rahim, S. L. Kristufek, S. Pan, J. J Richardson, F. Caruso "Phenolic building blocks for the assembly of functional materials" *Angew. Chemie - Int. Ed.,* 58 (2019), 1904–1927.

27. D. Wu, J. Zhou, M. N. Creyer, W. Yim, Z. Chen, P. B. Messersmith, J. V. Jokerst "Phenolic-enabled nanotechnology: versatile particle engineering for biomedicine" *Chem. Soc. Rev.,* 50 (2021), 4432–4483.

28. R. J. Robbins "Phenolic acids in foods: an overview of analytical methodology" *J. Agric. Food Chem.,* 51 (2003), 2866–2887.

29. H. El. Gharras "Polyphenols: food sources, properties and applications – a review" *Int. J. Food Sci. Technol.,* 44 (2009), 2512–2518.

30. A. N. Panche, A. D. Diwan, R. S. Chandra "Flavonoids: an overview" *J. Nutr. Sci.,* 5 (2016), e47.

31. A. Samanta, G. Das, S. K. Das "Roles of flavonoids in plants" *Int. J. Pharm. Tech.,* 6 (2011), 12–35.

32. M. C. Dias, D. C. G. Pinto, A. M. S. Silva "Plant flavonoids: chemical characteristics and biological activity" *Molecules,* 26 (2011), 5377.

33. M.-H. Pan, C.-S. Lai, C.-T. Ho "Anti-inflammatory activity of natural dietary flavonoids" *Food Funct.,* 1 (2010), 15–31.

34. M. G. L. Hertog, P. C. H. Hollman, D. P. Venema "Optimization of a quantitative HPLC determination of potentially anticarcinogenic flavonoids in vegetables and fruits" *J. Agric. Food Chem.,* 40 (1992), 1591–1598.

35. H. E. Khoo, A. Azian, S. T. Tang, S. M. Lim "Anthocyanidins and anthocyanins: colored pigments as food, pharmaceutical ingredients, and the potential health benefits" *Food Nutr. Res.,* 61 (2017), 1361779.

36. G. Mazza, E. Miniati "*Anthocyanins in fruits, vegetables, and grains*" (CRC Press, 1993).

37. A. Khoddami, M. A. Wilkes, T. H.Roberts "Techniques for analysis of plant phenolic compounds" *Molecules,* 18 (2013), 2328–2375.

38. I. Ignat, I. Volf, V. I. Popa "A critical review of methods for characterisation of polyphenolic compounds in fruits and vegetables" *Food Chem.,* 126 (2011), 1821–1835.

39. V. Saibabu, Z. Fatima, L.A. Khan, S. Hameed "Therapeutic potential of dietary phenolic acids" *Adv. Pharmacol. Sci.,* 2015 (2015), 823539.

40. S. Kiokias, C. Proestos, V. Oreopoulou "Phenolic acids of plant origin - a review on their antioxidant activity *in vitro* (O/W emulsion systems) along with their *in vivo* health" *Foods*, 9 (2020), 534.

41. O. Koroleva, A. Torkova, I. Nikolaev, E. Khrameeva, T. Fedorova, M.Tsentalovich, R. Amarowicz "Evaluation of the antiradical properties of phenolic acids" *Int. J. Mol. Sci.,* 15 (2014), 16351–16380.

42. R. Vinayagam, M. Jayachandran, B. Xu "Antidiabetic effects of simple phenolic acids: a comprehensive review" *Phyther. Res.,* 30 (2016), 184–199.

43. J. Prajna, J. Richa, C. Dipjyoti "HPLC quantification of phenolic acids from *Vetiveria zizanioides* (L .) Nash and its antioxidant and antimicrobial activity" *J.*

Pharm., 2013 (2013), 270472.

44. C. Cueva, M. V. Moreno-Arribas, P. J. Martín-Álvarez, G. Bills, M. F. Vicente, A. Basilio, C. L. Rivas, T. Requena, J. M.Rodríguez, B. Bartolomé "Antimicrobial activity of phenolic acids against commensal, probiotic and pathogenic bacteria" *Res. Microbiol.,* 161 (2010), 372–382.

45. R. Khalil, Q. Ali, M. Hafeez, A. Malik "Phenolic acid profiling by RP-HPLC: evaluation of antibacterial and anticancer activities of *Conocarpus erectus* plant extracts" *Biol. Clin. Sci. Res. J.,* 2020 (2020), e010.

46. M. Abotaleb, A. Liskova, P. Kubatka, D. Büsselberg "Therapeutic potential of plant phenolic acids in the treatment of cancer" *Biomolecules,* 10 (2020), 221.

47. A. Pieczykolan, W. Pietrzak, U. Gawlik-Dziki, R. Nowak "Antioxidant, anti-inflammatory, and anti-diabetic activity of phenolic acids fractions obtained from *Aerva lanata* (L.) juss" *Molecules,* 26 (2021), 3486.

48. J. Kang, K. M. Thakali, G. S. Jensen, X. Wu "Phenolic acids of the two major blueberry species in the US Market and their antioxidant and anti-inflammatory activities" *Plant Foods Hum. Nutr.,* 70 (2015), 56–62.

49. B. V. Fiod Riccio, B. Fonseca-Santos, P. Colerato Ferrari, M. Chorilli "Characteristics, biological properties and analytical methods of *trans*-resveratrol: a review. *Crit. Rev. Anal. Chem.,* 50 (2020), 339–358.

50. J. A. Sirerol, M. L. Rodríguez, S. Mena, M. A. Asensi, J. M. Estrela, A. L. Ortega "Role of natural stilbenes in the prevention of cancer" *Oxid. Med. Cell. Longev.,* 2016 (2016), 3128951.

51. S. Soares, E. Brandão, C. Guerreiro, S. Soares, N. Mateus, V. de Freitas "Tannins in food: insights into the molecular perception of astringency and bitter taste" *Molecules,* 25 (2020), 2590.

52. V. Koleckar, K. Kubikova, Z. Rehakova, K. Kuca, D. Jun, L. Jahodar, L. Opletal "Condensed and hydrolysable tannins as antioxidants influencing the health" *Mini Rev. Med. Chem.,* 8 (2008), 436–447.

53. N. Unusan "Proanthocyanidins in grape seeds: an updated review of their health benefits and potential uses in the food industry" *J. Funct. Foods,* 67 (2020), 103861.

54. D. G. Reid, S. L. Bonnet, G. Kemp, J. H. Van Der Westhuizen "Analysis of commercial proanthocyanidins. Part 4: solid state ^{13}C NMR as a tool for *in situ* analysis of proanthocyanidin tannins, in heartwood and bark of quebracho and acacia, and related species" *Phytochemistry,* 94 (2013), 243–248.

55. E. Haslam, Y. Cai "Plant polyphenols (vegetable tannins): gallic acid metabolism" *Nat. Prod. Rep.,* 11 (1994), 41–66.

56. A. Pizzi "Tannins: major sources, properties and applications" in *Monomers, Polymers and Composites from Renewable Sources* (2008), 179–199.

57. S. Ma, H. Qin, M. Jiang, J. Wang, W. Wang, G. Guo, L. Zhou, W. Chen, B. Han "Identification and comparison of tannins in gall of *Rhus chinensis* Mill. and gall of *Quercus infectoria* Oliv. by High-Performance Liquid Chromatography-Electrospray Mass Spectrometry" *J. Chromatogr. Sci.,* 58 (2020), 403–410.

58. E. Haslam "Natural polyphenols (vegetable tannins) as drugs: possible modes of action" *J. Nat. Prod.,* 59 (1996), 205–215.

59. A. Zalacain, M. Prodanov, M. C. Delgado, G. L. Alonso, G. L. "Optimisation of extraction and identification of gallotannins from sumac leaves" *Biosyst. Eng.,* 84 (2003), 211–216.

60. A. Aguilar-Galvez, G. Noratto, F. Chambi, F. Debaste, D. Campos "Potential of tara (*Caesalpinia spinosa*) gallotannins and hydrolysates as natural antibacterial compounds" *Food Chem.,* 156 (2014), 301–304.

61. S. Peng, A. Scalbert, B. Monties "Insoluble ellagitannins in *Castanea sativa* and *Quercus petraea* woods" *Phytochemistry,* 30 (1991), 775–778.

62. P. Comandini, M. J. Lerma-García, E. F. Simó-Alfonso, T. G. Toschi "Tannin analysis of chestnut bark samples (*Castanea sativa* Mill.) by HPLC-DAD-MS" *Food Chem.,* 157 (2014), 290–295.

63. A. Scalbert "Antimicrobial properties of tannins" *Phytochemistry,* 30 (1991), 3875–3883.

64. L. J. Porter "Tannins" *Methods Plant Biochem.,* 1 (1989), 389–419.

65. P. Buzzini, P. Arapitsas, M. Goretti, E. Branda, B. Turchetti, P.Pinelli, F. Ieri, A. Romani "Antimicrobial and antiviral activity of hydrolysable tannins" *Mini Rev. Med. Chem.,* 8 (2008), 1179–1187.

66. G. Hussain, J. Huang, A. Rasul, H. Anwar, A. Imran, J. Maqbool, A. Razzaq, N. Aziz, E. Ul H. Makhdoom, M. Konuk, T. Sun "Putative roles of plant-derived tannins in neurodegenerative and neuropsychiatry disorders: an updated review" *Molecules,* 24 (2019), 2213.

67. Y. Shirmohammadli, D. Efhamisisi, A. Pizzi "Tannins as a sustainable raw material for green chemistry: a review" *Ind. Crops Prod.,* 126 (2018), 316–332.

68. L. Falcão, M. E. M. Araújo "Vegetable tannins used in the manufacture of historic leathers" *Molecules,* 23 (2018), 1081.

69. A. Pizzi "Tannins: prospectives and actual industrial applications" *Biomolecules,* 9 (2019), 344.

70. K.Van Langenberg, W. Grigsby, G. Ryan "Green Adhesives : options for the Australian industry – summary of recent research into green adhesives from renewable materials and identification of those that are closest to commercial uptake*", Project No. PNB158-0910. Forest Wood Products Australia*.

71. I. Mueller-Harvey "Unravelling the conundrum of tannins in animal nutrition and

health" *J. Sci. Food Agric.,* 86 (2006), 2010–2037.

72. A. Pizzi, A. Baecker "A new boron fixation mechanism for environment friendly wood preservatives" *Holzforschung,* 50 (1996), 507–510.

73. A. G. Da Silveira, E. J. Santini, S. M. Kulczynski, R. Trevisan A. D. Wastowski, D. A. Gatto "Tannic extract potential as natural wood preservative of *acacia mearnsii*" *An. Acad. Bras. Cienc.,* 89 (2017), 3031–3038.

74. M. F. Thévenon, G. Tondi, A. Pizzi "Environmentally friendly wood preservative system based on polymerized tannin resin-boric acid for outdoor applications" *Maderas Cienc. y Tecnol.,* 12 (2010), 253–257.

75. M. F. Thevenon, G. Tondi, A. Pizzi "High performance tannin resin-boron wood preservatives for outdoor end-uses" *Eur. J. Wood Wood Prod.,* 67 (2009), 89–93.

76. C. Tascioglu, M. Yalcin, T. de Troya, H. Sivrikaya "Termicidal properties of some wood and bark exctracts used as wood preservatives" *BioRes.,* 7 (2012), 2960–2969.

77. G. Matamala, W. Smeltzer, G. Droguett "Comparison of steel anticorrosive protection formulated with natural tannins extracted from acacia and from pine bark" *Corros. Sci,.* 42 (2000), 1351–1362.

78. M. S. Noor Idora, L. K. Quen, H. S. Kang "Effect of tannin from *Rhizophora apiculate* as corrosion inhibitor for epoxy paint on mild steel" *J. Phys. Conf. Ser.,* 890 (2017), 012062.

79. A. Hadzich, S. Flores, J. Caprari, R. Romagnoli "Study of zinc tannates prepared with Tara powder (*Caesalpinia spinosa*) as anticorrosive pigments in alkyd paints and wash primer formulations" *Prog. Org. Coat.,* 117 (2018), 35–46.

80. M. Pérez, G. Blustein, M. García, B. Del Amo, M. Stupak "Cupric tannate: a low copper content antifouling pigment" *Prog. Org. Coat.,* 55 (2006), 311–315.

81. A. L. Missio, B. D. Mattos, D. de F. Ferreira, W. L. E. Magalhães, D. A. Bertuol, D. A. Gatto, A. Petutschnigg, G. Tondi "Nanocellulose-tannin films: from trees to sustainable active packaging" *J. Clean. Prod.,* 184 (2018), 143–151.

82. P. Li, J. A. Sirviö, A. Haapala, A. Khakalo, H. Liimatainen "Anti-oxidative and UV-absorbing biohybrid film of cellulose nanofibrils and tannin extract" *Food Hydrocoll.,* 92 (2019), 208–217.

83. A. L. Missio, B. D. Mattos, C. G. Otoni, M. Gentil, R. Coldebella, A. Khakalo, D. A. Gatto, O. J. Rojas "Cogrinding wood fibers and tannins: surfactant effects on the interactions and properties of functional films for sustainable packaging materials" *Biomacromolecules,* 21 (2020), 1865–1874.

84. A. Cano, M. Andres, A. Chiralt, C. González-Martinez "Use of tannins to enhance the functional properties of protein based films" *Food Hydrocoll.,* 100 (2020), 105443.

85. C. Peña-Rodriguez, J. F. Martucci, L. M. Neira, A. Arbelaiz , A. Eceiza, R. A.

Ruseckaite "Functional properties and in vitro antioxidant and antibacterial effectiveness of pigskin gelatin films incorporated with hydrolysable chestnut tannin" *Food Sci. Technol. Int.,* 21 (2015), 221–231.

86. A.-K. Koopmann, C. Schuster, J. Torres-Rodríguez, S. Kain, H. Pertl-Obermeyer, A. Petutschnigg, N. Hüsing "Tannin-based hybrid materials and their applications: a review" *Molecules,* 25 (2020), 4910.

87. M. Kleinert, T. Barth "Phenols from lignin" *Chem. Eng. Technol.,* 31 (2008), 736–745.

88. V. K. Ponnusamy, D. D. Nguyen, J. Dharmaraja, S. Shobana, J. R. Banu, R. G. Saratale, S. W. Chang, G. Kumar "A review on lignin structure, pretreatments, fermentation reactions and biorefinery potential" *Bioresour. Technol.,* 271 (2019), 462–472.

89. A. Lourenço, H. Pereira "Compositional variability of lignin in biomass" in *Lignin - Trends and Applications* (2018).

90. A. Tribot, G. Amer, M. A. Alio, H. de Baynast, C. Delattre, A. Pons, J.-D. Mathias, J.-M. Callois, C. Vial, P. Michaud, C.-G. Dussap "Wood-lignin: supply, extraction processes and use as bio-based material" *Eur. Polym. J.,* 112 (2019), 228–240.

91. W. Boerjan, J. Ralph, M. Baucher "Lignin biosynthesis" *Annu. Rev. Plant Biol.,* 54 (2003), 519–546.

92. L. A. Zevallos Torres, A. L. Woiciechowski, V. Oliveira de Andrade Tanobe, S. G. Karp, L. C. Guimarães Lorenci, C. Faulds, C. R. Soccol "Lignin as a potential source of high-added value compounds: a review" *J. Clean. Prod.,* 263 (2020), 121499.

93. Q. Liu, L. Luo, L. Zheng "Lignins: biosynthesis and biological functions in plants" *Int. J. Mol. Sci.,* 19 (2018), 335.

94. B. Baurhoo, C. A. Ruiz-Feria, X. Zhao "Purified lignin: nutritional and health impacts on farm animals - a review" *Anim. Feed Sci. Technol.,* 144 (2008), 175–184.

95. I. Spiridon, "Extraction of lignin and therapeutic applications of lignin-derived compounds. A review" *Environ. Chem. Lett.,* 18 (2020), 771–785.

96. S. Iravani, R. S. Varma "Greener synthesis of lignin nanoparticles and their applications" *Green Chem.,* 22 (2020), 612–636.

97. G. S. Raza, J. Maukonen, M. Makinen, P. Niemi, L. Niiranen, A. A. Hibberd, K. Poutanen, J. Buchert, K.-H. Herzig "Hypocholesterolemic effect of the lignin-rich insoluble residue of brewer's spent grain in mice fed a high-fat diet" *J. Agric. Food Chem.,* 67 (2019), 1104−1114.

98. J. J. Liao, N. H. A. Latif, D. Trache, N. Brosse, M. H. Hussin "Current advancement on the isolation, characterization and application of lignin" *Int. J. Biol. Macromol.,* 162 (2020), 985–1024.

99. E. Lizundia, M. H. Sipponen, L. G. Greca, M. Balakshin, B. L. Tardy, O. J. Rojas, D.

Puglia "Multifunctional lignin-based nanocomposites and nanohybrids" *Green Chem.,* 23 (2021), 6698–6760.

100. S.-J. Zhou, H.-M. Wang, S.-J. Xiong, J.-M. Sun, Y.-Y. Wang, S. Yu, Z. Sun, J.-L. Wen, T.-Q. Yuan "Technical lignin valorization in biodegradable polyester-based plastics (BPPs)" *Green Chem.,* 9 (2021), 12017−12042.

101. H.-M. Wang, T.-Q. Yuan, G.-Y. Song, R.-C. Sun "Advanced and versatile lignin-derived biodegradable composite film materials toward a sustainable world" *Green Chem.,* 23 (2021), 3790–3817.

102. R. Liu, L. Dai, C. Xu, K. Wang, C. Zheng, C. Si "Lignin-based micro- and nanomaterials and their composites in biomedical applications" *ChemSusChem,* 13 (2020), 4266–4283.

103. Q. Tang,Y. Qian, D. Yang, X. Qiu, Y. Qin, M. Zhou "Lignin-based nanoparticles: a review on their preparations and applications" *Polymers,* 12 (2020), 2471.

104. F. G. Fermoso, A. Serrano, B. Alonso-Fariñas, J. Fernández-Bolaños, R. Borja, G. Rodríguez-Gutiérrez "Valuable compound extraction, anaerobic digestion, and composting: a leading biorefinery approach for agricultural wastes" *J. Agric. Food Chem.,* 66 (2018), 8451–8468.

105. H. Xia, J. A. Houghton, J. H. Clark, A. S. Matharu "Potential utilization of unavoidable food supply chain wastes-valorization of pea vine wastes" *ACS Sustain. Chem. Eng.,* 4 (2016), 6002–6009.

106. V. G. Zuin, L. Z. Ramin "Green and sustainable separation of natural products from agro-industrial waste: challenges, potentialities, and perspectives on emerging approaches" *Top. Curr. Chem.,* 376 (2018), 3.

107. M. Macias Corral, Z. Samani, A. Hanson, G. Smith, P. Funk, H. Yu, J. Longworth "Anaerobic digestion of municipal solid waste and agricultural waste and the effect of co-digestion with dairy cow manure" *Bioresour. Technol.,* 99 (2008), 8288–8293.

108. R. C. Fierascu, E. Sieniawska, A. Ortan, I. Fierascu, J. Xiao "Fruits by-products – a source of valuable active principles. A short review" *Front. Bioeng. Biotechnol.,* 8 (2020), 319.

109. K. S. Ganesh, A. Sridhar, S. Vishali "Utilization of fruit and vegetable waste to produce value-added products: conventional utilization and emerging opportunities-a review" *Chemosphere,* 287 (2022), 132221.

110. C. Torres-León, N. Ramírez-Guzman, L. Londoño-Hernandez, G. A. Martinez-Medina, R. Díaz-Herrera, V. Navarro-Macias, O. B. Alvarez-Pérez, B. Picazo, M. Villarreal-Vázquez, J. Ascacio-Valdes, C. N. Aguilar "Food waste and byproducts: an opportunity to minimize malnutrition and hunger in developing countries" *Front. Sustain. Food Syst.,* 2 (2018), 52.

111. I. Mourtzinos, A. Goula "Polyphenols in agricultural byproducts and food waste" in *Polyphenols in Plants* (2019), 23–44.

112. L. Panzella, F. Moccia, R. Nasti, S. Marzorati, L. Verotta, A. Napolitano "Bioactive phenolic compounds from agri-food wastes: an update on green and sustainable extraction methodologies" *Front. Nutr.,* 7 (2020), 60.

113. A. Teixeira, N. Baenas, R. Dominguez-Perles, A. Barros, E. Rosa, D. A. Moreno, C. Garcia-Viguera "Natural bioactive compounds from winery by-products as health promoters: a review" *Int. J. Mol. Sci.,* 15 (2014), 15638–15678.

114. D. Panwar, P. S. Panesar, H. K. Chopra "Recent trends on the valorization strategies for the management of citrus by-products" *Food Rev. Int.,* 37 (2021), 91–120.

115. E. S. Dassoff, J. X. Guo, Y. Liu, S. C. Wang, Y. O. Li, "Potential development of non-synthetic food additives from orange processing by-products - a review" *Food Qual. Saf.,* 5 (2021), 1–14.

116. K. Tortora, A. P. Femia, A. Romagnoli, I. Sineo, M. Khatib, N. Mulinacci, L. Giovannelli, G. Caderni "Pomegranate by-products in colorectal cancer chemoprevention: effects in Apc-mutated pirc rats and mechanistic studies *in vitro* and *ex vivo*" *Mol. Nutr. Food Res.,* 62 (2018), 1700401.

117. M. Fourati, S. Smaoui, H. B. Hlima, K. Elhadef, O. B. Braïek, K. Ennouri, A. C. Mtibaa, L. Mellouli "Bioactive compounds and pharmacological potential of pomegranate (*Punica granatum*) seeds - a review" *Plants Foods Hum. Nutr.,* 75 (2020), 477–486.

118. A. Fazio, D. Iacopetta, C. La Torre, J. Ceramella, N. Muià, A. Catalano, A. Carocci, M. S. Sinicropi "Finding solutions for agricultural wastes: antioxidant and antitumor properties of recovery" *Foods Funct.,* 9 (2018), 6618–6631.

119. E. M. C.Alexandre, S. Silva, S. A. O. Santos, A. J. D. Silvestre, M. F. Duarte, J. A. Saraiva, M. Pintado "Antimicrobial activity of pomegranate peel extracts performed by high pressure and enzymatic assisted extraction" *Food Res. Int.,* 115 (2019), 167–176.

120. M. V. Eberhardt, C. Y. Lee, R. H. Liu "Antioxidant activity of fresh apples" *Nature,* 405 (2000), 903–904.

121. L. Panzella, M. Petriccione, P. Rega, M. Scortichini, A. Napolitano "A reappraisal of traditional apple cultivars from Southern Italy as a rich source of phenols with superior antioxidant activity" *Food Chem.,* 140 (2013), 672–679.

122. W. M. Hikal, A. A. Mahmoud, H. A. H. Said-Al Ahl, A. Bratovcic, K. G. Tkachenko, M. Kač niov R. M. Rodriguez "Pineapple (*Ananas comosus* L. Merr.), waste streams, characterisation and valorisation: an overview" *J. Ecol.,* 11 (2021), 610–634.

123. S. P. Kapadia, P. S. Pudakalkatti, S. Shivanaikar, "Detection of antimicrobial activity of banana peel (*Musa paradisiaca* L.) on *Porphyromonas gingivalis* and *Aggregatibacter actinomycetemcomitans*: an *in vitro* study" *Contemp. Clin. Dent.,* 6 (2015), 496–499.

124. J. Lee, R. E. Wrolstad "Extraction of anthocyanins and polyphenolics from blueberry processing waste" *J. Food Sci.,* 69 (2004), 564–573.

125. E. M. Azman, A. House, D. Charalampopoulos, A. Chatzifragkou "Effect of dehydration on phenolic compounds and antioxidant activity of blackcurrant (*Ribes nigrum* L.) pomace" *Int. J. Food Sci. Technol.,* 56 (2021), 600–607.

126. M. A. Varo, M. Jacotet-Navarro, M. P. Serratosa, J. Mérida, A.-S. Fabiano-Tixier, A. Bily, F. Chemat "Green ultrasound-assisted extraction of antioxidant phenolic compounds determined by high performance liquid chromatography from bilberry (*Vaccinium Myrtillus* L .) juice by-products" *Waste and Biomass Valorization,* 10 (2019), 1945–1955.

127. S. Mildner-Szkudlarz, J. Bajerska, P. Górnaś, D. Segliņa, A. Pilarska, T. Jesionowski "Physical and bioactive properties of muffins enriched with raspberry and cranberry pomace powder: a promising application of fruit by-products rich in biocompounds" *Plants Foods Hum. Nutr.,* 71 (2016), 165–173.

128. Q. Y. Zafra-Rojas, B. E. González-Martínez, N. del Socorro Cruz-Cansino, M. López-Cabanillas, Á. Suárez-Jacobo, A. Cervantes-Elizarrarás, E. Ramírez-Moreno "Effect of ultrasound on *in vitro* bioaccessibility of phenolic compounds and antioxidant capacity of blackberry (*Rubus fruticosus*) residues cv. Tupy" *Plants Foods Hum. Nutr.,* 75 (2020), 608–613.

129. E. Villamil-Galindo, F. Van de Velde, A. M. Piagentini "Strawberry agro-industrial by-products as a source of bioactive compounds: effect of cultivar on the phenolic profile and the antioxidant capacity" *Bioresour. Bioprocess.,* 8 (2021), 61.

130. E. Robles, N. Izaguirre, A. Martin, D. Moschou, J. Labidi "Assessment of bleached and unbleached nanofibers from pistachio shells for nanopaper making" *Molecules,* 26 (2021), 1371.

131. S. Er an, O. G. st nda , R. Carle, R. M. Schweiggert "Identification of phenolic compounds in red and green pistachio (*Pistacia vera* L.) hulls (Exo- and Mesocarp) by HPLC-DAD-ESI-(HR)-MS" *J. Agric. Food Chem.,* 64 (2016), 5334−5344.

132. A. S. Sonmezdag, H. Kelebek, S. Selli "Characterization and comparative evaluation of volatile, phenolic and antioxidant properties of pistachio (*Pistacia vera* L.) hull" *J. Essent. Oil Res.,* 29 (2016), 262–270.

133. J. Qiu, L. Chen, Q. Zhu, D. Wang, W. Wang, X. Sun, X. Liu, F. Du "Screening natural antioxidants in peanut shell using DPPH – HPLC – DAD – TOF/MS methods" *Food Chem.,* 135 (2012), 2366–2371.

134. O. Bobet, S. Nassio, M. Seynou, B. Remy, L. Zerbo, I. Sanou, M. Sawadogo, Y. Millogo, E. Gilles "Characterization of peanut shells for their valorization in earth brick" *J. Miner. Mater. Charact. Eng.,* 8 (2020), 301–315.

135. V. Silva, V. Falco, M. I. Dias, L. Barros, A. Silva, R. Capita, C. Alonso-Calleja, J. S. Amaral, G. Igrejas, I. C. F. R. Ferreira, P. Poeta "Evaluation of the phenolic profile of *Castanea sativa* Mill. by-products and their antioxidant and antimicrobial activity

against multiresistant bacteria" *Antioxidants,* 9 (2020), 87.

136. L. Cruz-Lopes, I. Domingos, J. V. Ferreira, B. Esteves "Chemical composition and study on liquefaction optimization of chestnut shells" *Open Agric.,* 5 (2020), 905–911.

137. M. Hu, X. Yang, X. Chang "Bioactive phenolic components and potential health effects of chestnut shell: a review" *J. Food Biochem.,* 45 (2021), e13696.

138. E. Alvarez-Parrilla, L. A. de la Rosa, R. Urrea Lopez "Bioactive components and health effects of pecan nuts and their byproducts: a review" *J. Food Bioact.,* 1 (2018), 56–92.

139. J. Villasante, E. Pérez-Carrillo, E. Heredia-Olea, I. Metón, M. P. Almajano "*In vitro* antioxidant activity optimization of nut shell (*Carya illinoinensis*) by extrusion using response surface methods" *Biomolecules,* 9 (2019), 883.

140. B. Yuan, M. Lu, K. M. Eskridge, L. D. Isom, M. A. Hanna "Extraction, identification, and quantification of antioxidant phenolics from hazelnut (*Corylus avellana* L.) shells" *Food Chem.,* 244 (2018), 7–15.

141. H. Kelebek, S. Selli, P. Kadiro lu, O. Kola, S. Kesen, B. Uçar, B. Çetiner "Bioactive compounds and antioxidant potential in tomato pastes as affected by hot and cold break process" *Food Chem.,* 220 (2017), 31–41.

142. F. Shahidi, V. Varatharajan, W. Y. Oh, H. Peng "Phenolic compounds in agri-food by-products, their bioavailability and health effects" *J. Food Bioact.,* 5 (2019), 57–119.

143. K. Szabo, F. V. Dulf, Z. Diaconeasa, D. C. Vodnar "Antimicrobial and antioxidant properties of tomato processing byproducts and their correlation with the biochemical composition" *Lwt,* 116 (2019), 108558.

144. H. Akyol, Y. Riciputi, E. Capanoglu, M. F. Caboni, V. Verardo "Phenolic compounds in the potato and its byproducts: an overview" *Int. J. Mol. Sci.,* 17 (2016), 835.

145. R. Azmat, S. Moin, A. Saleem "Remediation of Cu metal-induced accelerated Fenton reaction by potato peels bio-sorbent" *Environ. Monit. Assess.,* 188 (2016), 674.

146. P. S. Murthy, M. M. Naidu "Recovery of phenolic antioxidants and functional compounds from coffee industry by-products" *Food Bioprocess Technol.,* 5 (2012), 897–903.

147. F. J. Barba, E. Roselló-Soto, M. Brncic, J. M. Lorenzo "*Green extraction and valorization of by-products from food processing" (CRC Press, 2019).*

148. T. Conde, S. I. Mussatto "Isolation of polyphenols from spent coffee grounds and silverskin by mild hydrothermal pretreatment" *Prep. Biochem. Biotechnol.,* 46 (2016), 406–409.

149. A. S. P. Moreira, F. M. Nunes, M. R. Domingues, M. A.Coimbra "Coffee melanoidins: structures, mechanisms of formation and potential health impacts" *Food Funct.,* 3 (2012), 903–915.

150. L. Panzella, P. Cerruti, V.Ambrogi, S. Agustin-Salazar, G. D'Errico, C. Carfagna, L. Goya, S. Ramos, M. A. Martín, A. Napolitano, and M. d'Ischia "A superior all-natural antioxidant biomaterial from spent coffee grounds for polymer stabilization, cell protection, and food lipid preservation" *ACS Sustain. Chem. Eng.,* 4 (2016), 1169–1179.

151. A. Panusa, A. Zuorro, R. Lavecchia, G. Marrosu, R. Petrucci "Recovery of natural antioxidants from spent coffee grounds" *J. Agric. Food Chem.,* 61 (2013), 4162–4168.

152. C. Monente, I. A. Ludwig, A. Irigoyen, M. P. De Peña, C. Cid "Assessment of total (free and bound) phenolic compounds in spent coffee extracts" *J. Agric. Food Chem.,* 63 (2015), 4327–4334.

153. I. Okur, B. Soyler, P. Sezer, M. H. Oztop, H. Alpas "Improving the recovery of phenolic compounds from spent coffee grounds (SCG) by environmentally friendly extraction techniques" *Molecules,* 26 (2021), 613.

154. J. J. Rochín-Medina, K. Ramírez, J. G. Rangel-Peraza, Y. A. Bustos-Terrones "Increase of content and bioactivity of total phenolic compounds from spent coffee grounds through solid state fermentation by *Bacillus clausii*" *J. Food Sci. Technol.,* 55 (2018), 915–923.

155. S. I. Mussatto, L. F. Ballesteros, S. Martins, J. A. Teixeira, "Extraction of antioxidant phenolic compounds from spent coffee grounds" *Sep. Purif. Technol.,* 83 (2011), 173–179.

156. D. Pujol, C. Liu, J. Gominho, M.À. Olivella, N. Fiol, I. Villaescusaa, H. Pereira "The chemical composition of exhausted coffee waste" *Ind. Crops Prod.,* 50 (2013), 423–429.

157. G. V. de Melo Pereira, D. P. de Carvalho Neto, A. I Magalhães J., F. Guilherme do Prado, M. G. B. Pagnoncelli, S. G. Karp, C. R. Soccol "Chemical composition and health properties of coffee and coffee by-products" *Adv. Food Nutr. Res.*, 91 (2020), 65-96.

158. L. Bresciani, L. Calani, R. Bruni, F. Brighenti, D. Del Rio "Phenolic composition, caffeine content and antioxidant capacity of coffee silverskin" *Food Res. Int.,* 61 (2014), 196–201.

159. N. J. Salazar-López, C. V. López-Rodríguez, D. A. Hernández-Montoya, R. Campos-Vega "Health benefits of spent coffee grounds *Coffea Arabica* L" in *Food Waste and by-products* (2020), 327–351.

160. N. García-Gutiérrez, M. E. Maldonado-Celis, M. Rojas-López, G. F. Loarca-Piña, R. Campos-Vega "The fermented non-digestible fraction of spent coffee grounds induces apoptosis in human colon cancer cells (SW480)" *J. Funct. Foods,* 30 (2017),

237–246.

161. D. M. López-Barrera, K. Vázquez-Sánchez, M. G. F. Loarca-Piña, R. Campos-Vega "Spent coffee grounds, an innovative source of colonic fermentable compounds, inhibit inflammatory mediators *in vitro*" *Food Chem.,* 212 (2016), 282–290.

162. B. Fernandez-Gomez, A. Lezama, M. Amigo-Benavent, M. Ullate, M. Herrero, M. Á. Martín, M. D. Mesa, M. D. del Castillo "Insights on the health benefits of the bioactive compounds of coffee silverskin extract" *J. Funct. Foods,* 25 (2016), 197–207.

163. A. Iriondo-DeHond, M. B. Rios, T. Herrera, A. Rodriguez-Bertos, F. Nuñez, M. I. San Andres, S. Sanchez-Fortun, M. D. Del Castillo "Coffee silverskin extract: nutritional value, safety and effect on key biological functions" *Nutrients,* 11 (2019), 2693.

164. F. Rodrigues, A. Palmeira-de-Oliveira, J. das Neves, B. Sarmento, M. H. Amaral, M. B. P. P. Oliveira "Coffee silverskin: a possible valuable cosmetic ingredient" *Pharm. Biol.,* 53 (2015), 386–394.

165. P. Ferreira-Santos, E. Zanuso, Z. Genisheva, C. M. R. Rocha, J. A. Teixeira "Green and sustainable valorization of bioactive phenolic compounds from *Pinus* by-products" *Molecules,* 25 (2020), 2931.

166. A. Greinert, M. Mzowczynska, W. Szefner "The use of waste biomass from the wood industry and municipal sources for energy production" *Sustainability,* 11 (2019), 3083.

167. S. Djilas, J. Čanadanović-Brunet, G. Ćetković "By-products of fruits processing as a source of phytochemicals" *Chem. Ind. Chem. Eng. Q.,* 15 (2009), 191–202.

168. V. Sukruansuwan, S. C. Napathorn "Use of agro-industrial residue from the canned pineapple industry for polyhydroxybutyrate production by *Cupriavidus necator* strain A-04" *Biotechnol. Biofuels,* 11 (2018), 202.

169. M. S. N. dos Santos, G. L. Zabot, M. A. Mazutti, M. V. Tres "Potential applications of pecan residual biomasses: a review" *Biointerface Res. Appl. Chem.,* 10 (2020), 5524–5531.

170. I. Sepelev, R. Galoburda "Industrial potato peel waste application in food production: a review" *Res. Rural Dev.,* 1 (2015), 130–136.

171. T. Løvdal, B. Van Droogenbroeck, E. C. Eroglu, S. Kaniszewski, G. Agati, M. Verheul, D. Skipnes "Valorization of tomato surplus and waste fractions: a case study using Norway, Belgium, Poland, and Turkey as examples" *Foods,* 8 (2019), 229.

172. H. Cory, S. Passarelli, J. Szeto, M. Tamez, J. Mattei "The role of polyphenols in human health and food systems: a mini-review" *Front. Nutr.,* 5 (2018), 87.

173. S. Ben-Othman, I. Jõudu, R. Bhat "Bioactives from agri-food wastes: present insights and future challenges" *Molecules,* 25 (2020), 510.

174. L. Verotta, L. Panzella, S. Antenucci, V. Calvenzani, F. Tomay, K. Petroni, E. Caneva, A. Napolitano "Fermented pomegranate wastes as sustainable source of ellagic acid: antioxidant properties, anti-inflammatory action, and controlled release under simulated digestion conditions" *Food Chem.,* 246 (2018), 129–136.

175. P. Goupy, C. Dufour, M. Loonis, O. Dangles "Quantitative kinetic analysis of hydrogen transfer reactions from dietary polyphenols to the DPPH radical" *J. Agric. Food Chem.,* 51 (2003), 615–622.

176. V. Gökmen, A. Serpen, V. Fogliano "Direct measurement of the total antioxidant capacity of foods: the 'QUENCHER' approach" *Trends Food Sci. Technol.,* 20 (2009), 278–288.

177. I. F. F. Benzie, J. J. Strain The ferric reducing ability of plasma (FRAP) as a measure of "antioxidant power": the FRAP assay" *Anal. Biochem.,* 239 (1996), 70–76.

178. N. Seifzadeh, M. A. Sahari, M. Barzegar, H. A. Gavlighi, L. Calani, D. Del Rio, G. Galaverna "Evaluation of polyphenolic compounds in membrane concentrated pistachio hull extract" *Food Chem.,* 277 (2019), 398–406.

179. L. Panzella, T. Eidenberger, A. Napolitano, M. D'Ischia "Black sesame pigment: DPPH assay-guided purification, antioxidant/antinitrosating properties, and identification of a degradative structural marker" *J. Agric. Food Chem.,* 60 (2012), 8895–8901.

180. A. Javed, A. Ahmad, A. Tahir, U. Shabbir, M. Nouman, A. Hameed "Potato peel waste—its nutraceutical, industrial and biotechnological applacations" *AIMS Agric. Food,* 4 (2019), 807–823.

181. L. Panzella, S. Pérez-Burillo, S.Pastoriza, M. Á. Martín, P. Cerruti, L.Goya, S. Ramos, J. Á. Rufián-Henares, A. Napolitano, M. d'Ischia "High antioxidant action and prebiotic activity of hydrolyzed spent coffee grounds (HSCG) in a simulated digestion-fermentation model: toward the development of a novel food supplement" *J. Agric. Food Chem.,* 65 (2017), 6452–6459.

182. J.-X. Sun, X.-F. Sun,. R.-C. Sun, P. Fowler, M. S. Baird "Inhomogeneities in the chemical structure of sugarcane bagasse lignin" *J. Agric. Food Chem.,* 51 (2003), 6719–6725.

183. L. Panzella, T. Eidenberger, A. Napolitano "Anti-Amyloid aggregation activity of black sesame pigment: toward a novel Alzheimer's disease preventive agent" *Molecules,* 23 (2018), 676.

184. R. García-Villalba, J. C. Espín, K. Aaby, C. Alasalvar, M. Heinonen, G. Jacobs, S. Voorspoels, T. Koivumäki, P. A. Kroon, E. Pelvan, S. Saha, F. A. Tomás-Barberán "A validated method for the characterization and quantification of extractable and non-extractable ellagitannins after acid hydrolysis in pomegranate fruits, juices, and extracts" *J. Agric. Food Chem.,* 63 (2015), 6555–6566.

185. W. Yang, G. Qi, J. K. Kenny, D. Puglia, P. Ma "Effect of cellulose nanocrystals and lignin nanoparticles on mechanical, antioxidant and water vapour barrier properties

of glutaraldehyde crosslinked PVA films" *Polymers,* 12 (2020), 1364.

186. M. A. Ortenzi, S. Gazzotti, B. Marcos, S. Antenucci, S. Camazzola, L. Piergiovanni, H. Farina, G. Di Silvestro, L. Verotta "Synthesis of polylactic acid initiated through biobased antioxidants: towards intrinsically active food packaging" *Polymers,* 12 (2020), 1183.

187. V. Ambrogi, L. Panzella, P. Persico, P. Cerruti, C. A. Lonz, C. Carfagna, L. Verotta, E. Caneva, A. Napolitano, M d'Ischia "An antioxidant bioinspired phenolic polymer for efficient stabilization of polyethylene" *Biomacromolecules,* 15 (2014), 302–310.

188. S. Antenucci, L. Panzella, H. Farina, M. A. Ortenzi, E. Caneva, S. Martinotti, E. Ranzato, B. Burlando, M. d'Ischia, A. Napolitano, L. Verotta "Powering tyrosol antioxidant capacity and osteogenic activity by biocatalytic polymerization" *RSC Adv.,* 6 (2016), 2993–3002.

189. D. Liberti, M. L. Alfieri, D. M. Monti, L. Panzella, A. Napolitano "A melanin-related phenolic polymer with potent photoprotective and antioxidant activities for dermo-cosmetic applications" *Antioxidants,* 9 (2020), 270.

190. K. Zheng, H. Tang, Q. Chen, L. Zhang, Y. Wu, Y. Cui "Enzymatic synthesis of a polymeric antioxidant for efficient stabilization of polypropylene" *Polym. Degrad. Stab.,* 112 (2015), 27–34.

191. K. Zheng, L. Zhang, Y. Gao, Y. Wu, W. Zhao, Y. Cui "Enzymatic oxidative polymerization of pyrogallic acid for preparation of hindered phenol antioxidant" *J. Appl. Polym. Sci.,* 132 (2014), 41591.

192. L. Panzella, G. D'Errico, G. Vitiello, M. Perfetti, M. L. Alfieri, A. Napolitano, M. d'Ischia "Disentangling structure-dependent antioxidant mechanisms in phenolic polymers by multiparametric EPR analysis" *Chem. Commun.,* 54 (2018), 9426–9429.

193. P. Sarti "*Nitric oxide in human health and disease*" eLS, 2013.

194. O. Mustafa, K. Gu, C. Esra "Antioxidant activity/capacity measurement. 1. Classification, physicochemical principles, mechanisms, and electron transfer (ET)-based assays" *J. Agric. Food Chem.,* 64 (2016), 997–1027.

195. P. Meredith, T. Sarna "The physical and chemical properties of eumelanin" *Pigment Cell Res.,* 19 (2006), 572–594.

196. A. B. Mostert, G. R. Hanson, T. Sarna, I. R. Gentle, B. J. Powell, P. Meredith "Hydration-controlled X-band EPR spectroscopy: a tool for unravelling the complexities of the solid-state free radical in eumelanin" *J. Phys. Chem. B,* 117 (2013), 4965–4972.

197. L. Panzella, G. Gentile, G. D'Errico, N. F. Della Vecchia, M. E. Errico, A. Napolitano, C. Carfagna, M. d'Ischia "Atypical structural and π-electron features of a melanin polymer that lead to superior free-radical-scavenging properties" *Angew. Chem. Int. Ed. Engl.,* 125 (2013), 12916–12919.

198. S. Moussouni, M.-L. Saru, E. Ioannou, M. Mansour, A. Detsi, V. Roussis, P. Kefalas

"Crude peroxidase from onion solid waste as a tool for organic synthesis. Part II: oxidative dimerization-cyclization of methyl *p*-coumarate, methyl caffeate and methyl ferulate" *Tetrahedron Lett.,* 52 (2011), 1165–1168.

199. A. B. Muñoz-García, F. Sannino, G. Vitiello, D. Pirozzi, L. Minieri, A. Aronne, P. Pernice, M. Pavone, G. D'Errico "Origin and electronic features of reactive oxygen species at hybrid zirconia-acetylacetonate interfaces" *ACS Appl. Mater. Interfaces,* 7 (2015), 21662–21667.

200. L. Marcocci, J. J. Maguire, M. T. Droy-Lefaix, L. Packer "The nitric oxide-scavenging properties of Ginkgo biloba extract EGb 761" *Biochem. Biophys. Res. Commun.,* 201 (1994), 748–755.

201. C. Xu, S. Liu, Z. Liu, F. Song, S. Liu "Superoxide generated by pyrogallol reduces highly water-soluble tetrazolium salt to produce a soluble formazan: a simple assay for measuring superoxide anion radical scavenging activities of biological and abiological samples" *Anal. Chim. Acta,* 793 (2013), 53–60.

202. P. K. Sadh, P. Chawla, J. S. Duhan "Fermentation approach on phenolic, antioxidants and functional properties of peanut press cake" *Food Biosci.,* 22 (2018), 113–120.

203. S. Maicas "The role of yeasts in fermentation processes" *Microorganisms,* 8 (2020), 1142.

204. R. Luedeking, E. L. Piret "A kinetic study of the lactic acid fermentation. Batch process at controlled pH" *Biotechnol. Bioeng.,* 67 (2000), 636–644.

205. A. Pandey "Solid-state fermentation" *Biochem. Eng. J.,* 13 (2003), 81–84.

206. P. K. Sadh, S. Kumar, P. Chawla, J. S. Duhan "Fermentation: a boon for production of bioactive compounds by processing of food industries wastes (by-products)" *Molecules,* 23 (2018), 2560.

207. B. M. Silva, P. B. Andrade, F. Ferreres, A. L. Domingues, R. M. Seabra, M. A. Ferreira "Phenolic profile of quince fruit (*Cydonia oblonga* Miller) (pulp and peel)" *J. Agric. Food Chem.,* 50 (2002), 4615−4618.

208. F. Russo, N. Caporaso, A. Paduano, R. Sacchi "Phenolic compounds in fresh and dried figs from Cilento (Italy), by considering breba crop and full crop, in comparison to Turkish and Greek dried figs" *J. Food Sci.,* 79 (2014), 1278-1284.

209. M. I. Gil, F. A. Tomás-Barberán, B. Hess-Pierce, A. A. Kader "Antioxidant capacities, phenolic compounds, carotenoids, and vitamin C content of nectarine, peach, and plum cultivars from California" *J. Agric. Food Chem.,* 50 (2002), 4976–4982.

210. K. Aaby, D. Ekeberg, G. Skrede "Characterization of phenolic compounds in strawberry (*Fragaria* × *ananassa*) fruits by different HPLC detectors and contribution of individual compounds to total antioxidant capacity" *J. Agric. Food Chem.,* 55 (2007), 4395–4406.

211. Apak, R., zy rek, M., G çl , K. & Çapano lu, E. "Antioxidant activity/capacity measurement. 2. Hydrogen atom transfer (HAT)-based, mixed-mode (Electron Transfer (ET)/HAT), and lipid peroxidation assays" *J. Agric. Food Chem.,* 64 (2016), 1028−1045.

212. İ. Gulcin "Antioxidants and antioxidant methods: an updated overview" *Arch. Toxicol.,* 94 (2020), 651–715.

213. P. Sharma, S. F. McClees, F. Afaq "Pomegranate for prevention and treatment of cancer: an update" *Molecules,* 22 (2017), 177.

214. W. R. García-Niño, C. Zazueta "Ellagic acid: pharmacological activities and molecular mechanisms involved in liver protection" *Pharmacol. Res.,* 97 (2015), 84–103.

215. J.-Y. Bae, J.-S. Choi, S.-W. Kang, Y.-J. Lee, J. Park, Y.-H. Kang "Dietary compound ellagic acid alleviates skin wrinkle and inflammation induced by UV-B irradiation" *Exp. Dermatol., 19* (2010), 182–190.

216. W. Grigsby, D. Steward "Applying the protective role of condensed tannins to acrylic-based surface coatings exposed to accelerated weathering" *J. Polym. Environ. Degrad*., 26 (2018), 895–905.

217. W. J. Grigsby "Photooxidative stability provided by condensed tannin additives in acrylic-based surface coatings on exterior exposure" *J. Coatings Technol. Res.,* 15 (2018), 1273–1282.

218. M. R. da Silveira, R. S. Peres, V. F. Moritz, C. A. Ferreira "Intumescent coatings based on tannins for fire protection" *Mater. Res.,* 22 (2019), e20180433.

219. L. Palou, S. A. Valencia-Chamorro, M. B. Pérez-Gago "Antifungal edible coatings for fresh citrus fruit: a review" *Coatings,* 5 (2015), 962–986.

220. J. M. Krochta "Proteins as raw materials for films and coatings: definitions, current status, and opportunities" in *Protein-Based Films and Coatings* (CRC Press, 2002), 1–41.

221. L. J. Bastarrachea, D. E. Wong, M. J. Roman, Z. Lin, J. M. Goddard "Active packaging coatings" *Coatings* 5 (2015), 771–791.

222. S. Yoa, J. Kim "A Study on the properties of silk and nylon 6 fabrics by tannic acid treatment" J. *Fash. Bus.,* 20 (2016), 119–132.

223. Y. Liu, K. Ai, L. Lu "Polydopamine and its derivative materials: synthesis and promising applications in energy, environmental, and biomedical fields" *Chem. Rev.,* 114 (2014), 5057–5115.

224. M. L. Alfieri, L. Panzella, S. L. Oscurato, M. Salvatore, R. Avolio, M. E. Errico, P. Maddalena, A. Napolitano, M. d'Ischia "The chemistry of polydopamine film formation: the amine-quinone interplay" *Biomimetics,* 3 (2018), 26.

225. A. Andersen, Y. Chen, H. Birkedal "Bioinspired metal-polyphenol materials: self-

healing and beyond" *Biomimetics,* 4 (2019), 30.

226. S. Y. Han, S.-P. Hong, E. K. Kang, B. J. Kim, H. Lee, W. I. Kim, I. S. Choi "Iron gall ink revisited: natural formulation for black hair-dyeing" *Cosmetics,* 6 (2019), 23.

227. G. Crini "Non-conventional low-cost adsorbents for dye removal: a review" *Bioresour. Technol.,* 97 (2006), 1061–1085.

228. M. Sulyman, J. Namiesnik, A. Gierak "Low-cost adsorbents derived from agricultural by-products/wastes for enhancing contaminant uptakes from wastewater: a review" *Polish J. Environ. Stud.,* 26 (2017), 479–510.

229. H. A. Alalwan, M. A. Kadhom, A. H. Alminshid "Removal of heavy metals from wastewater using agricultural byproducts" *J. Water Supply Res. Technol. - AQUA,* 69 (2020), 99–112.

230. L. Panzella, P. Manini, A. Napolitano, M. d'Ischia "The acid-promoted reaction of the green tea polyphenol epigallocatechin gallate with nitrite ions" *Chem. Res. Toxicol.,* 18 (2005), 722–729.

231. J. Tošović, U. Bren "Antioxidative action of ellagic acid—A kinetic DFT study" *Antioxidants,* 9 (2020), 587.

232. J. Mo, P. Panichayupakaranant, N. Kaewnopparat, S. Songkro, W. Reanmongkol "Topical anti-inflammatory potential of standardized pomegranate rind extract and ellagic acid in contact dermatitis" *Phyther. Res.,* 28 (2014), 629–632.

233. W. S. Tavares, A. G. Tavares-Júnior, F. J. Otero-Espinar, M. Martín-Pastor, F. F. O. Sousa "Design of ellagic acid-loaded chitosan/zein films for wound bandaging" *J. Drug Deliv. Sci. Technol.,* 59 (2020), 101903.

234. V. B. Rahimi, V. R. Askari, S. H. Mousavi "Ellagic acid reveals promising anti-aging effects against D-galactose-induced aging on human neuroblastoma cell line, SH-SY5Y: a mechanistic study" *Biomed. Pharmacother.,* 108 (2018), 1712–1724.

235. G. Gorgisen, H. Ozkol, Y. Tuluce, A. Arslan, Y. Ecer, S. Keskin, Z. Kaya, M. C. Ragbetli "Silibinin and ellagic acid increase the expression of insulin receptor substrate 1 protein in ultraviolet irradiated rat skin" *Biotech. Histochem.,* 95 (2020), 641–646.

236. O. Özer, B. Mutlu, B. Kivçak "Antityrosinase activity of some plant extracts and formulations containing ellagic acid" *Pharm. Biol.,* 45 (2007), 519–524.

237. I. Ertam, B. Mutlu, I. Unal, S. Alper, B. Kivçak, O. Ozer "Efficiency of ellagic acid and arbutin in melasma: a randomized, prospective, open-label study" *J. Dermatol.,* 35 (2008), 570–574.

238. H. Shimogaki, Y. Tanaka, H. Tamai, M. Masuda "*In vitro* and *in vivo* evaluation of ellagic acid on melanogenesis inhibition" *Int. J. Cosmet. Sci.,* 22 (2000), 291–303.

239. I. Nyamba, A. Lechanteur, R. Semdé, B. Evrard "Physical formulation approaches for improving aqueous solubility and bioavailability of ellagic acid: a review" *Eur. J.*

Pharm. Biopharm., 159 (2021), 198–210.

240. C. Ceci, G. Graziani, I. Faraoni, I. Cacciotti "Strategies to improve ellagic acid bioavailability: from natural or semisynthetic derivatives to nanotechnological approaches based on innovative carriers" *Nanotechnology,* 31 (2020), 382001.

241. M. A. Ortenzi, S. Antenucci,S. Marzorati, L. Panzella, S. Molino, J. Á. Rufián Henares, A. Napolitano, L. Verotta "Pectin-based formulations for controlled release of an ellagic acid salt with high solubility profile in physiological media" *Molecules* 26 (2021), 433.

242. H. Tokutomi, T. Takeda, N. Hoshino, T. Akutagawa "Molecular structure of the photo-oxidation product of ellagic acid in solution" *ACS Omega,* 3 (2018), 11179–11183.

243. R. Haywood, F. Rogge, M. Lee "Protein, lipid, and DNA radicals to measure skin UVA damage and modulation by melanin" *Free Radic. Biol. Med.,* 44 (2008), 990–1000.

244. C. Pezzella, V. G. Giacobelli, V. Lettera, G. Olivieri, P. Cicatiello, G. Sannia, A. Piscitelli "A step forward in laccase exploitation: recombinant production and evaluation of techno-economic feasibility of the process" *J. Biotechnol.,* 259 (2017), 175–181.

245. L. Panzella, P. Manini, O. Crescenzi, A. Napolitano, M. d'Ischia "Nitrite-induced nitration pathways of retinoic acid, 5,6-epoxyretinoic acid, and their esters under mildly acidic conditions: toward a reappraisal of retinoids as scavengers of reactive nitrogen species" *Chem. Res. Toxicol.,* 16 (2003), 502–511.

246. L. Panzella, L. Melone, A. Pezzella, B. Rossi, N. Pastori, M. Perfetti, G. D'Errico, C. Punta, M. d'Ischia "Surface-functionalization of nanostructured cellulose aerogels by solid state eumelanin coating" *Biomacromolecules,* 17 (2016), 564–571.

247. P. Manini, L. Panzella, T. Eidenberger, A. Giarra, P. Cerruti, M. Trifuoggi, A. Napolitano "Efficient binding of heavy metals by black sesame pigment: toward innovative dietary strategies to prevent bioaccumulation" *J. Agric. Food Chem.,* 64 (2016), 890–897.

248. C. D. Stalikas "Extraction, separation, and detection methods for phenolic acids and flavonoids" *J. Sep. Sci.,* 30 (2007), 3268–3295.

249. M. Ikeda "Public health problems of organic solvents" *Toxicol. Lett.,* 64–65 (1992), 191–201.

250. K. Shanab, C. Neudorfer, E. Schirmer, H. Spreitzer "Green solvents in organic synthesis: an overview" *Curr. Org. Chem.,* 17 (2013), 1179–1187.

251. A. Paiva, R. Craveiro, I. Aroso, M. Martins, R. L. Reis, A. R. C. Duarte "Natural deep eutectic solvents - Solvents for the 21st century" *ACS Sustain. Chem. Eng.,* 2 (2014), 1063–1071.

252. M. Ruesgas-Ramón, M. C. Figueroa-Espinoza, E. Durand "Application of deep

eutectic solvents (DES) for phenolic compounds extraction: overview, challenges, and opportunities" *J. Agric. Food Chem.,* 65 (2017), 3591–3601.

253. A. P. Abbott, G. Capper, D. L. Davies, R. L. Rasheed, V. Tambyrajah "Novel solvent properties of choline chloride/urea mixtures" *Chem. Commun.,* 9 (2003), 70–71.

254. K. Radoševića, M. C. Bubalo, V. G. Srček, D. Grgas, T. L. Dragičević, I. R. Redovniković "Evaluation of toxicity and biodegradability of choline chloride based deep eutectic solvents" *Ecotoxicol. Environ. Saf.,* 112 (2015), 46–53.

255. E. L. Smith, A. P. Abbott, K. S. Ryder "Deep eutectic solvents (DESs) and their applications" *Chem. Rev.,* 114 (2014), 11060–11082.

256. Q. Zhang, K. De Oliveira Vigier, S. Royer, F. Jérôme "Deep eutectic solvents: syntheses, properties and applications" *Chem. Soc. Rev.,* 41 (2012), 7108–7146.

257. M. Francisco, A. Van Den Bruinhorst, M. C. Kroon "Low-transition-temperature mixtures (LTTMs): a new generation of designer solvents" *Angew. Chemie - Int. Ed.,* 52 (2013), 3074–3085.

258. S. L. Perkins, P. Painter, C. M. Colina "Experimental and computational studies of choline chloride-based deep eutectic solvents" *J. Chem. Eng. Data,* 59 (2014), 3652−3662.

259. A. Kovács, E. C. Neyts, I. Cornet, M. Wijnants, P. Billen "Modeling the physicochemical properties of natural deep eutectic solvents" *ChemSusChem,* 13 (2020), 3789–3804.

260. B. Soares, D. J. P. Tavares, J. L. Amaral, A. J. D. Silvestre, C. S. R. Freire, J. A. P. Coutinho "Enhanced solubility of lignin monomeric model compounds and technical lignins in aqueous solutions of deep eutectic solvents" *ACS Sustain. Chem. Eng.,* 5 (2017), 4056–4065.

261. J. P. Wojeicchowski, C. Marques, L. Igarashi-Mafra, J. A. P. Coutinho, M. R. Mafra "Extraction of phenolic compounds from rosemary using choline chloride – based deep eutectic solvents" *Sep. Purif. Technol.,* 258 (2021), 117975.

262. C. Ma, A. Laaksonen, C. Liu, X. Lu, X. Ji "The peculiar effect of water on ionic liquids and deep eutectic solvents" *Chem. Soc. Rev.,* 47 (2018), 8685–8720.

263. O. S. Hammond, D. T. Bowron, K. L. Edler "The effect of water upon deep eutectic solvent nanostructure: an unusual transition from ionic mixture to aqueous solution" *Angew. Chemie*, 56 (2017), 9782–9785.

264. L. Rock, N. Brunswick "Standardized methods for the determination of antioxidant capacity and phenolics in foods and dietary supplements" *J. Agric. Food Chem.,* 53 (2005), 4290–4302.

265. M. Kawaguchi, R. Ito, K. Saito, H. Nakazawa "Novel stir bar sorptive extraction methods for environmental and biomedical analysis" *J. Pharm. Biomed. Anal.,* 40 (2006), 500–508.

266. R. C. Andeme Ela, L. Spahn, N. Safaie, R. C. Ferrier Jr., R. G. Ong "Understanding the effect of precipitation process variables on hardwood lignin characteristics and recovery from black liquor" *ACS Sustain. Chem. Eng.,* 8 (2020), 13997–14005.

267. S. Wang, S. Su, L.-P. Xiao, B. Wang, R.-C. Sun, G. Song "Catechyl lignin extracted from castor seed coats using deep eutectic solvents: characterization and depolymerization" *ACS Sustain. Chem. Eng.,* 8 (2020), 7031–7038.

268. Q. Xia, Y. Liu, J. Meng, W. Cheng, W. Chen, S. Liu, Y. Liu, J. Lia , H. Yu "Multiple hydrogen bond coordination in three-constituent deep eutectic solvents enhances lignin fractionation from biomass" *Green Chem.,* 20 (2018), 2711–2721.

269. M. Francisco, A. Van Den Bruinhorst, M. C. Kroon "New natural and renewable low transition temperature mixtures (LTTMs): screening as solvents for lignocellulosic biomass processing" *Green Chem.,* 14 (2012), 2153–2157.

270. Y.-H. Ci, F. Yu, C.-X. Zhou, H.-E Mo, Z.-Y. Li, Y.-Q. Ma, L.-H. Zang "New ternary deep eutectic solvents for effective wheat straw deconstruction into its high-value utilization under near-neutral conditions" *Green Chem.* 22 (2020), 8713–8720.

271. S. Goriparti, M. N. K. Harish, S. Sampath "Ellagic acid – a novel organic electrode material for high capacity lithium ion batteries" *Chem. Commun.,* 49 (2013), 7234–7236.

272. K. Miki, H. Kamitakahara, A. Yoshinaga, Y. Tobimatsu, T. Takano "Methylation-triggered fractionation of lignocellulosic biomass to afford cellulose-, hemicellulose-, and lignin-based functional polymers: via click chemistry" *Green Chem.,* 22 (2020), 2909–2928.

273. L. S. Kocheva, A. P. Karmanov, M. V. Mironov, V. A. Belyy, I. N. Polina, S. A. Pokryshkin "Characteristics of chemical structure of lignin biopolymer from *Araucaria* relict plant. Questions and answers of evolution" *Int. J. Biol. Macromol.,* 159 (2020), 896–903.

274. C. B hrle, T. U. Nick, M. Bennati, G. Jeschke, F. Vogel "High-field electron paramagnetic resonance and density functional theory study of stable organic radicals in lignin: influence of the extraction process, botanical origin, and protonation reactions on the radical g tensor" *J. Phys. Chem. A.,* 119 (2015), 6475–6482.

275. V. Vinciguerra, S. Spina, M. Luna, G. Petrucci, M. Romagnoli "Structural analysis of lignin in chestnut wood by pyrolysis-gas chromatography/mass spectrometry" *J. Anal. Appl. Pyrolysis,* 92 (2011), 273–279.

276. A. Boukir, S. Fellak, P. Doumenq "Structural characterization of *Argania spinosa* Moroccan wooden artifacts during natural degradation progress using infrared spectroscopy (ATR-FTIR) and X-Ray diffraction (XRD)" *Heliyon,* 5 (2019), e02477.

277. S. Agustin-Salazar, N. Gamez-Meza, L. Á. Medina-Juárez, L., M. Malinconico, P. Cerruti "Stabilization of polylactic acid and polyethylene with nutshell extract: efficiency assessment and economic evaluation" *ACS Sustain. Chem. Eng.,* 5 (2017),

4607–4618.

278. J. Živković, I. Mujić, Z. Zeković, G. Nikolić, S. Vidović, A. Mujić "Extraction and analysis of condensed tannins in *Castanea sativa* mill" *J. Cent. Eur. Agric.,* 10 (2009), 283–288.

279. T. J. Herald, P. Gadgil, R. Perumal, S. R., Bean, J. D. Wilson "High-throughput micro-plate HCl-vanillin assay for screening tannin content in sorghum grain" *J. Sci. Food Agric.,* 94 (2014), 2133–2136.

280. B. Bayram, G. Ozkan, T. Kostka, E. Capanoglu, T. Esatbeyoglu "Valorization and application of fruit and vegetable wastes and by-products for food packaging materials" *Molecules,* 26 (2021), 4031.

281. M. Corrales, J. H. Han, B. Tauscher "Antimicrobial properties of grape seed extracts and their effectiveness after incorporation into pea starch films" *Int. J. Food Sci. Technol.,* 44 (2009), 425–433.

282. J.-W. Han, L. Ruiz-Garcia, J.-P. Qian, X.-T. Yang "Food packaging: a comprehensive review and future trends" *Compr. Rev. Food Sci. Food Saf.,* 17 (2018), 860–877.

283. A. Valdés, A. C. Mellinas, M. Ramos, M. C. Garrigós, A. Jiménez "Natural additives and agricultural wastes in biopolymer formulations for food packaging" *Front. Chem.,* 2 (2014), 6.

284. EUROSTAT. Packaging Waste Statistics. European Union Statistical System. 2019. Available online: https://ec.europa.eu/ eurostat/statistics-explained/index.php?title=Packagingwastestatistics (accessed.

285. M. Asgher, S. A. Qamar, M. Bilal, H. M. N. Iqbal "Bio-based active food packaging materials: sustainable alternative to conventional petrochemical-based packaging materials" *Food Res. Int.,* 137 (2020), 109625.

286. F. Debeaufort "Active biopackaging produced from by-products and waste from food and marine industries" *FEBS Open Bio,* 11 (2021), 984–998.

287. S. Shankar, J.-W. Rhim "Bionanocomposite films for food packaging applications" *Ref. Modul. Food Sci.* (2018), 1-10.

288. F. Luangapai, M. Peanparkdee, S. Iwamoto "Biopolymer films for food industries: properties, applications, and future aspects based on chitosan" *Rev. Agric. Sci.,* 7 (2019), 59–67.

289. J. F. Rubilar, R. M. S. Cruz, "Grape seed extract antioxidant and antimicrobial properties: use in active packaging" in *Grapes: production, phenolic composition and potential biomedical effects* (2014), 165–179.

290. Y. Guo, J. Huang, Y. Chen, Q. Hou, M. Huang "Effect of grape seed extract combined with modified atmosphere packaging on the quality of roast chicken" *Poult. Sci.,* 99 (2020), 1598–1605.

291. P. Vostrejs, D. Adamcová, M. D. Vaverková, V. Enev, M. Kalina, M. Machovsky, M. Šourkov I. Marova, A. Kovalcik "Active biodegradable packaging films modified with grape seeds lignin" *RSC Adv.,* 10 (2020), 29202–29213.

292. T. de Moraes Crizel, A. de Oliveira Rios, V. D. Alves, N. Bandarra, M. Moldão-Martins, S. Hickmann Flôres "Active food packaging prepared with chitosan and olive pomace" *Food Hydrocoll.,* 74 (2018), 139–150.

293. G. Oliveira, C. P. Passos, P. Ferreira, M. A. Coimbra, I. Gonçalves "Coffee by-products and their suitability for developing active food packaging materials" *Foods,* 10 (2021), 683.

294. G. F. Nogueira, R. A. de Oliveira, J. I. Velasco, F. M. Fakhouri "Methods of incorporating plant-derived bioactive compounds into films made with agro-based polymers for application as food packaging: a brief review" *Polymers,* 12 (2020), 2518.

295. A. Orsuwan, S. Shankar, L.-F. Wang, R. Sothornvit, J. W. Rhim "Preparation of antimicrobial agar/banana powder blend films reinforced with silver nanoparticles" *Food Hydrocoll.,* 60 (2016), 476–485.

296. Y. Qin, Y. Liu, L. Yuan, H. Yong, J. Liu "Preparation and characterization of antioxidant, antimicrobial and pH- sensitive films based on chitosan, silver nanoparticles and purple corn extract" *Food Hydrocoll.,* 96 (2019), 102–111.

297. E. Alvarez-Parrilla, R. Urrea-López, L. A. de la Rosa "Bioactive components and health effects of pecan nuts and their byproducts: a review" *J. Food Bioact.,* 1 (2018), 56–92.

298. L. A. de La Rosa, E. Alvarez-Parrilla, F. Shahidi "Phenolic compounds and antioxidant activity of kernels and shells of mexican pecan (*Carya illinoinensis*)" *J. Agri. Food Chem.,* 59 (2011), 152–162.

299. S. Agustin-Salazar, P. Cerruti, L. Á. Medina-Juárez, G. Scarinzi, M. Malinconico, H. Soto-Valdez, N. Gamez-Meza "Lignin and holocellulose from pecan nutshell as reinforcing fillers in poly (lactic acid) biocomposites" *Int. J. Biol. Macromol.,* 115 (2018), 727–736.

300. M. Leon-Bejarano, Y. Durmus, M. Ovando-Martínez, S. Simsek "Physical, barrier, mechanical, and biodegradability properties of modified starch films with nut by-products extracts" *Foods,* 9 (2020), 226.

301. J. Xu, D. Sagnelli, M. Faisal, A. Perzon, V. Taresco, M. Mais, C. V. L. Giosafatto, K. H. Hebelstrup, P. Ulvskov, B. Jørgensen, L. Chen, S. M. Howdle, A. Blennow "Amylose/cellulose nanofiber composites for all-natural, fully biodegradable and flexible bioplastics" *Carbohydr. Polym.,* 253 (2021), 117277.

302. A. Gea, E. Stringano, R. H. Brown, I. Mueller-Harvey "In situ analysis and structural elucidation of sainfoin (*Onobrychis viciifolia*) tannins for high-throughput germplasm screening" *J. Agric. Food Chem.,* 59 (2011), 495–503.

303. J. A. Kennedy, G. P. Jones "Analysis of proanthocyanidin cleavage products following acid-catalysis in the presence of excess phloroglucinol" *J. Agric. Food Chem.,* 49 (2001), 1740–1746.

304. L. Goya, M. A. Martín, S. Ramos, R. Mateos, L. Bravo "A cell culture model for the assessment of the chemopreventive potential of dietary compounds" *Curr. Nutr. Food Sci.,* 5 (2009), 56–64.

305. A. Patras, N. P. Brunton,C. O'Donnell, B. K. Tiwari "Effect of thermal processing on anthocyanin stability in foods; mechanisms and kinetics of degradation" *Trends Food Sci. Technol.,* 21 (2010), 3–11.

306. L. Ngamwonglumlert, S. Devahastin, N. Chiewchan "Natural colorants: pigment stability and extraction yield enhancement via utilization of appropriate pretreatment and extraction methods" *Crit. Rev. Food Sci. Nutr.,* 57 (2017), 3243–3259.

307. V. O. Silva, A. A. Freitas, A. L. Maçanita, F. H. Quina "Chemistry and photochemistry of natural plant pigments: the anthocyanins" *J. Phys. Org. Chem.,* 29 (2016), 594–599.

308. P. Trouillas, J. C. Sancho-García, V. De Freitas, J. Gierschner, M. Otyepka, O. Dangles "Stabilizing and modulating color by copigmentation: insights from theory and experiment" *Chem. Rev.,* 116 (2016), 4937–4982.

309. R. Boulton "The copigmentation of anthocyanins and its role in the color of red wine: a critical review" *Am. J. Enol. Vitic.,* 52 (2001), 67–87.

310. C. C. Gras, H. Bogner, R. Carle, R. M. Schweiggert "Effect of genuine non-anthocyaninic phenolics and chlorogenic acid on color and stability of black carrot (*Daucus carota* ssp. *sativus* var. *atrorubens* Alef.) anthocyanins" *Food Res. Int.,* 85 (2016), 291–300.

311. L. Fan, Y. Wang, P. Xie, L. Zhang, Y. Li, J. Zhou "Copigmentation effects of phenolics on color enhancement and stability of blackberry wine residue anthocyanins: chromaticity, kinetics and structural simulation" *Food Chem.,* 275 (2019), 299–308.

312. C. C. Gras, K. Bause, S. Leptihn, R. Carle, M. Ralf "Effect of chlorogenic acid on spectral properties and stability of acylated and non-acylated cyanidin-3-O-glycosides" *Food Chem.,* 240 (2018), 940–950.

313. Ö. Süfer "Poly (lactic acid) films in food packaging systems" *Food Sci. Nutr. Technol.,* 2 (2017), 000131.

314. L. K. Ncube, A. U. Ude, E. N. Ogunmuyiwa, R. Zulkifli, I. N. Beas "Environmental impact of food packaging materials: a review of contemporary development from conventional plastics to polylactic acid based materials" *Materials,* 13 (2020), 4994.

315. S. Kandasamy, J. Yoo, J. Yun, H.-B. Kang, K.-H. Seol, H.-W. Kim, J.-S. Ham "Application of whey protein-based edible films and coatings in food industries: an updated overview" *Coatings,* 11 (2021), 1056.

316. M. Abdalrazeq, C. V. L. Giosafatto, M. Esposito, M. Fenderico, P. Di Pierro, R. Porta "Glycerol-plasticized films obtained from whey proteins denatured at alkaline pH" *Coatings,* 9 (2019), 322.

317. I. Corrado, M. Abdalrazeq, C. Pezzella, R. Di Girolamo, R. Porta, G. Sannia, C. V. L.Giosafatto "Design and characterization of poly (3-hydroxybutyrate-co-hydroxyhexanoate) nanoparticles and their grafting in whey protein-based nanocomposites" *Food Hydrocoll.,* 110 (2021), 106167.

318. P. R. Salgado, M. E. Lopez-Caballero, M. C. Gomez-Guillen, A. N. Mauri, P. Montero "Exploration of the antioxidant and antimicrobial capacity of two sunflower protein concentrate films with naturally" *Food Hydrocoll.,* 29 (2012), 374–381.

319. M. Freire, S. Cofrades, J. Pérez-Jiménez, J. Gómez-Estaca, F. Jiménez-Colmenero, R. Bou "Emulsion gels containing n-3 fatty acids and condensed tannins designed as functional fat replacers" *Food Res. Int.,* 113 (2018), 465–473.

320. H. Soto-Valdez, R. Auras, E. Peralta "Fabrication of poly(lactic acid) films with resveratrol and the diffusion of resveratrol into ethanol" *J. Appl. Polym. Sci.,* 121 (2011), 970–978.

321. F. Iñiguez-Franco, H. Soto-Valdez, E. Peralta, J. F. Ayala-Zavala, R. Auras, N. Gámez-Meza "Antioxidant activity and diffusion of catechin and epicatechin from antioxidant active films made of poly(L-lactic acid)" *J. Agric. Food Chem.,* 60 (2012), 6515–6523.

322. S. Agustin-Salazar, N. Gamez-Meza, L. A. Medina-Juàrez, H. Soto-Valdez, P. Cerruti "From nutraceutics to materials: effect of resveratrol on the stability of polylactide" *ACS Sustain. Chem. Eng.,* 2 (2014, 1534–1542).

323. D. Battegazzore, S. Bocchini, J. Alongi, A. Frache, F. Marino "Cellulose extracted from rice husk as filler for poly (lactic acid): preparation and characterization" *Cellulose,* 21 (2014), 1813–1821.

324. S. He, C. Gu, D. Wang, W. Xu, R. Wang, Y. Ma "The stability and *in vitro* digestion of curcumin emulsions containing Konjac glucomannan" *Lwt-Food Sci. Technol.* 117 (2020), 108672.

325. A. Hejna "Potential applications of by-products from the coffee industry in polymer technology – current state and perspectives" *Waste Manag.,* 121 (2021), 296–330.

326. D. Baiocco, R. Lavecchia, S. Natali, A. Zuorro "Production of metal nanoparticles by agro-industrial wastes: a green opportunity for nanotechnology" *Chem. Eng. Trans.,* 47 (2016), 67–72.

327. S. Rawal, M. M. Patel "Threatening cancer with nanoparticle aided combination oncotherapy" *J. Control. Release,* 301 (2019), 76–109.

328. Z. A. Raza, A. Rehman, M. Mohsin, S. Z. Bajwa, F. Anwar, A. Naeem, N. Ahmad "Development of antibacterial cellulosic fabric via clean impregnation of silver nanoparticles" *J. Clean. Prod.,* 101 (2015), 377–386.

329. J. W. Rhim, L. F. Wang, S. I. Hong "Preparation and characterization of agar/silver nanoparticles composite films with antimicrobial activity" *Food Hydrocoll.,* 33 (2013), 327–335.

330. M. C. Moulton, L. K. Braydich-Stolle, M. N. Nadagouda, S. Kunzelman, S. M. Hussain, R. S. Varma "Synthesis, characterization and biocompatibility of “green” synthesized silver nanoparticles using tea polyphenols" *Nanoscale,* 2 (2010), 763–770.

331. H. Wu, L. He, M. Gao, S. Gao, X. Liao, B. Shi "One-step in situ assembly of size-controlled silver nanoparticles on polyphenol-grafted collagen fiber with enhanced antibacterial properties" *New J. Chem.,* 35 (2011), 2902–2909.

332. H.-W. Chien, C.-J. Kuo, L.-H. Kao, G.-Y. Lin, P.-Y. Chen "Polysaccharidic spent coffee grounds for silver nanoparticle immobilization as a green and highly efficient biocide" *Int. J. Biol. Macromol.,* 140 (2019), 168–176.

333. H. Wang, J. Qian, F. Ding "Emerging chitosan-based films for food packaging applications" *J. Agric. Food Chem.,* 66 (2018), 395–413.

334. M. N. V. R. Kumar "A review of chitin and chitosan applications" *React. Funct. Polym.,* 46 (2000), 1–27.

335. S. Kumar-Krishnan, E. Prokhorov, M. Hernández-Iturriaga, J. D. Mota-Morales, M. Vázquez-Lepe, Y. Kovalenko, I. C. Sanchez, G. Luna-Bárcenas "Chitosan/silver nanocomposites: synergistic antibacterial action of silver nanoparticles and silver ions" *Eur. Polym. J.,* 67 (2015), 242–251.

336. D. Kadam, B. Momin, S. Palamthodi, S. S. Lele "Physicochemical and functional properties of chitosan-based nano- composite films incorporated with biogenic silver nanoparticles" *Carbohydr. Polym.,* 211 (2019), 124–132.

337. S. J. Chipera, D. L. Bish "Fitting full X-ray diffraction patterns for quantitative analysis: a method for readily quantifying crystalline and disordered phases" *Adv. Mater. Phys. Chem.,* 3 (2013), 47–53.

338. L. Lutterotti, S. Matthies, H. Wenk "MAUD: a friendly Java program for material analysis using diffraction" *IUCr Newsl. CPD,* 21 (1991), 14–15.

339. R. Micillo, J. Sirés-Campos, J. C. García-Borrón, L. Panzella, A. Napolitano, C. Olivares "Conjugation with dihydrolipoic acid imparts caffeic acid ester potent inhibitory effect on dopa oxidase activity of human tyrosinase" *Int. J. Mol. Sci.,* 19 (2018), 2156.

340. R. Micillo,V. Pistorio, E. Pizzo, L. Panzella, A. Napolitano, M. d’Ischia "2-S-Lipoylcaffeic acid, a natural product-based entry to tyrosinase inhibition via catechol manipulation" *Biomimetics,* 2 (2017), 15.

341. R. Gaglione, E. Dell'Olmo, A. Bosso, M. Chino, K. Pane, F. Ascione, F. Itri, S. Caserta, A. Amoresano, A. Lombardi, H. P. Haagsman, R. Piccoli, E. Pizzo, E. J. A. Veldhuizen, E. Notomista, A. Arciello "Novel human bioactive peptides identified in

Apolipoprotein B: evaluation of their therapeutic potential" *Biochem. Pharmacol.,* 130 (2017), 34–50.

342. A. Vollaro, M. R. Catania, M. R. Iesce, R. Sferruzza, B. D'Abrosca, G. Donnarumma, A. De Filippis, F. Cermola, M. DellaGreca, E. Buommino "Antimicrobial and anti-biofilm properties of novel synthetic lignan-like compounds" *New Microbiol.,* 42 (2019), 21–28.

343. C. Jacqueline, J. Caillon, V. Le Mabecque, A.-F. Miegeville, P.-Y. Donnio, D. Bugnon, G. Potel "*In vitro* activity of linezolid alone and in combination with gentamicin , vancomycin or rifampicin against methicillin-resistant *Staphylococcus aureus* by time – kill curve methods" *J. Antimicrob. Chemother.,* 51 (2003), 857–864.

344. O. Catanzano, V. D'Esposito, G. Pulcrano, S. Maiolino, M. R. Ambrosio, M. Esposito, A. Miro, F. Ungaro, P. Formisano, M. R. Catania, F. Quaglia "Ultra-small silver nanoparticles loaded in alginate-hyaluronic acid hybrid hydrogels for treating infected wounds" *Int. J. Polym. Mater. Polym. Biomater.,* 66 (2017), 626–634.

345. C. Queiroz, M. L. Mendes Lopes, E. Fialho, V. L. Valente-Mesquita, "Polyphenol oxidase: characteristics and mechanisms of browning control" *Food Rev. Int.,* 24 (2008), 361–375.

346. J. Nourooz-Zadeh, J. Tajaddini-Sarmadi, S. P. Wolff "Measurement of hydroperoxides in edible oils using the ferrous oxidation in xylenol orange assay" *J. Agric. Food Chem.,* 43 (1995), 17–21.

347. A. V. Nand, S. Swift, B. Uy, P. A. Kilmartin "Evaluation of antioxidant and antimicrobial properties of biocompatible low density polyethylene/polyaniline blends" *J. Food Eng.,* 116 (2013), 422–429.

348. A. Castañeda-Ovando, M. de Lourdes Pacheco-Hernández, M. E. Páez-Hernández, J. A. Rodríguez, C. A. Galán-Vidal "Chemical studies of anthocyanins: a review" *Food Chem.,* 113 (2009), 859–871.

349. S. Wahyuningsih, L. Wulandari, M. W. Wartono, H. Munawaroh, A. H. Ramelan "The effect of pH and color stability of anthocyanin on food colorant" *IOP Conf. Ser. Mater. Sci. Eng.,* 193 (2017), 012047.

350. S. Kumar, A. K. Pandey "Chemistry and biological activities of flavonoids: an overview" *Sci. World J.,* 2013 (2013), 162750.

351. R. Mattioli, A. Francioso, L. Mosca, P. Silva "Anthocyanins: a comprehensive review of their chemical properties and health effects on cardiovascular and neurodegenerative diseases" *Molecules,* 25 (2020), 3809.

352. X.-Y. Chen, J. Zhou, L.-P. Luo, B. Han, F. Li, J.-Y. Chen, Y.-F. Zhu, W. Chen, X.-P. Yu "Black rice anthocyanins suppress metastasis of breast cancer cells by targeting RAS/RAF/MAPK pathway" *Biomed Res. Int.,* 2015 (2015), 414250.

353. D. Li, P. Wang, Y. Luo, M. Zhao, F. Chen "Health benefits of anthocyanins and

molecular mechanisms: update from recent decade" *Crit. Rev. Food Sci. Nutr.,* 57 (2017), 1729–1741.

354. J. Fang "Bioavailability of anthocyanins" *Drug Metab. Rev.,* 46 (2014), 508–520.

355. C. Czank, A. Cassidy, Q. Zhang, D. J. Morrison, T. Preston, P. A. Kroon, N. P. Botting, C. D. Kay "Human metabolism and elimination of the anthocyanin, cyanidin-3-glucoside: a ^{13}C-tracer study" *Am. J. Clin. Nutr.,* 97 (2013), 995–1003.

356. R. M. De Ferrars, C. Czank, Q. Zhang, N. P. Botting, P. A. Kroon, A. Cassidy, C. D. Kay "The pharmacokinetics of anthocyanins and their metabolites in humans" *Br. J. Pharmacol.,* 171 (2014), 3268–3282.

357. F. J. Olivas-Aguirre, J. Rodrigo-García, N. Del R Martínez-Ruiz, A. I. Cárdenas-Robles, S. O. Mendoza-Díaz, E. Álvarez-Parrilla, G. A. González-Aguilar, L. A. de la Rosa, A. Ramos-Jiménez, A. Wall-Medrano "Cyanidin-3-O-glucoside: physical-chemistry, foodomics and health effects" *Molecules,* 21 (2016), 1264.

358. H. Oliveira, I. Fernandes, N. F. Brás, A. Faria, V. De Freitas, C. Calhau, N. Mateus "Experimental and theoretical data on the mechanism by which red wine anthocyanins are transported through a human MKN-28 fastric cell model" *J. Agric. Food Chem.,* 63 (2015), 7685–7692.

359. S. Kamiloglu, E. Capanoglu, C. Grootaert, J. Van Camp "Anthocyanin absorption and metabolism by human intestinal Caco-2 cells - a review" *Int. J. Mol. Sci.,* 16 (2015), 21555–21574.

360. L. Tian, Y. Tan, G. Chen, G. Wang, J. Sun, S. Ou, W. Chen, W. Bai "Metabolism of anthocyanins and consequent effects on the gut microbiota" *Crit. Rev. Food Sci. Nutr.,* 59 (2019), 982–991.

361. U. Hribar, N. Poklar Ulrih "The Metabolism of Anthocyanins" *Curr. Drug Metab.,* 15 (2014), 3–13.

362. P. Vitaglione, G. Donnarumma, A. Napolitano, F. Galvano, A. Gallo, L. Scalfi, V. Fogliano "Protocatechuic acid is the major human metabolite of cyanidin-glucosides" *J. Nutr.,* 137 (2007), 2043–2048.

363. M. Garcia-Alonso, A. M. Minihane, G. Rimbach, J. C. Rivas-Gonzalo, S. de Pascual-Teresa "Red wine anthocyanins are rapidly absorbed in humans and affect monocyte chemoattractant protein 1 levels and antioxidant capacity of plasma" *J. Nutr. Biochem.,* 20 (2009), 521–529.

364. C. D. Kay, G. Pereira-Caro, I. A. Ludwig, M. N. Clifford, A. Crozier "Anthocyanins and flavanones are more bioavailable than previously perceived: a review of recent evidence" *Annu. Rev. Food Sci. Technol.,* 8 (2017), 155–180.

365. S. Schmitt, S. Tratzka, A. Schieber, M. Passon "Hemisynthesis of anthocyanin phase II metabolites by porcine liver enzymes" *J. Agric. Food Chem.,* 67 (2019), 6177–6189.

366. M. Bouktaib, S. Lebrun, A. Atmani, C. Rolando "Hemisynthesis of all the O-

monomethylated analogues of quercetin including the major metabolites, through selective protection of phenolic functions" *Tetrahedron Lett.,* 58 (2002), 10001–10009.

367. C. Cren-Olivé, S. Lebrun, C. Rolando "An efficient synthesis of the four mono methylated isomers of (+)-catechin including the major metabolites and of some dimethylated and trimethylated analogues through selective protection of the catechol ring" *J. Chem. Soc. Perkin Trans. 1,* 2 (2002), 821–830.

368. J. Kozłowska, B. Potaniec, B. Zarowska, M. Anioł "Synthesis and biological activity of novel O-alkyl derivatives of naringenin and their oximes" *Molecules,* 22 (2017), 1485.

369. S. Straßmann, M. Passon, A. Schieber "Chemical hemisynthesis of sulfated cyanidin-3-O-glucoside and cyanidin metabolites" *Molecules,* 26 (2021), 2146.

370. S. Straßmann, T. Brehmer, M. Passon, A. Schieber "Methylation of cyanidin-3-O-glucoside with dimethyl carbonate" *Molecules,* 26 (2021), 1342.

371. R. Mouselmani, E. Da Silva, M. Lemaire "Dimethyl sulfite a potential agent for methylation" *Tetrahedron,* 71 (2015), 8905–8910.

372. R. L. Prior, X. Wu "Anthocyanins: structural characteristics that result in unique metabolic patterns and biological activities" *Free Radic. Res.,* 40 (2006), 1014–1028.

373. P. W. Needs, P. A. Kroon "Convenient syntheses of metabolically important quercetin glucuronides and sulfates" *Tetrahedron,* 62 (2006), 6862–6868.

374. A. Courtois, M. Jourdes, A. Dupin, C. Lapèze, E. Renouf, B. Biais, P.-L. Teissedre, J.-M. Mérillon, T. Richard, S. Krisa "*In vitro* glucuronidation and sulfation of ϵ-viniferin, a resveratrol dimer, in humans and rats" *Molecules,* 22 (2017), 733.

375. A. Burrows "Palette of our palates: a brief history of food coloring and its regulation" *Compr. Rev. Food Sci. Food Saf.,* 8 (2009), 394–408.

376. G. T. Sigurdson, P. Tang, M. M. Giusti "Natural colorants: food colorants from natural sources" *Annu. Rev. Food Sci. Technol.,* 8 (2017), 261–280.

377. M. Iacomino, F. Weber, M. Gleichenhagen, V. Pistorio, L. Panzella, E. Pizzo, A. Schieber, M. d'Ischia, A. Napolitano "Stable benzacridine pigments by oxidative coupling of chlorogenic acid with amino acids and proteins: toward natural product-based green food coloring" *J. Agric. Food Chem.,* 65 (2017), 6519–6528.

378. V. Bongartz, L. Brandt, M. L. Gehrmann, B. F. Zimmermann, N. Schulze-Kaysers, A. Schieber "Evidence for the formation of benzacridine derivatives in alkaline-treated sunflower meal and model solutions" *Molecules* 21, 91 (2016).

379. A. Napolitano, A. Pezzella, G. Prota "6,7-Dihydroxy-1,2,3,4-tetrahydroisoquinoline formation by iron mediated dopamine oxidation: a novel route to endogenous neurotoxins under oxidative stress conditions" *Tetrahedron Lett.,* 40 (1999), 2833–2836.

380. M. Iacomino, J. I. Paez, R. Avolio, A. Carpentieri, L. Panzella, G. Falco, E. Pizzo, M. E. Errico, A. Napolitano, A. del Campo, M. d'Ischia "Multifunctional thin films and coatings from caffeic acid and a cross-linking diamine" *Langmuir,* 33 (2017), 2096–2102.

381. S. V. E. Prigent, A. G. J. Voragen, F. Li, A. J. W. G. Visser, G. A.Van Koningsveld, H. Gruppen "Covalent interactions between amino acid side chains and oxidation products of caffeoylquinic acid (chlorogenic acid)" *J. Sci. Food Agric.,* 88 (2008), 1748–1754.

382. J. A. Fernández-López, J. M. Angosto, P. J. Giménez, G. León "Thermal stability of selected natural red extracts used as food colorants" *Plant Foods Hum. Nutr.,* 68 (2013), 11–17.

383. F. Mastrogiovanni, A. Mukhopadhya, N. Lacetera, M. T. Ryan, A. Romani, R. Bernini, T. Sweeney "Anti-inflammatory effects of pomegranate peel extracts on in vitro human intestinal caco-2 cells and *ex vivo* porcine colonic tissue explants" *Nutrients,* 11 (2019), 548.

La borsa di dottorato è stata cofinanziata con risorse del
Programma Operativo Nazionale Ricerca e Innovazione 2014-2020 (CCI 2014IT16M2OP005),
Fondo Sociale Europeo, Azione I.1 "Dottorati Innovativi con caratterizzazione Industriale"

UNIONE EUROPEA
Fondo Sociale Europeo

Ministero dell'Istruzione, dell'Università e della Ricerca

PON RICERCA E INNOVAZIONE 2014 - 2020